Marine Applications for Structural Adhesives.

Esther M. Knox B. Eng.

Submitted for the Degree of Ph. D.
Glasgow University

Department of Mechanical Engineering
Faculty of Engineering

July 1996

Abstract

Modern structural adhesives are now available that are potentially suitable for the bonding of both metallic components and fibre reinforced polymer materials for structural marine applications. Pultruded grp specimens are increasingly available which together with mass produced grp panels form the building blocks for a wide range of fabricated composite polymer structures. The trends in advanced marine technology are to make greater use of prefabricated components. A major problem in the use of polymer composite materials for large structures is the joining of sub assemblies and laminate panels. This thesis considers the understanding and development of the use of bonded structures and adhesive applications in the offshore and marine industries. The study includes the production, thermal and fatigue performance of bonded grp components and the problem of butt joining of laminates as well as the performance of steel sandwich structures. The results of a small scale experimental study of various detailed design options for panels are supported by finite element analysis. The discussion highlights the advantages and disadvantages of various types of butt joints. Possible failure mechanisms are discussed and include a ranking of joining methods with respect to the strength of the basic laminate. Sandwich panels offer a practical substitute for traditional stiffened plating and, with careful consideration of face and core parameters may be more structurally efficient than stiffened single skin structures. Both analytical and experimental techniques were utilised to study the performance characteristics of steel corrugated core sandwich beam elements under static and fatigue loading. Comparisons between the viable alternative fabrication methods showed adhesive bonding to be very acceptable, especially where structures are subjected to fatigue loading. Transverse to the corrugations, the failure modes are complex and dependent on the combination of geometry of the face and core material. The performance of the necessary bonded joints is particularly influenced by the type of the adhesive used and the form of surface preparation prior to bonding. Small scale experiments have highlighted the importance of suitable surface preparation to promote short term static strength and durability. Investigation of the effect of aging in a wet environment is particularly important in a marine environment as a major concern is the sensitivity of the adhesive to the effects of water. The research has shown that a primer can make an important contribution to both the strength and durability of the joint. Other factors influencing overall joint performance are the type of surface preparation chosen for the substrate, geometric details including joint orientation, spew fillet removal and load. Adhesion at the interface between the adhesive and substrate and also bulk adhesive hydrolytic degradation were also investigated to determine the role each has in influencing the overall durability of an adhesively bonded connection. A novel form of test was successfully developed to rapidly grade the adhesion durability performance at the interface. The results of this research should improve confidence regarding adhesive bonding of materials of types, sections and sizes suitable for marine structures.

Contents

page number

Abstract 2
List of Figures 7
List of Tables 14
Acknowledgements 15

1.0 Introduction 16

2.0 Section A: Durability Performance of Adhesively Bonded Joints
2.1 Introduction 19
2.2 Background 21
2.2.1 Stress Distribution in Adhesively Bonded Joints 21
2.2.1.1 Introduction 21
2.2.1.2 Theory 22
2.2.2 Adhesion 26
2.2.3 Failure of Adhesively Bonded Joints in Wet Environments 27
2.2.3.1 Failure Mechanisms 27
2.2.4 Surface Treatments 31
2.2.4.1 Adherend Surface Preparation 31
2.2.4.2 Bonding Pretreatments 32
2.2.5 Summary of Factors Influencing Durability of Adhesively Bonded Joints 34
2.3 Experimental Procedures 35
2.3.1 Small-Scale Joint Testing 35
2.3.2 Bulk Adhesive Specimen Manufacture 38
2.3.3 Experimental Programme 38
2.3.3.1 Stress Distribution on Adhesively Bonded Joints 38
2.3.3.2 Surface Preparation 38
2.3.3.3 Durability: Accelerated Aging 39
2.3.3.3.1 Bonded Joint Physical Geometric Details 40
2.3.3.3.2 Primer Selection 41
2.3.3.3.3 Bulk and Interface Phenomena 42
2.3.3.3.3.1 Study of Bulk Adhesive Properties 42
2.3.3.3.3.2 Interface Study 42
2.3.3.3.4 Bonded Grp Durability Performance 43
2.3.3.3.4.1 Primer Adhesive Compatibility 43
2.3.3.3.4.2 Grp Joint Durability 44
2.3.3.3.4.3 Grp Surface Preparation 44
2.3.3.3.4.4 Selected Adhesive/Grp/Primer Compatibility 44

page number

2.4 Results 45
2.4.1 Stress Distribution in Bonded Joints 45
2.4.2 Surface Preparation 45
2.4.3 Durability: Accelerated Aging 45
2.4.3.1 Bonded Joint Physical Geometric Details 45
2.4.3.2 Primer Selection 46
2.4.3.3 Bulk and Interface Phenomena 46
2.4.3.3.1 Study of Bulk Adhesive Properties 46
2.4.3.3.2 Interface Study 47
2.4.3.4 Bonded Grp Durability Performance 48
2.4.3.4.1 Primer Adhesive Compatibility 48
2.4.3.4.2 Grp Joint Durability 48
2.4.3.4.3 Grp Surface Preparation 48
2.4.3.4.4 Selected Adhesive/Grp/Primer Compatibility 48
2.5 Finite Element Stress Analysis 49
2.6 Discussion 51
2.6.1 Surface Preparation 51
2.6.2 Stress Distribution in Adhesively Bonded Joints 54
2.6.3 Durability: Accelerated Aging 59
2.6.3.1 Geometric Details 60
2.6.3.2 Primer Effects 67
2.6.3.3 Interface and Bulk Performance 69
2.6.3.3.1 Bulk Performance 69
2.6.3.3.2 Interface Performance 70
2.6.3.4 Grp Bonded Joint Performance 72
2.6.4 Final Comments 75
2.7 Conclusions 78

3.0 Section B: Application of Adhesives for Joining Grp

3.1 Introduction 111
3.2 Background 112
3.2.1 Grp Sandwich Construction 115
3.2.2 Adhesive Selection 115
3.2.3 Health and Safety 117
3.2.4 Bonded Joint Design 118
3.2.5 Thermal Performance 121
3.2.6 Fatigue 122
3.2.7 Failure Theories for Finite Element 123
3.3 Experimental Programme 125
3.3.1 Testpiece Preparation 125

page number

3.3.2 Adhesive Selection 125
3.3.3 Selected Adhesive Performance on Pultruded Material 126
3.3.4 Revised Adhesive Performance 126
3.3.5 Pultrusion Surface Treatment 126
3.3.6 Thermal Performance 127
3.3.6.1 Adhesive Joint High Temperature Performance 127
3.3.6.2 Grp Thermal Performance 128
3.3.6.3 Adhesive Joint Low Temperature Performance 128
3.3.6.4 Thermal Creep Performance 128
3.3.6.5 Post Cure Effect 129
3.3.7 Adhesive Handling Characteristics 129
3.3.7.1 Manual Mixing 129
3.3.7.2 Pot Life 129
3.3.7.3 Cure Schedule 130
3.3.8 Bonded Butt Joint Performance 130
3.3.9 Fatigue Performance 130
3.3.10 Bulk Adhesive Data for Finite Element Analysis 131
3.4 Results 132
3.4.1 Adhesive Selection 132
3.4.2 Selected Adhesive Performance on Pultruded Material 132
3.4.3 Revised Adhesive Performance 132
3.4.4 Pultrusion Surface Treatment 132
3.4.5 Thermal Performance 133
3.4.5.1 Adhesive Joint High Temperature Performance 133
3.4.5.2 Grp Thermal Performance 133
3.4.5.3 Adhesive Joint Low Temperature Performance 133
3.4.5.4 Thermal Creep Performance 133
3.4.5.5 Post Cure Effect 134
3.4.6 Adhesive Handling Characteristics 134
3.4.6.1 Manual Mixing 134
3.4.6.2 Pot Life 134
3.4.6.3 Cure Schedule 134
3.4.7 Bonded Butt Joint Performance 135
3.4.8 Fatigue Performance 135
3.4.9 Bulk Adhesive Data for Finite Element Analysis 135
3.5 Finite Element Stress Analysis 136
3.5.1 Bonded Butt Joint Performance 136
3.5.2 Fatigue Specimens 137
3.6 Discussion 138
3.6.1 Adhesive Selection 138

page number

3.6.2 Health and Safety Issues 139
3.6.3 Adhesive Performance 140
3.6.3.1 Thermal Performance 140
3.6.4 Production Environment 145
3.6.5 Structural Performance 145
3.6.5.1 Butt Joint Numerical Analysis 146
3.6.5.1.1 Tensile Results 147
3.3.5.1.2 Three Point Bend Results 148
3.6.6 Fatigue 150
3.7 Summary Outline Design Guidance 156

4.0 Section C: Steel Corrugated Core Sandwich Construction
4.1 Introduction 199
4.2 Background 200
4.3 Simple Sandwich Theory 203
4.4 Parametric Study 209
4.5 Experimental Work 211
4.5.1 Geometries 211
4.5.2 Experimental Procedures 211
4.5.2.1 Study of Stiffness and Ultimate Capacity 211
4.5.2.2 Fatigue Performance 212
4.6 Results 214
4.6.1 Static Performance 214
4.6.2. Fatigue Performance 215
4.7 Numerical Analysis 216
4.7.1 Complete Structure 216
4.7.2 Single Element 216
4.8 Discussion 218
4.9 Conclusion 226

5.0 Conclusion 240

6.0 References 241

List of figures

2.0 Section A: Durability Performance of Adhesively Bonded Joints

Figure 2.1 Simple lap shear joint used in Volkersen's analysis

Figure 2.2 Volkersen's shear stress distribution as calculated for the specimen shown in figure 2.3

Figure 2.3 Thick steel adherend lap shear connection used in close-form analysis

Figure 2.4 Goland and Reissner tensile stress distribution as calculated for the specimen shown in figure 2.3

Figure 2.5 Finite element analysis results showing the effect of a fillet

Figure 2.6 Various geometries of thick adherend small scale test pieces used throughout this thesis

Figure 2.7 Preloaded cleavage specimen used for accelerated durability tests

Figure 2.8 Bulk material tensile test specimens

Figure 2.9 Scrape jig and specimen

Figure 2.10 Modified grp bonded lap shear specimen and adapters for tensile testing

Figure 2.11 Effect of various mechanical surface preparation techniques have on tensile strength (XSA 25x25mm)

Figure 2.12 Effect of various mechanical surface preparation techniques have on shear strength (XSA 15x25mm)

Figure 2.13 Accelerated (T=30°C,100%R.H.) durability performance of Araldite 2007 bonded steel lap shear joints (XSA 15x25mm) showing the effect of a fillet and preload (15% UTS 19.7kN)
a) all inclusive results
b) the effect of a fillet
c) the effect of a preload

Figure 2.14 Accelerated (T=30°C,100%R.H.) durability performance of Araldite 2007 bonded steel lap shear joints (XSA 15x25mm) showing the effect of an adequate surface preparation prior to the application of a primer (A187)

Figure 2.15 Accelerated (T=30°C,100%R.H.) durability performance of Araldite 2007 bonded steel lap shear joints (XSA 15x25mm) showing the effect of various bonding primers

Figure 2.16 Accelerated (T=30°C,100%R.H.) durability performance of Araldite 2007 bonded steel lap shear joints (XSA 15x25mm) showing the effect of a primer

Figure 2.17 Accelerated (T=30°C,100%R.H.) durability performance of Araldite 2007 bulk tensile samples with and without the application of a preload (20% UTS 1800N)
a)no preload
b) with and without a preload

Figure 2.18 Accelerated (T=30°C,100%R.H.) durability performance of Araldite 2007 interfacial strength on steel adherends with and without the application of a primer (A187)

Figure 2.19 Accelerated (T=30°C,100%R.H.) durability performance of Redux 410 bonded steel lap shear joints (XSA 15x25mm) with and without the application of a primer (A187)

Figure 2.20 Accelerated (T=30°C,100%R.H.) durability performance of Araldite 2005 bonded grp lap shear joints (XSA 15x25mm) on peel ply surfaces with and without a preload (20% UTS 6000N) and a primer (A187)

Figure 2.21 Accelerated (T=30°C,100%R.H.) durability performance of Araldite 2005 bonded grp lap shear joints (XSA 15x25mm) with various surface preparations

Figure 2.22 Accelerated (T=30°C,100%R.H.) durability performance of Redux 420 bonded grp lap shear joints (XSA 15x25mm) with a primer (SiP) on a peel ply surface

Figure 2.23 Principal tensile stress distribution through the adhesive layer for an Araldite 2007 bonded steel lap shear joint (XSA 25x25mm) for a nominal load (20kN)

Figure 2.24 Principal shear stress distribution through the adhesive layer for an Araldite 2007 bonded steel lap shear joint (XSA 25x25mm) for a nominal load (20kN)

Figure 2.25 Principal tensile stress distribution through the adhesive layer for an Araldite 2007 bonded steel lap shear joint of various overlap lengths for a nominal load (20kN)

Figure 2.26 Principal shear stress distribution through the adhesive layer for an Araldite 2007 bonded steel lap shear joint of various overlap lengths for a nominal load (20kN)

Figure 2.27 Principal failure tensile stress distribution through the adhesive layer for an Araldite 2007 bonded steel lap shear joint of various overlap lengths

Figure 2.28 Principal failure shear stress distribution through the adhesive layer for an Araldite 2007 bonded steel lap shear joint of various overlap lengths

Figure 2.29 Co-ordinate system used in the finite element analysis

Figure 2.30 Schematic representation of a failure in a lap shear joint with no fillet

Figure 2.31 Failure surface showing good adhesion of a shot blast Araldite 2007 bonded steel lap shear joint

Figure 2.32 Failure surface showing poor adhesion of an Araldite 2007 bonded steel lap shear joint
a)black oxide surface
b)primer surface

Figure 2.33 Typical failure surface of a 100mm overlap Araldite 2007 bonded steel lap shear joint

Figure 2.34 Experimental load/time plot for 100mm overlap Araldite 2007 bonded steel lap shear joint

Figure 2.35 Typical failure surface of a 100mm overlap Araldite 2007 bonded steel lap shear joint when the adhesive is applied in discrete strips

Figure 2.36 Typical failure surface of an Araldite 2007 bonded steel lap shear joint after accelerated aging (T=30°C,100%R.H.) with the fillet left intact and no preload

Figure 2.37 Typical failure surface of an Araldite 2007 bonded steel lap shear joint after accelerated aging (T=30°C,100%R.H.) with the fillet removed and no preload

Figure 2.38 Typical failure surface of an Araldite 2007 bonded steel lap shear joint after accelerated aging (T=30°C,100%R.H.) with the a preload (15%UTS 19.7kN)
a) spew fillet intact
b) spew fillet removed

Figure 2.39 Plot of water penetration depth into an Araldite 2007 bonded steel lap shear joint with fillet removed (XSA 15x25mm) during accelerated aging (T=30°C,100%R.H.)

Figure 2.40 Typical failure surface of an Araldite 2007 bonded steel lap shear joint primed with a silane (A187) after accelerated aging (T=30°C,100%R.H.)

Figure 2.41 Load displacement plots obtained from bulk tensile samples (see figure 2.8) of Araldite 2007 after accelerated aging (T=30° C,100%R.H.)

Figure 2.42 Typical failure surfaces obtained from the scrape test after accelerated aging (T=30°C,100%R.H.)
a) phase 1 failure
b) phase 2 failure

Figure 2.43 Typical failure surface of an Araldite 2005 bonded grp lap shear joint after accelerated aging (T=30°C,100%R.H.) showing a resin failure

Figure 2.44 Araldite 2007 bonded steel lap shear joint exposed to natural climatic conditions (submerged under load in the Clyde Estuary) to asses aging

3.0 Section B: Application of Adhesives for Joining Grp

Figure 3.1 Several common joint geometries for composite panels

Figure 3.2 Shear failure strength of three adhesives tested at elevated temperatures on steel adherends (XSA15x25mm)

Figure 3.3 Grp thermal performance at elevated temperatures

Figure 3.4 Shear failure strength of three adhesives tested at subzero temperatures on steel adherends (XSA15x25mm)

Figure 3.5 Thermal creep performance of adhesively bonded tensile shear connections (XSA15x25mm)

Figure 3.6 Post cure effect on Redux 420 bonded tensile shear connections (XSA15x25mm)

Figure 3.7 Variation in static strength due to manual mixing of Redux 410 bonded steel shot blast lap shear specimens (XSA15x25mm)

Figure 3.8 Cure schedule at ambient temperatures for Redux 410 bonded steel lap shear joint (XSA15x25mm)

Figure 3.9 A)Recessed strap joint
B)Best experimental butt joint: Bonded hybrid joint of tapered steel straps and 9mm grp adherends

Figure 3.10 Redux 410 adhesively bonded pultruded stiffener/grp plate connection used for fatigue testing in transverse bending

Figure 3.11 Fatigue performance of composite/pultrusion Redux 410 bonded attachments in bending (R=0.2) and marine grade woven roving polyester laminate

Figure 3.12 Three dimensional 20 noded solid element model of a recessed strapped joint.

Figure 3.13 Three dimensional 20 noded solid element model of a steel tapered strapped joint

Figure 3.14 Finite element stress analysis results for the recessed strap joint (tension)
a) S11
b) S22
c) S33

Figure 3.15 Adhesive stress (s12, s22) at the grp/adhesive interface at the position indicated in figure 3.14 of the recessed strap joint (tension)
Figure 3.16 Finite element stress analysis results for the steel tapered strap joint (tension)
Figure 3.17 Detailed stress distribution (s12, s22) through the grp at the tip of the tapered strap (tension)
Figure 3.18 Finite element stress analysis results for the steel tapered strap joint (three point bend)
Figure 3.19 Detailed stress distribution (s22) of the recessed strap joint in the adhesive at the end of the straps (three point bend)
Figure 3.20 Finite element stress analysis results (s11) for the unstressed attachment fatigue specimen
Figure 3.21 Finite element stress analysis results (s22) for the unstressed attachment fatigue specimen
Figure 3.22 Maximum bending stress distribution in the grp plate of the fatigue specimens
Figure 3.23 Finite element stress analysis results (s11) for the stressed attachment fatigue specimen
Figure 3.24 Finite element stress analysis results (s22) for the stressed attachment fatigue specimen
Figure 3.25 Experimental load - displacement curves obtained for Redux 410 and Araldite 2007 bonded steel lap shear joints at elevated temperatures (XSA 15x25mm)
Figure 3.26 Experimental load - displacement curves obtained for Redux 410 and Araldite 2007 bonded steel lap shear joints at sub zero temperatures (XSA 15x25mm)
Figure 3.27 Creep curves for Redux 410 bonded grp/steel tensile shear specimens sustaining various loads at 100°C displayed on a log time graph (XSA 15x25mm)
Figure 3.28 Creep curves for Redux 410 bonded grp/steel tensile shear specimens sustaining various loads at 100°C displayed on a linear time graph (XSA 15x25mm)
Figure 3.29 Failure surface of a Redux 410 bonded grp/steel tensile shear specimen
Figure 3.30 Recessed strap joint tested in tension demonstrating an adhesive failure
Figure 3.31 Double strap grp joint tested in tension demonstrating a resin type failure
Figure 3.32 H - section steel strap joint demonstrating an interply delamination failure

Figure 3.33 Steel tapered strap joint demonstrating an interply delamination failure
Figure 3.34 Fatigue failure surfaces in the pultrusion of the stressed attachment
Figure 3.35 Fatigue failure surfaces of the unstressed attachment
Figure 3.36 Detailed variation of stresses across the plate top surface and at the first ply level of the unstressed fatigue specimen
Figure 3.37 Detailed variation of stresses across the top surface and the middle area of the pultrusion material of the stressed fatigue specimen
Figure 3.38 Detailed variation of stresses at the adhesive/grp interface in the adhesive

4.0 Section C: Steel Corrugated Core Sandwich Construction

Figure 4.1 All steel adhesively bonded (Araldite 2007) corrugated core sandwich beam
Figure 4.2 Simple sandwich beam and sign convention for sandwich theory
Figure 4.3 Influence of various parameters on the longitudinal structural efficiency of the corrugated core
Figure 4.4 Effect of core web angle on longitudinal modulus and structural efficiency for a given core depth, face plate thickness and flange length
Figure 4.5 Comparison of the longitudinal structural efficiency of the corrugated sandwich structure versus traditional single sided stiffening
Figure 4.6 Comparison of the longitudinal structural efficiency of the corrugated sandwich structure versus alternative forms of stiffening
Figure 4.7 Terminology diagram and experimental sandwich dimensions
Figure 4.8 Axial compression test
Figure 4.9 Load versus displacement curves for experimental sandwich beams tested in static three point bending transverse to the corrugations
Figure 4.10 Fatigue experimental results of sandwich beams in the form of a S-N diagram tested in bending transverse to the corrugations
Figure 4.11 Finite element transverse in plane stress distribution across the face plate surfaces of a bonded steel corrugated core sandwich construction
Figure 4.12 Schematic representation of the tensile transverse bending stress from simple sandwich beam theory.
Figure 4.13 Single element model for finite element stress analysis
Figure 4.14 Finite element axial stress results for a single corrugation unit
Figure 4.15 Resultant axial stress distribution at bond edge for an increase in flange length

Figure 4.16 Model C demonstrating permanent plastic deformation of the beam element after loading transverse to the corrugations in bending

Figure 4.17 Model B demonstrating failure by web buckling after loading transverse to the corrugations in bending

Figure 4.18 Model A demonstrating shear failure of a bond to allow the face plate to slip after loading transverse to the corrugations in bending

List of tables

2.0 Section A: Durability Performance of Adhesively Bonded Joints

Table 2.1 Ultimate failure load for thick adherend steel lap shear joints bonded with Araldite 2007 of varying overlap lengths

Table 2.2 Accelerated (T=30°C,100%R.H.) durability performance of Araldite 2007 bonded preloaded (50% UTS 13kN) steel cleavage specimens (XSA 25x25mm)

Table 2.3 Accelerated (T=30°C,100%R.H.) durability performance of Araldite 2007 preloaded bulk adhesive tensile specimens as shown in figure 2.8 (50% UTS 1800N)

Table 2.4 Accelerated (T=30°C,100%R.H.) durability performance of Araldite 2007 preloaded bulk adhesive tensile specimens (20% UTS 1800N)

Table 2.5 Linear elastic material properties used in finite element stress analysis of thick adherend lap shear joints.

3.0 Section B: Application of Adhesives for Joining Grp

Table 3.1 Performance of cold cure adhesives on grp polyester shot blast adherends

Table 3.2 Performance of Redux 410 on grp/pultrusion polyester shot blast adherends

Table 3.3 Performance of Redux 420 on grp polyester shot blast adherends

Table 3.4 Lap shear strength of Redux 420 bonded polyester pultrusion joints using various surface roughening techniques (XSA 15x25mm)

Table 3.5 Influence of pot life on shear strength of Redux 410 bonded steel adherends (XSA 15x25mm)

Table 3.6 Experimental butt joints tensile and bending performance (bond overlap length = 100mm, total length = 300mm, width = 25mm)

Table 3.7 Redux 410 experimental bulk properties

Table 3.8 Material data input for finite element analysis

4.0 Section C: Steel Corrugated Core Sandwich Construction

Table 4.1 Sandwich static performance transverse to corrugations (three point bending)

Table 4.2 Sandwich static performance parallel to corrugations (three point bending)

Table 4.3 Sandwich static performance (axial compression)

Table 4.4 Data input for finite element stress analysis

Acknowledgements

I would like to thank Professor M.J. Cowling for his supervision and endless encouragement throughout the study. I would also like to thank the technicians, Alex Torry, Sandy Erwin, Denis Kearns and Alan Birkbeck for their assistance in the experimental work, Lynn Cullen for secretarial assistance and Yishan Xia for some help in the numerical studies.

The work was supported in part funding by SERC, MTD, MoD, adhesive manufacturers and fabrication and oil industry sponsors. Such support is gratefully acknowledged.

1.0 Introduction

An adhesive may be defined as a material which, when applied to surfaces of a material, can join them together and resist separation[1]. Adhesives as a means of joining materials have been used by mankind for centuries. However, it is only in the last fifty years that the science and technology of adhesives and adhesion have really progressed.

There are many practical advantages which adhesives can offer:

- ability to join thin sheets
- improved stress distribution
- enables novel design concepts
- ability to join dissimilar materials
- improves aesthetic appeal

to mention but a few. But of course there are also disadvantages:

- unknown durability performance in a hostile (wet) environment
- high temperature resistance may be low
- underlying low strength when compared directly to metallic materials
- limited non destructive test methods.

However, there are wide and varied applications for adhesives in many sectors of industry. While the aerospace industry has realised the full potential of the adhesive technology available, the heavier industries are slow to follow. After all, it was many years before welding was widely accepted in the shipyards as opposed to riveting. Thus progress is cautious and slow. The Glasgow Marine Technology Centre has over ten years research experience in adhesive bonding for marine structural applications and has demonstrated the distinct practical applications and benefits which can be offered[2]. The potential for adhesive exploitation is vast in the marine sector. It is becoming increasingly clear that the topside of vessels are determined not only by the loads imposed in service, but also the need to achieve structural integrity and aesthetic appeal. The weld distortion and consequent rework on thin plate structures can make welding an expensive option. Reworking steel components that have been distorted by conventional welding can involve thousands of man-hours. Shipbuilders estimate that removing distortion in 6 to 8 mm plates and modules accounts for 33% of the labour costs of a passenger ship or fast naval craft, and 25% with large tankers and commercial carriers which contain a significant number of parts made from 20mm thick steel.[3] With a reduction in distortion, it may be possible to reduce

actual plate thickness. The effects of weight reduction for superstructure construction can mean higher speeds and increased stability due to reduced top weight. Further distinct potential benefits include possible increased fatigue performance of the components due to the low stress distribution. Fatigue can be a main issue in marine structural service life. The use of adhesives for repair may reduce the need for hot work permits offshore if a cold cure adhesive is used. It is believed that the relatively simple bonding operations with repetitive components will produce labour saving which will thus compensate for any increase in material cost. The performance of structural adhesives has progressed to such a point that it is possible to consider the use of new material combinations together with the opportunity of novel construction for use in the demanding marine and offshore environment. The use of adhesives in technically demanding applications has provided the incentive for research and development and investigations of the fundamental aspects of adhesion science.

The underlying theme throughout this thesis is the use of adhesives for structural applications in the marine and offshore environment. There are three main areas of research:

1. durability performance of the adhesives in a wet (marine) environment

2. the use of adhesives to fabricate glass reinforced plastics (grp) structural panels

3. the use of adhesives to fabricate novel steel corrugated core structural sandwich panels

Section A: Durability Performance of Adhesively Bonded Joints

A main concern, as with any polymer system in a wet environment, is the durability performance of an adhesive connection. It is well known that the most common and important factor influencing the long term behaviour of unprotected adhesively bonded metal joints is the presence of high humidity or liquid water. The effect of prolonged stressing of a steel bonded connection in a humid environment has been the subject of numerous investigations which were predominantly for thin section applications. Although initial bond strengths between different methods of joint preparation can often be similar and appear to give satisfactory strengths, once the joints are introduced to a stressed and humid environment bond strengths can rapidly deteriorate. Consequently, experiments to validate thick section joint parameters are vital. The main bulk of this study uses accelerated ageing procedures (high temperature and humidity) to grade

influencing factors on the performance of both bulk epoxy adhesive material and thick section bonded connections. The main conclusion from this work is that the interface appears to be the moisture critical area in a bonded steel connection which has been shot blasted prior to bonding. This area can be improved by the correct use of an appropriate bonding primer. From this work, a new method of rapidly grading interfacial properties has been developed and proven successful.

Section B: Adhesive Application of Adhesives for Joining Grp.

This section explores the practical considerations of using adhesively bonded grp sections for structural panels. Investigations here included adhesive selection procedures for grp thick sections, health and safety issues, adhesive thermal and fatigue performance. The work included experimental testing of structural sections including panel/panel butt joints. This experimental research was correlated with numerical analyses.

Section C: Steel Corrugated Core Sandwich Constructions

The concept of sandwich construction is to use the material efficiently and where it is required. Corrugated core sandwich panels are believed to be structurally efficient. Steel corrugated core sandwich panels are a specific form of sandwich panel which can only be fabricated using through thickness laser welding, riveting, spot welding or adhesive bonding. This research explored the performance of such bonded panels under static and fatigue loading and their failure mechanisms using both experimental work and finite element stress analysis. It was found that under fatigue loading in the high cycle, low stress regime, an adhesively bonded sandwich panel can out-perform the equivalent laser welded sandwich construction.

2.0 Section A:

Durability Performance of Adhesively Bonded Joints

2.1 Introduction

It is well known that the most common and most important factor influencing the long term behaviour of unprotected adhesively bonded metal joints is the presence of high humidity or liquid water[1]. This has been a subject of concern for many years. Whereas the initial strength of a structural adhesive is fairly high and can be predicted from the vast amount of data available, subsequent time-dependent failure as catastrophic as total delamination of a joint, particularly in tropical conditions, may be observed. This type of failure is less predictable due to limited test data and the relatively short time adhesives have been in common use, which gives rise to a shortage of long term data.

The performance of adhesively bonded joints, as with any other material, is a critical factor for reliable applications in-service. Accelerated environmental testing is a means of estimating service life or of providing data to rank influencing factors in terms of resistance to degradation but the problem is that such environmental testing does not necessarily reflect the degradation mechanisms in the service environment.

In contrast with the technology used in the aerospace industry, the development of adhesives for bonding steel in marine type applications has been governed not only by considerations of the highest possible strength and good durability performance, but more by the consideration of simple and economic process techniques. Sophisticated chemical surface treatment procedures are too expensive, autoclaves for curing process at high temperatures and pressures are mostly not practicable and curing cycles requiring hours to complete are not compatible with the conditions of modern manufacturing production processes.

For marine type applications, an important limitation that has been recognised is the degenerative effect that moisture may have upon the strength of an adhesively bonded joint. Such effects are pronounced when the component is also subject to conditions of high temperature and stress[1].

The aims of this section of work were:

1. To investigate the performance of various surface pretreatment techniques suitable for bonding mild steel adherends for marine type applications, using small scale testing techniques.

2. To investigate the durability performance of thick adherend epoxy bonded joints which are suitable for marine applications. This work involved:

   a) investigation of the stress distribution within an unaged thick adherend lap shear joint to elucidate possible failure mechanisms.

   b) investigation of the durability performance of thick adherend steel lap shear joints using acceptable accelerated aging techniques (30°C, 100% relative humidity). This study involved a review of various practical geometric details which may influence performance. Factors investigated included the application of a prestress, the effect a spew fillet and the effectiveness of various surface pretreatments.

   c) An attempt to isolate the relative influence which the adhesive within the joint and the interface have on durability performance.

   To fully explore (c) two additional pieces of work were undertaken.

      (i) a study of the intrinsic performance of the bulk adhesive after accelerated aging (including the effect prestressing).

      (ii) the formulation of a novel test technique to examine the effect of aging on the adhesive/adherend interface.

   d) investigation of the durability performance of thick adherend epoxy bonded grp specimens subjected to accelerated aging. This work took a similar format to the metallic adherend study and included investigation of various surface pretreatments, (peel plies, shot blasting, the application of a bonding primer) and the application of a prestress.

2.2 Background

This section of work is an essential precursor to the following study on the durability performance of adhesively bonded joints. In order to aid understanding of failure after ageing it is first necessary to examine joint failure, including stress and strain distributions within the bonded joint, before stress redistribution due to ageing has occurred.

2.2.1 Stress Distribution in Adhesively Bonded Joints.

2.2.1.1 Introduction

The ability of an engineer to predict loads and stresses is the basis of any structural engineering design. One of the most common adhesively bonded joint designs employed in industry as a quality control test is the simple lap shear joint. The bonded connection consists of two adherends bonded together by an overlap. However simple in geometry this connection is, the stresses occurring within the adhesive layer are highly complex when a load is applied to the joint. Volkersen[2] carried out the initial work to analyse the stresses occurring within a lap shear joint. His results were later supplemented by those of Goland and Reissner[3] whose study was based on an analytical elastic approach which is still useful today for describing the stresses in an adhesively bonded joint. The key results from these studies are the non-uniform stress distributions across the layer of adhesive and high stress concentrations occurring at the extremities of the overlap. Today, however, there are improved methods of obtaining the stresses involved. Finite element (f.e.) stress analysis is one such tool that can be used to evaluate the detailed stress distribution in the whole of the adhesive layer. The variation in stress alone is however insufficient to predict and explain failure of the adhesive bond. A satisfactory failure criterion has yet to be established[4] but the following being various criteria proposed:

global yielding
yielding of the adherends
a fracture mechanics parameter
local or global failure
critical stress or strain levels in the adhesive over a distance

The purpose of this section of work is to examine the failure of lap shear joints in greater detail and to correlate the experimental study with the results of f.e. analysis with the aim of increasing understanding of the failure processes.

2.2.1.2 Theory

For a simple lap shear joint as shown in figure 2.1, on the most basic level, the average adhesive shear stress, τ, may be calculated from

$$\tau = \frac{P}{bl}$$

where P is the applied load, b is the joint width and l is the overlap length. In this simple analysis the adherends are considered to be rigid and the adhesive only to deform in shear.

In practice the adhesive layer may be regarded as 'thin' and is considered more flexible than the adherends, thus it is reasonable to ignore the axial stresses (cleavage stresses) in the adhesive layer. Thus equilibrium of stresses forbids the shear stress τ_{xy} from varying in the y direction, i.e. over the thickness of the adhesive layer. Following these assumptions, Volkersen[2] produced a simple theoretical elastic stress analysis to determine the distribution of the shearing stresses in the adhesive layer. He assumed that these stresses arise solely from differential straining of the adhesive in the lap joint and the elongation of the adhesive. According to Volkersen[2], the ratio of maximum shearing stress to the mean shear stress is given by

$$\frac{\tau_x}{\tau_m} = \frac{\omega}{2}\frac{\cosh \omega X}{\sinh \omega/2} + \left(\frac{\psi - 1}{\psi + 1}\right)\frac{\omega}{2}\frac{\sinh \omega X}{\cosh \omega/2}$$

where

$$\omega^2 = (1 + \psi)\phi$$

$$\psi = \frac{t_1}{t_2}$$

$$\phi = \frac{Gl^2}{Et_1t_3}$$

$$X = \frac{x}{l}, \qquad -1/2 \le x \le 1/2$$

G = shear modulus of the adhesive
E = Young's modulus of the adherends
t_1, t_2 = the thickness of the adherends
t_3 = the thickness of the adhesive

l = length of the joint

If the adherends are of equal thickness, $\psi = 1$ and $\omega = \sqrt{(2\phi)}$

The maximum adhesive shear stress which occurs at the ends of the joint is

$$\frac{\tau_{max}}{\tau_m} = \sqrt{\frac{\phi}{2}} \coth \sqrt{\frac{\phi}{2}}$$

and the distribution $\frac{\tau_{max}}{\tau_m}$ is shown in figure 2.2 as calculated for the typical thick steel adherend lap shear connection shown in figure 2.3, overlap length of 15mm using values of E=210000N/mm^2, G=1150N/mm^2, t_3=0.5mm and t_1,t_2=6mm. The shear stress at the ends of the joint is 28.47N/mm^2 where the ratio $\frac{\tau_{max}}{\tau_m}$ is 1.07 for a nominal load of 10kN. This would indicate the joint is likely to first fail at the ends. This cannot occur since it implies complementary shear stress on a free surface and no free shear stress can exist on a free surface. The maximum shear stress must occur near the ends of the overlap, but not at the end.

Thus, Volkersen's theory neglects several important factors. As a result of eccentricity of loading of the lap shear joint, there will be a bending moment applied to the joint in addition to the in-plane tension. This bending moment will cause the adherends to bend and allow the joint to rotate. This rotation alters the direction of the load line in the region of the overlap causing a geometrically non-linear problem. Furthermore, the theorem of complimentary shears means that the shear stress at the end of the adhesive must be zero to accommodate the free edge.

Goland and Reissner[3] considered the bending deformation of the adherends as well as the transverse strains ε_y in the adhesive and the associated cleavage stress σ_y. The bending of the adherends outside the joint region has a significant effect on the stress distribution in the joint. The effect is expressed via a bending moment factor k and associated rotational factor k'. k relates the bending moment on the adherend at the end of the overlap, M_0, to the in-plane loading by the relationship

$$M_0 = kP\frac{t}{2}$$

where P is the load and t is the adherend thickness (assuming equal thickness adherends)

The parameters k and k' are not independent of one and other but k is usually dominant. If the load on the joint is very small, $M_0 \approx pt/2$ and $k \approx 1$ so an insignificant rotation of the joint takes place. As the load increases, the overlap rotates and brings the line of action of the load closer to the centre line of the adherends and thus reduces the magnitude of the bending moment factor.

The stress distribution in the joint due to these end loads is then calculated by using one of two separate theories: the first theory neglects completely the flexibility of the adhesive layer and assumes the layer to be extremely thin, of similar elastic stiffness to the adherends so that the deformations are of little importance. The second theory neglects the transverse flexibility of the adherends and assumes the adhesive layer is thin, but that its deformation makes a distinct contribution to the stress pattern of the joint (as in bonded metal to metal joints). The choice of appropriate methods depends on the elastic and geometric properties of the joint under consideration. The problem with these theories is the difficulty of deciding on the appropriate method. Furthermore, both theories are unable to satisfy the stress boundary conditions at the joint edges.

Goland and Reissner[3] treated the adhesive layer as a infinite number of shear springs with an infinite number of tension/compression springs in the y direction and derived expressions for the adhesive shear stress τ_x and the normal stress σ_y. The shear stress is similar to that predicted previously by Volkersen and the normal stress is given by

$$\sigma_y = \frac{pt^2}{L^2 R_3}\left((R_2\lambda^2\frac{k}{2} - \lambda k'\cosh\lambda\cos\lambda)\cosh\frac{\lambda x}{L}\cos + (R_1\lambda^2\frac{k}{2} - \lambda k'\sinh\lambda\sin\lambda)\sinh\frac{\lambda x}{L}\sin\frac{\lambda x}{L}\right)$$

where

F = force per unit width

$p =$ F/t

l=overlap length

L=l/2

$\nu =$ Poisson's ratio

$$\gamma^4 = \sqrt{\frac{6E_a t(1-\upsilon^2)}{Et_a}}$$

$$\lambda = \gamma\frac{L}{t}$$

$$m = \sqrt{\frac{3(1-\upsilon^2)}{2}}$$

$$\xi = \frac{L}{t}\sqrt{\frac{F}{Et}}$$

$$k = \frac{1}{1+2\sqrt{2}\tanh(m\xi)}$$

$$k' = \sqrt{2m\xi}k$$

$$R_1 = \cosh\lambda\sinh\lambda + \sinh\lambda\cos\lambda$$
$$R_2 = \sinh\lambda\cos\lambda - \cosh\lambda\sin\lambda$$
$$R_3 = (\sinh 2\lambda + \sin 2\lambda)/2$$

The tensile stress distribution for this theory is illustrated in figure 2.4 for the similar joint configuration considered previously in this study (15mm overlap & 10kN load). Peak stresses occur at the joint edge with a lower stress level carried within the remaining portion of the joint. The maximum stress per unit load in the joint decreases as the load increases. Lubkin and Reissner[5] considered the calculated results of the above theories in relation to tubular joints and showed that the bounds of this theory are conservative for all but the shortest overlaps, due to the stress relief afforded by the inelastic deformation of the adhesive, but give no indication of the true bounds.

Both of these analyses are limited in their application because the shear and peel stresses are assumed constant through the adhesive thickness, the shear is considered to be at a maximum at the overlap ends and shear deformation of the adherends are neglected. The shear stress at the joint end must be zero because the end face of the adhesive is a free surface.

Recently, a number of authors have developed and updated the theories of Volkersen, Goland and Reissner using both closed-form analytical and finite element analyses, and have developed elastic analyses which take account of the above discrepancies, although the results of Goland and Reissner are found to be relatively accurate.[6]

In general, practical adhesive joints do not have a square edge as considered in the above theories but may in most cases have a spew fillet which has been squeezed out during manufacture. Thus the assumption that the adhesive layer has a square edge is unrealistic in practical applications. It has been shown by Adams[7], figure 2.5, using f.e. stress analysis techniques, that the presence of a fillet causes changes in the adhesive stress distribution in the highly stressed region at the joint end. He concluded that investigation of these stresses is only

possible using finite element methods and that no other modelling technique can accurately represent the stresses and hence be used to predict joint strength.

2.2.2 Adhesion

The mechanisms of adhesion and mechanisms which improve adhesion are not fully understood and many theories have been proposed. The main mechanisms which have been proposed are[1]:

- mechanical interlocking, which suggests that the main source of adhesion is through interlocking or keying of the adhesive into irregularities of the substrate surface[8],

- diffusion of the adhesive polymer molecules across the interface to produce adhesion[9],

- electronic theory presumes that if the adhesive and the adherend have different electronic band structures there is likely to be some electron transfer on contact and this will result in a double layer of electrical charge at the interface and so forming an adhesive bond[10],

- adsorption where adherence is due to the surface forces acting between the atoms in the two surfaces. These forces may be due to weak van der Waals forces or stronger ionic, covalent and metallic bonds due to chemisorption at the interface[11].

- chemical reaction which states that the adhering materials undergo chemical reaction with each other to form primary valence bonds at the interface[79].

- boundary layer theory which states that whatever the cause of interfacial adhesion, the strength of the adhesive joint is determined by the mechanical properties of the materials making up the joint and the local stresses in the joint. It is not determined by interfacial forces because clear failures in the adhesive is highly uncommon. Failure is essentially always cohesive, in the adhesive or adherend or both, or in some boundary layer.[44]

2.2.3 Failure of Adhesively Bonded Joints in Wet Environments.

2.2.3.1 Failure Mechanisms.

Whilst the locus of failure of unaged structural joints usually involve a cohesive type fracture process in the adhesive layer, after environmental attack failure often occurs at or very close to the interface between the adhesive and the adherend[12]. However, whether the failure path is at the interface or whether it is in the oxide, in a weak boundary layer or within the primer (if used) is a matter of some controversy[1]. The exact failure path probably depends upon the particular joint under examination[13]. Thus the type of stress developed in a relatively thin steel adherend used in the automotive industry and the stress developed in a thick steel adherend for a marine type application can produce apparently different failure processes before and after environmental ageing, due to the different stress pattern within the joints.

Water is the substance which causes the greatest problems in the environmental stability of adhesive joints. There are two fundamental problems with water, its abundance and the fact that adhesives are hydrophilic. (The polar groups which confer adhesive properties on a substance are inherently hydrophilic[14]). In a marine application the majority of bonded structural components will be exposed to moist air and if the relative humidity is high then over a period of time the strength of the joint will usually decline. There are many studies in the literature which have demonstrated this by exposing adhesive joints to higher humidity, natural climates or laboratory environments[15,16,17,18].

Water may enter and affect adhesively bonded joints by one or a combination of the following processes:[14]

1. diffusion through the adhesive[19]
2. transport along the interface[20]
3. capillary action through cracks and crazes in the adhesive
4. diffusion through the adherend if it itself, permeable[21]

This may cause weakening by one or a combination of the following actions[14]:

a. altering the adhesive properties in a reversible manner, such as by platicisation[22].
b. altering the adhesive properties in an irreversible manner either by causing it to hydrolyse, crack, or craze[23]

c. attacking the interface, either by displacing the adhesive or hydrating the metal or metal oxide[24]

Knowledge about reactions in the boundary zone, especially those at the interface between the adhesive and the metal surface, is relatively poor. This is also the case for the fracture mechanisms after ageing processes. Generally, it is understood that whilst the bonding in the boundary zone between a polymer and metal surface is of high strength, it is not necessarily stable against the effects of water[25].

The first research into the application of continuum fracture mechanics to the failure of adhesive joints was undertaken by Ripling and co workers[26]. They developed the double cantilever joint geometry which is a constant compliance geometry. This results in the adhesive fracture energy being independent of crack length and thus is well suited to environmental studies where crack growth will be a function of the applied load and environment. They found that a specimen containing a cohesive starter crack, loaded and placed in water, showed interfacial rather than cohesive failure. This interfacial failure occurred within the stress field generated by the original cohesive crack and eventually propagated along the adhesive/metal oxide interface. The fracture energy required, G_{Ic}, to cause crack growth in an aqueous environment is much lower than that needed in a relatively dry environment[27]. However the measured adhesive fracture energies required for this crack growth are much higher than the thermodynamic work of adhesion. This is because under an applied load, mechanical strain energy is available to assist environmental cracking. This is reflected in the inelastic energy dissipative process e.g. plastic flow occurring in the regions of the adhesive around the crack tip. The thermodynamic work of adhesion does not allow for such processes.

Mostovoy et al[27] concluded that there was a minimum G_{Ic} below which slow crack growth would not occur in aqueous environments. This would imply that there is a stress below which no environmental attack will occur. However, the evidence is conflicting. The timescale over which the experiments were conducted was insufficiently long to be able to state, with confidence, that the true minimum value of G_{Ic} had been attained. It is well established that joints under no externally applied stress may still suffer environmental attack[1]. Thus, whether the presence of a stress is essential for environmental attack to occur has yet to be definitely established, but it is obvious that stresses including applied, swelling and shrinkage stresses may accelerate environmental decay mechanisms. Cherry and Thomas[28] have also argued that, the presence of a stress is essential for environmental attack but consider that in the absence of an

externally applied stress, internal shrinkage stresses provide the necessary strain energy requirements. However, this hypothesis has yet to be proven, especially since;

(a) hot cure adhesives are associated with the highest shrinkage stresses[95] but generally result in the most durable joints, and

(b) any shrinkage stresses will probably be rapidly diminished by stress relaxation processes in the adhesives, accelerated by plasticisation due to the presence of water and swelling stresses due to water absorption.

The above observations highlight the importance of the interface when considering environmental failure mechanisms. Corrosion environmental attack on the metallic adherend material can cause a loss of joint strength[29] but this is not generally a common failure mechanism. Corrosion of the surface of a metal adherend is often a post failure occurrence after the displacement of adhesive on the metal by water[19].

In a review by Kinloch[30], the various parameters associated with environmental degradation of structural adhesive connections and a qualitative model was proposed for the overall failure mechanisms were considered. The key steps were as follows:

Initially, there is an accumulation of the critical water concentration in the interface region. The rate of attaining this concentration appears to be controlled by the rate of water diffusion through the adhesive in most cases. This can be accelerated by temperature and possibly stress. Several groups have shown that the kinetics of the environmental failure mechanism may be governed by the rate of diffusion of water into the joint. Brewis and co-workers[31] have also demonstrated that a linear relationship often exists between loss of joint strength and total water content of the adhesive layer. De Neve and Shanahan[32] indicate that the adsorption behaviour is essentially Fickian. The glass transition temperature, Tg, and the elastic modulus corresponding to the rubbery state both decrease with water uptake. The phenomena are probably related to plasticisation of the polymer. To show that the water diffusion process was the rate determining stage for an epoxy system, Bowditch et al[33] took modulus measurements on an epoxy formulation filled with 180phr (parts per hundred resin by weight) of titanium oxide when dry and after equilibration with an environment of 81% relative humidity. It was shown that the full extent of disruption of the adhesion interface was rapidly achieved and was not subsequently progressive. If water enters a joint by diffusion through the adhesive

layer then it is possible to calculate the distribution of water using standard equations (Fick's Law)[34] up to a point.

Whilst studying epoxy-bonded grit-blasted mild steel butt joints, Gledhill, Kinloch and Shaw[24] noted that the exposure to 55% relative humidity at 20°C for 2500 hours failed to result in any loss of strength, although exposure to liquid water at progressively higher temperatures led to increasing loss of joint strength. Information of this type led to the introduction of the concept of a critical water concentration which must be present before degradation may occur. Contradictory evidence was found for the existence of a limiting equilibrium water content[35,36] below which joints were unaffected by water. Here[35], it was concluded that attack of adhesion interfaces by water was reversible and that, at any given equilibrium water content, the full potential of water for degradation of adhesive joints was modified by the partitioning of water between the adhesive and the interface.

Following water penetration[30], there is a loss of integrity of the interfacial regions. The precise mechanism responsible for this will depend upon the combination of adhesive and adherend. Two common mechanisms are:

(i) rupture of interfacial bonds by either displacement of the adhesive by water to cause failure of interfacial secondary bonds or possible hydrolysis of interfacial covalent bonds. The stability of any adhesive/adherend interface in the presence of liquid environment may be assessed from the thermodynamic arguments of Gledhill and Kinloch[19]. The thermodynamic work of adhesion is defined as the energy required to separate a unit area of two phases forming an interface, if only secondary forces, e.g. Van der Waals, are acting across the interface, which is believed by many to be the main mechanism of adhesion for most adhesives. Kinloch[37] has given a table in which the work of adhesion of adhesive interfaces are compared to their tendency to debond interfacially in an unstressed condition. The fact that interfacial debonding only occurs when the thermodynamic work of adhesion is negative is very strong evidence of the validity of thermodynamics in predicting the durability of the adhesive bonds. The thermodynamics as stated above take no account of intrinsic interfacial forces arising from primary bonds or mechanical interlocking.

(ii) changes occurring in the oxide structure e.g. hydration causing mechanical weakening of the oxide layer[36].

The rate of strength loss in the interfacial regions may be faster if a stress is present[1]. This stress can be an externally applied stress, internal stress produced

by shrinkage during cure, or by adhesive swelling induced by water uptake. For a joint to fracture or lose strength upon testing it is not necessary for complete weakening of the interfacial regions. From basic fracture mechanics considerations, only a relatively small crack is required to have developed before a substantial decrease in failure time at constant load is produced.

2.2.4 Surface Treatments

2.4.1.1 Adherend Surface Preparation

It has been recognised for many years that the establishment of intimate molecular contact at the interface is a necessary, though sometimes insufficient, requirement for developing strong adhesive joints[1]. This means that the adhesive needs to spread over the solid substrate, or adherend surface and needs to displace air and any other contaminants that may be present on the surface. Furthermore, the adherend or substrate requires to be a receptive site for the formation of a strong bond, i.e. free from gross contamination and weak surface layers.

In marine applications involving the adhesive bonding of steel adherends, surface preparation plays an important role in both the initial strength of a joint and its long term durability. In contrast to the case of aluminium and titanium, where an oxide usually exists, chemical etching procedures are not recommended for steel adherends due to cost, complexity and practicality, except for the case of stainless steels[25]. The best results in previous studies[38] have been obtained using shot blasting or mechanical roughening of steel surfaces.

The mechanical roughening process removes surface oxide scale which is essentially chemically passive and produces a fissured surface. The nascent surface reoxidises almost immediately but the consequences of the roughening treatment are an increase in surface area for bonding purposes and the formation of chemically active oxide layers[39]. In the immediate absence of liquid water, this enhancement of the surface appears to be relatively stable[40] for timescales sufficient to allow production bonding processes to be completed. It appears that some form of solvent based degreasing treatment prior to and/or after mechanical treatment is beneficial[38,41]. Some hot cured epoxy adhesives are, however, capable of producing reasonable results on as-received oiled steel[41] due to an inherent ability to absorb some oil, thus displacing it from the interface with the adherend.

In the quest for good durability in wet environments, the use of primers of various types has been promoted and investigated over a number of years. In studies of

the boundary layer[42] between an adhesive and a steel adherend and the consequences for long term durability, it has become clear that there is a 'weak boundary layer' phenomenon which is affected by surface treatment. It is also clear that water ingress can destroy chemical bonds in this boundary region. Hence chemical treatments involving silane primers[43] have been studied as a means of increasing the chemical stability in this region through the production of covalent bonds at the interface[25].

2.2.4.2 Bonding Pretreatments

Results of some experiments[25] have led to the conclusion that the invading water at the glueline can also destroy the chemical bonds in the boundary zone by hydrolytic reactions. If such a mechanism exists, it should be possible to increase the stability of the boundary zone by replacing the original water-unstable chemical bonds by stable systems. This situation can be achieved by using substances with the metal oxides to form more stable chemical compounds which after this react, via the other chemical groups, with the adhesive to form covalent bonds. Classical substances which can react more readily with the metal oxide or with the polymers and build up water stable bonds are organic silanes. They have been used as finishes on glass fibres and in the matrix resins in fibre reinforced plastics for many years[44].

If such a primer, based upon reactive silanes, is used on mild steel adherends, a marked improvement in durability can be achieved[12]. Reactive silanes can also be mixed directly in the bulk adhesive and thus will not only be present on the boundary layer. Each primer has a specific chemical makeup and may only be suitable for a range of specific adhesive and adherends.

It has been shown that the following conditions, associated with the use of primers, have a major effect on joint strength[45]:

- the combined choice of primer and adhesive
- the solvent for the primer
- the pH of the primer solution
- the drying conditions of the primer.

This work[45] has shown how a primer can make an essential contribution to the strength and durability of a joint but that its choice and use are critical as that of the adhesive itself.

For a silane primer, which resulted in increased joint durability, there was some evidence for chemical rather than a purely secondary bonding between the primer and the metal oxide and it is postulated that the presence of the interfacial chemical bonds were responsible for the greatly increased durability[46]. Further work using Auger and X-ray photoelectron spectroscopy has shown that a silane often increases joint durability and the polysiloxane metal oxide interface is resistant to water attack. The primer layer itself is now the weakest part of the joint and fracture may occur by cohesive failure of that layer. Thus, to increase joint durability, further attention should be focused on increasing the intrinsic strength of the silane based primers commonly employed[30].

The effect on the adhesive of mixing a reactive silane into the adhesive is not due to the permeability coefficient and diffusion constant being reduced[25]. Measurements of water diffusion in the adhesive, with and without reactive silanes, showed that a silane content of 2% did not change the diffusion properties of the epoxy resin. On the other hand this does not exclude the possibility that the silane content within the adhesive causes positive effects in a, supposedly, weak boundary layer which itself is produced by the influence of the state of the metal surface. A silane mixed with the adhesive may improve the wetting of the substrate by the adhesive and therefore improve adhesion.

The deleterious effect of water on the joint strength and post-failure corrosion of the substrate could be avoided if the integrity of the interface regions could be maintained. Thus, water must be either prevented from reaching the interface in sufficient concentrations to cause damage or the intrinsic durability of the interface must be increased.

Most organic polymers are permeable to water to a varying extent[47]. Epoxy and phenolic adhesives are at the lower end of the spectrum and, whilst there is undoubtedly room for improvement, the other properties of any adhesive such as wetting, adhesion characteristics, process ability, toughness and cost must be balanced against the need for low coefficients of permeability and diffusivity.

A second approach has been to use sealants[48] (which are usually based upon organic polymers) to coat the edges of the exposed joints. This will obviously only slow down the penetration of water but it is often not possible to apply a thick enough layer to be effective.

2.2.5 Summary of Factors Affecting Durability of Adhesively Bonded Joints.

If the service environment physically or chemically attacks the adhesive to any extent, then the joint may well be weakened. However, loss of strength in the adhesive is not usually a major mechanism of attack in an aqueous environment. While the locus of failure of well-prepared joints is invariably by cohesive fracture in the adhesive layer, after environmental attack it is usually via apparent interfacial failure between the adhesive and substrate. The main aspects of the durability of structural adhesive joints are:[30]

1. Water is a particularly aggressive environment, especially when joints are exposed to hot/wet environments. Such exposure can impair performance by producing a loss of strength in the joints and these effects can be accelerated by the presence of a stress.

2. Adherends which posses high surface free energies are associated with environmental failure at the interface.

3. Mechanisms of environmental degradation which have been identified are:

   (i)displacement of the adhesive on the adherend by water, owing to the rupture of secondary bonds at the adhesive adherend interface. This may be predicted from thermodynamic considerations.

   (ii)subtle changes occurring in the oxide structure on the metallic adherend e.g. hydration which causes mechanical weakening and eventually failure of the oxide layer. This process may be inhibited or accelerated by the presence of trace elements in the oxide layer.

   (iii)hydrolysis in a boundary layer of the adhesive, adjacent to the adherend surface, the properties of this boundary layer being different from those of the bulk adhesive.

   (iv)in special circumstances there is gross corrosion of the adherends, but usually such corrosion is a post-failure occurrence.

4. The kinetics of environmental failure are influenced by the diffusion of water through the adhesive and, in some cases, this may be the rate determining stage.

5. To increase service performance a surface pre-treatment and/or a surface primer must be employed to ensure the generation of stable oxide layers and thus the formation of strong interfacial forces which are resistant to rupture by water.

2.3 Experimental Procedures

2.3.1 Small Scale Joint Testing

A variety of specimen geometries as per figure 2.6 were used to apply shear, tensile, shear, cleavage and peel loading as appropriate. Some of the experimental studies included in this thesis involved steel adherends which were prepared from BS4360 Grade 43A mild steel. Other studies included a marine grade grp (E-glass isothalic polyester resin composite) which were prepared from laminates produced by Vosper Thornycroft UK Ltd.

The adherend and the type of adhesives used for each study are listed in the table below. In the majority of studies using steel adherends, a standard surface preparation was employed which involved shot blasting and solvent degreasing with acetone. Adhesive dispensing was done manually and applied to the adherend surface using a spatula. Bond line thickness was controlled by wires, shims and/or careful clamping with spacers. For the case of the single part heat cured epoxy adhesive (Araldite 2007 from Ciba Geigy[49]) curing was performed using an oven at 180°C for twenty minutes according to the manufacturer's recommendations. The temperature of the adhesive during cure was monitored by a thermocouple. The sample was then allowed to cool at ambient temperatures in the laboratory. For the two part cold curing adhesives (Araldite 2005, Redux 410 and Redux 420 all from Ciba Geigy[49]) curing was carried out at ambient laboratory temperatures for a period of 48 hours or seven days.

Unless otherwise stated, the adhesive spew fillets were left removed. The individual components of the study, testpieces and adhesives used are summarised below.

study/section	testpiece/adherend/figure	adhesive
stress distribution in bonded joints/2.3.3.1	lap shear/s*/fig2.6	2007
surface preparation/2.3.3.2	lap shear/s/fig2.6	2007
	tensile/s/fig2.6	2007
bonded joint physical geometric details/2.3.3.3.1	lap shear/s/fig2.6	2007
	cleavage/s/fig2.7	2007
primer selection/2.3.3.3.2	lap shear/s/fig2.6	2007
bulk adhesive properties/2.3.3.3.3.1	bulk tensile//fig2.8	2007

study/section	testpiece/adherend/figure	adhesive
interface performance/2.3.3.3.3.2	scrape test/s/fig2.9	2007
primer adhesive compatibility/2.3.3.3.4.1	lap shear/s/fig2.6	Redux410
grp bonded joint/2.3.3.3.4.2	lap shear/grp*/fig2.10	2005
grp surface preparation/2.3.3.3.4.3	lap shear/grp/fig2.10	2005
Redux/grp/primer compatibility/2.3.3.3.4.4	lap shear/grp/fig2.10	Redux420
adhesive selection/3.3.2	lap shear/grp/fig2.6 tensile/grp/fig2.6 cleavage/grp/fig2.6 impact/grp/fig2.6	various
selected adhesive performance on pultrusion/3.3.3	lap shear/grp,p*/fig2.6 tensile/grp,p/fig2.6 cleavage/grp,p/fig2.6 impact/grp,p/fig2.6	Redux410
revised adhesive performance/3.3.4	lap shear/grp/fig2.6 tensile/grp/fig2.6 cleavage/grp/fig2.6 impact/grp/fig2.6	Redux420
pultrusion surface treatment/3.3.5	lap shear/p/fig2.6	Redux420
adhesive high temperature performance/3.3.6.1	lap shear/s/fig2.6	Redux410 2007 Autostic[50]
grp thermal performance/3.3.6.2	tensile/grp/fig2.8	Not Applicable

study/section	testpiece/adherend/figure	adhesive
adhesive low temperature performance/3.3.6.3	lap shear/s/fig2.6	Redux410 2007 Autostic[50]
thermal creep performance/3.3.6.4	tensile shear/s,grp/fig2.6	Redux410 Redux420
post cure effect/3.3.6.5	lap shear/s/fig2.6	Redux420
manual mixing/3.3.7.1	lap shear/s/fig2.6	Redux410
pot life/3.3.7.2	lap shear/s/fig2.6	Redux410
cure schedule/3.3.7.3	lap shear/s/fig2.6	Redux410
butt joint performance/3.3.8	butt joints/grp/table3.6	Redux410 2005
fatigue performance/3.3.9	stiffener connection/grp,p/fig3.10	Redux410
bulk adhesive performance/3.3.10	bulk tensile//fig2.8	Redux410
sandwich static performance/4.5.2.1	sandwich construction/s/fig4.7	2007
sandwich fatigue performance/4.5.2.2	sandwich construction/s/fig4.7	2007

*s=steel
grp=glass reinforced plastic
p=pultrusion

2.3.2 Bulk Adhesive Specimen Manufacture

This method was used to produce bulk adhesive specimens of hot curing one part paste adhesive, Araldite 2007.

1. Heat adhesive to approximately 40°C to reduce viscosity and increase wetability, especially if the adhesive has been stored in a refrigerator.
2. Spread adhesive into the pre-treated PTFE mould. (The mould is made from a heat sink base and aluminium sides for good heat transfer. The sides are approximately 4mm in height)
3. Heat adhesive and mould to approximately 40°C.
4. Apply vacuum over mould.
5. Respread adhesive into mould using a warm spatula.
6. Repeat 3,4 & 5 as necessary until no further air can be removed from the bulk material.
7. Place a thermocouple in a corner of the adhesive.
8. Control temperature rise by 10°C increments until equilibrium is reached at 120°C.
9. Increase temperature to 140°C and cure for 80 minutes.
10. Machine the cured adhesive to the required dimensions as stated in BS18: 1987 (see figure 2.8).

2.3.3 Experimental Programme

2.3.3.1 Stress Distribution in Bonded Joints

For the purpose of this study, a series of thick adherend steel lap shear Araldite 2007 bonded specimens (figure 2.6) with varying overlap lengths from 15mm to 100mm were prepared using standard techniques in 2.3.1 above and tested. The tests were performed in a 250kN Instron tensile testing machine at a constant crosshead speed (0.2mm/minute) at ambient temperatures.

2.3.3.2 Surface Preparation

To investigate the effects of a range of common mechanical surface preparation methods a series of standard (15mm overlap) thick adherend steel lap shear and tensile, square section, specimens (X.S.A 25x25mm), see figure 2.6, were prepared as specified in section 2.3.1 above and tested for their ultimate failure load.

The specimens were subjected to a range of different surface treatments prior to bonding with Araldite 2007, including:

as-received surface with a heavy oxide layer,
abraded using abrasive paper grade p400,
ground using a surface grinder,
shot blast using aluminium oxide medium,
milled on a milling machine using a carbide cutter,
oily.

Experiments included each of these surface treatments with and without acetone degreasing and including a single surface condition with a bonding primer addition. The bonding primer used was Redux 113[49], which is a two-component corrosion-inhibiting hot-cure epoxy resin primer solution, that may also be used as a general purpose primer. Such a primer, is perhaps, more suitable for use with a lower strength adhesive where the primer adhesion strength is more compatible with that of the adhesive. The primer was applied as a solution with a brush.

The tests were performed in a 250kN Instron tensile testing machine at a constant crosshead speed (0.2mm/minute) at ambient temperatures.

2.3.3.3 Durability: Accelerated Aging

The durability of bonded joints in any environment is related to a range of parameters involving a series of complex processes. To be able to understand these processes, and hence the adhesive performance, the strategy adopted in this thesis involves separating out particular variables. Thus, the overall study had the aim of predicting performance of bonded connections through a range of substudies. This included using steel adherends and hot cure adhesives to compare and calibrate the performance of several variables easily. The effect of water diffusion into the adhesive can be clearly seen from the strength behaviour of bonded joints in humid environments. It is usual to investigate the ageing properties in bonded steel joints by measuring the initial dry strength and the residual strength after ageing. All the samples were bonded with Araldite 2007 and aged in an environmental cabinet maintained at 30°C and 100% relative humidity. Each subseries of experiments had a duration of twelve weeks. Within the twelve week period two samples of each test condition were tested (wet) to their ultimate failure load at two week intervals. This environmental treatment is referred to as "standard ageing" in the remainder of this thesis.

2.3.3.3.1 Bonded Joint Physical Geometric Details

In this work two types of specimens were used - thick adherend steel lap shear joints (15mm overlap) and preloaded steel cleavage specimens, (X.S.A 25x25mm) see figures 2.6 and 2.7. All the specimens were bonded with Araldite 2007, using standard procedures in section 2.3.1 above.

Four variations of the standard thick adherend lap shear specimen were investigated. These were:

type A:a fully cleaned joint edge and no load on the joint

type B:a joint left with the excess adhesive on the bond edge and no load applied.

type C:as in A but with 15% of the initial failure load applied to the joint.

type D:as in B and with 15% of the initial failure load applied to the joint. (Dry initial failure load is approximately 19.7 kN and 21.4 kN without and with fillet respectively.)

Forty eight lap shear specimens were involved in this phase of the work. The load was applied to the lap shear specimens using stress tubes. Two specimens were placed in each tube which was then torqued to the required load level. The loaded stress tubes and unloaded specimens were then placed in the environmental cabinet where conditions were maintained at standard ageing conditions. Two specimens of each type were tested wet for their residual static strength at two weekly intervals for a total of 12 weeks.

The tests were performed in a 250kN Instron tensile testing machine at a constant crosshead speed (0.2mm/minute) at ambient temperatures.

Two types of preload cleavage specimens were investigated, both preloaded at 50% of their initial failure load (approx. 13kN):

1. A fully cleaned joint edge with all spew fillets removed.

2. A joint with all spew fillets retained.

The static preload was applied very simply to the cleavage specimen using a bolt (see figure 2.7). Each cleavage specimen was first loaded to the required level in

a testing machine and the bolt was then touch tightened before the applied load was removed. The specimens were then suspended in the cabinet at standard ageing conditions. Two specimens of each type were removed and tested (wet) to destruction each month over a period of ten months. In all cases the specimens were tested immediately on removal from the cabinet while the bonds were fully saturated.

The tests were performed in a Lloyd 10000L tensile testing machine at a constant crosshead speed (0.2mm/minute) at ambient temperatures.

2.3.3.3.2 Primer Selection

Standard thick adherend steel lap shear joints (see figure 2.6) and a typical hot cure single-part structural epoxy paste adhesive, Araldite 2007, were used to investigate the role an adhesive primer has in improving joint strength and durability. Two silanes (A187[51] and SiP[52]) and two corrosion inhibitors (Albritec[53] and Accomet-c[54]) were chosen as pretreatment primers for bonding. Two different surface preparations were also incorporated in this study:

(i) shot blasting:- found to be the best form of mechanical roughening on steel adherends to produce high short term strength;

(ii) black oxide layer:- (steel left in the as-received state from the steel mill) this is the worst form of surface conditioning for short term static strength as the thick oxide layer forms a weak link between the adherend and the adhesive and this will be the site of failure initiation.

The surface primers were prepared as solutions according to the manufacturers' instructions. They were applied to the steel surfaces prior to the adhesive application by a brush and allowed to dry on the adherend surface. It is also possible, in certain cases, to premix the adhesive and the primer for application in one stage but this was not attempted here. The experiments in section 2.3.3.3.1 have shown the benefits that a spew fillet has in increasing joint durability and therefore all further experiments had their spew fillets left intact.

After ageing in the environmental cabinet at standard conditions, two specimens of each type were tested (wet) for their residual static strength at two weekly intervals for a total of 12 weeks.

The tests were performed in a 250kN Instron tensile testing machine at a constant crosshead speed (0.5mm/minute) at ambient temperatures.

2.3.3.3.3. Bulk and Interface Phenomena

It is thought that the interfacial zone is an important parameter affecting joint durability. This is supported by the improvement in durability performance when the surface to be bonded is modified using a primer. In an attempt to isolate the roles which the bulk adhesive within the joint and the interfacial zone have on durability performance two additional pieces of work were undertaken:

(i) A study of the intrinsic performance of bulk adhesive after ageing.

(ii) The effect of ageing on the adhesion of the adhesive at a steel interface.

2.3.3.3.3.1 Study of Bulk Adhesive Properties

To investigate the sensitivity of a typical hot cure epoxy adhesive in the overall joint performance, bulk adhesive samples of Araldite 2007, in the form of tensile specimens, see figure 2.8, were subjected to the standard ageing conditions. The bulk adhesive samples were cast using the technique in section 2.3.2 to minimise void content and to ensure a uniform cure of the adhesive. Two conditions were investigated with the standard ageing cycle:

(i) Bulk samples subjected to ageing alone.

(ii) Bulk samples preloaded in stress tubes and subjected to ageing. Initial preload was approximately 50% ultimate static failure strength. Further experiments included a preload level of 20% ultimate static failure strength. (Ultimate static failure load is 1800N)

The tests were performed in a Lloyd 10000L tensile testing machine at a constant crosshead speed (0.2mm/minute) at ambient temperatures.

2.3.3.3.3.2 Interface Study

To investigate the effect of ageing on the adhesion strength of Araldite 2007 at the interface, a jig was designed, figure 2.9, to strip the adhesive from a steel adherend, see figure 2.9. The force required to remove the adhesive after the sample has undergone ageing is recorded. Two surfaces were considered

initially, a shot blast surface and a shot blast surface primed with a silane. These specimens are prepared by hot curing a single part paste adhesive on a steel substrate to produce a thick film. The adhesive thickness was controlled to approximately 0.4mm, which is similar to the thickness in the standard lap shear specimens used in the earlier specimens. The sample thickness was then measured after cure.

To fabricate the specimens used in the scrape tests the procedure is as follows:

1. The required area on the metal substrate is prepared for bonding. This may include shot blasting of the surface followed by pretreatment with a primer.

2. The adhesive is applied to the metal adherend surface. Heat resistant masking tape is used to give a clean working edge.

3. The specimen is laid up in a jig to maintain a constant bondline thickness. An adjacent adherend surface is sprayed with PTFE which the test sample is placed against.

4. The specimen is cured according to manufacturer's instructions.

The specimens were subjected to standard accelerated environmental ageing and tested at half week intervals on a 250kN Instron tensile testing machine at a constant crosshead speed (0.5mm/minute) at ambient temperatures.

2.3.3.3.4 Bonded Grp Durability Performance

Several experiments were undertaken to investigate the performance of composite bonded cold cure epoxy joints with and without silane pretreatment. All the tests were performed in a 250kN Instron tensile testing machine at a constant crosshead speed (0.5mm/minute) at ambient temperatures. To minimise the required machining and increase the number of samples in a stress tube a modified grp lap shear specimen was used as shown in figure 2.10. This specimen type required grip adapters for use in the Instron tensile machine as also shown in figure 2.10. In all grp bonded specimens the spew fillet were left.

2.3.3.3.4.1 Primer/Adhesive Compatibility

Initial tests were used to ascertain the compatibility of a silane treated surface with an adhesive 'Redux 410' (selected for its good mechanical properties used

with polyester grp adherends, see section 3.3.2). Initially, thick adherend steel lap shear specimens (see figure 2.6) were prepared with a shot blast surface and a silane treated surface (A187) as in section 2.3.1 and subjected to standard accelerated environmental ageing with spew fillet intact.

2.3.3.3.4.2 Grp Joint Durability

Composite modified grp lap shear adherends, see figure 2.10, were similarly aged under standard conditions and tested with a peel ply surface and a silane treated surface. The adhesive used in this case was Araldite 2005 from Ciba Geigy. Araldite 2005 is a cold curing two part epoxy adhesive of the same adhesive family as Araldite 2007 (used in the earlier experiments on steel adherends). Araldite 2005 was expected to have similar durability performance characteristics as Araldite 2007 with good mechanical performance characteristics. The specimens were fabricated according to the procedure in section 2.3.1 with spew fillet intact, Initially, four conditions were considered:

(i) A bonded grp joint using peel ply surfaces.

(ii) A bonded grp joint using peel ply surfaces and a silane primer suitable for both the adhesive and the adherend.

(iii) Preloaded grp joints of types (i) and (ii). The preload was applied to the joint using a stress tube. This was approximately 20% of their ultimate static failure load of 6000N.

2.3.3.3.4.3 Grp Surface Preparation

A shot blast grp modified lap shear (see figure 2.10) surface with and without a silane primer was further investigated under standard environmental ageing conditions. These tests were used to ascertain whether shot blasting provided a more beneficial site for the silane pretreatment. The specimens were produced by the procedure outlined in section 2.3.1 with spew fillet intact.

2.3.3.3.4.4 Selected Adhesive/Grp/PrimerCompatibility

A final series of tests examined the performance of a grp substrate with the selected adhesives (refer to section 3.3.2) Redux 420 using peel ply surfaces and an alternative silane treatment (SiP^{52}) on modified lap shear specimens, see figure 2.10. The specimens were fabricated according to the method in section 2.3.1 with spew fillet intact.

2.4 Results

2.4.1 Stress Distribution in Bonded Joints.

The series of mild steel lap shear specimens of varying overlap lengths were tested for their ultimate tensile strength. A record of force versus time was taken for all specimens. Table 2.1 shows the ultimate failure load and average shear stress for each overlap length tested. During testing, especially of the longer overlap lengths, longitudinal rotation of the specimen between the grips was observed. It is easily demonstrated from the results here that increasing the overlap length does not increase proportionally the load carrying capacity of the joint.

2.4.2 Surface Preparation Study

The results are presented as histograms in figures 2.11 and 2.12 which show average results from two tests. The tensile results follow the same general trends as the lap shear results. Clearly a form of mechanical surface roughening improves the short term bond strength and there are some small differences in the results arising from different forms of mechanical treatment. The results from joints containing contamination, e.g. oil, heavy oxide layer or epoxy primer are inferior. Examination of the failure surfaces showed that in these cases adhesive failure had occurred whilst all the other surface-roughened specimens produced a combination of adhesive/cohesive failure.

2.4.3 Durability Performance : Accelerated Aging

2.4.3.1 Bonded Joint Physical Geometric Details

The results obtained from the preloaded cleavage specimens proved to be subject to considerable scatter, see table 2.2. Results from the lap shear specimens were more consistent and are presented in figures 2.13a-c. As might be expected there is a reduction in ultimate tensile strength after accelerated ageing. It appears an application of a preload reduces residual strength as does removal of a spew fillet. Generally, all of the specimens degrade gradually over the 12 week exposure time after an initial larger decrease in strength in the first two week period. This initial decrease in strength for the nonloaded specimens was approximately 21%. For the loaded samples with fillets there was a decrease in strength of approximately 24% and for the clean loaded samples a decrease in strength of 21%. If a line is fitted through the data for a nonloaded sample, see figure 2.13b, for the period between 2 and 12 weeks, it can be seen that the filleted samples tend to degrade slower than the cleaned samples. This is demonstrated by the shallower slope of the line and would indicate that their

durability performance is better. The durability performance of the loaded samples cannot be analysed in a similar manner due to a larger scatter in the test result data, see figure 2.13c. However, from figure 2.13a we can see that the application of a nominal load increases the rate of strength degradation and the influence of the fillet is minimised.

2.4.3.2 Primer Selection

Figure 2.14 shows the benefits of using primers on a well pre-prepared (shot blast) steel adherend compared to a treatment which has poor short term static strength. The black oxide layer forms a weak link and failure occurs between the steel surface, as also seen in the unaged samples, see figure 2.32. The test results in figure 2.15 indicate that, on steel adherends, both silane primers have generally superior performance over the two corrosion inhibitors although the difference is small. Using a silane primer on a steel surface has been shown to significantly increase durability performance compared to a similar shot blast non-treated surface (see figure 2.16).

2.4.3.3 Bulk and Interface Phenomena

2.4.3.3.1 Study of Bulk Adhesive Properties

In figure 2.17a, bulk samples subjected to ageing alone showed both a small reduction in Young's modulus and ultimate failure stress over the exposure period. There was approximately a 20% reduction in adhesive ultimate failure stress and a 10% reduction in Young's modulus after this period of ageing. All the samples were tested in their fully saturated condition. The 50% preloaded bulk samples failed prior to their test date, see table 2.3. In retrospect the preload level (50% of the ultimate static failure load) was unrealistically high as a general service load. But this work indicated that there must be a critical preload level. The first phase of preload tests also highlighted a problem in the method of loading in the stress tubes. The bulk specimens were drilled with a hole at either end to allow a small shackle to be used for loading and connection. This hole tended to elongate during loading due to creep and therefore this reduced the load level on the specimen chain. This problem was overcome by designing special grips to hold the bulk samples in the tubes. A second batch of preloaded bulk samples was then tested. These samples were preloaded to 20% of their ultimate static failure load and were successfully tested. During the exposure period the specimens in the stress tubes required to be retorqued regularly and indicated that the specimens were undergoing creep deformation over this period. The results from these experiments are shown in table 2.4. The general trend from these results is a decrease in modulus of elasticity with increased exposure

time while the failure stress does not appear to show a similar reduction over the same duration. Comparison between the stressed and unstressed samples shows that the stressed samples retain a higher level of residual strength over the same exposure period (see figure 2.17b). The results of the stressed bulk samples (20% preload) cannot be directly compared in absolute terms to the unstressed samples where extension measurements are involved in the calculated properties. This is due to the fact that two different methods of sample elongation measurement were made. For the unstressed bulk sample a 10mm gauge length linear voltage displacement transducer was used which could measure +- 0.5mm. This was attached directly to the centre of the sample using clips. This method of extension measurement is thought to be extremely accurate. When the stressed samples were first tested it was found that there extension under test was outwith the range of the surface mounted linear voltage displacement transducer. Thus the specimen extension was then measured using the internal extensometer on the tensile test machine. This measured the total displacement of the crosshead and will not therefore be as accurate. Thus direct comparisons in the load/displacement plots, Young's modulus, extension to failure etc. cannot be made between the stressed and unstressed samples.

2.4.3.3.2 Interface Study

After ageing in the environmental cabinet specimens were tested at half weekly intervals for up to 4 weeks. Originally the experiments had a planned duration of up to 12 weeks with testing at two weekly intervals. However, initial results showed clearly that within four weeks the failure mechanisms occurring had changed. Thus the programme was revised to monitor these changes over a shorter time span, at half weekly intervals. In these experiments the adhesive layer was subjected to cleavage/peel loading, using a razor like tool, until adhesive failure occurred. Figure 2.18 shows the results from these experiments. Although there is a large amount of scatter, it is possible to see a general trend of two distinct failure patterns. Initially, both surface preparations show a similar failure load and failure surface. After a period of approximately three days the failure load for the standard shot blast preparation decreases and the type of failure changes due to the loss of integrity at the interface. The silane treated surfaces continue in the initial failure mode until finally, after approximately 17 days, they too change failure mode and fail at a lower load. This indicates a longer interfacial resistance to degradation by water.

2.4.3.4 Bonded Grp Durability Performance

2.4.3.4.1 Primer/Adhesive Compatibility

These results are shown in figure 2.19. They indicate that the adhesive Redux 410 and the silane primer A187 appear to be compatible and are not detrimental to durability performance. Over the 12 week exposure period there does not appear to be the same significant benefits from using a silane primer with this adhesive as seen on a steel surface with a hot cure epoxy adhesive (see section 2.4.3.2).

2.4.3.4.2 Grp Joint Durability

Similar experiments were undertaken on grp adherends using the two part cold cure adhesive 2005, a peel ply surface preparation and silane A187. The results from these experiments were similarly disappointing as significant benefits were not obtained when using a silane on a peel ply surface (see figure 2.20). Although the scatter in these results makes definitive interpretation of the results difficult. It can, however, be seen from the general trends over the 12 week exposure period, that there is very little change in the residual shear strength and that the application of a preload does not significantly affect durability performance.

2.4.3.4.3 Grp Surface Preparation

Shot blasting a grp surface will expose glass fibres from beneath the resin rich outer layer but will also cause some damage to the glass fibres themselves. Figure 2.21 shows a sub-series of tests which was performed to investigate the potential benefits from using a shot blasted surface with a silane treatment instead of a peel ply surface. Shot blasting the grp surface did not significantly change durability performance and it would appear that a peel ply surface with and without the application of a primer produces the best performance. Again, the trend shows very little change in residual strength but there is a degree of scatter in the results.

2.4.3.4.4 Selected Adhesive/Grp/Primer Compatibility

Results from these experiments are shown in figure 2.22. They indicate that the performance of a silane treated grp Redux 420 bonded joint is not significantly improved over an untreated surface and both demonstrate a general retention of residual strength over the exposure time.

2.5 Finite Element Stress Analysis

As discussed in section 2.2.1.2 it is possible to predict the general behaviour of lap shear joints to a limited extent using the Goland and Reissner[3] stress analysis, it is not possible to use such techniques to determine detailed stress distributions through the thickness of the adhesive layer. To overcome this difficulty a finite element stress analysis was used to investigate the behaviour of the range of overlaps tested in the experimental stage as in section 2.4.1. These models were loaded under a static tensile load in an attempt to simulate the realistic test situation. The analysis assumed plane strain, linear elastic materials and the adhesive properties given in table 2.5. The adhesive in this model is assumed to be 0.2mm thick and was modelled as three layers of elements through the adhesive thickness using 20-noded brick elements. The package used was SESAM[55].

Two load cases were considered for the four different overlap lengths:

i) The ultimate failure load for each length of overlap. The value of this load was obtained from the experimental work,
ii) A nominal load to investigate joint sensitivity to overlap length.

It must be noted that the larger aspect ratio of the elements in the adhesive layer in the longer overlap lengths were not ideal but did produce adequate results.

The results of the analyses performed are shown in figures 2.23 to 2.28. Figure 2.29 shows the co-ordinate system which was used.

A typical stress distribution through the adhesive layer for an adhesively bonded lap shear obtained using a finite element model is shown in figures 2.23 and 2.24. This stress distribution is obtained from an analysis of a 25mm overlap length with a nominal applied load of 20 kN.

From this typical plot various interesting points should be noted:

- the maximum stresses are at the joint end x = l at the upper adherend interface and at x = 0 at the lower adherend interface.
- the maximum stresses are the tensile stresses at x = 0 and x = l.
- most of the joint carries a relatively low level of tensile and shear stress.
- only approximately 1/5 of the joint is highly stressed.

Figures 2.25 and 2.26 represent the comparative principal stress distribution at the upper adherend interface obtained when a nominal load of 20kN is applied to each length of overlap. It can be seen that:

•the maximum stress which occurs at x=l does not proportionally decrease for an increase in overlap.
•the centre portion of the joint carries a low level of stress which is of similar magnitude of each overlap length.
•the proportional length of the joint under a low level of stress is of similar magnitude.

Comparison of the principal tensile and shear failure stress distributions for the four lengths of overlap is shown in figures 2.27 and 2.28 at the interface of the upper adherend. From these distributions it should be noted that

•the maximum shear and tensile stress levels for all lengths of overlaps are similar at final failure.
•the tensile stresses are greater than the shear stresses at the joint extremities.

These results compare well with the experimental fracture surfaces found after failure of the joint. A schematic representation of the type of failure predicted is shown in figure 2.30 and this is similar to that found by Adams[56] neglecting the effect of the fillet.

2.6 Discussion

2.6.1 Surface Preparation

In this study suitable surface preparation techniques have been selected which can be undertaken in a structural fabrication environment. Thus they must be simple and economic while producing the highest possible strengths and durability. No attempt has been made to maintain ultra-clean laboratory conditions. The methods available included shot blasting, sanding, brushing and machining.

The thick adherend shear results in figure 2.12 compare very favourably with previous thin adherend results using hot cured epoxy adhesives and mild steel adherends without the use of a solvent[38]. A form of mechanical roughening, shot blasting and machining by grinding or milling produces the best results. Good adhesion is visible in figure 2.31 for a shot blast surface. It is difficult to extract the independent effects of surface topography and the volume of material removed by these methods when compared to abrasion or wire brushing techniques.

For tensile loading there is a much more marked benefit from using shot blasted or ground surface finishes followed by a solvent degrease compared to abraded or milled and hence these results should be used to determine preferences (figure 2.11). Others[57] have performed experiments on polished and roughened surfaces of aluminium alloy and stainless steel substrates with an epoxy-polyamide adhesive and showed that the rougher surfaces gave the highest butt joint strengths with a shot blast surface producing the best result. It is often observed that some form of mechanical abrasion will improve joint strength. However, such treatments do not generally result in a surface topography with cavities suitable for establishing mechanical interlocking with the adhesive[58]. One effect of mechanical surface roughening in an industrial environment is usually to ensure the surface is free from contamination and weak surface layers etc. It has been suggested that increases in joint strength might be attributed to extra interfacial bonding area available typically about 5 to 30%[59] or to changes in stress distribution. There is evidence[60] that the state of the metal surface on which the adhesive cures has a distinct effect on the cured adhesive in the boundary layer adjacent to the adherend. Such studies involve the etching away of the steel from cured joints and hence the observed adhesive surface morphologies are a combination of the differential effects of the original cure against the surface and the differential stability of the adhesive in the etching solution. More work is needed in this area to ascertain the effect and quantify various surface roughness but it is clear from figures 2.11 and 2.12 that a form of mechanical roughening of the surface produces an inherently superior result both

for initial joint strength and potentially for long term durability. The results of these tests also demonstrate the influence of the surface treatment on the stability of the boundary zone. Others have found the influence of a particular surface treatment on the aging behaviour of bonded steel joints is not equivalent with all (different) adhesives.[61]

The results of the current study on both oiled steel, black oxide mill scale and the epoxy primed samples are similar and show an interfacial type of failure, see figure 2.32. The hot cure epoxy adhesive used is capable of transporting oil from the interface with the adherend to produce strength results similar to the as-received oxide coated condition, thus minimising the effect of the oily film. Fay and Maddison[41] similarly show that the initial strength difference between various pre treatments on thin steel adherend hot cure epoxy joints is very small, with the oily joint giving a lower value but point out that bond durability can be seriously impaired. Adhesive manufacturing compatibility claims should thus not be based solely on initial strength data. The strength of joints which were primed with the epoxy primer is governed by the inherent strength and adhesion of the primer, in this case relatively low strength and poor adhesion as shown in figures 2.11 and 2.12. However, it was pointed out at a later date[62] that the thickness of this type of surface primer treatment is critical to performance and may explain the lower joint strengths attained. The purpose of any particular surface treatment may be manifold but the main aims are to remove and prevent formation of any weak surface layer on the adherend. Obviously if any weak surface boundary layer initially on the substrate is not removed the loci of failure is likely to be through this region and relatively low joint strength is observed, as in the case of the weak oxide scale on the steel substrates and protective oils and grease. Kinloch[63] points out that after processing, protective oils can be oxidised and very firmly attached and ingrained on the metal oxide. Such layers may require several degreasing treatments or even acid etching to completely remove them.

It is apparent from figures 2.11 and 2.12 that an economical and simple surface preparation prior to bonding gives an adequate short term static strength. Roughening the surface may lead to improved joint strengths. This may be due to an increased surface area for bonding, increased mechanical interlocking or improved kinetics of wetting and an effective surface cleaning process. It may also slightly change the stress distribution. Where a primer is used it should ideally match the adhesive system chemistry. Further work, to investigate the use of silane and alternative primers, examining their long term effects on joint strength is presented in section 2.6.3.2.

The purpose of a solvent degrease is to remove any surface contamination e.g. oil, grease or abrasive dust etc. which may occur through the steel fabrication process or surface preparation treatments and potentially act as a weak boundary layer. Sometimes adding a solvent to a high molecular weight resin may simply increase spreadability. Thus unevaporated solvent on a steel surface may possibly increase wettability of the adhesive at the interface. The use of a solvent after the surface roughening process for the thick adherend lap shear specimens case appears to have no substantial effect on short term strength, see figure 2.12.

However, from figure 2.11, it appears that the use of a solvent can improve the short term tensile strength of a mechanically roughened surface. The use a solvent on a shot blast and ground surface produces a significant increase in tensile strength compared to other roughening surface treatments with a solvent degrease. Brockmann[38] does not appear to use a solvent degrease after a surface roughening treatment on epoxy steel shear joints although a surface treatment of degreasing alone appears to attain an adequate short term strength relative to a shot blast surface. However, the state of the steel surface is not stated prior to solvent application. Similarly, Fay and Maddison[41] also show the short term strength of a degreased steel surface to be adequate. For long term strength Brockmann[61] has shown that a simple degrease may not give adequate long term performance and a surface roughening treatment gives better results.

In a production environment such as in the shipbuilding industry, where assembly cycles are relatively long, there would be considerable merit in surface treatments which would also provide long term protection for a mechanically cleaned surface, prior to bonding. This treatment should be compatible with the adhesive system to be used and require a minimum of subsequent surface preparation prior to the final bonding process. Most fabricators use solvent based shop primers formulated from epoxy resins as corrosion inhibitors and paint system keys on all surfaces. At present it is generally recommended that these are removed prior to bonding to achieve maximum adhesion. Reformulation of these materials as chemically curing high adherence polymers may, however, offer considerable advantages for the future of bonding technology. Recent discussions[64] have indicated a possible coupling agent which could have superior hydrolytic stability than silane based primers. These coupling agents, Titanate/Zirconate and Zircoaluminates are normally used in the corrosion protection of steel by adding them to the protective marine coating and have as yet not been tried as a specific bonding primer.

2.6.2 Stress Distribution in Adhesively Bonded Joints.

The purpose of this section of the thesis is to investigate the performance of an unaged lap shear joint with view to aid understanding of an aged joint in a wet environment which was used in the following sections in this study. It is not intended as a comprehensive study on failure analysis and criteria. The experimental results of various overlap lengths of equivalent widths and adherend and adhesive thickness showed that increasing the overlap length did not proportionally increase the ultimate failure load and that the calculated average ultimate failure stress decreased as the ultimate overlap length increased, see table 2.1. This would indicate that the load carrying capacity is determined by the initial failure at a local stress or strain concentration. Thus these local effects must be accounted for when predicting joint failure. Generally, failures in the shorter overlap lengths (15,25,50mm) are rapid and catastrophic. For the longer overlap lengths (75,100mm) failures are less rapid. In a single lap joint which is very long or wide the appearance of initial cracks will not necessarily indicate that the ultimate load carrying capacity has been reached, alternatively a short lap joint made with a brittle adhesive will almost certainly fail when the first single crack appears[65]. The occurrence of the first crack normally leads to total failure since the crack tip forms a stress concentration which is higher than that which caused the adhesive to crack in the first instance. Thus the initial failure in many instances coincides with final failure. The initial failure is caused by local high stress concentration in the adhesive as a consequence of the joint geometry, loading and mechanical properties of the adhesive and the adherend. It is vital to understand that failure is not related to the average stress but rather to local high stresses[65]. Thus it is pointless to consider the calculated average failure stress as demonstrated in table 2.1.

The Goland and Reissner[3] stress analysis for steel joints predicts the fundamental stress distribution occurring in the adhesive of a lap shear joint when all the materials involved are considered to be elastic. However, several important factors are omitted from their analysis which include:

- the stress will vary through the thickness of the adhesive layer.
- stresses in two dimensions only are considered.
- adherend shear strains are neglected.
- the longitudinal in-plane tensile stress cannot always be deduced.

Finite element analysis is an important tool to overcome many of the difficulties of the closed formed solutions. However, finite element analysis predicts stresses and strains not joint strength. The question of how to interpret these results for

strength predictions remains largely unsolved and no universal criterion has gained acceptance[4]. From the results obtained using finite element stress analysis in this thesis, see figures 2.23 and 2.24, several important aspects of lap shear behaviour can be pinpointed. It would appear that failure is initiated by a high tensile stress occurring at the end of the overlap at x=l and x=0 see figure 2.29. Adams and Peppiat[66] were one of the first to examine lap shear end geometries use finite element stress analysis. In their model of a square edge lap shear joint they show peak principal tensile stresses to occur at the corner of the adhesive at the interface adjacent to the loaded adherend. The magnitude of which is approximately ten times the applied shear stress. This tensile stress is caused by the eccentricity of load path which tends to cause the specimen to rotate (to alleviate this effect) by bringing the line of action of the load closer to the centre-line of the adherends. This effect is highlighted especially in the longer overlap lengths, being observed as significant rotation of the specimen under test. Adams and Panes[67] reported that lap shear joints tested to their ultimate failure were limited by one of two factors. Either yield in the adherend or the maximum shear properties of the adhesive. The combination of tension and bending moments caused by localised yielding of the adherends of the adherends on the bonded surface at the end of the overlap. This gives rise to large strains in the adhesive leading to failure. These tensile stresses are extremely important and tend to lead to failure of the joint by enabling cracks to initiate and propagate. In thin metallic adherends or long lengths of overlap these tensile stresses are often sufficiently high enough to exceed the metallic yield stress. Thus, after fracture of the joint, the substrates are observed to be plastically deformed as was seen in the longer overlap lengths (75mm and 100mm) in this research. In the case of bonding fibre reinforced plastics the presence of high tensile stresses frequently causes joint failure due to delamination of the substrates and is further discussed in section 3.6.6.

Variation of stresses occur through the adhesive thickness. The maximum stresses occur at/close to the adherend/adhesive interface (see figures 2.23 and 2.24). The variation of stresses close to the unloaded adherend end are similar to those at the loaded adherend end but are very much reduced[68]. This is verified through the f.e. stress analysis results and the test specimen fracture surfaces. On examination of a fracture surface, see figure 2.33, failure occurs at or very close to the adherend surface leaving an almost completely exposed steel adherend surface after failure. Similarly, it was found by Adams et al[69] that there is a considerable variation of stress across the adhesive layer in the elastic case showing an increase in principal stress as the corner (singularity) is approached. Since failure occurs in this region of these very high stresses it is clear that the

averaged stresses in this region cannot give an accurate indication of onset of failure.

Figure 2.25 and 2.26 demonstrate a significant portion of the joint, approximately $0.2< x/l <0.8$, is carrying a very low level of uniform stress and this is the case in all lengths of overlap. The centre portion of the joint is almost redundant. Hart Smith[70] shows, using a elastic-plastic analysis, that the central portions of loaded joints are under low stress levels. He demonstrated that a large flaw can be present and yet there will be no loss of joint strength because there was little load to be transferred from this region. Increasing the overlap length does not increase proportionally the load carrying capacity of the joint. This is easily verified in the experimental stage, see table 2.1, since doubling the overlap length does not proportionally increase the ultimate failure load. The failure of the joint is based on the level of tensile (cleavage) stress attained at the outer edges of the overlap as shown in figure 2.27 and 2.28. In Hart Smith's[70] analyses he demonstrated that if a flaw occurs at the outside edge the effect is merely to move the high load transfer area inwards into the previously lightly loaded area. There is no increase in the peak adhesive shear stress or strain and therefore there would be no loss of strength. The global effect is to reduce the effective length of the joint. This observation supports the finite element stress analysis results. In figure 2.27 and 2.28 the ultimate failure stresses at the joint extremities for the varying overlap length are similar, approximately 300 N/mm^2. However, a value of 300N/mm^2 is extremely high as the tensile failure stress of the bulk adhesive is less than 60 N/mm^2. The basic problem is that in all practical joints a stress/strain concentration exists. At a square or sharp corner the local stress is predicted as infinite. Many analyses have shown that the strain/stress predicted at certain areas of joints can become theoretically infinite due to strain/stress concentration effects such as sharp corners and material and geometric discontinuities[68]. These effects make the application of simple maximum values at a point difficult because the value generated from the analysis, and which is compared to the critical value, depends on the proximity of the point under consideration, to the concentrator. Any attempt to use bulk properties will fail to work as the singularity is due to difference in material properties which the bulk property does not take account of[68]. In fact the state of stress and strain in this region is unknown. Using a failure criterion based on a critical value of peak average centre line stress or strain would appear unjustified as it neglects the presence of the stress singularity[65]. Zhao and Adams[68] suggest using a rounded corner has the ability to fill this knowledge gap as it will remove the singularity and application of a maximum value of stress/strain related criteria to predict joint strength will then be appropriate. In reality, this criterion may be suitable for real joints since there will always be some degree of rounding and singularities will not necessarily exist.

For brittle adhesives, a failure criterion based on stress is appropriate and for adhesives demonstrating more ductility in their stress strain behaviour a value of peak strain may be more applicable[71]. In this work, it would appear to be appropriate to take as a failure criterion, the maximum tensile principal stress at the interface of 300 N/mm^2. In other, earlier, studies, the peak stress from an elastic analysis were used to asses joint strength. Only qualitative and not quantitative results were obtained[4] and also the assumed end geometry at the end of the overlap region significantly affected stress distribution without affecting joint strength. In this study the end geometry of the samples are all the same and modelled the same thus can not be considered to affect the stress distribution from specimen to specimen. Obviously, this is not a universal criterion and is limited to these specific joints at various overlap lengths. This may appear at first over simplistic. The singularities make the application of simple maximum value at a point difficult because the value of stress or strain at a point depends on the proximity to the singularity. Criteria which depend upon a critical value occurring over a prescribed distance provide a means to overcome this problem of the infinite stress or strain, but there is no apparent physical basis for these criteria. However, this type of criterion has been found to produce reasonable predictions of joint strength within a joint type and over a limited range of dimensions[73]. It must be pointed out that the maximum point stress value obtained in this study is in effect at a prescribed distance from a singularity i.e. as the stress is calculated at the integration points of the finite element and then extrapolated to the node points. Thus the value of 300N/mm^2 is effectively a stress calculated at a proportional distance within the bond at the element adjacent to the singularity. Of course, the value will then depend upon the mesh density at the area of the singularity. For this study, the density was unaltered for the various overlap lengths and therefore it is possible to use this stress value as a failure criteria. A recent study[73] concluded that there is no evidence that failure criteria based on stress or strains at a distance work between joint types and for joints of the same type with large variations in geometry. However, a reasonable correlation was found within joint types and for limited ranges of geometries i.e. a criterion which has been demonstrated for a particular joint type and size may be used to predict the strength of joints of the same type which are of similar dimensions.

If we consider the longer overlap lengths, where failure may not be immediate, it is shown that towards the joint extremities, the there is a rapid increase in both tensile and shear stresses, see figures 2.27 and 2.28. Similarly, Adams[74] and others[75,76] report a large stress gradient occurring towards the overlap ends. This may cause a failure pattern as shown in figure 2.30. High principal tensile stresses only occur in a small proportion of the bonded area, at the joint extremities. The peak stress is close to the interface and near the end of overlap.

These peak stresses are partially due to both geometric and material discontinuity and a stress concentration may be expected in this area. The tensile stress level decreases away from the joint end and thus the failure mechanism changes. The tensile and shear stresses in the central region are of similar magnitudes and it is mainly the shear stresses which produce failure propagation. Examination of the adherend surface, adjacent to the adhesive showed that a very thin layer of adhesive remained on the adherend surface suggesting that a cohesive failure occurred in this region. During the course of failure of a long overlap joint, crack propagation may not be continuous and this has often been recorded on the load/time plot as small steps, approximately 750N to 3750N, in an otherwise smooth graph, see figure 2.34. The specimen under test is seen to have two initial tensile bond failures from either end of the joint, for a distance of approximately 15mm of the 100mm overlap length. Chiu and Jones[75] expect the tensile stresses (peel) to have a significant influence on joint failure and it is from here they also expect failure to initiate. The remaining bond area does not fail until the load has reached the required stress level to produce re-initiation and failure in the remainder of the joint. When this is attained, the cracks propagate from either end of the joint until they meet in the centre, causing complete failure. Adams and Wake[56] illustrate a similar type of failure pattern of a single lap joint. They describe how, when a lap joint fails, the initial crack in the fillet turns to propagate near or at the adherend interface. When this crack meets a similar crack running in the opposite direction complete joint failure occurs. This failure scenario is well shown in figure 2.33. Examination of the failure surfaces shows that the cracks do appear to propagate by means of this arrest and re-initiation mechanism. The acceleration of the fracture gives rise to instability, causing crack forking (see figure 2.33) This occurs when the fracture divides into two separate branches and is either halted or slowed down before one of the branches continues to propagate. Periodic markings, concentric with the fracture origin at the thumbnail shaped portion, oriented at 90 degrees to the direction of loading, are found on the fracture surface. The stress distribution at the tip of the crack is such that propagation along two loci is possible. This forking leaves a typical undercut on the fracture surface. This type of failure is highlighted when small discrete strips of adhesive are applied to the joint instead of a continuous strip, see figure 2.35. Further work carried out at Glasgow University[77] examined in detail the failure surfaces of lap shear joints under an optical microscope. Examination of the adhesive adjacent to the thumbnail shape on the metal adherend surface, see figure 2.33, metal particles were found to be present in the adhesive. These have been pulled from the opposite adherend surface and explain the presence of the 'silvery' thumbnail area of metal. Any oxidised layers or shot blast particles on the surface of the adherend are mechanically weak, or only loosely attached to the substrate and therefore may remain embedded in the adhesive on failure.

Bickerman[78] first introduced the theory of the existence of 'weak boundary layers'. He suggested that the idea of two phases in contact with one another which were entirely isotropic and of uniform composition up to their boundaries was mistaken. Of course, materials of different moduli and Poisson's ratio when joined will develop a stress concentration at the edge of the joint in response to the applied load. This stress concentration will be higher the greater the disparity in moduli and Poisson's ratio[79] and may be the true cause of failure. There is general controversy as to the existence of weak boundary layers and their role in failure[79]. As the failure surfaces in the longer overlap lengths show, a concentric type of crack marking from the initial thumbnail point indicates that the failure appears to propagate at a greater rate in the centre portion of the testpiece. Similarly, Adams and Panes[67] report that the more important phase of failure is marked by the appearance of a crack in the bulk adhesive in the plain strain area of a lap joint which rapidly grows to cause failure.

The effect of a fillet was not investigated in this study and it is acknowledged that a fillet has a pronounced effect on the stress pattern within the adhesive and therefore failure initiation and ultimate failure load. Adams and Peppiat[80] show that a full depth fillet reduces the shear stress by approximately 40% at the tension end of a double lap joint. The effect a fillet has on durability performance is investigated in the next section.

This experimental and numerical analysis has shown that in a thick adherend lap shear joint the area of failure initiation occurs at the joint extremities near the interfaces where both high tensile and shear stresses occur. Failure initiation is thought to be due to the tensile (cleavage) stresses produced due to the bending moment causing plastic deformation of the adherends. A large proportion of the joint is effectively redundant as it is carrying a very low proportion of the load. This may be an important factor when considering the durability performance of an adhesively bonded lap shear joint from the size effect point of view. The high degree of eccentricity may limit the use of thick adherend composite joints or very thin metallic joints. From this numerical study, it is believed that a critical tensile stress at the end of the overlap in the adhesive of approximately 300N/mm^2 for this type of adhesive and adherend combination, indicates failure initiation.

2.6.3 Durability: Accelerated Aging

As discussed in section 2.2.2 the most common and most important factor influencing the long term behaviour of unprotected adhesively bonded metal joints is the presence of a high humidity or liquid water. The durability of such joints in these environments is related to a range of parameters involving a series of

complex processes. To increase understanding of these processes, and hence the adhesive performance, the strategy adopted in this thesis involves separating out particular variables. Degradation of the bulk adhesive or the substrate itself may lead to reduction of mechanical strength of the bonded joint. Alternatively, modification of the interfacial region or the interphase may suffice to lead to premature failure of the joint. With the aim of understanding better the mechanisms of joint degradation, experimental work has been effected both on bonded joints and on bulk adhesives.

2.6.3.1 Geometric Details

The results obtained from the preloaded cleavage specimens, table 2.2, proved to be subject to considerable scatter. This scatter was attributed to the sensitivity of the joint to alignment and the method of preloading the joint. The durability results on the cleavage specimens will thus be disregarded in the rest of this discussion. A similar test to the preloaded cleavage specimen is the wedge test. The wedge test consists of specimens which are cut from two metal sheets which are bonded together. After bonding the metal plates are separated by driving a steel wedge into one end of the adhesive layer. The wedge produces a crack in the unaged specimen for a few millimetres down the adhesive layer which causes a very high stress pattern at the tip of the initial crack in the adhesive layer. This test produces results which are only of a qualitative nature is it is not possible to distinguish quantitatively between different grades of interface stability[25]. Thus the preloaded cleavage specimens may be more suitable for qualitative results, i.e. distinguishing between various surface pretreatments and not to measure the degradation of properties with time.

Results from the lap shear specimens, figure 2.13a-c, were more consistent. In general, all the results follow a similar trend. The ultimate failure load decreases as the ageing time in the environmental cabinet increases, but there is some scatter in the results. This trend is as might be expected. Numerous studies have been carried out showing the decrease of residual strength of bonded metallic substrates with epoxy adhesives after aging in both natural environments and accelerated aging in wet or humid surroundings[15,16,17,18]. It has been reported elsewhere[81], in a current research programme investigating the durability performance of 2007 adhesively bonded metallic joints in water at 60°C, that after an initial drop in strength after three weeks, there is a increase in strength after 12 weeks. This work has not yet been fully reported and there is no explanation given for this reported result. General trends from the results in the current study indicate specimen types B, A, D and finally C (see section 2.3.3.3.1) are listed in order of decreasing durability performance. This would indicate that cleaning the

joint and/or applying a load to a joint has a detrimental effect on durability performance. Others[1] have found that a hot wet environment was by far the more hostile environment and that the presence of an applied load increased the rate of loss of strength. However, the most damaging environment depends on the exact system which is being investigated[47]. Although there is a decrease in the ultimate failure load over a 12 week time span for all the specimens. The failure load for type B has decreased to approximately 72% of the original strength. The largest reduction in durability performance was obtained after 12 weeks from loaded specimens when the ultimate failure load had fallen to approximately 65% of the original strength.

Adams and Peppiat[80] show that a full depth fillet reduces the shear stress by approximately 40% at the tension end of an unaged double lap joint. Hashim[82] demonstrated experimentally that a fillet left intact on a thick adherend adhesively bonded lap shear joint of 2007, of the type used in this study, can increase practical joint strength by about 10%. Thus, the excess adhesive left intact after the bonding process firstly increases overall initial joint strength by a similar magnitude as reported by Hashim[82] but does it increase durability performance? Considering first the results relating to unstressed samples, see figure 2.13b, it can be seen that the initial drop in strength in the first two week period (of approximately 21%), is followed by a much slower decline in joint strength over the next ten weeks. This trend in results has been found by other workers[19,41]. If a line is fitted through the results after the initial strength reduction, using regression analysis, the rate of decline in the filleted sample is less than that of the cleaned sample and thus this would suggest that a fillet is beneficial to durability performance. The difference between the filleted and the non filleted stressed sample is less distinctive and there is also a larger amount of scatter in the results. The general trend for the stressed samples is similar to the unstressed sample, showing first a large reduction in strength followed by a much slower decline in joint strength (see figure 2.13c). It may be concluded that a stressed sample has a poorer durability performance than a unstressed sample, see figure 2.13a, and that the fillet has little influence on stressed sample performance. Furthermore, it seen that a stressed joint with a fillet has a similar failure surface as a stressed, filleted and cleaned joint, see figures 2.37 and 2.38. Therefore an applied stress of 15% ultimate failure strength of an unaged joint is more detrimental to adhesive joint durability performance than removing the fillet. The stressed interfacial bonds increase water penetration.

As to whether the spew fillet seals the joint, i.e. limits diffusion at the interface between the substrate and the adhesive of the effective working joint area or increases the diffusion path length is a difficult question. Various studies

demonstrate that water distribution in joints with impermeable adherends and good surface preparation can be accounted for by assuming Fickian diffusion in the adhesive layer. Comyn[14] demonstrated that water uptake is linear with joint strength to a degree as long as the water does not attack the interface. Where one or more of the adherends are permeable and / or the surface preparation is less rigorous, this provides further paths for water diffusion into the joint[14]. Gledhill and Kinloch[19] showed that the kinetics of failure are governed by the rate of diffusion of water throughout the adhesive to the interface. Therefore, to limit the diffusion of water through the joint, a sealant may be used. Minford[48] used a silicone sealant at the bond edges and showed that it effectively protected joints from a sea coast exposure for eight years, but was relatively ineffectual in the (hotter) jungle environment. While a silicone sealant may be a barrier to liquid water, it is not an effective vapour barrier. The use of a sealant may only inhibit primary corrosion and delay slightly the diffusion process[25]. Removal of the spew fillet after cure also modifies the exposed adhesive surface texture. Initially, after cure, the adhesive has a glossy appearance. When the spew fillet is removed, the surface texture of the exposed adhesive is rougher and of a matt finish, exposing any voids or cracks in the adhesive layer which may act as entry sites for the water penetration. It is also possible that the surface gloss may act as a surface seal to decrease diffusion of water through the joint. Since (figure 2.13b) the rate of strength loss for the joints with a fillet is less than the clean samples, this indicates that water ingress to the interface is reduced, implying that the spew fillet must be sealing the joint and limiting water diffusion whilst also increasing the diffusion path length. Furthermore, it is shown later, see page 65 and 66, that water penetrates a joint to a maximum depth of 5mm in 12 weeks. Thus indicating that a filleted specimen can be effected by water in the test time span, but due to the fillet, the joint edge is sealed in the unstressed filleted specimen.

Zanni Deffranges and Shanahan[20] proposed that the phenomenon of capillary diffusion exacerbates water ingress. Surface tension effects near the metal oxides/polymer interfacial region increase the effective driving force of water penetration. They tested bulk adhesive at 70°C under 100% relative humidity and showed as diffusion progresses, the elastic modulus decreases. By testing torsional joints with the same adhesive, they showed that the elastic modulus decreased more quickly in torsional joints. They also found that the diffusion constant, D, is significantly higher for a torsional joint and concluded that water penetration within the adhesive joint was occurring by another route as well as by conventional diffusion within the polymer. It would seem that water was entering the system by seepage close to the interface or interphase region. They proposed[20] a phenomenon of capillary diffusion at the joint interface. Such a mechanism has been reported in the degradation of composite materials[83].

Where water enters along the interphase between the matrix and fibre. Adams and Wake[84] alternatively argued that wicking as a primary mode of entry at the interface is extremely improbable and that entry is normally by diffusion through the exposed boundary surface. The rate of transport of moisture through the adhesive to the interface is given by the permeability. Wicking assumes that the adhesive is displaced from the substrate at the exposed edge, the rate of wicking being the rate of displacement or shrinkage of the adhesive away from the adherend occurs. The area available for entry of moisture may be very small in absolute measurement as it is determined by the thickness of the glueline, width and length of the overlap and interfacial atomic or molecular distances. In most studies, the assumption made is that the adhesive zone is a 2D area between the metal adherends with the presence of one phase not affecting the other. This is clearly not the real situation. The adhesive zone is 3D extending from the base of the material through oxide layers of different structures into adhesive layers possessing different properties of the bulk adhesive. The resistance of the boundary zone is influenced mainly by the type of steel, its surface treatment before application and the type of adhesive[61]. Most previous studies have employed ultra clean surface preparation techniques whereas, in this case, preparation was deliberately less rigorous and therefore water transport along the adhesive interface and would seem likely. Interfacial transportation cannot be excluded as a possible mechanism of water entry into the joint and is believed to be a significant factor in determining thick adherend lap shear durability performance.

The diffusion mechanism is split into two parts. Water diffuses into the thickness of the bulk polymer causing aging and reduction in mechanical properties. In addition, water seeps or spreads close to the interface at a faster rate and may in turn diffuse towards the bulk adhesive of the glue line. Clearly the second process may play an important role by also provoking the failure of interfacial bonding. This second process is slowed down by leaving the spew fillet intact.

Type B (section 2.3.3.3.1) demonstrated the best durability performance (no load and a fillet) and did not show visual evidence of typical interfacial debonding, see figure 2.36, but there was possibly limited water penetration, especially where there is a reduced size spew fillet on the sides of the specimens. The performance of the joints did decline with exposure time therefore some degradation must be occurring. It may be suggested that the degradation is solely due to degradation of the adhesive itself as the properties of unstressed bulk adhesive specimens also degrade over the 12 week period, see figure 2.17a. There is contradictory evidence from similar research as to whether the bulk epoxy adhesive degrades at these temperatures and humidity. Gledhill and

Kinloch[19] reported the breaking stress of bulk epoxy adhesive is not affected by even prolonged exposure in water at temperatures of 20, 40 and 60°C and clearly demonstrated that the observed losses of joint strength under these conditions could not be directly attributed to degradation of the adhesive in the joints. Whereas the experimental work in the current study showed degradation of adhesive performance at 30°C and 100% relative humidity. However, the percentage drop in adhesive bulk properties over the same total time span is less (20% drop in tensile stress and 10% drop in modulus of elasticity) than that in the lap shear joint (28% drop in strength) (see figure 2.17a). Thus, it appears that the durability performance of the bulk adhesive has only minor influence on the overall joint strength where interfacial failure is the main mechanism of failure. Furthermore, it will be shown in the next section that the durability performance of this type of specimen can be improved by using a surface primer. This also indicates that the durability performance is improved due to modification of the interface and thus most degradation must be occurring here.

After fracture, the nature and topography of the joint fracture was observed visually. Specimens of types C, D and A (see section 2.3.3.3.1) were all observed to have similar interfacial failure surfaces, see figures 2.37 and 2.38, whereas type B, see figure 2.36, had a failure surface similar to that observed in a lap shear joint which has not been subjected to ageing conditions. In an unaged sample, see figure 2.31, the adhesive fracture surfaces appear to leave a ragged edge, as also seen in type B samples indicating good interfacial adhesion, whereas the failure fracture surface of the degraded samples leaves smooth, clean edges, see figures 2.37 and 2.38 indicating poor adhesion as also shown by the samples in figure 2.32.

In specimen types A, C and D over the 12 week time period water molecules are believed to diffuse throughout the joint to the interface. This is indicated by 'shadows' which show on the edge of the failure surfaces, see figures 2.37 and 2.38. The water molecules appear to degrade the steel bond interfacial zone and this causes adhesive failure, as shown in figures 2.37 and 2.38. Failure occurs at the interface leaving the steel adherend exposed. This is a classic symptom of environmental attack. Research by Gledhill and Kinloch[19] reported that the mechanism of environmental failure of steel epoxy butt joints is the displacement of adhesive on the oxide metal surface, by water, and this can be predicted from thermodynamic considerations. On fracture water is seen glistening on the adherend surface 'shadows' and this area soon corrodes after exposure to air. In the current research, in no case was the fresh fracture failure surface corroded whereas the external surfaces of the joint were corroded. The presence of corrosion on the failure surface does not necessarily mean corrosion was a failure

mechanism. In many cases corrosion only occurs after the interface has failed by the ingress of water, the adherend surface now exposed and a liquid present so that post failure corrosion may occur. Gledhill and Kinloch[19] established that substrate corrosion was not an operative mechanism but rather a post operative phenomenon. The rate of advance of corrosion product on the metal oxide surface was measured and was slower than the interfacial failure region itself. However, others[29] have reported corrosion as a mechanism of failure of thin adherend lap shear joints. As yet, there is no explanation why this difference should exist.

A further conclusion from this research is that a loaded joint is more affected by water degradation than one that is not, although a critical preload level cannot be specified from this study and further work is recommended. This is contradictory to what is found when bulk samples are stressed at a low nominal load. When the bulk samples were prestressed and aged, it was found that their residual stress was greater than that of a an unstressed sample (see figure 2.17b). Evidence from other research demonstrated conflicting evidence as to the influence an applied stress can have on durability performance of adhesive bonded joints. Fay and Maddison[41] showed that the application of stress may, in some cases, result in rapid joint failure. Their results also show that, where prestressed joints survive long periods of exposure in a humid environment, they can do so without exhibiting stress related losses of strength. Other work[15] showed that double lap joints became weaker with aging exposure, but stressed and unstressed samples were weakened to the same extent. Some loaded specimens may even show an increased level of residual strength due to an increased plasticity effect of invading water in the low strain adhesive. There is evidence[14] which indicates that stress does not increase the diffusion rate through the adhesive. Uptake remains Fickian at all levels of stress[14] but whilst equilibrium uptake was not significantly altered by stress, there is a tendency for the diffusion coefficient, D, to increase. The enhanced diffusion rate for stressed samples could be due to stress causing microscopic or interfacial separation. Alternatively, the interfacial bonds could be stressed[14] and any chemical reaction involving the destruction of these bonds would be accelerated if the bonds were so stressed. Bowditch et al[33] proposed that the influence an applied stress has on the durability performance is a trade off between the plasticisation of the adhesive and the interfacial attack by water. The plasticisation will reduce in-built stresses following cure, and thus increase joint strength. As the interface degrades it will negate the benefits from plasticisation. As the bulk properties are not degraded further with the application of a preload, this would further indicate that the interface is the dominant factor in determining joint uptake of water and also joint degradation.

Visual examination of the aged failure surface showed 'shadows' on the fractured surfaces, see figures 2.37 and 2.38, which increased in size as exposure time increased. It is thought that these shadows correspond to water penetration at the interface. All the surfaces were photographed and the size of water shadow was measured, using a ruler, from the photographs. If a plot of this water shadow is made against the square root of exposure time, see figure 2.39, it shows that the size of water shadow for a cleaned specimen, increases with time. On this graph, the plot for the stressed and unstressed, cleaned, samples shows that the rate of water penetration into the joint is increased when a nominal load is applied, as demonstrated by a steeper slope. It is difficult to plot similar graphs for the filleted, loaded and unloaded samples as there is no distinct edge to measure a base line from and in the case of the filleted, unloaded specimens there is no distinct water shadow from the fillet edge. What should also be noted is that the water shadow is more pronounced at the end of the overlap compared to the sides of the joint, see figures 2.37 and 2.38. This demonstrates that at the areas of high stress in the joint (see section 2.6.2) increased water penetration to the interface occurs. Similarly, Gledhill and Kinloch[19] plotted the fractional depth of penetration of water against the immersion time and showed that the rate of ingress of this type of failure pattern is constant at constant temperature but increases as the immersion temperature increases. As the immersion time increased, the interfacial failure region increased at the expense of the cohesive region. De Neve and Shanahan[32] noticed that, after aging, a circular white line concentric with the cylinder appears in fractured joints which apparently corresponds to water penetration within the glue line. As the depth of penetration increased with time until the line of separation became indistinct, a plot of penetration versus $\sqrt{t}$ was a reasonably straight line, thus leading them to the supposition that water ingress was Fickian. This type of relationship can also be seen from the results in the current study. A graph of water ingress shadow size against root time, see figure 2.39, is reasonably linear, indicating Fickian behaviour for the water ingress. The test specimens in the current study were all suspended vertically in an environmental cabinet which allowed condensation of water on an upper edge of the joint. In this area, on the outer steel surface, there is increased corrosion and also greater penetration of the water molecules into the bonded region, as shown in figure 2.38 by the increased size of 'water shadow'. If the diffusion process is Fickian, the diffusion velocity and the amount of water invading the interface are dependent on the concentration gradient of water and temperature. Thus, the higher water concentration on the condensation surface explains the larger water shadow.

2.6.3.2 Primer Effects

To ensure initially, reasonably strong joints in the case of bonding high energy substrates such as metals, glasses and ceramics it is generally sufficient to remove surface contamination and weak oxides which may act as weak boundary layers, see section 2.6.1. However, to produce durable joints, it is necessary to form stable oxides which are receptive to the adhesive and to establish strong, stable, intrinsic forces at the adhesive or the primer and oxide surface. A preliminary set of experiments reviewed the potential for a silane primer on a shot blasted surface and on an unprepared surface, i.e. with the mill scale still intact. These results, see figure 2.14 show that, for a primer to be effective, it must first be applied to a clean surface. Fay and Maddison[41] found similar results. They investigated the use of Accomet C and a silane primer on thin steel lap shear joints. They concluded that these processes require application to clean surfaces which may be difficult to attain in volume manufacturing.

Brockmann[85] studied the change in strength and deformability of the adhesive layer itself under hot and humid environmental conditions and concluded that, for aluminium bonds, the water stability is dependent on the adhesive and surface treatment. It was pointed out that the two most effective ways to increase stability were to change the surface condition through special surface preparation and to use corrosion resistant primers. Thus the first stage of this section of the current work reviewed the potential of adhesive primers to increase interfacial joint strength and durability. Since the primer used in structural joints must essentially permit the joint strength to approach the cohesive strength of the adhesive, the primers must also be of equivalent high strength.

Four primers were tested, two silanes and two corrosion inhibitors and all improved durability performance compared to a shot blasted surface. Generally, it can be shown that all four primers under test on a shot blasted surface improve joint durability compared to a standard shot blasted surface, see figures 2.15 and 2.16. The residual strength of an aged shot blasted surface may be compared to that of the unaged shot blasted treated filleted specimen to facilitate the assessment of the effects of the various surface treatments. This shows (figure 2.16) that the silane treated surface is superior to the standard shot blasted sample and loss in strength is negligible over the 12 week exposure period. This would indicate that a primer, such as SiP, is beneficial for short and long term performance. If the surfaces of these samples are examined visually, see figure 2.40, it can be seen that there is very little interfacial damage and that the failure is similar in visual appearance to the unaged standard shot blasted sample (see figure 31) where the adhesive shows a ragged edge type of failure. Similar results

have been found by Fay and Maddison[41] who report that stressed samples showed enormous durability performance when treated with Accomet C or a silane. The silanes gave the better performance on a steel adherend (figure 2.15). The actual mechanism by which the primer improves performance is not entirely understood. When a silane is used to improve durability it has been demonstrated that they produce polysiloxane coatings on steel[46]. This may lead to a more durable interface but may also greatly assist the entry of water into adhesive joints. This is due to the fact that polysiloxanes are about the most permeable polymers known and may possibly increase the rate of diffusion of water to the interface by 2×10^4 faster than diffusion through the adhesive. Throughout the work on primer selection, no consideration was given to the curing procedure, application method, layer thickness etc. Recent studies[45] have shown that many processing parameters can affect the performance of the primer and, therefore, the performance of the adhesive joint. The effectiveness of silane treatments is well established and it is thought to involve the formation of primary bonds at the substrate/silane and adhesive/silane interface.

Joint failure after aging appears to be intimately related to plasticisation of the polymer by water and weakening of the steel substrate adhesive interfacial zone. As the durability performance of a shot blasted filleted sample can be improved by using a surface bonding pretreatment, this would indicate that, although no surface degradation of this type of sample is observed visually it must be occurring. This again would suggest that the interfacial failure region in these specimens is the dominant failure mechanism.

In this study, the sample size was small. However, it is felt that the results demonstrate trends and that they represent a valid assessment of the relative durability of various conditions. Arnold[86] emphasised the importance of large scale testing for design verification while test procedures using small scale specimens can be used for research and quality assurance. Recent research[81] has shown that sample size can affect durability performance. A larger sample appears to degrade less than a small sample. Obviously, as the ingress of water affects durability performance and is Fickian, a smaller sample of the same specimen type will have, in percentage terms, a larger affected area than a larger joint with greater surface area. Thus, it is important to consider full scale tests to establish higher confidence levels in real term data in a marine environment.

2.6.3.3 Interface and Bulk Performance

If it is possible to increase understanding between the predominant failure mechanisms of aged joints, then it may be possible to increase performance. There were two areas to investigate:

(i) intrinsic bulk adhesive material performance,

(ii) the interface phenomena.

2.6.3.3.1 Bulk Performance

In this work, aged samples of bulk adhesive material showed approximately 20% reduction in ultimate failure stress and a corresponding small reduction in Young's modulus (10%) as a result of the accelerated ageing process, see figure 2.17. This may indicate a possible plastisication effect, see figure 2.41. These results are similar to those of Shanahan and Neve[32] who concluded that the hydrothermal aging of the bulk adhesive leads to marked changes in the mechanical properties of the material due, presumably, to a large extent to plasticisation effects. However, the current study showed that these bulk samples are not further degraded, in the accelerated environment, by the application of a preload if the magnitude is low (approximately 20% of the UTS) see figure 2.17b. No critical preload level can be specified from these experiments but 50% preload of the UTS can cause rapid degradation and failure (compare table 2.3 and table 2.4). Davis and Fay[17] reported that adhesive joint degradation is dependent on the applied stress. All of the mild steel joints which were continuously loaded at 3kN failed within a year but those loaded at 1.2kN survived considerably longer. The level of applied stress therefore affects the failure mode of mild steel joints. At high stress levels creep is the major factor influencing joint survival time and leads to cohesive failure. At low stress levels, when creep rates are lower, corrosion effects were reported to dominate. However, when a nominal, low preload is used, as in this current study, bulk adhesive specimens undergo creep deformation. This phenomenon was observed when the stress tubes used to apply the preload, utilising a spring arrangement, required retorquing. Small et al[87] found that the creep rate was much higher in humid aged joints rather than dry joints. Under conditions of high humidity, the failure processes are accelerated. Firstly, the adhesive is more compliant and therefore exhibits a higher creep deformation. Secondly, the peeling from the adherends appears to be essentially actuated by the presence of moisture which penetrates the interfacial areas and further debonds the adhesive. Small et al[87] also reported that, despite higher creep rates under humid conditions, the elongation to failure

is no greater than that measured in dry tests. From this evidence, it would appear that creep deformation of the bulk specimens in a humid environment is a dominant factor in degradation. If the preload is high, the creep rate will be significant and cause failure in relatively short periods of time (see table 2.3). At lower preloads, creep deformation still occurs but does not cause failure. Furthermore, when the low prestressed specimens were tested, the elongation to failure was increased and the ultimate tensile stress at failure was greater than the non stressed samples for a given exposure time, see figure 2.17b. Gledhill[88] considered that a self toughening mechanism may be occurring when an epoxy adhesive is subjected to an applied load. It is suggested that there is an increase in severity of crack tip blunting which is responsible for the rise in adhesive fracture energy and the associated change in crack propagation behaviour from stable to unstable.

Although the present study demonstrates how bulk properties of the adhesive may be influenced by water ingress, failure behaviour cannot be explained by this phenomenon. Present experimental evidence suggests that failure occurs completely in a low strength interface or weak boundary layer in the adhesive but near the substrate. Bowditch et al[33] proposed that the water partitions between the adhesive matrix and the adherend surface and suggested that, with a given adhesive, susceptibility to interfacial hydrolytic attack increases with hydrophilicity of the adherend surface. Thus, it might be concluded that the shot blasted mild steel surface used in this study shows a high degree of hydrophilic properties since, although the bulk adhesive does degrade, it does not do so to the same extent as the joint itself.

2.6.3.3.2 Interface Performance

The generation of adhesive bond durability data with the conventional lap shear joints requires undesirablely long periods of environmental exposure. With developments in adhesives and improvements in bonding technology, even longer periods of exposure will be required, unless durability testing can be modified. More severe environments at higher temperatures and loads, whilst reducing test time, may give unrealistic failure modes which would not predominate under service conditions. With the known correlation of service disbonds with warm moist environments, a major consideration is therefore the role of water ingress and the influence of the bond geometry on the role of loss of strength, whether adhesive or pre-treatment dependent. Arrowsmith and Maddison[89] proposed a smaller bond area than standard and predrilled holes to reduce the diffusion path length but at the expense of the initial strength and sensitivity.

A new type of experiment has therefore been developed rapidly to quantify the interface durability phenomena by increasing the diffusion of water to the interface. This experimental method measured the force required to remove the adhesive from a steel adherend (section 2.4.3.3.2) after accelerated ageing. This technique attempted to grade the strength of adhesion to the steel adherend. A similar type of experiment[90] was undertaken where coupling agents were screened as primers for typical epoxy formulations, by comparing the time to failure of the thin films of polymers (cured on primed microscope slides) soaked in water until interfacial failure could be induced by prying with a razor blade. The primers were rated according to the length of time the film retained adhesion.

After ageing in the environmental cabinet, specimens in the current study were tested at half weekly intervals for up to 4 weeks. Originally, the experiments had a planned duration of up to 12 weeks with testing at two-weekly intervals. However, initial results showed clearly that, within four weeks, the failure mechanisms had changed. Thus, the programme was revised to monitor these changes over a shorter time span. In these experiments, the adhesive layer was subjected to cleavage/peel loading, using a razor like tool, until adhesive failure occurred. Figure 2.18 shows the results from these experiments. Although there is a large amount of scatter, it is possible to see a trend. Initial failure strengths, labelled phase 1, for both silane and shot blasted surfaces are similar, but after only 7 days exposure the strength of a shot blasted surface was reduced to a lower level and maintained this level throughout further exposure and testing (phase 2). The silane treated surface maintained the phase 1 level for a longer time but at approximately 17 days, the form of failure changed to the lower load level (phase 2). At the transition point, in both cases, the failure mode also changed. Phase 1 failure involves the adhesive becoming detached in small strips. However the adhesive detaches spontaneously as a complete sheet or in large segments in phase 2. These failure surfaces are shown in figure 2.42. In this type of test the failure mechanism is a trade off between the change in adhesive properties versus the change in bulk adhesive properties due to aging. Initially, in a phase 1 failure, there are high adhesion forces and the epoxy adhesive is relatively brittle. Thus, failure occurs due to the adhesive, in effect, being chipped off the surface. The adhesive material is too brittle, and adhesion still high enough to allow the scrape tool to remove the adhesive as a complete strip. As the adhesion strength is reduced due to degradation and the adhesive is plasticised and becomes tougher, the adhesive may be removed from the adherend surface as a single strip as seen in a phase 2 failure.

The results of these studies into bulk and adhesion strength would suggest that the type of failure occurring within an adhesive joint after accelerated ageing is caused by reduction in the adhesion strength at the interface. This is indicated by the slow changes in properties of the bulk adhesive, see figure 2.17, compared to a relatively fast reduction of the adhesion performance shown in figure 2.18. Of course, it must be considered that, in this form of testing, diffusion of water to the adherend surface is rapid as it can enter via the top adhesive surface, at the adhesive edges, and at the interface of the steel and the adhesive. But it does show that the adhesion mechanisms are rapidly degraded once penetrated by water. The silane primer will increase the stability of the adhesive/adherend interface against displacement and/or penetration by water molecules. This effect is indicated by a retention of a higher residual adhesion strength by a silane treated surface as shown in figure 2.18. Secondary weakening of a joint is due to the change in properties of the bulk adhesive within the joint. This secondary process occurs more gradually than the interfacial effect. Similarly, Zanni-Deffranges and Shanahan[20] demonstrated that the bulk properties of the adhesive may be influenced by water ingress, but that failure behaviour cannot be explained by this phenomenon. Their work suggests also that fracture occurs near the interface, perhaps in a low strength interface or weak boundary layer.

The most critical aspect of environmental durability testing is the assessment of the test results and the extrapolation of those results to predicted service life. The new test described here is ideal for rapidly discriminating between the improved structural adhesives and surface treatments now being developed, if not for predicting service life. The use of these experiments considerably reduces the time required to evaluate the durability of adhesively bonded metallic substrates and allows comparison between different treatments and adhesive.

2.6.3.4 Grp Bonded Joint Durability Performance

The object here was to investigate the durability performance of an adhesive bond in a composite joint and review ways of improving joint strength. This section of research is contained within the durability section for completeness. Extensive work on bonding of grp is discussed in further detail in the following section. Similar accelerated aging experiments to those on steel adherends were undertaken on grp adherends using a peel ply surface preparation and silane A187 pretreatment. Silane A187 was recommended as a suitable bonding primer for both steel and grp adherends while using an epoxy adhesive. The results from these experiments were disappointing as significant benefits were not obtained when using a silane on a peel ply surface (see figure 2.20). This is contrary to work by Lees[91] who reported that the durability of the adhesive composite

interface can be improved by the use of silane based primers and, furthermore, under hot humid environmental conditions an adhesive/composite interface is much more stable than the equivalent adhesive/metal interface. Generally, in the current work, all of the trends are similar for all the tests on the grp bonded joints and show very little change in residual strength after 12 weeks exposure, although there is a significant degree of scatter in the results. Silanes are often used as an adhesive promoter in composites materials. The silane acts as a coupling agent between the uncured resin and the glass in composite manufacture. When peel plies are used, there is neither an exposed glass surface nor any uncured resin and, consequently, this seems to explain the poor performance seen in the tests. To take advantage of silane primers, a method needs to be found which will expose the glass surface while not damaging the glass unduly.

Shot blasting or other mechanical preparation of a grp surface will expose glass fibres from the resin rich outer skin, but will also cause some damage the glass fibres themselves. Figure 2.21 shows a sub-series of tests which was performed to investigate the potential benefits from using a shot blasted surface with a silane treatment instead of a peel ply surface. Comparison of figures 2.20 and 2.21 do not indicate any significant benefits to be gained from using a shot blasted surface or silane treatments. Although it would indicate that a peel ply surface generally gives greater durability performance than a shot blasted surface. When using a silane surface pretreatment, it is vital to ensure that the silane primer type is compatible with the type of adhesive and is not, in fact, detrimental to the static short and long term performance. Redux 410 (this adhesive was selected for use on grp adherends for its good mechanical properties - see section 3.6.1) showed no such problems when tested on steel lap shear adherends and subjected to ageing, see figure 2.19. The adhesive Redux 410 is a modified epoxy and is thus not typical of the epoxy adhesives for which silane pretreatment is recommended and therefore it was necessary to perform such tests. The primer it is not detrimental to performance but it did not show the significant benefits seen when using a primer in earlier studies on steel adherends, see section 2.6.3.2.

Final experiments investigated the durability performance of the revised, preferred adhesive for composite adherends (Redux 420, see section 3.6.1) on a grp peel ply adherend using an alternative SiP silane treatment. These experiments were performed to investigate the performance of the selected adhesive using an alternative silane treatment on specified grp laminates adherends using a peel ply surface. The results did not increase confidence in the use of silane on the peel ply surface to increase durability performance (see figure 2.22). In the accelerated durability experiments, silane treatments did not give significantly increased

(repeatable) performance on grp adherends, as is expected on a steel substrate. This can be explained by visual examination of the grp failure surfaces. In all of the experimental cases (figures 2.20, 2.21 and 2.22), the failure occurred through the resin rich surface at the top fibre interface. This is a similar scenario to that found later in the thesis in terms of unaged static failure of composite joints. Even after a 12 week exposure with an applied preload, failure was still at the fibre interface in the grp adherend, see figure 2.43. Bowditch et al[92] reported similar mechanisms, depending on the exposure duration. Thus, the adhesive durability performance, both in terms of adhesive and cohesive strength, is not an issue here and pretreatment is relatively unimportant. Joints to plastics have been reported elsewhere[93] to be far less susceptible to environmental attack than for high energy substrates such as steel. Although, when attack does occur, the composite material itself may be more readily degraded than the adhesive layer or the interfacial regions[94] as demonstrated here. General degradation of the mechanical properties of polyester resin composites are attributed to[83] plasticisation and consequent loss of stiffness in the resin, to debonding stresses across the fibre-resin interface induced by resin swelling (which may explain the type of degradation occurring here) and to osmotic pressure and to chemical attack by water on the fibre resin bond. A recent study at Glasgow University[96] demonstrated that polyester composite materials show general degradation in properties in a number of environments relevant to marine applications. As the failure mechanism in the current study does not alter pre and post exposure, alternative experiments would be required to examine the durability performance of the adhesive in a composite joint. In the following section of this thesis, the design of composite joints and their failure mechanisms are discussed. It is apparent that, in many cases, the interlaminar strength is the main issue in joint performance and not the adhesive. It is possible that experiments run for a longer duration might show a change in failure mechanism as reported by Bowditch and Stannard[92]. They reported that composite lap shear joints exposed at 70°C and 90% relative humidity to accelerate aging, first showed a high rate of strength loss but then the residual strength tended to level out. At short exposure times, failure was generally within the grp substrate, but this was replaced by adhesive failures at intermediate times. At long times, however, there was a return to substrate failure. It was proposed that these different failure mechanisms were due to the different rates at which the adhesive and the polyester matrix degraded. Measurement of changes in grp laminate with exposure support this. Thus the experiments in this study may be too short to produce a significant change in the adhesive performance to affect the failure mechanism of the composite joint after aging. In fact, it may be that the experiments are simply monitoring the durability performance of the interface region between the top fibres and the resin. This would indicate that a peel ply outer surface layer is the most durable under these

conditions (see figure 2.21). Hashim[82] found that a peel ply surface also gave better short term strength when compared to a shot blasted surface. To improve durability performance of this joint type, consideration must be given to the composite adherend by improving the interlaminar strength both in short and long term performance.

2.6.4 Final Comments

The durability of thick adherend steel epoxy joints is obviously a highly complex subject. A large amount of work has been carried out on various aspects of durability. However, it is often difficult to compare the results of different workers because of the many variables involved. Also, on many occasions insufficient practical details are published to permit a detailed analysis of the results for comparison purposes. Furthermore, the adhesive, adherend, and primer processing parameters can contribute to a significant difference in performance.

Adhesive bonding is an important joining method in many areas of engineering. However the lack of a universally applicable criterion for predicting the static load carrying capacity of adhesive joints makes predicting durability performance even harder[4]. From this study on a thick adherend steel lap shear joint, it would appear that unaged failure initiation is produced by a high, tensile (cleavage) stress occurring at the ends of the overlaps at or near the interface. Most of the load transfer occurs in the narrow zones adjacent to the ends of the bonded overlaps. These load transfer zones are separated by a lightly loaded elastic trough. Prediction of the service life of adhesive joints exposed to a hostile environment requires a knowledge of the mechanisms and kinetics of attack, the identified mechanisms being the rupture of secondary forces and the kinetics being governed by the diffusion of water through the adhesive to the interface, as long as the surface preparation is relatively good. For a shot blasted surface, water may enter the joint along the interface also. Thus, for failure of a lap shear joint to occur in a wet environment, water must first penetrate the joint system through the adhesive or along the interface and reach sufficient concentration at the interface region to cause an effect. With the lap shear joint used for the majority of this study, the critical area for failure initiation is at the overlap edges and, unfortunately, this is the area of the joint where water molecules will first enter the interface. Moisture distribution in adhesive sandwiches show peak concentrations at the joint edge and are lowest in the centre[97].The combination of high stresses at the joint ends and the fact that this is the area of initial water penetration make this type of unprotected joint susceptible to water degradation in a wet environment. Joint protection can be increased by leaving a spew fillet intact and the application of a suitable bonding primer.

To obtain a qualitative comparison of performance between a silane primed surface and a untreated surface, a new test method described in the previous text was successfully used. This method scraped an adhesive strip from a steel adherend and recorded the load required after various accelerated ageing times. Thus, it is possible to measure the decrease in interfacial forces caused by water penetration over a period of time. Within the current study, it was shown that, after a relatively short period of time of exposure to a humid environment, the integrity of the interface of the non-primed surface was lost. After a further period of time even the integrity of the primed surface is reduced. Ultimately, both failure surfaces appear to be similar although it is thought that originally the chemical bonding is different i.e. a non primed surface has secondary bonding whereas a primed surface produces primary covalent bonding. Furthermore, the ultimate peak failure load of both surfaces are equivalent. This type of scrape testing appears to be very useful for rapidly detecting changes in interfacial strength of an adhesive/adherend system within days. With the steel interface being under attack by water molecules, it might be expected to corrode and initiate joint failure. Throughout this work, only post failure corrosion was observed.

Throughout this study, high humidity and temperature have been use to accelerate the aging process. This is an established means of grading durability performance. But how do such joints perform in a real environment? A chain of lap shear specimens was deposited in the Clyde Estuary[76]. These specimens were bonded in the usual manner with Araldite 2007 (some with silane primer) and further coated with a protective paint. The specimens were suspended under load (approximately 10 - 15 % of the ultimate static failure load) from a pier, see figure 2.44, into the sea. The exact load on the specimens will vary dynamically due to the currents and prevailing weather conditions. Due to the tidal variation, the top specimens could be exposed to the splash zone. After a period of two years, samples were removed from the specimen chain and tested for their residual strength. It was found to have only decreased by 10 - 15 % and there was no difference between the silane treated surface performance and the untreated surfaces[76]. At five years, all of the remaining specimens were tested and found to show approximately 50% reduction in strength. This would appear to be relatively poor performance but it must be noted that, due to the type of aggressive exposure, the actual steel specimen was very badly eroded and corroded whilst the adhesive bond still remained intact. If the specimens had not been tested at this time it was felt that the specimens may have been lost due to severe degradation around the shackle holes. Furthermore, due to the significant degradation of the steel substrates, the thickness of the adherend was reduced. Thus, the stress distribution in the specimens will be somewhat altered under the

preload. If such materials were used on the topside of marine structures, they would be maintained by painting etc. to reduce corrosion. Thus, this test was particularly aggressive although performed in a 'real' environment and may give an over-pessimistic picture of the durability of such joints. Similar samples were tested in a laboratory environment[98] at ambient temperatures submerged in distilled water sustaining a 40% load and showed no failures after more than three years. Thus, care must be taken in interpreting results, whether from accelerated aging or 'real' world exposure.

2.7 Conclusions

From the work discussed in the previous section several conclusions can be drawn:

1. A solvent-degreased, shot-blasted surface produces a joint which is effective, efficient and of adequate short term strength for fabrication in an industrial environment.
2. Steel adherend epoxy bonded thick lap shear joints are degraded by water in an accelerated aging environment (30°C and 100% relative humidity).
3. Bulk adhesive properties are degraded by water in an accelerated aging environment but to a lesser extent than the joint (30°C, 100% relative humidity).
4. The application of a preload accelerates aging in a epoxy bonded joint. The application of a low nominal load to a bulk adhesive sample does not accelerate aging. Creep is thought to be a significant mechanism thus the level of the preload is critical.
5. Durability performance is determined primarily by the performance of the interface. The degradation of the bulk adhesive is a secondary effect.
6. The interface is the critical zone in determining durability performance of a shot blast steel epoxy bonded joint and is affected by a preload. Highly tensile stressed areas in the joint show increased water penetration.
7. Corrosion at the interface did not appear to be a failure mechanism.
8. Modifying the shot blasted interface by using a bonding primer will improve durability performance. A suitable surface treatment on a steel surface is required first for a primer to be effective.
9. A spew fillet will improve durability performance by sealing the joint edges.
10. A new, rapid durability test method has been developed qualitatively to grade interfacial performance of metallic adherends/adhesive systems.
11. Bonded grp durability performance is more difficult to assess due to the permeable adherends. Grp adherends are not suitable for the new test method due to their inherent surface roughness.
12. The adhesive performance and surface pretreatment is not often an issue in the durability performance of a composite joint since failure frequently occurs at the interface between the top fibre layer and the resin rich surface.

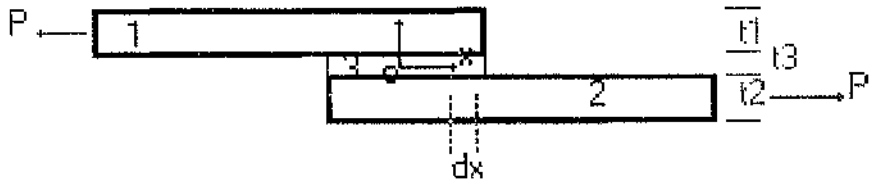

Figure 2.1 Simple lap shear joint used in Volkersen's analysis

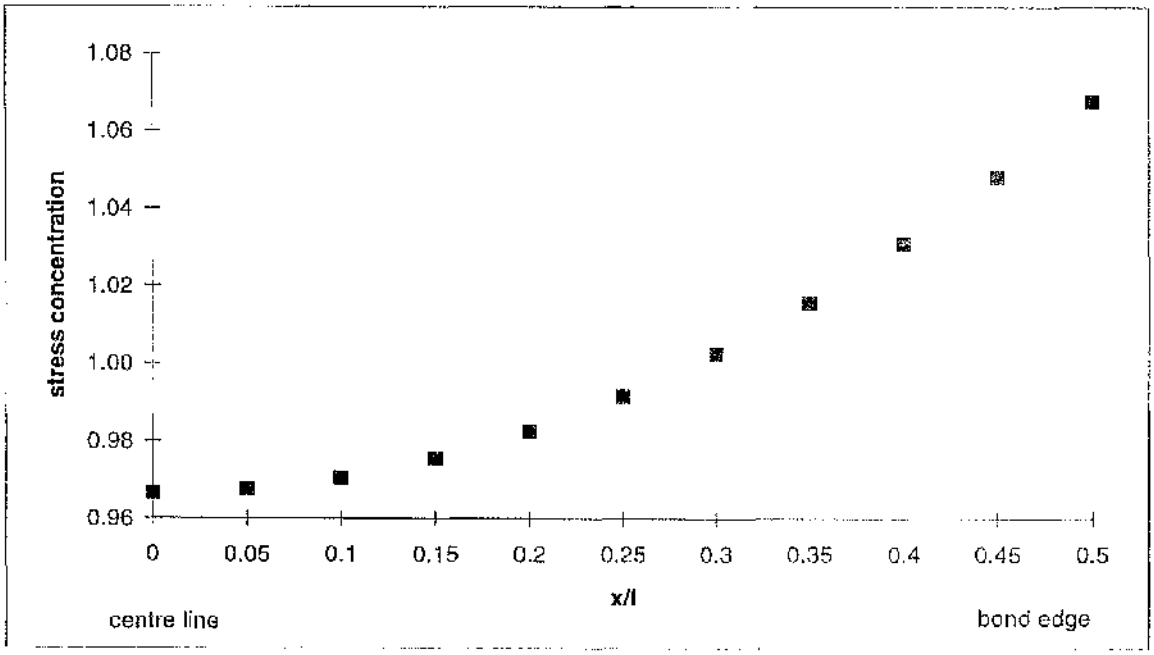

Figure 2.2 Volkersen's shear stress distribution as calculated for the specimen shown in figure 2.3

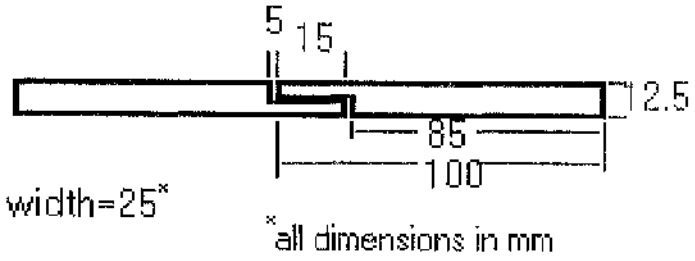

Figure 2.3 Thick steel adherend lap shear connection used in close-form analysis

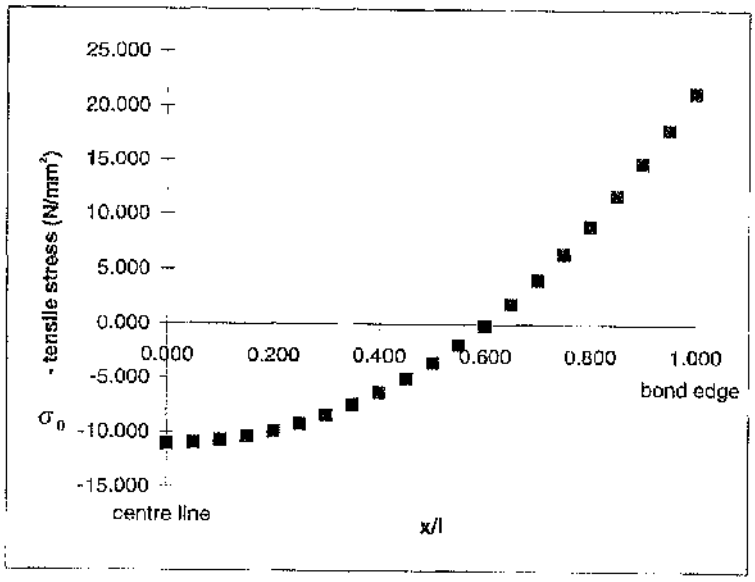

Figure 2.4 Goland and Reissner tensile stress distribution as calculated for the specimen shown in figure 2.3

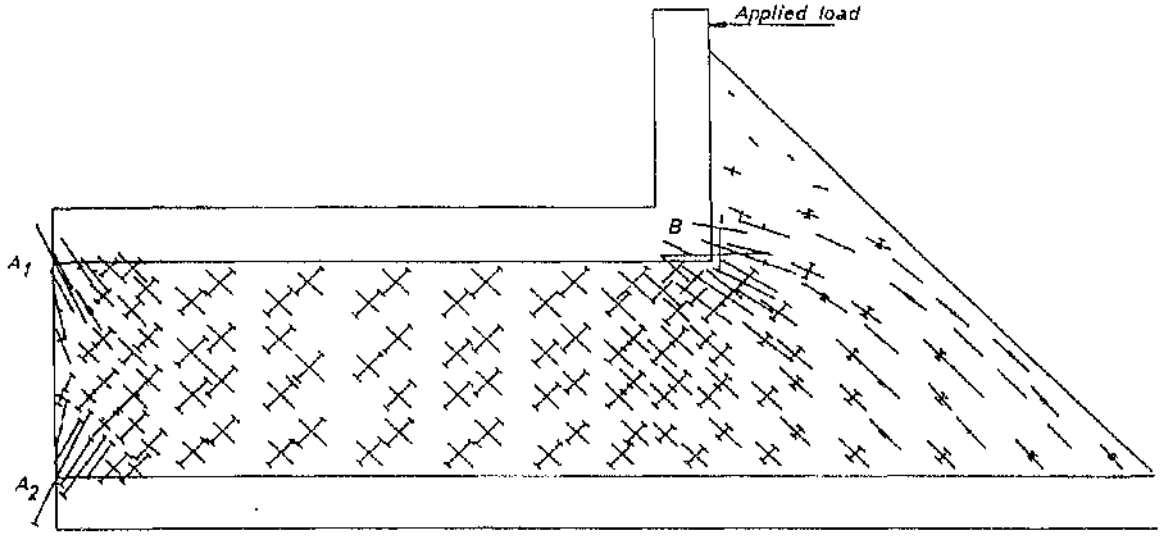

Principal stress pattern for silicone rubber model showing end effects. Lines indicate principal stresses in magnitude and direction. Bars at the ends of the lines indicate compressive stress

Figure 2.5 Finite element analysis results showing the effect of a fillet[7]

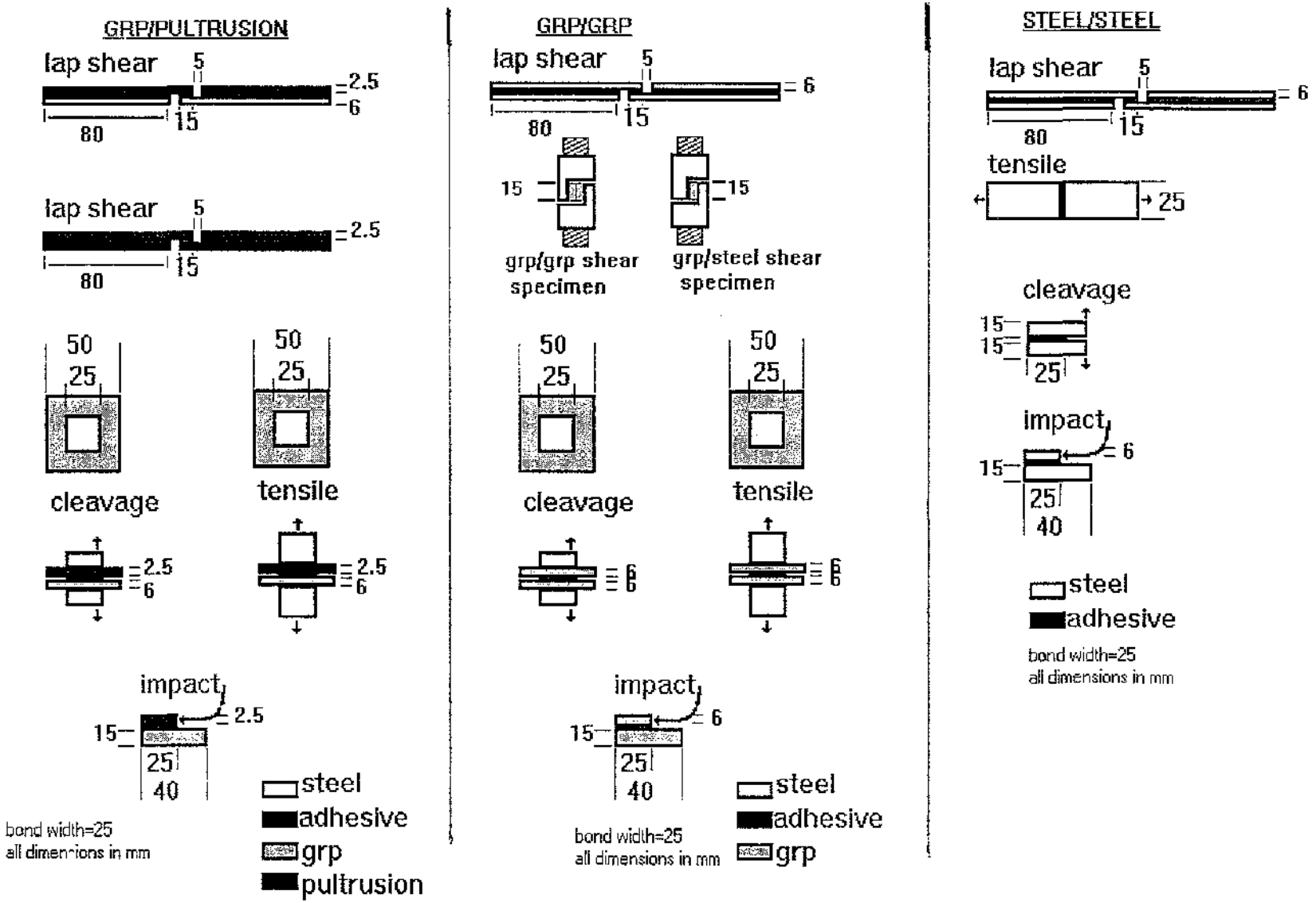

Figure 2.6 Various geometries of thick adherend small scale test pieces used throughout this thesis

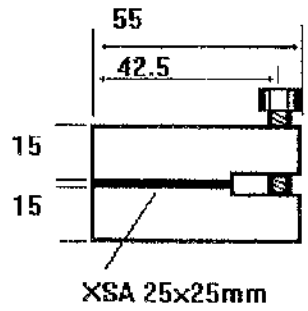

Figure 2.7 Preloaded cleavage specimen used for accelerated durability tests

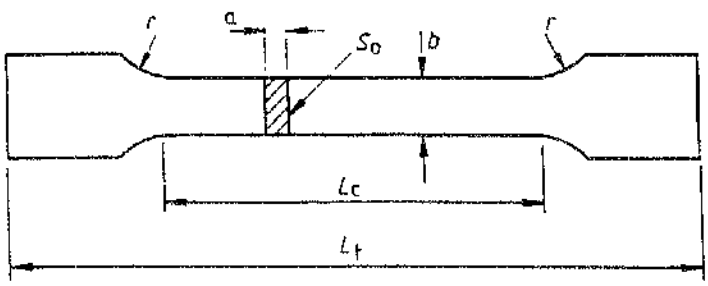

L_t =180mm
L_c =65mm
b =12.5mm
r =25mm
a =3mm
S_o=37.5mm^2

Figure 2.8 Bulk material tensile test specimens

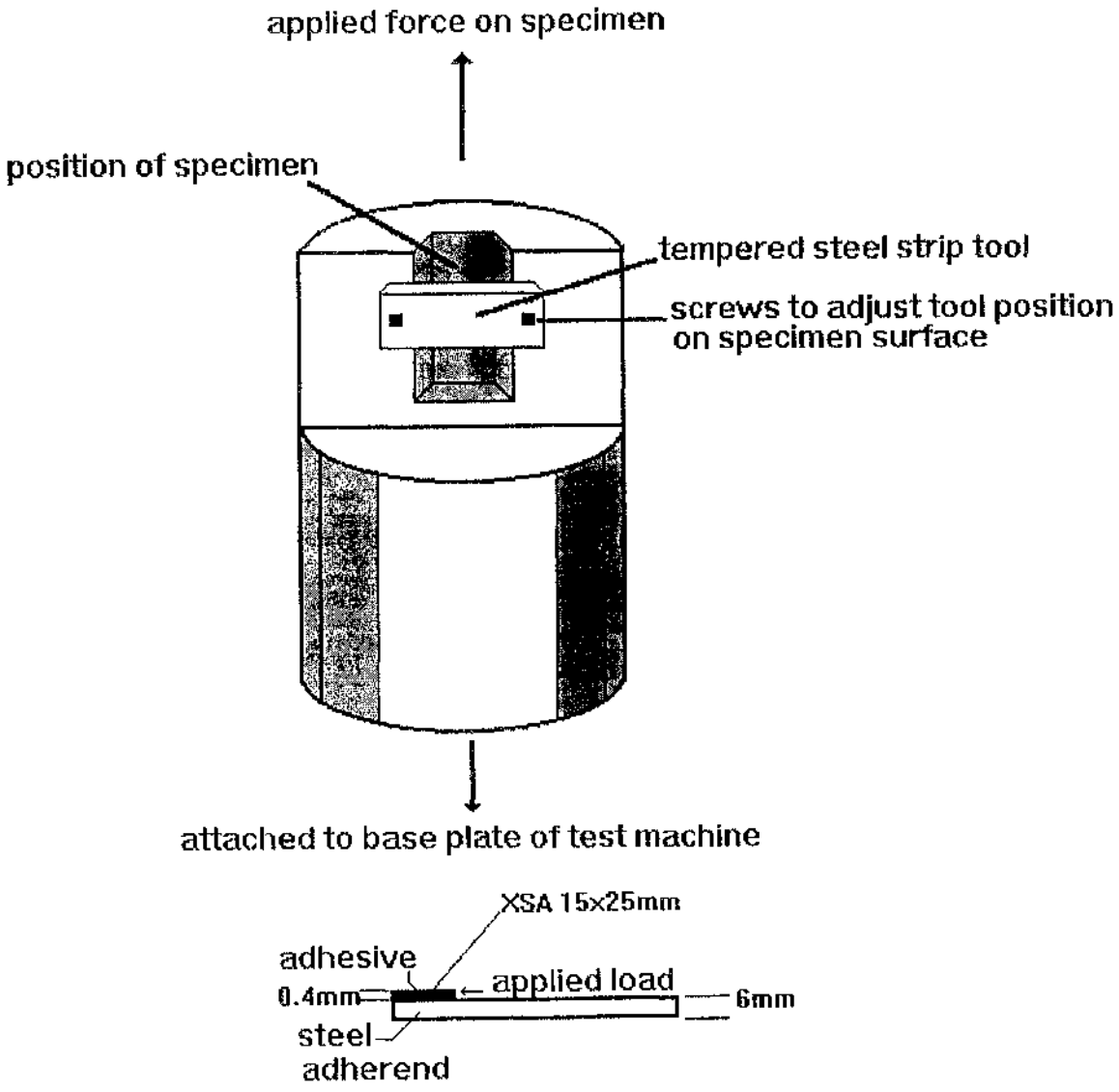

Figure 2.9 Scrape jig and specimen

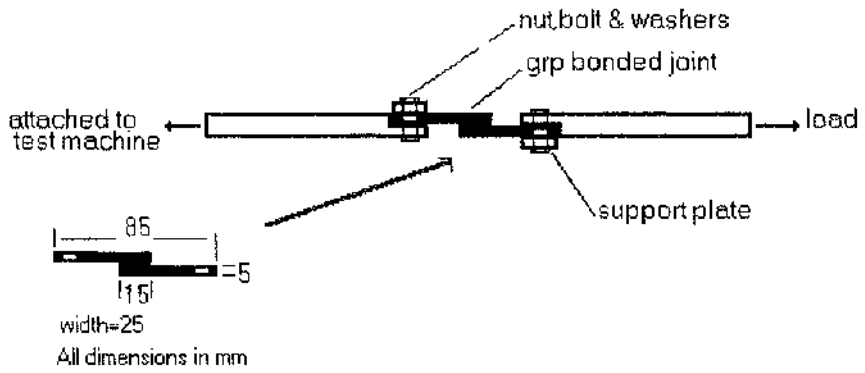

Figure 2.10 Modified grp bonded lap shear specimen and adapters for tensile testing

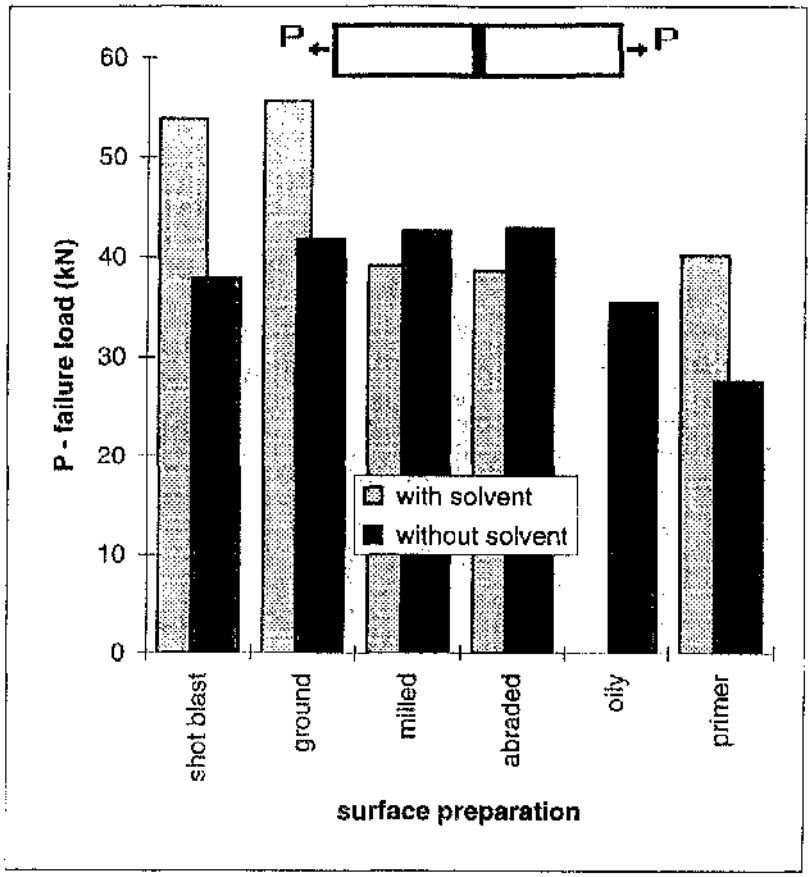

Figure 2.11 Effect of various mechanical surface preparation techniques have on tensile strength (XSA 25x25mm)

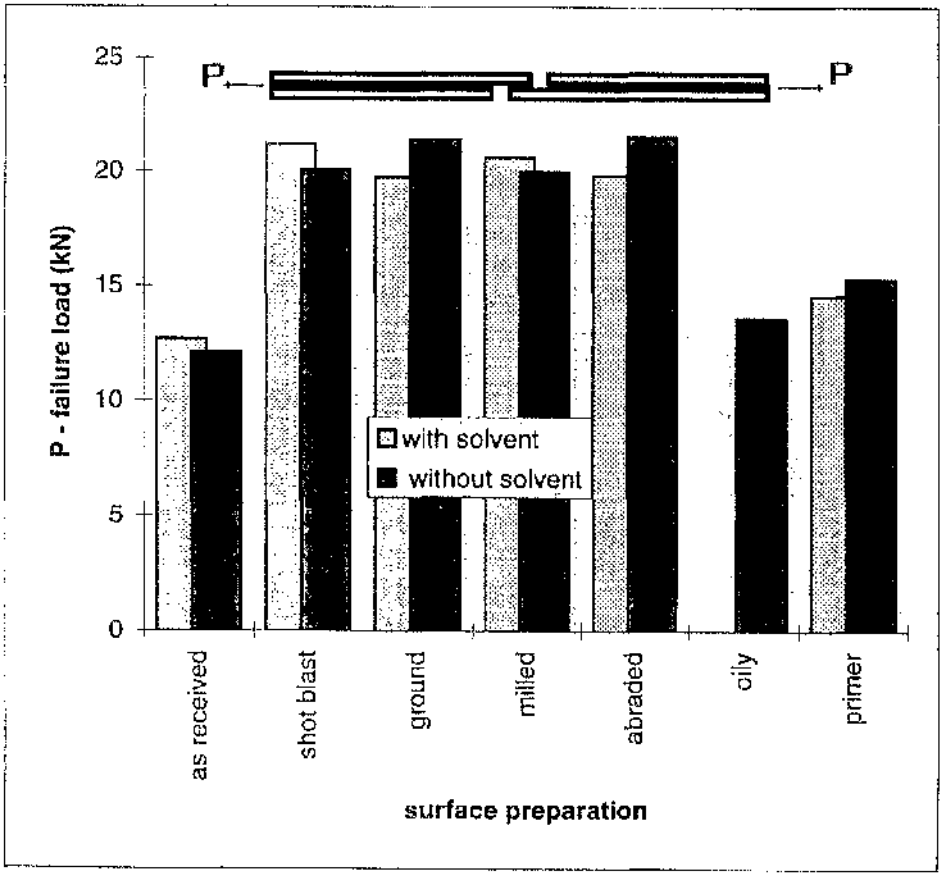

Figure 2.12 Effect of various mechanical surface preparation techniques have on shear strength (XSA 15x25mm)

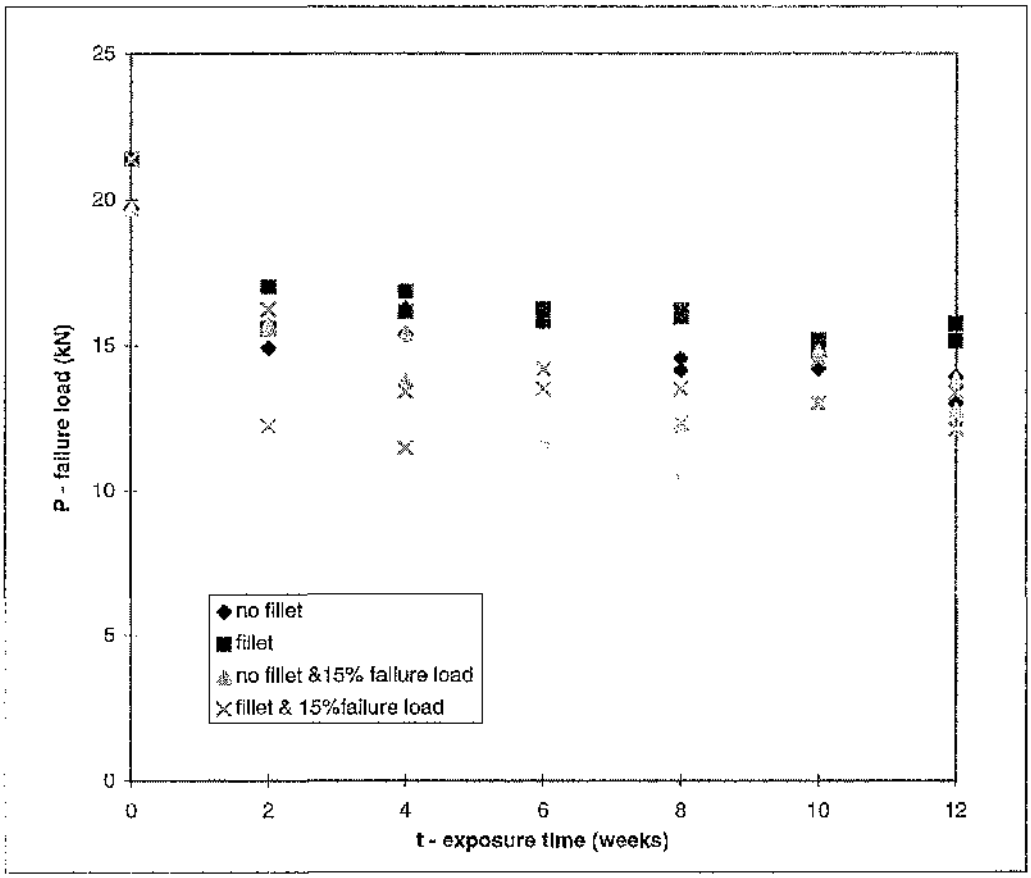

a) all inclusive results

Figure 2.13 Accelerated (T=30°C,100%R.H.) durability performance of Araldite 2007 bonded steel lap shear joints (XSA 15x25mm) showing the effect of a fillet and preload (15% UTS 19.7kN)

a) all inclusive results

b) the effect of a fillet

c) the effect of a preload

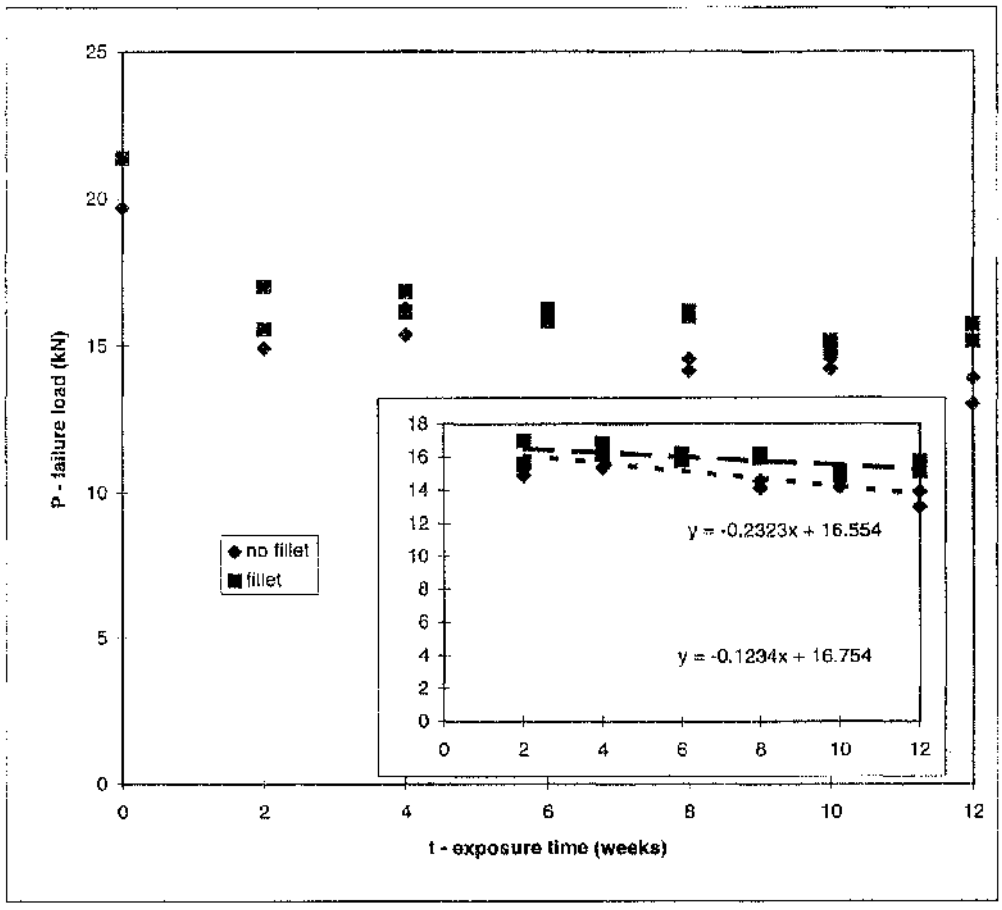

b) the effect of a fillet

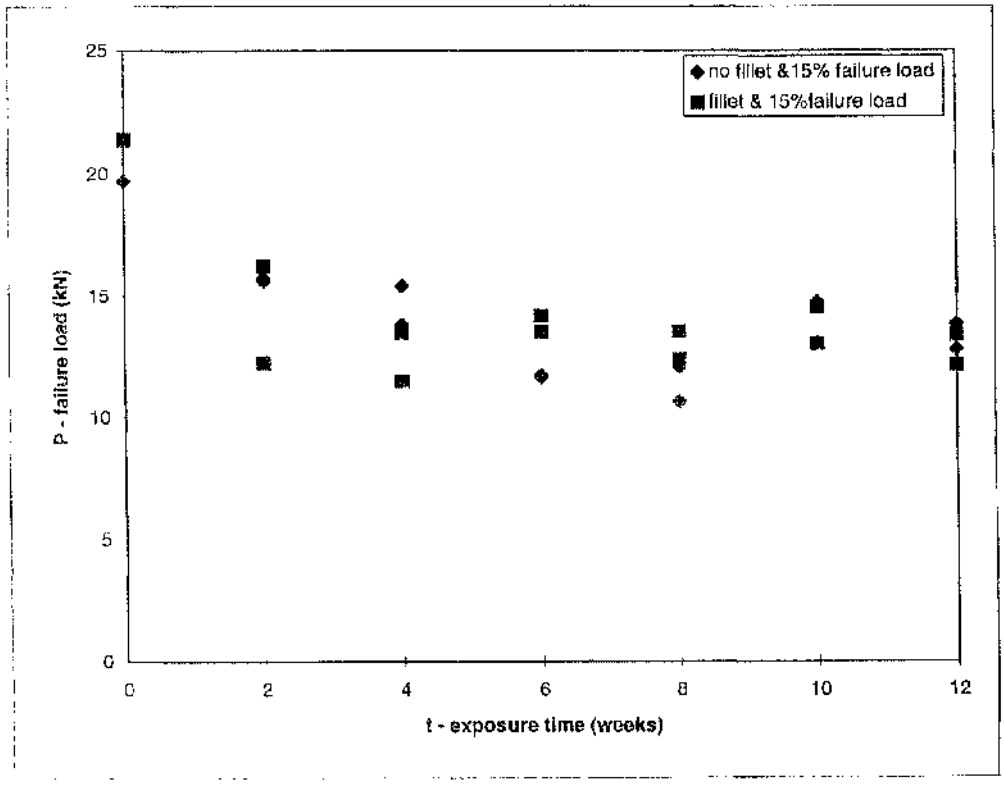

c) the effect of a preload

Figure 2.13 Accelerated (T=30°C,100%R.H.) durability performance of Araldite 2007 bonded steel lap shear joints (XSA 15x25mm) showing the effect of a fillet and preload (15% UTS 19.7kN)

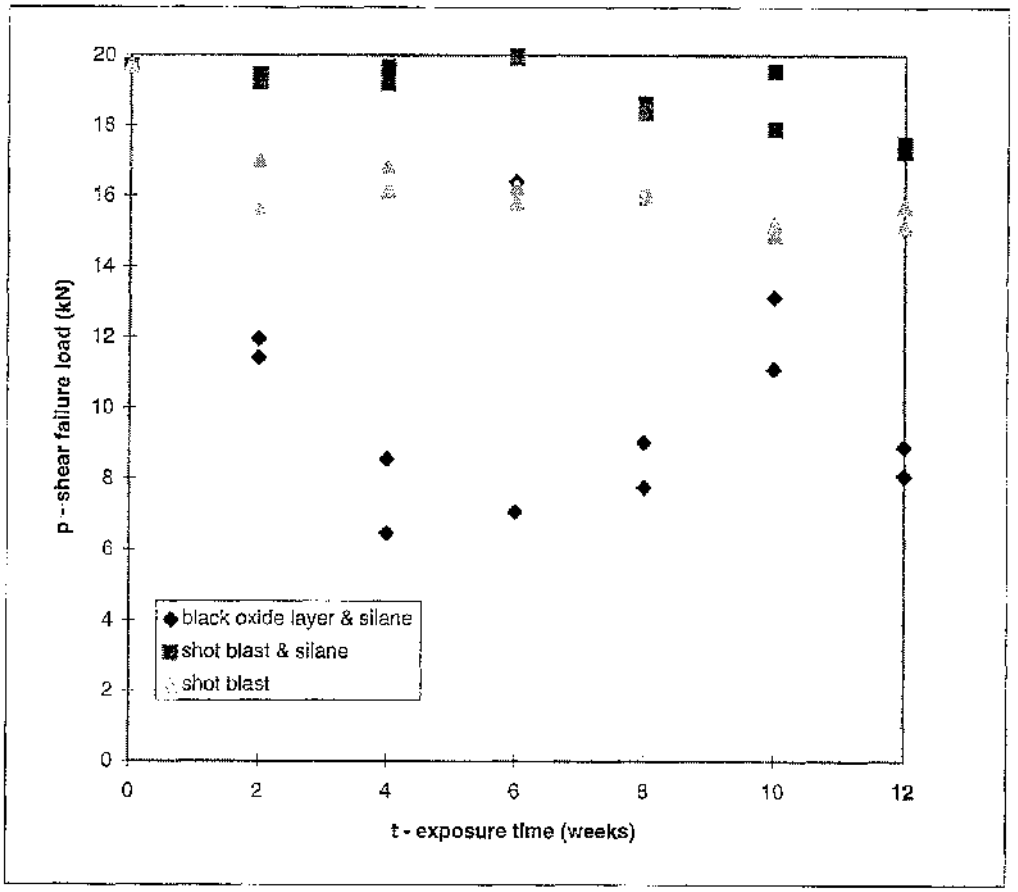

Figure 2.14 Accelerated (T=30°C,100%R.H.) durability performance of Araldite 2007 bonded steel lap shear joints (XSA 15x25mm) showing the effect of an adequate surface preparation prior to the application of a primer (A187)

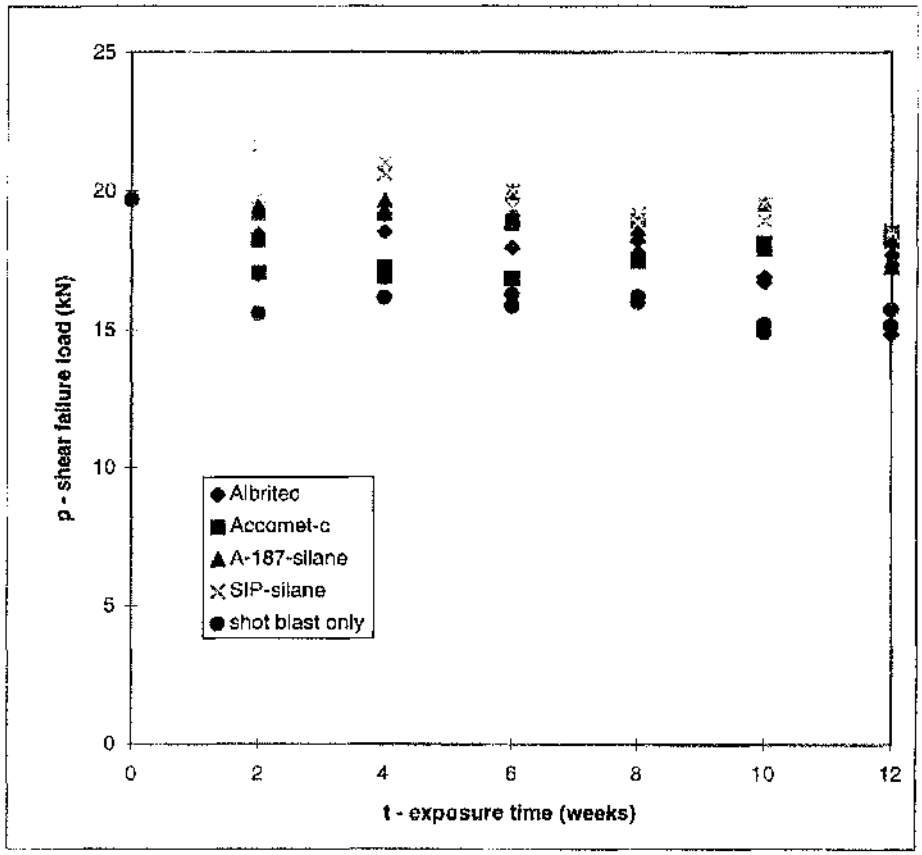

Figure 2.15 Accelerated (T=30°C,100%R.H.) durability performance of Araldite 2007 bonded steel lap shear joints (XSA 15x25mm) showing the effect of various bonding primers

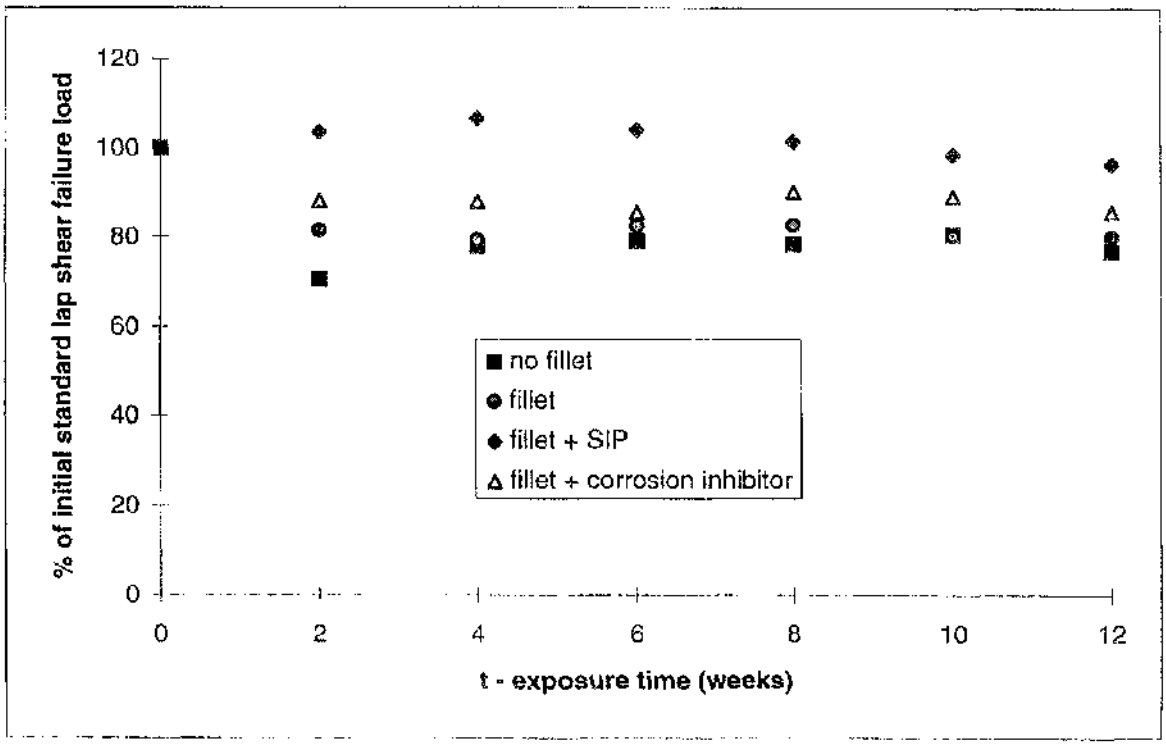

Figure 2.16 Accelerated (T=30°C,100%R.H.) durability performance of Araldite 2007 bonded steel lap shear joints (XSA 15x25mm) showing the effect of a primer

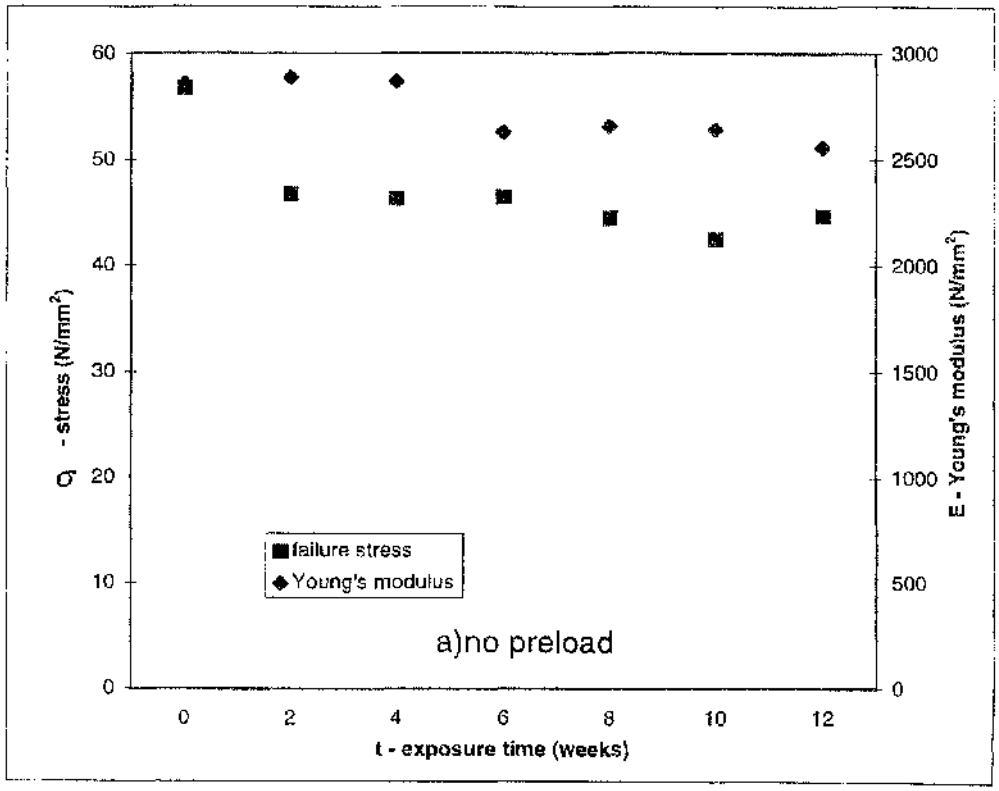

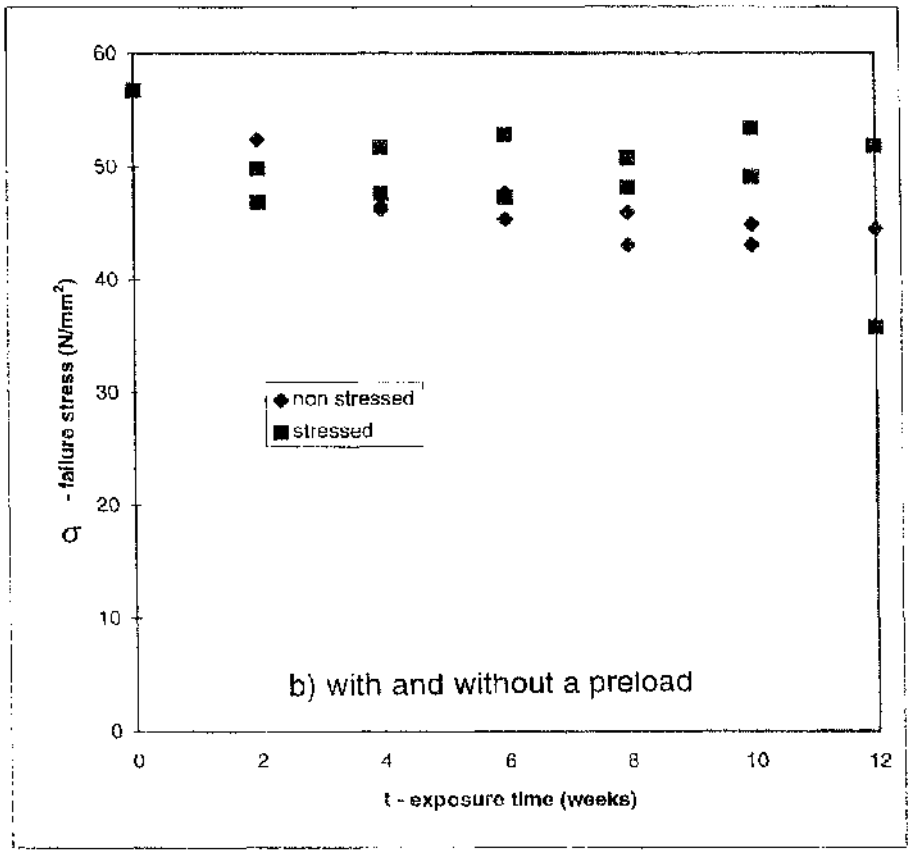

Figure 2.17 Accelerated (T=30°C,100%R.H.) durability performance of Araldite 2007 bulk tensile samples with and without the application of a preload (20% UTS 1800N)
a)no preload
b) with and without a preload

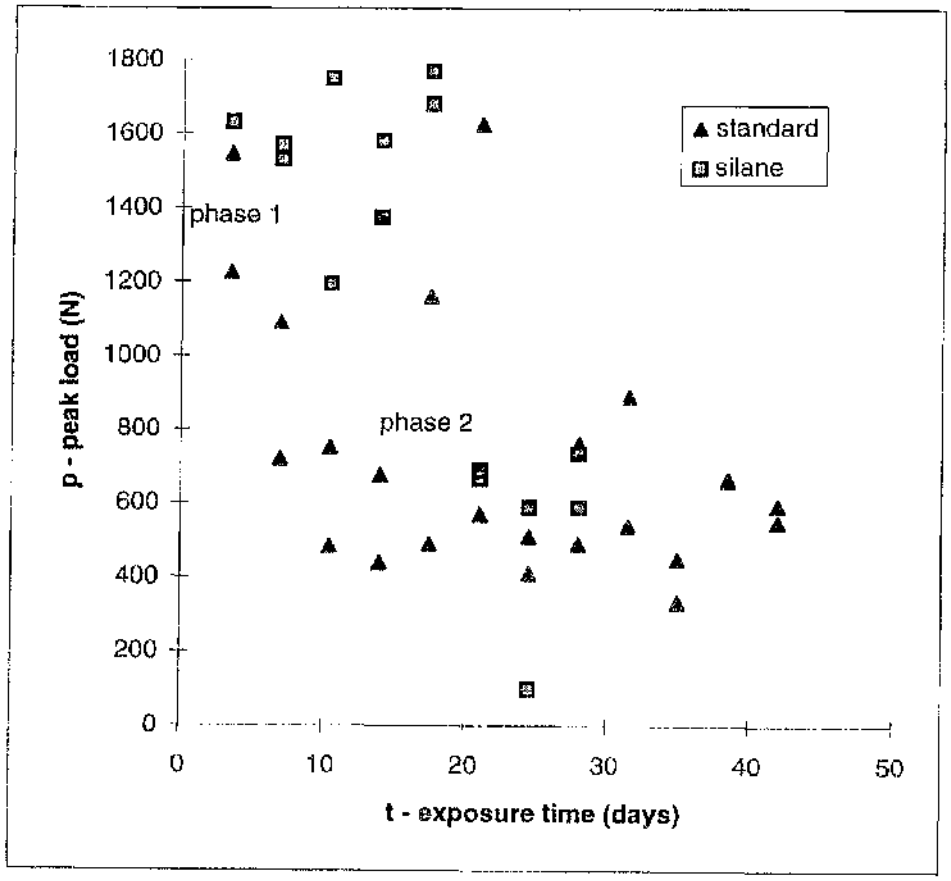

Figure 2.18 Accelerated (T=30°C,100%R.H.) durability performance of Araldite 2007 interfacial strength on steel adherends with and without the application of a primer (A187)

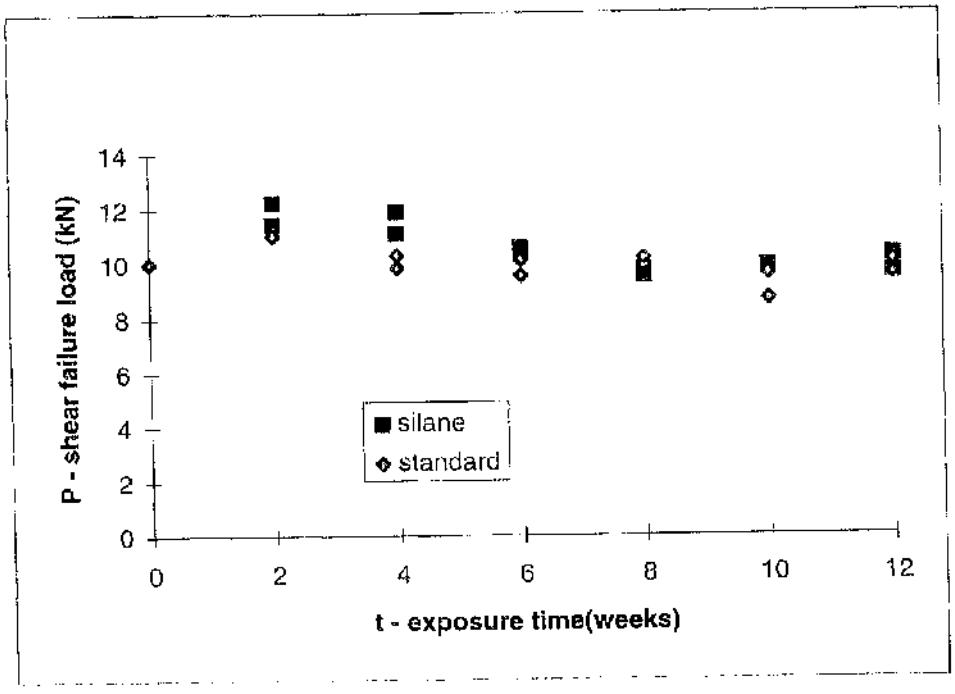

Figure 2.19 Accelerated (T=30°C,100%R.H.) durability performance of Redux 410 bonded steel lap shear joints (XSA 15x25mm) with and without the application of a primer (A187)

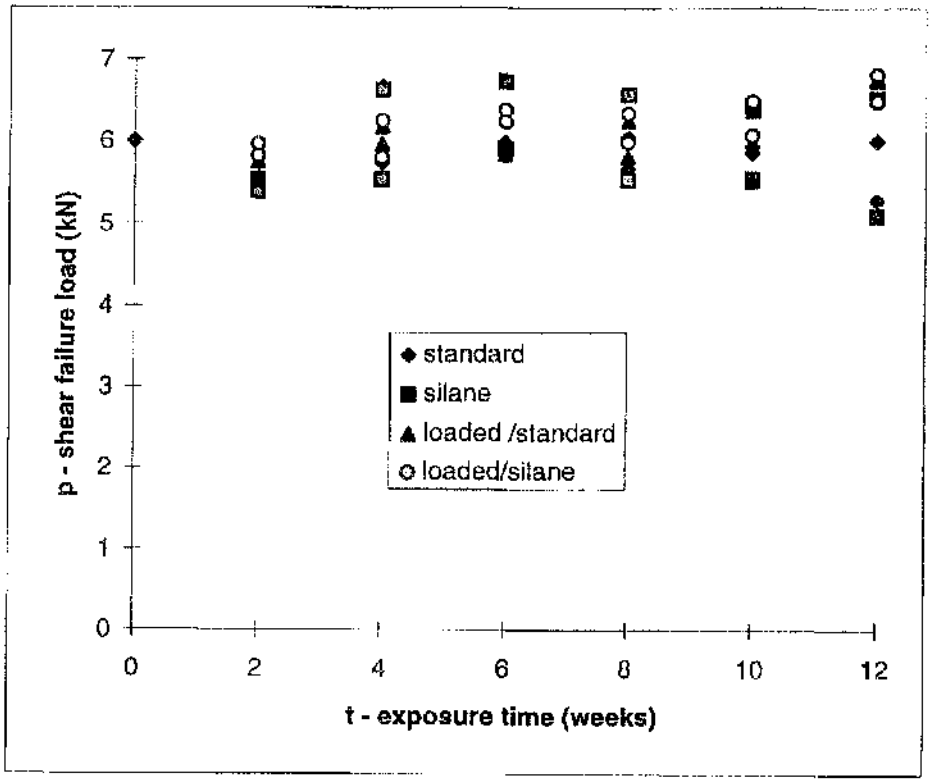

Figure 2.20 Accelerated (T=30°C,100%R.H.) durability performance of Araldite 2005 bonded grp lap shear joints (XSA 15x25mm) on peel ply surfaces with and without a preload (20% UTS 6000N) and a primer (A187)

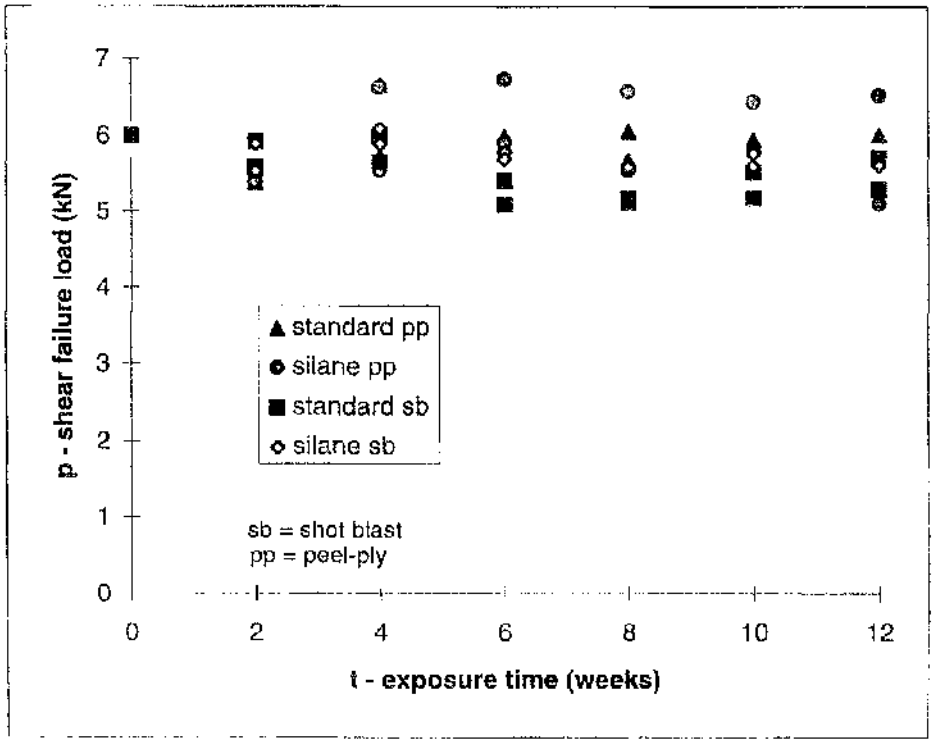

Figure 2.21 Accelerated (T=30°C,100%R.H.) durability performance of Araldite 2005 bonded grp lap shear joints (XSA 15x25mm) with various surface preparations

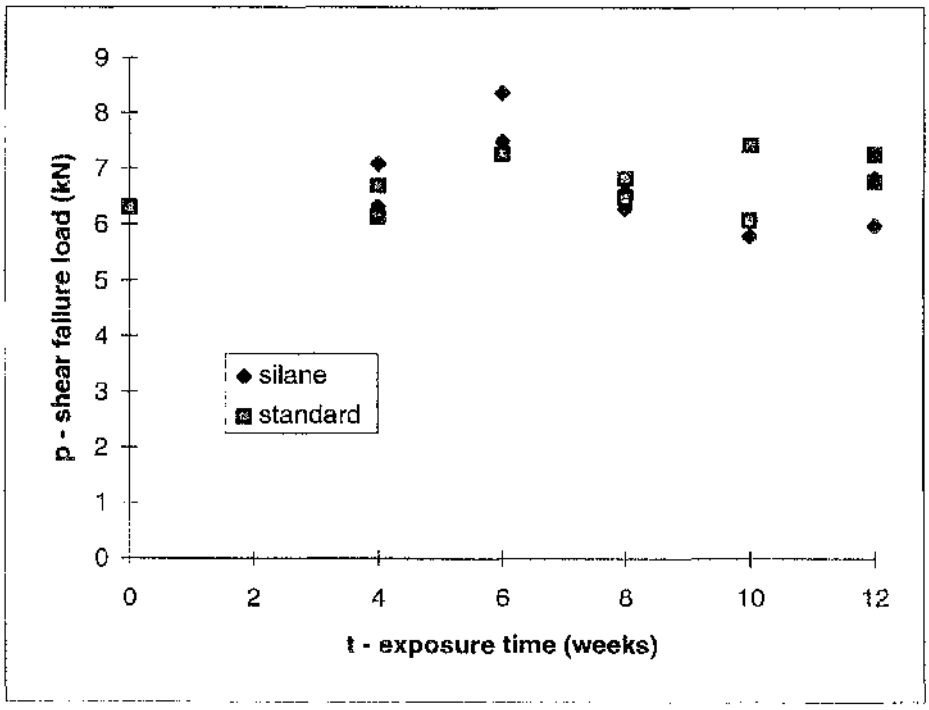

Figure 2.22 Accelerated (T=30°C,100%R.H.) durability performance of Redux 420 bonded grp lap shear joints (XSA 15x25mm) with a primer (SiP) on a peel ply surface

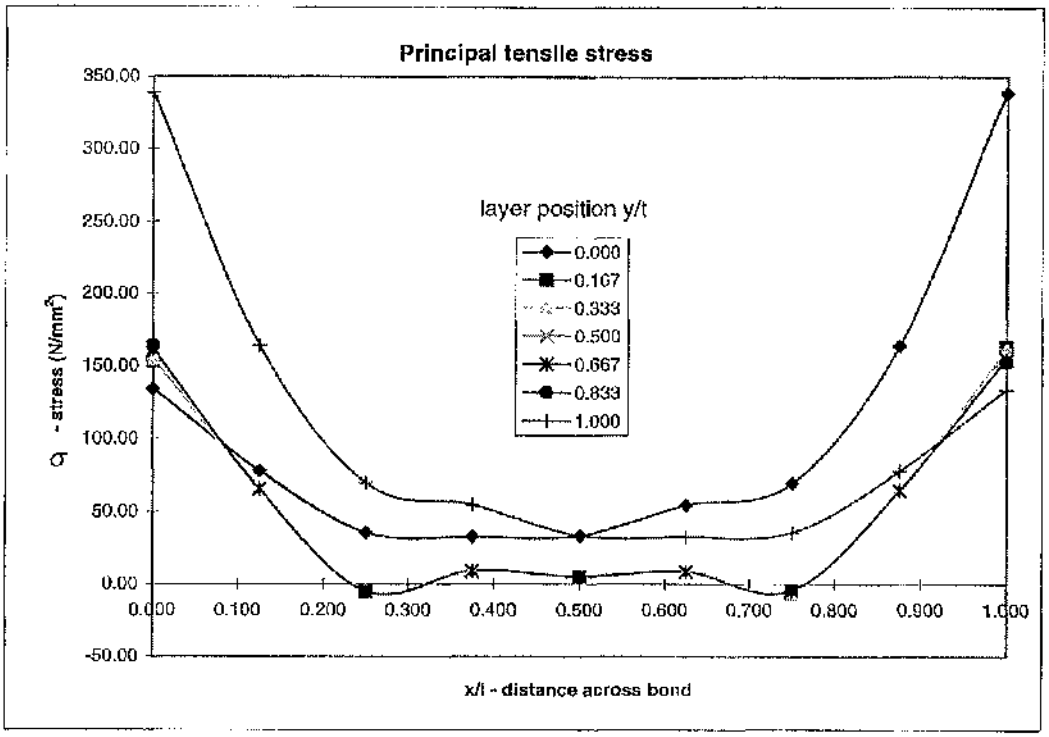

Figure 2.23 Principal tensile stress distribution through the adhesive layer for an Araldite 2007 bonded steel lap shear joint (XSA 25x25mm) for a nominal load (20kN)

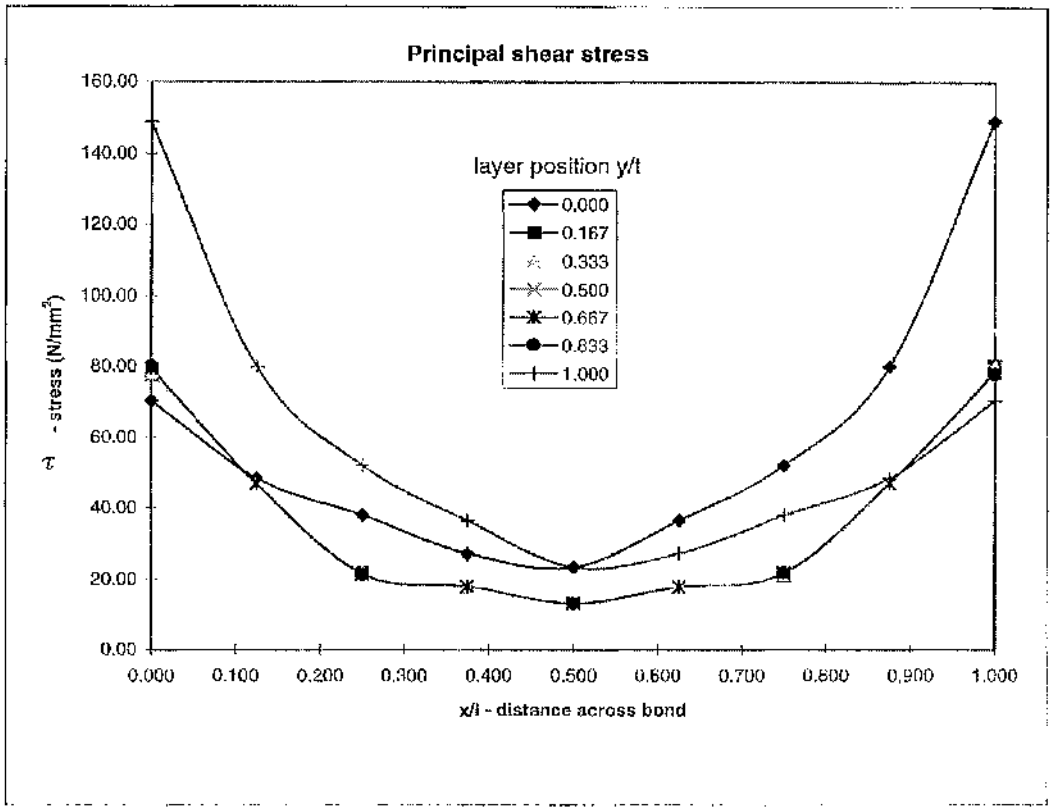

Figure 2.24 Principal shear stress distribution through the adhesive layer for an Araldite 2007 bonded steel lap shear joint (XSA 25x25mm) for a nominal load (20kN)

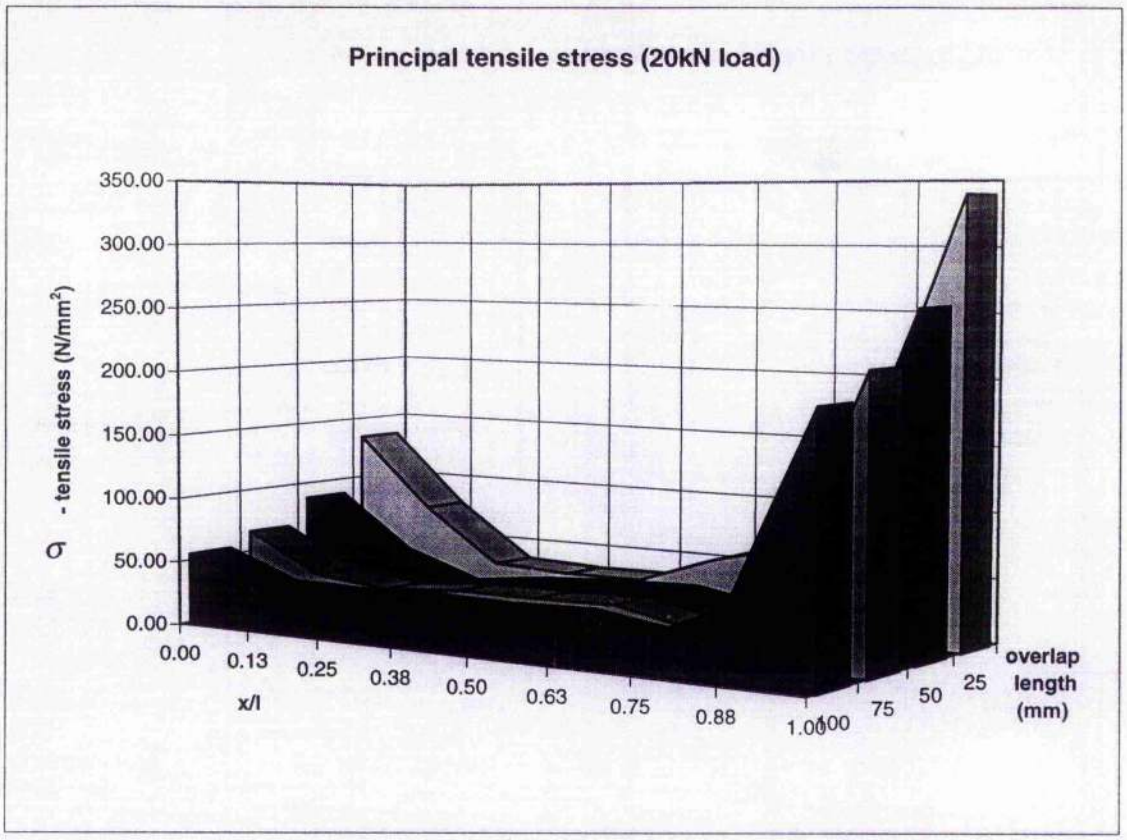

Figure 2.25 Principal tensile stress distribution through the adhesive layer for an Araldite 2007 bonded steel lap shear joint of various overlap lengths for a nominal load (20kN)

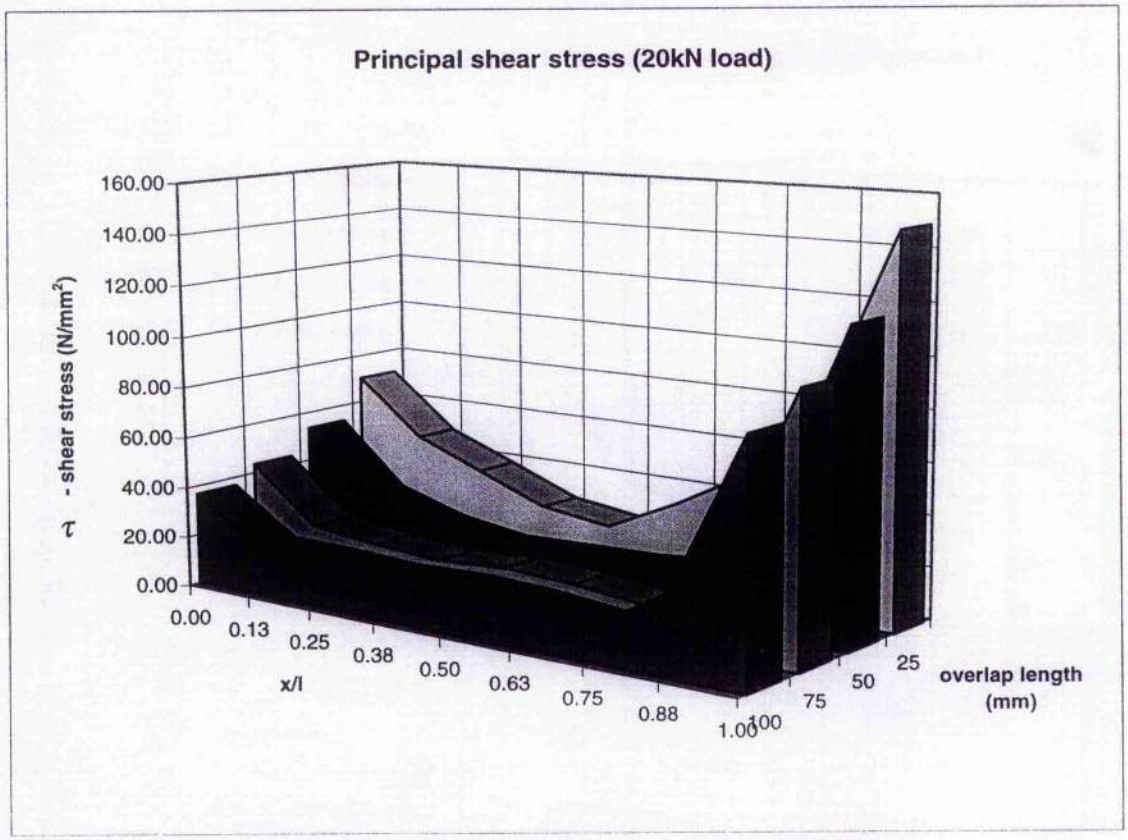

Figure 2.26 Principal shear stress distribution through the adhesive layer for an Araldite 2007 bonded steel lap shear joint of various overlap lengths for a nominal load (20kN)

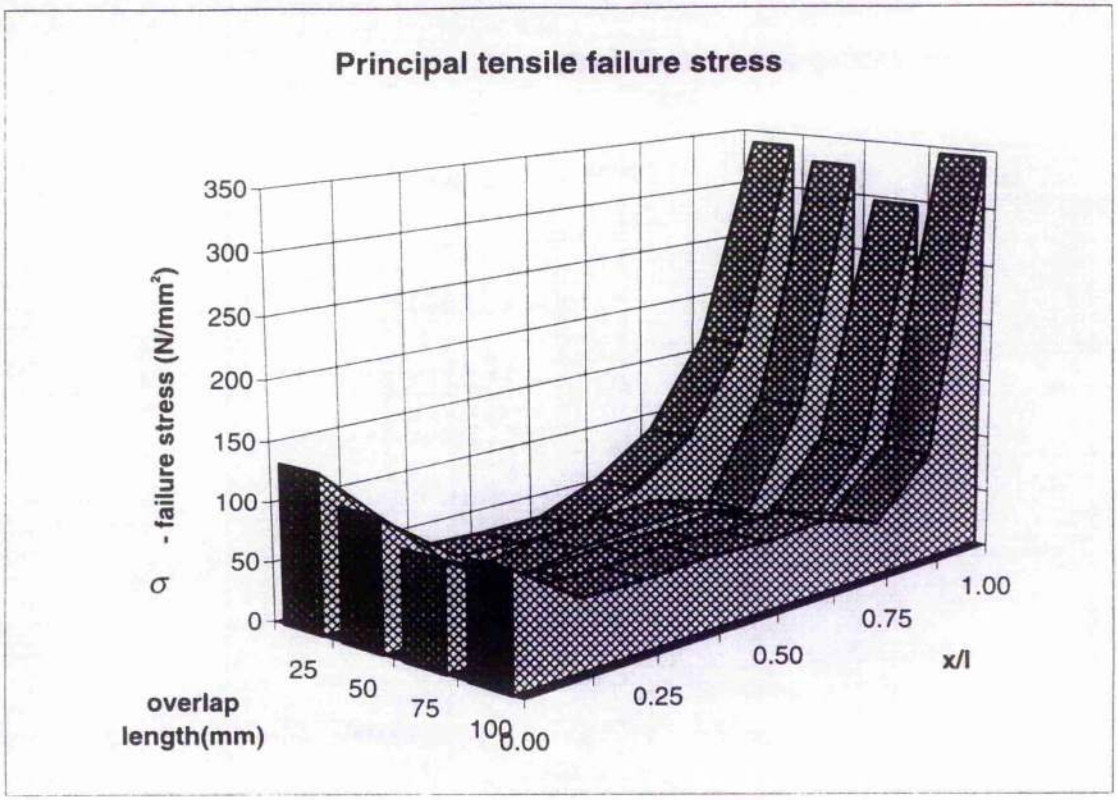

Figure 2.27 Principal failure tensile stress distribution through the adhesive layer for an Araldite 2007 bonded steel lap shear joint of various overlap lengths

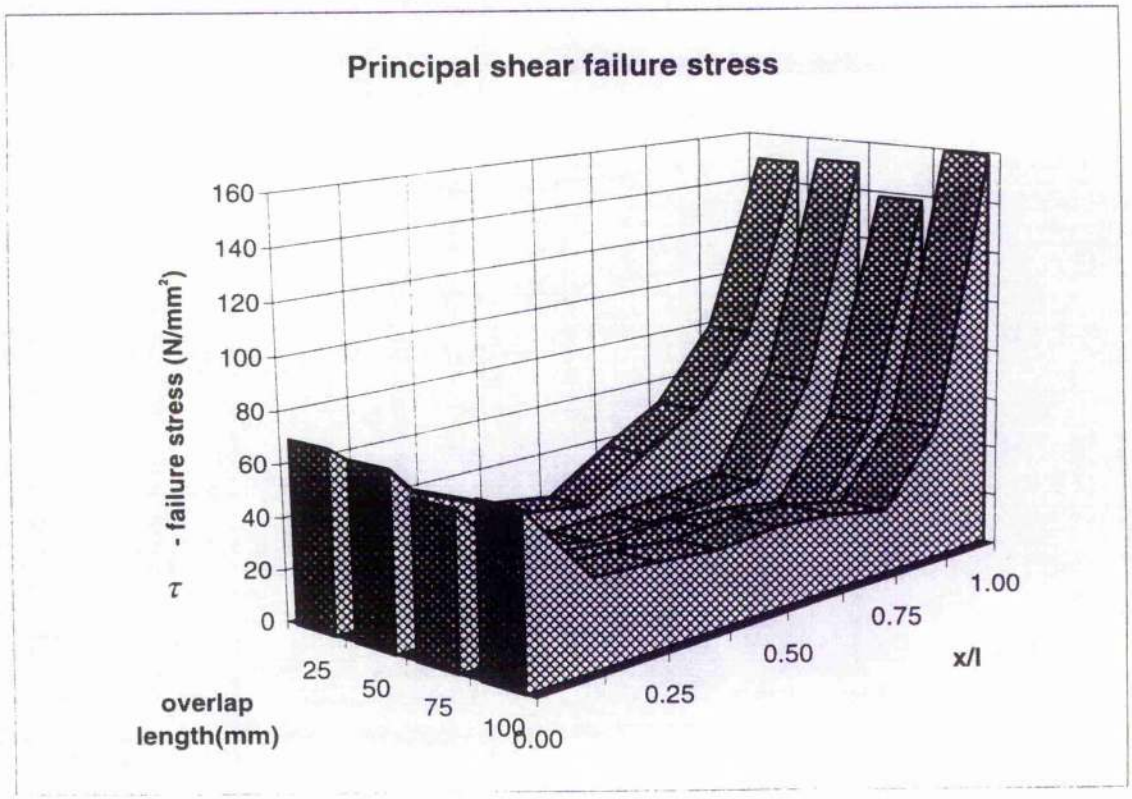

Figure 2.28 Principal failure shear stress distribution through the adhesive layer for an Araldite 2007 bonded steel lap shear joint of various overlap lengths

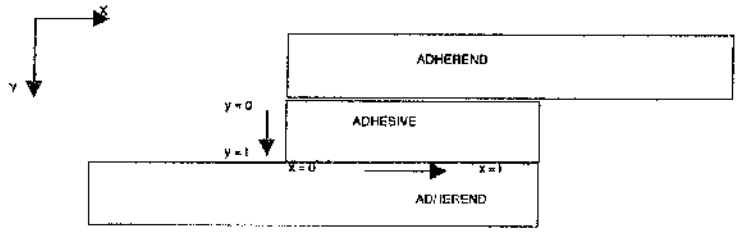

Figure 2.29 Co-ordinate system used in the finite element analysis

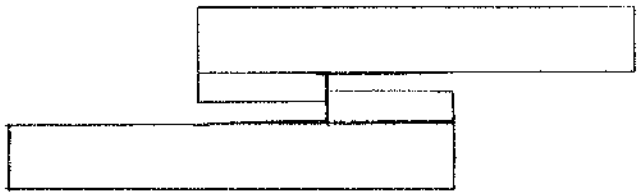

Figure 2.30 Schematic representation of a failure in a lap shear joint with no fillet

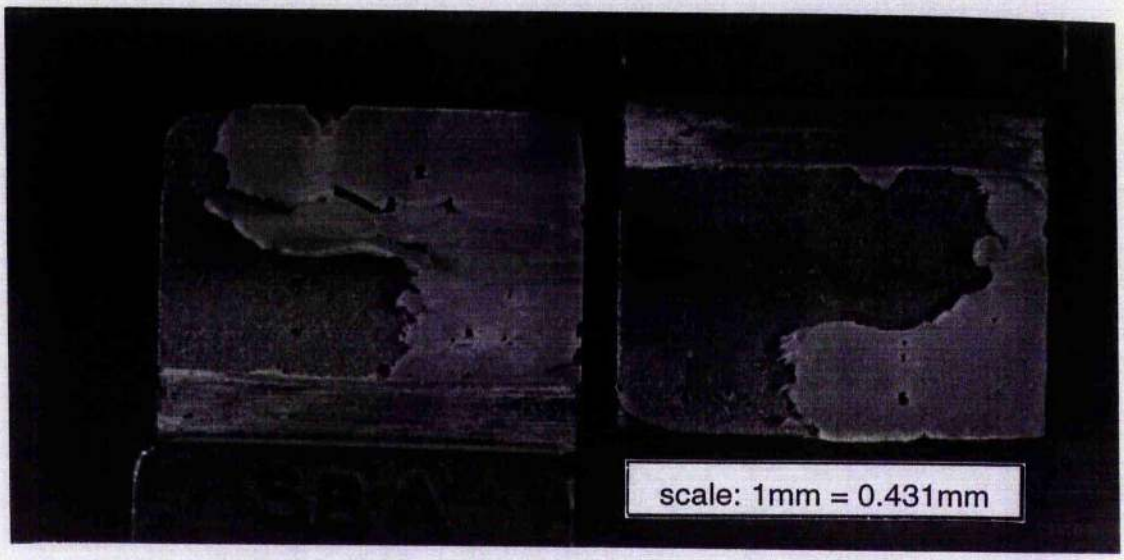

Figure 2.31 Failure surface showing good adhesion of a shot blast Araldite 2007 bonded steel lap shear joint

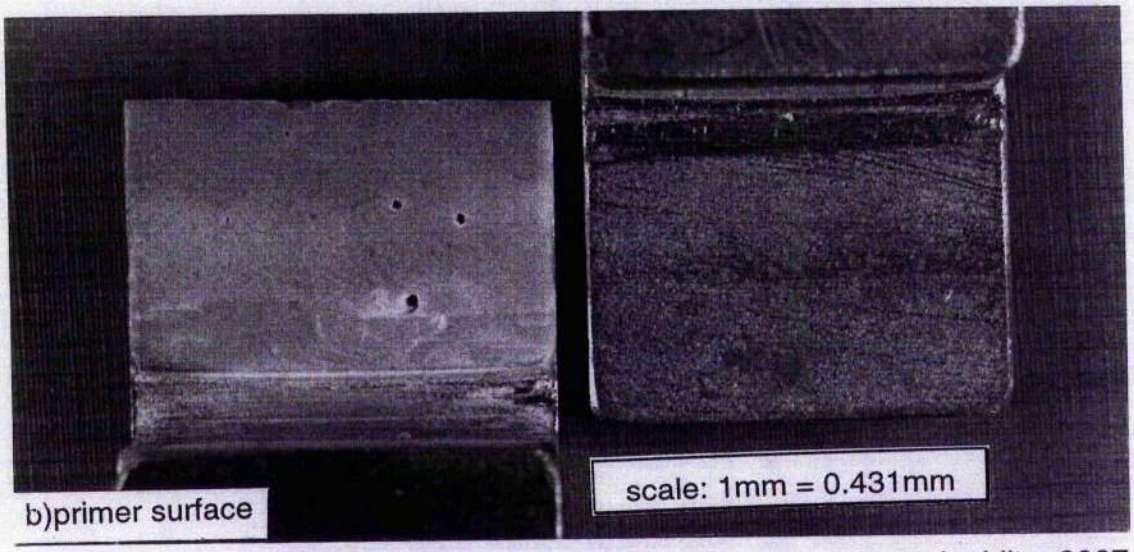

Figure 2.32 Failure surface showing poor adhesion of an Araldite 2007 bonded steel lap shear joint

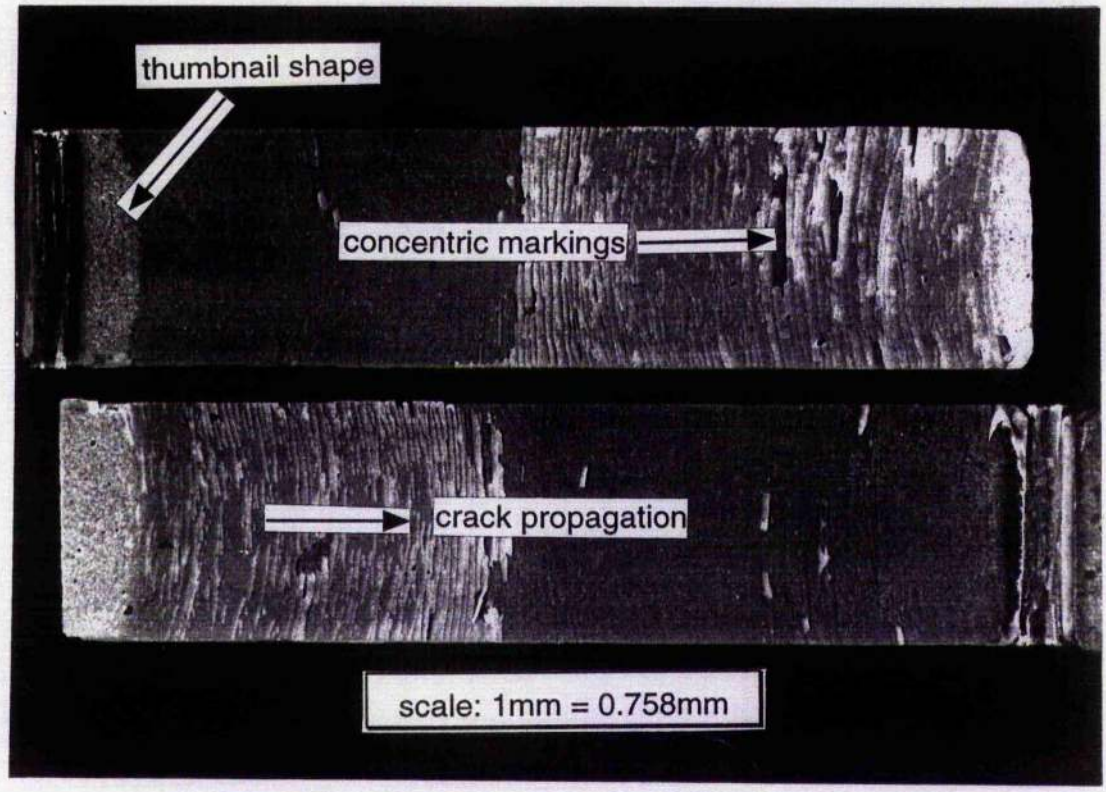

Figure 2.33 Typical failure surface of a 100mm overlap Araldite 2007 bonded steel lap shear joint

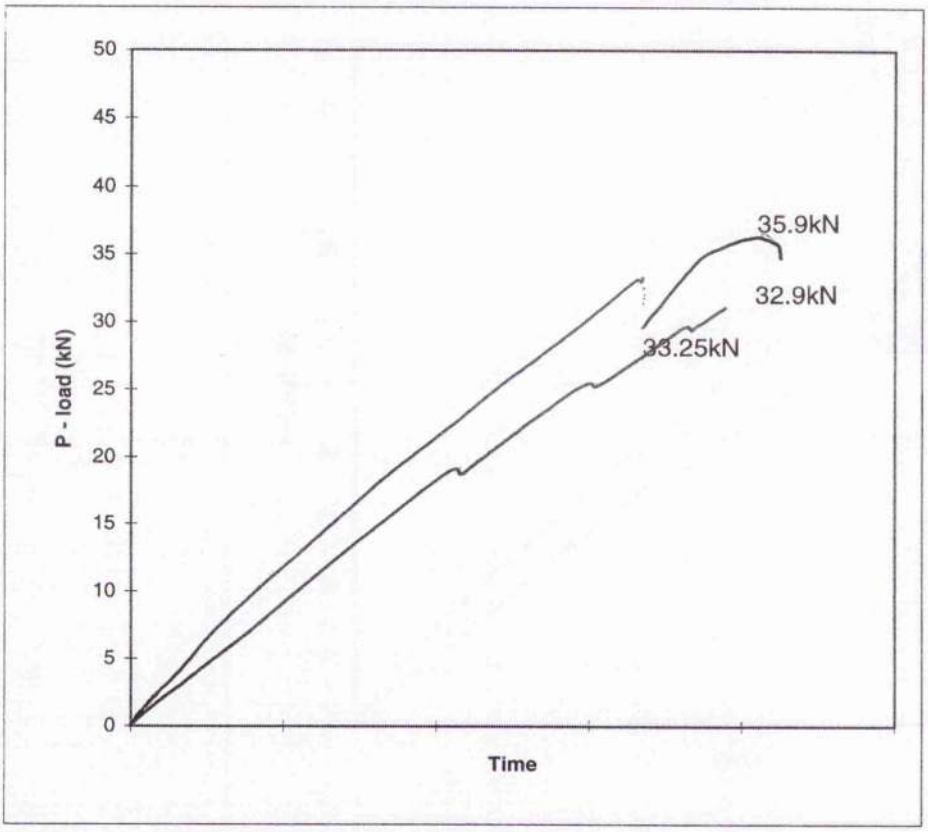

Figure 2.34 Experimental load/time plot for 100mm overlap Araldite 2007 bonded steel lap shear joint

Figure 2.35 Typical failure surface of a 100mm overlap Araldite 2007 bonded steel lap shear joint when the adhesive is applied in discrete strips

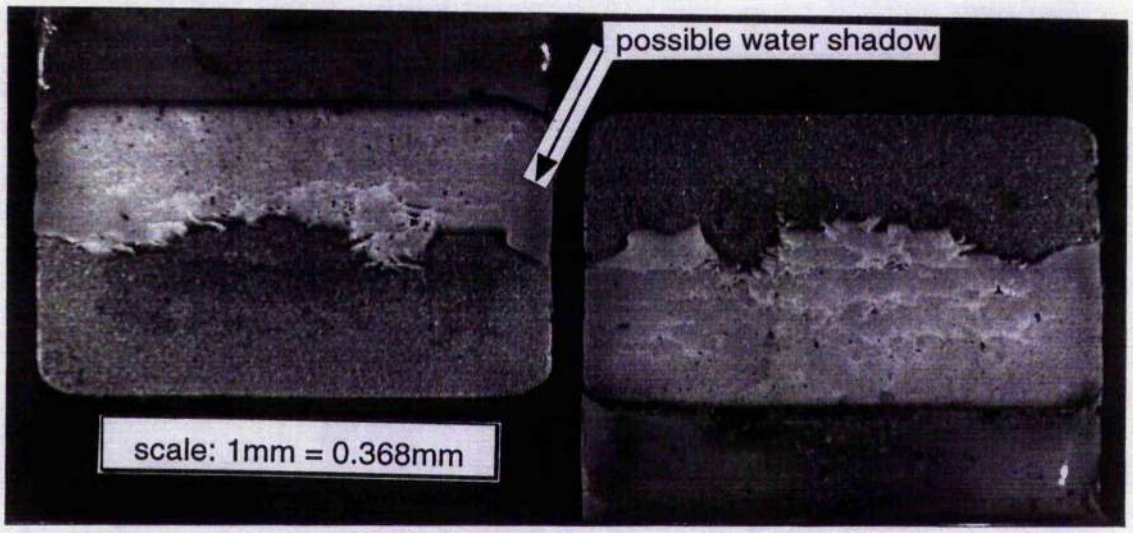

Figure 2.36 Typical failure surface of an Araldite 2007 bonded steel lap shear joint after accelerated aging (T=30°C,100%R.H.) with the fillet left intact and no preload

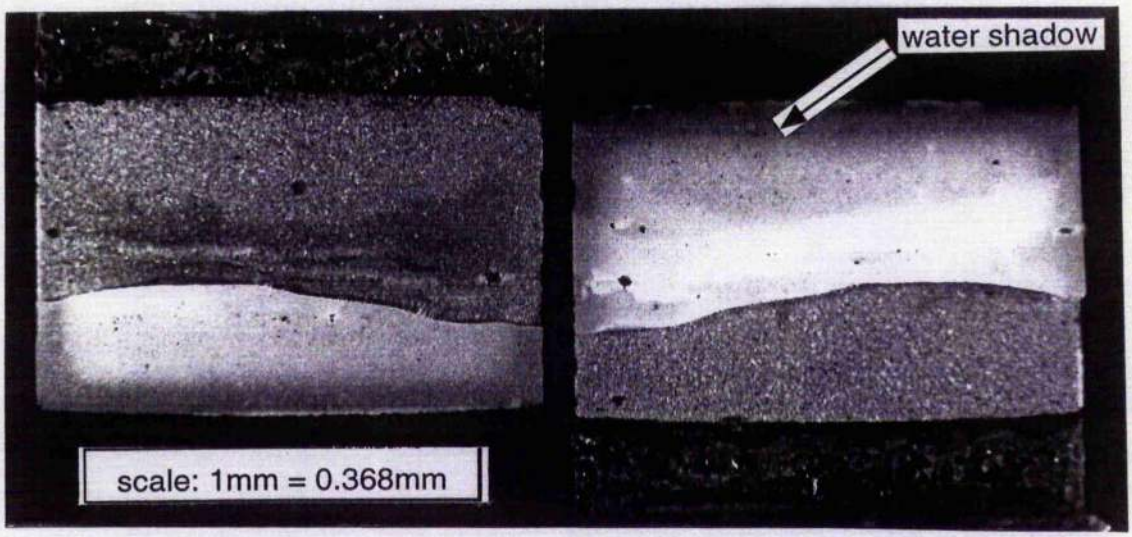

Figure 2.37 Typical failure surface of an Araldite 2007 bonded steel lap shear joint after accelerated aging (T=30°C,100%R.H.) with the fillet removed and no preload

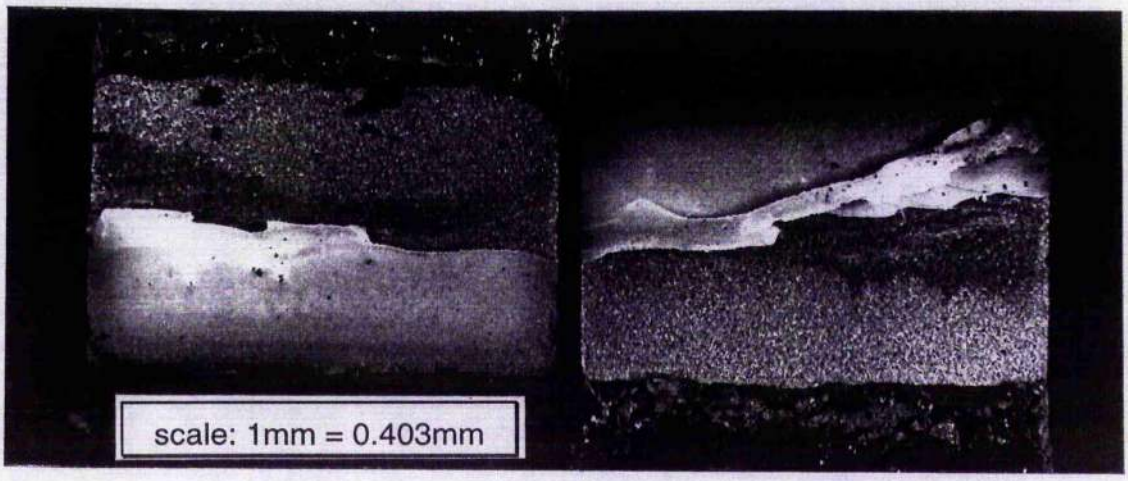

a) spew fillet intact

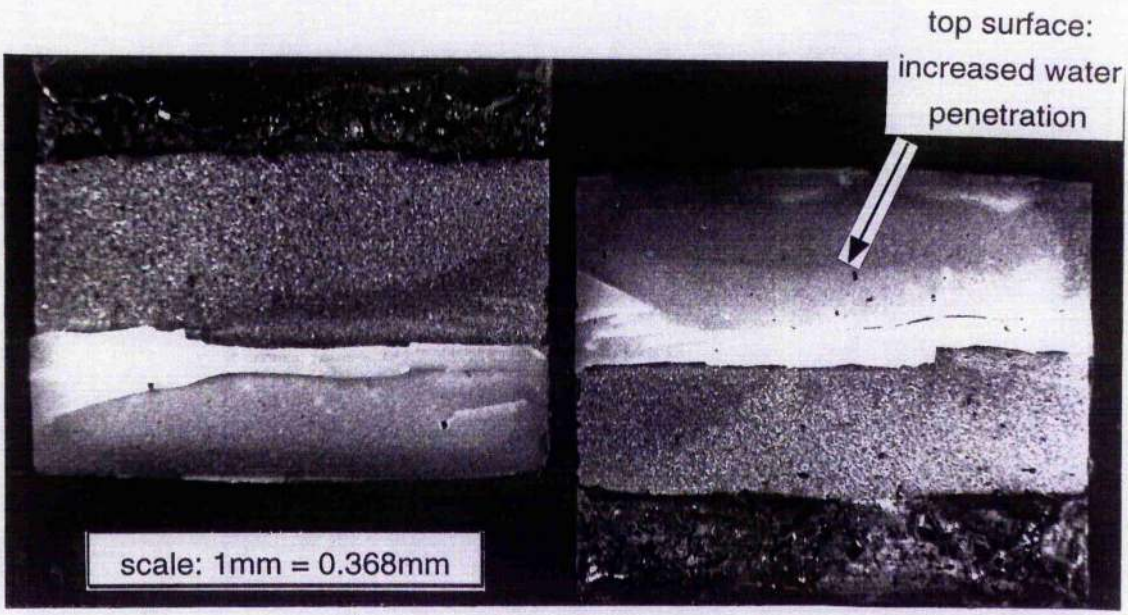

b) spew fillet removed

Figure 2.38 Typical failure surface of an Araldite 2007 bonded steel lap shear joint after accelerated aging (T=30°C,100%R.H.) with the a preload (15%UTS 19.7kN)
a) spew fillet intact
b) spew fillet removed

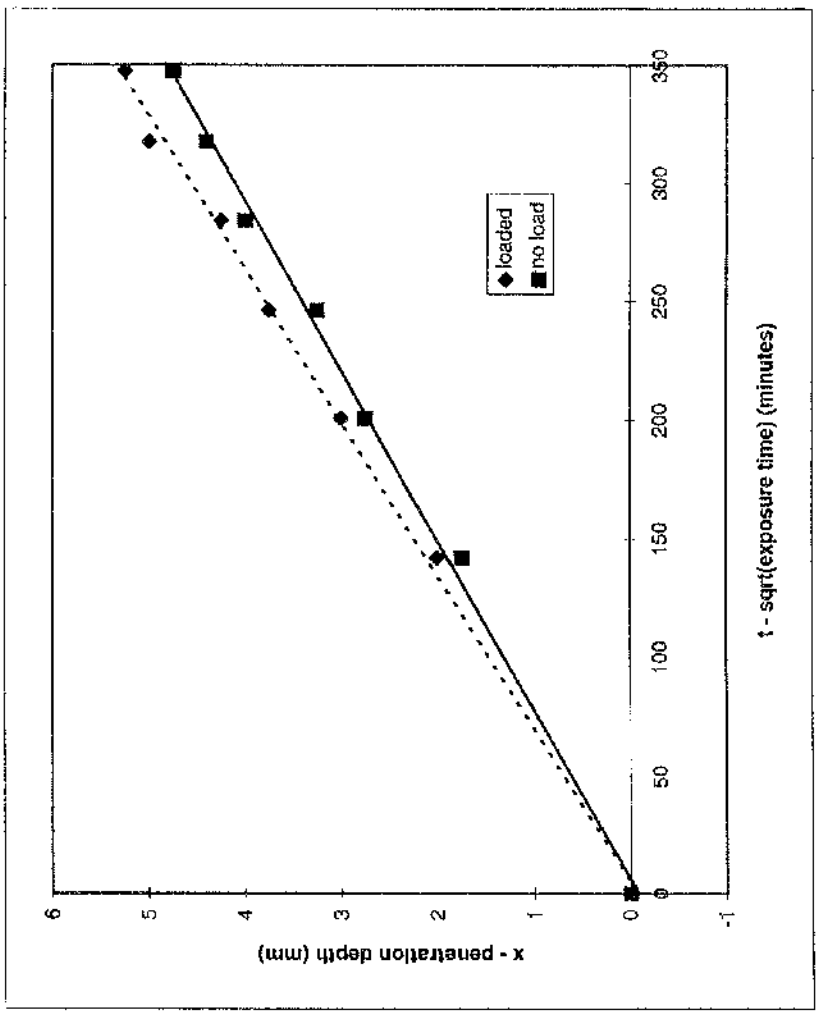

Figure 2.39 Plot of water penetration depth into an Araldite 2007 bonded steel lap shear joint (XSA 15x25mm) during accelerated aging (T=30°C,100%R.H.)

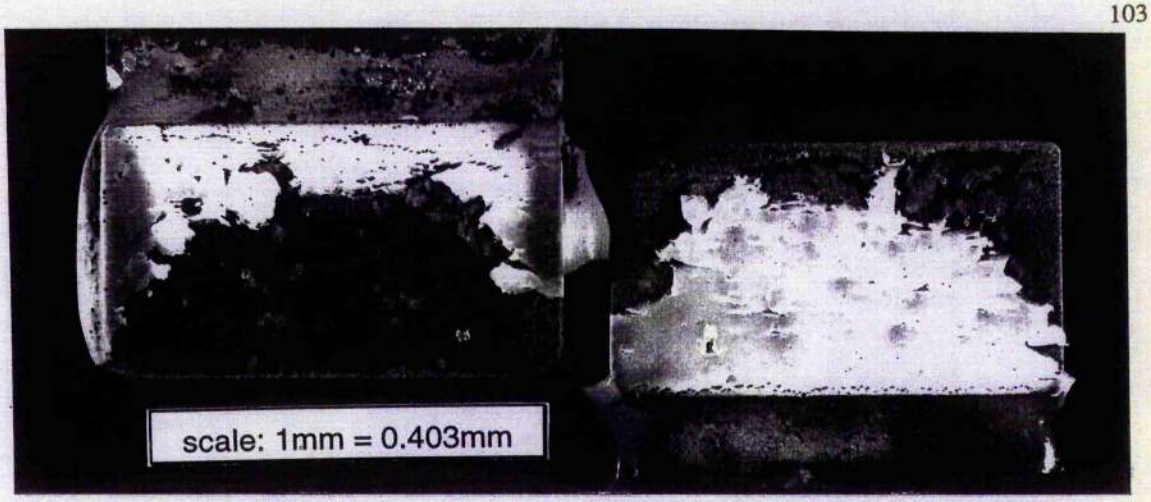

Figure 2.40 Typical failure surface of an Araldite 2007 bonded steel lap shear joint primed with a silane (A187) after accelerated aging (T=30°C,100%R.H.)

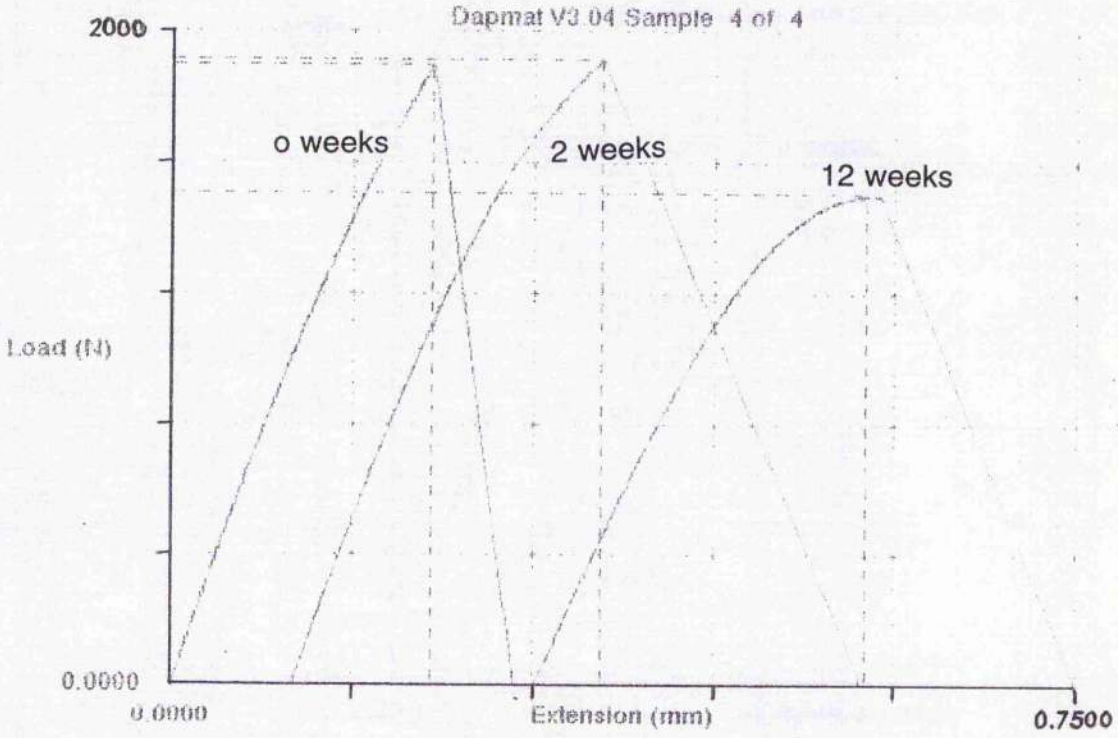

Figure 2.41 Load displacement plots obtained from bulk tensile samples (see figure 2.8) of Araldite 2007 after accelerated aging (T=30° C,100%R.H.)

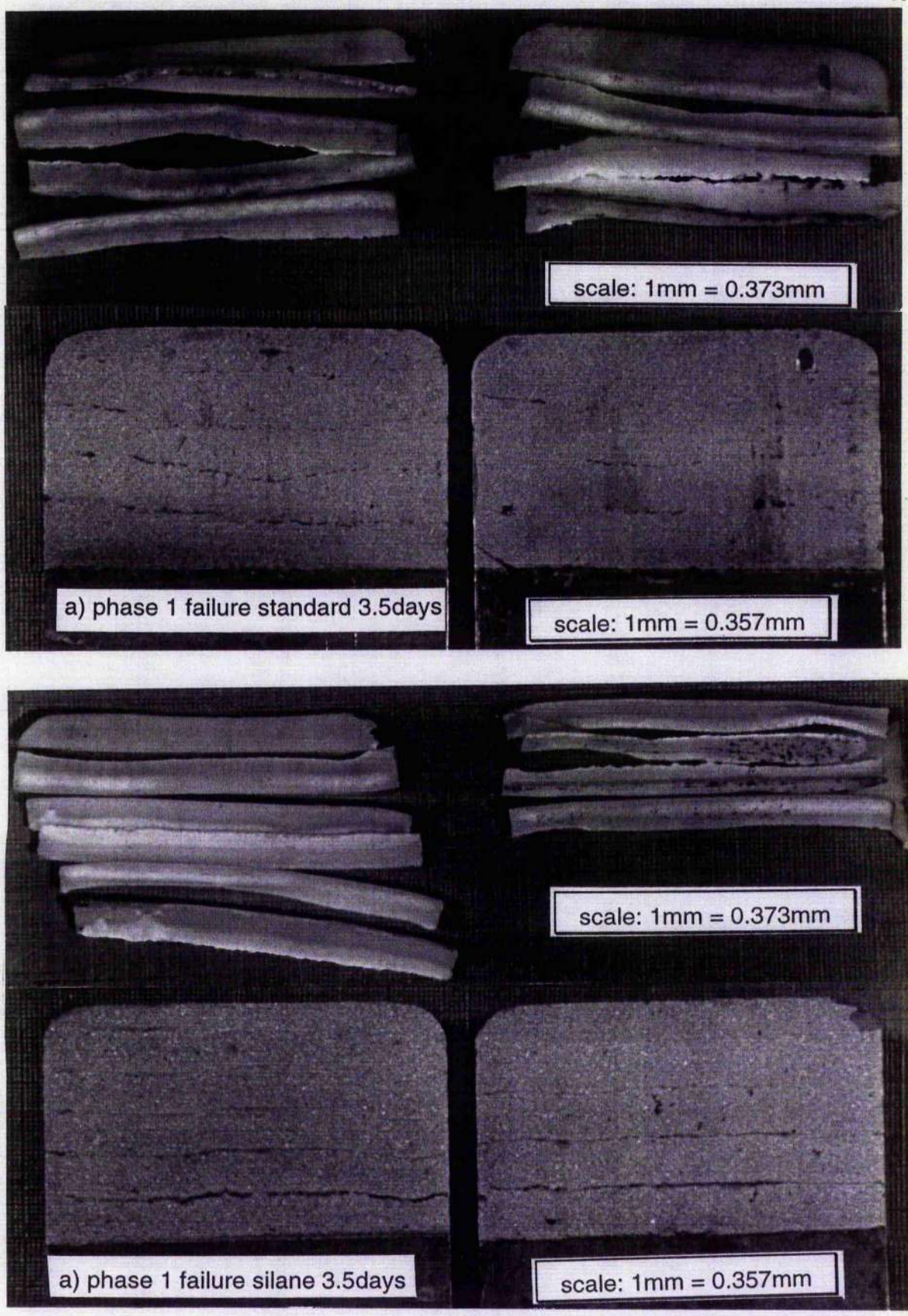

Figure 2.42 Typical failure surfaces obtained from the scrape test after accelerated aging (T=30°C,100%R.H.)

a) phase 1 failure

b)phase 2 failure

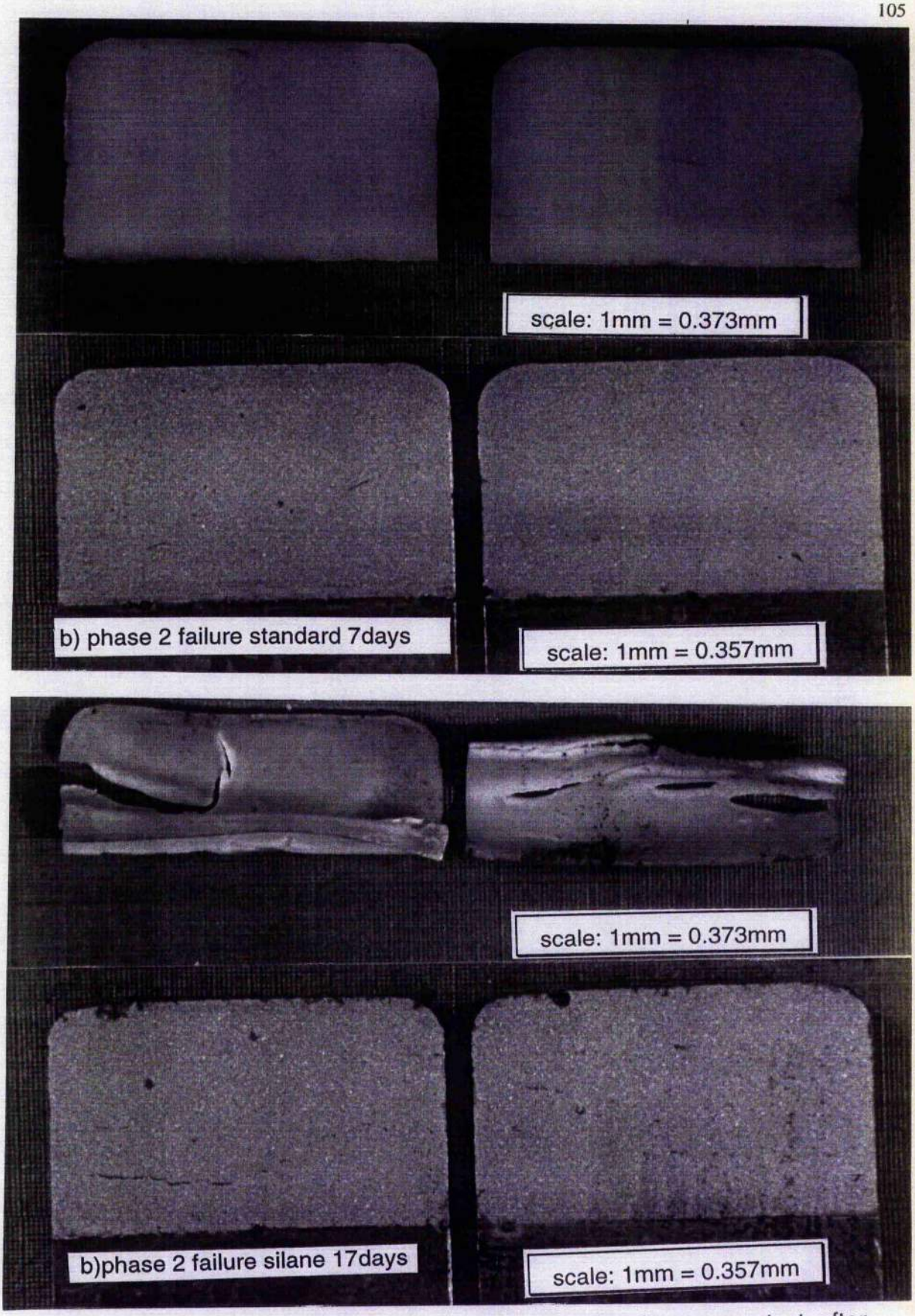

Figure 2.42 Typical failure surfaces obtained from the scrape test after accelerated aging (T=30°C,100%R.H.)

a) phase 1 failure

b)phase 2 failure

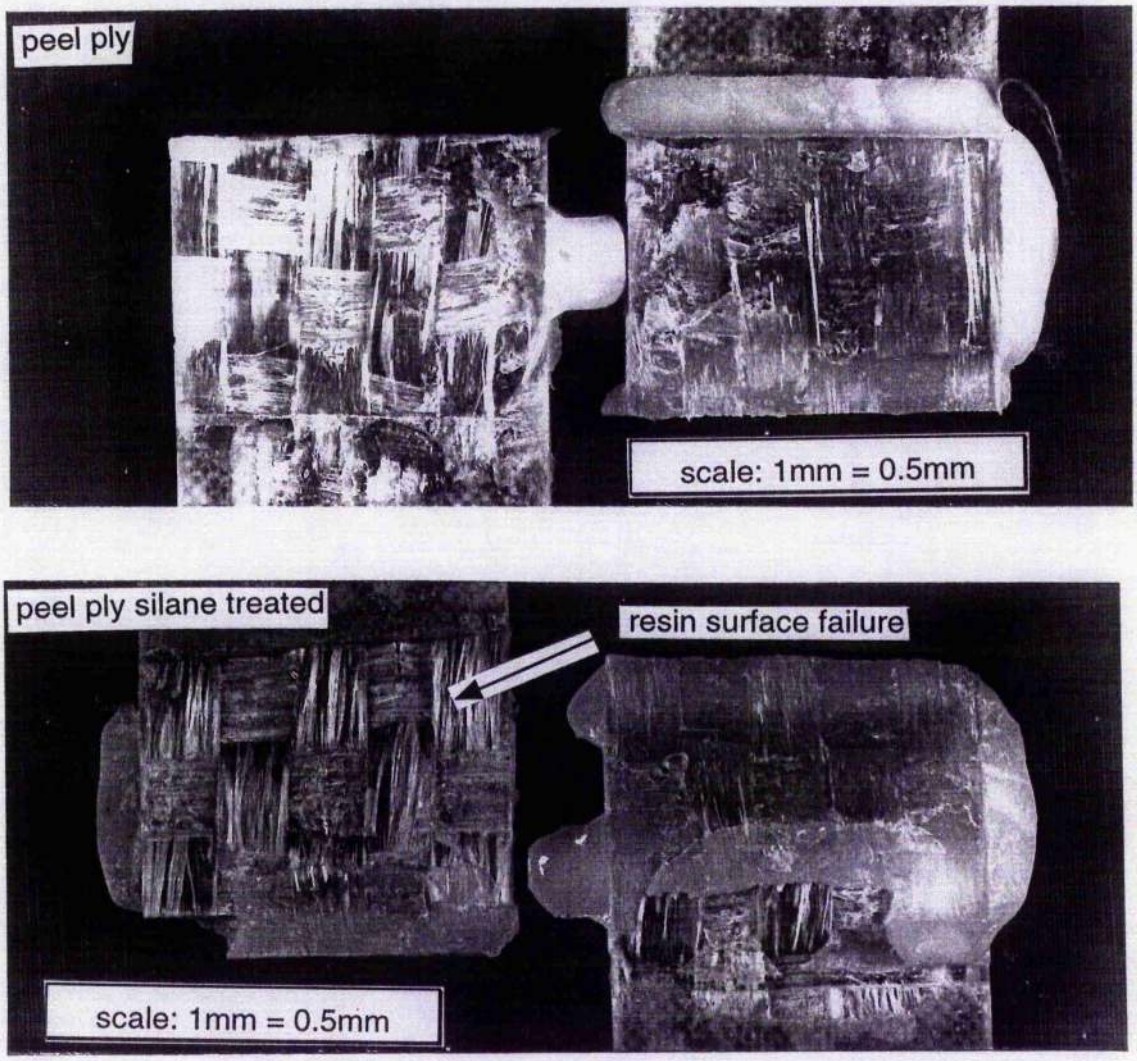

Figure 2.43 Typical failure surface of an Aradite 2005 bonded grp lap shear joint after accelerated aging (T=30°C,100%R.H.) showing a resin failure

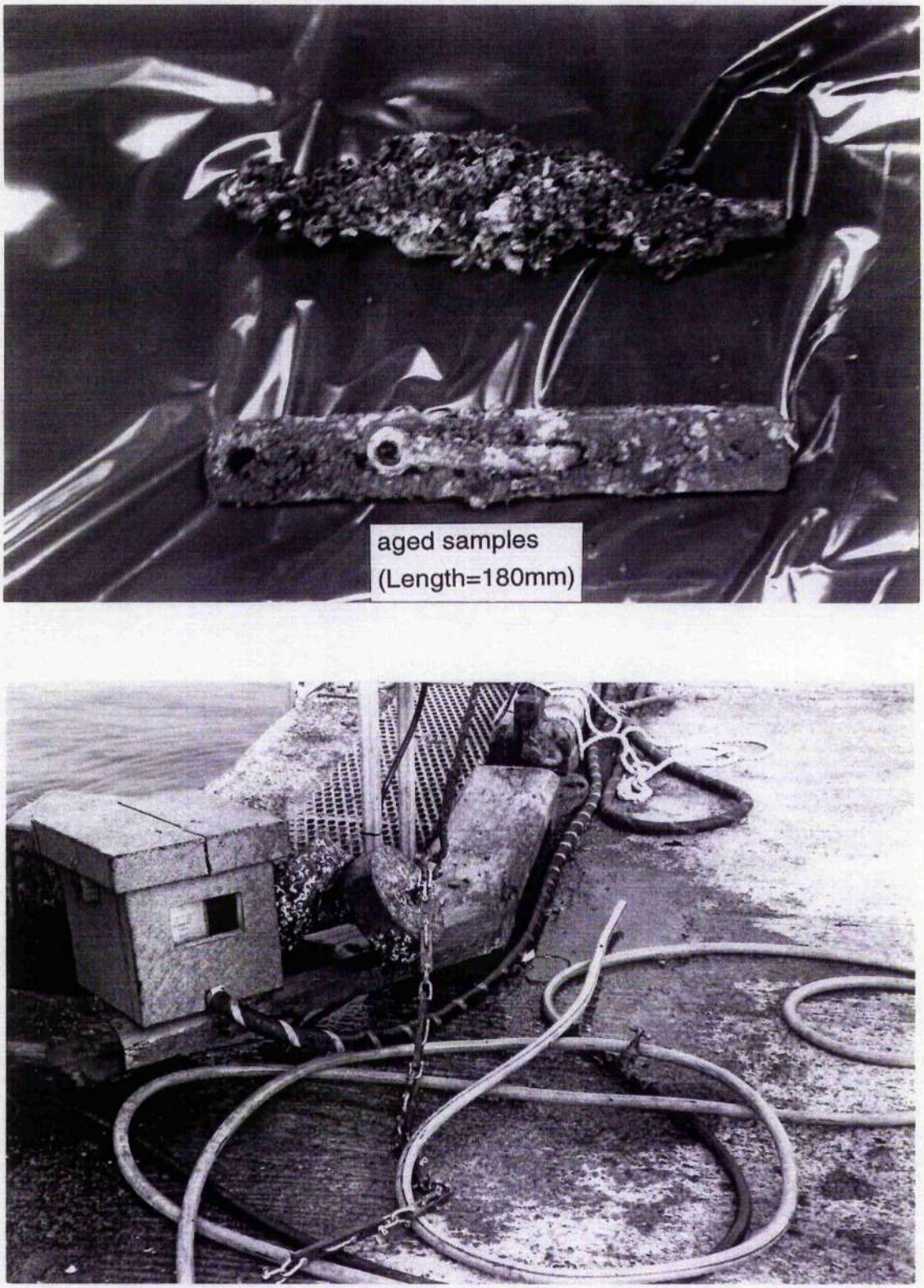

Figure 2.44 Araldite 2007 bonded steel lap shear joint exposed to natural climatic conditions (submerged under load in the Clyde Estuary) to asses aging

Bond Area mm	Failure Load kN	Average Failure Stress N/mm²
15X25	21.05 21.30 19.00 19.75 18.70 18.40	52.53
25X25	26.75 19.90 20.00 21.65 22.40 20.95	30.09
50X25	27.50 24.55 22.50 24.35 23.20	19.536
75X25	39.70 26.70	17.76
100X25	32.90 24.70 35.90 26.70	12.02

Table 2.1 Ultimate failure load for thick adherend steel lap shear joints bonded with Araldite 2007 of varying overlap lengths

Time	preload=50%failure load			
	no fillet		fillet	
Months	failure load kN		failure load kN	
1				
2	6.44	8.98	5.00	10.04
3	8.28	7.32	9.40	10.30
4	9.64	8.24	9.14	8.12
5	10.58	8.44	10.54	9.48
6	5.48	7.96	6.20	6.44
7	8.32	10.26	9.38	8.10
8	5.32	5.42	6.38	5.38
9	9.76	8.70	11.72	11.18
10	8.32	xxx	10.34	11.02

Table 2.2 Accelerated (T=30°C,100%R.H.) durability performance of Araldite 2007 bonded preloaded (50% UTS 13kN) steel cleavage specimens (XSA 25x25mm)

planned duration (wks)	failure time (wks)	failure load (N)
2	1	xxx
2	1	xxx
4	3.57	xxx
4	xxx	1549
6	4.57	xxx
6	xxx	1873
8	2.857	xxx
8	1.86	xxx
10	4.14	xxx
10	0.86	xxx
12	12.57	xxx
12	12.71	

Table 2.3 Accelerated (T=30°C,100%R.H.) durability performance of Araldite 2007 preloaded bulk adhesive tensile specimens as shown in figure 2.8 (50% UTS 1800N)

duration (weeks)	original dimensions (mm)	original mass (g)	final dimensions (mm)	final mass (g)	change in mass (g)	maximum load (N)	maximum stress (N/mm2)	mod. of elasticity (N/mm2)
2	12.4x3.00	12.20	12.38x3.00	12.37	0.17	1808.00	46.83	1573.00
2	12.45x3.00	12.24	12.43x3.00	12.40	0.16	1858.00	49.82	1433.00
4	12.45x3.00	12.25	12.35x2.98	12.54	0.29	1904.00	51.72	1457.00
4	12.45x3.00	12.24	12.38x3.00	12.53	0.29	1770.00	47.66	1504.00
6	12.50x3.06	12.21	12.38x2.99	12.58	0.37	1808.00	47.27	1429.00
6	12.45x2.88	10.98	12.24x2.63	11.36	0.38	1762.00	52.82	1360.00
8	12.45x3.00	12.20	12.17x2.94	12.68	0.48	1816.00	50.75	1353.00
8	12.47x3.00	12.20	12.25x2.95	12.64	0.44	1740.00	48.14	1377.00
10	12.40x3.00	12.19	11.85x2.85	12.70	0.51	1804.00	53.43	1273.00
10	12.40x3.00	12.12	11.55x2.84	12.69	0.57	1610.00	49.08	1133.00
12	12.50x3.00	12.08	12.00x2.89	12.64	0.56	1183.00	35.77	1109.00
12	12.50x3.00	12.15	11.60x2.85	12.72	0.57	1797.00	51.81	1264.00

Table 2.4 Accelerated (T=30°C,100%R.H.) durability performance of Araldite 2007 preloaded bulk adhesive tensile specimens (20% UTS 1800N)

MATERIAL	YOUNG'S MODULUS (N/mm^2)	POISSON'S RATIO
Mild steel	210000	0.3
Epoxy adhesive Araldite 2007[99]	5000	0.37

Table 2.5 Linear elastic material properties used in finite element stress analysis of thick adherend lap shear joints

3.0 Section B:

Application of Adhesives for Joining Grp

3.1 Introduction

The fundamental purpose of this section of this thesis is to explore the structural capability of current grp composites when joined with methods which will impart high levels of properties to the connections. When this occurs, both the base grp material and the connection may be more fully utilised structurally than is the case for many of the current applications of grp composites in offshore or marine applications. The simultaneous purpose of this section is to explore the practicality of using adhesives to join preformed grp components, so as to provide an economical and more efficient use of both materials and labour, in comparison with hand-laid composite structures.

Consequently, the purpose is to provide fundamental data and information which can be used as the basis for the next generation of composite applications offshore and in marine structures. In particular, it focuses on the issues associated with structural adhesive bonding as the prime joining process, since such joining is structurally more satisfactory for composite materials than is mechanical fastening. The underlying ethos of the work is to explore the capabilities of adhesive bonding of appropriate grp materials, not just in terms of mechanical properties, but also possible production processes for use in the industrial environment and to address issues such as the inevitable concerns (albeit of little practical significance) regarding health and safety.

The aims of the work were to apply adhesive bonding technology to the development of composite components for the topsides of offshore structures and marine applications in advanced ships. Many aspects of composite bonded joint performance will be investigated including joint design, temperature effects, creep, fatigue and adhesive processing characteristics, each of which could justify a full scale study in its own right. This is not the intention. The fundamental purpose of this study is to explore the structural capability of grp bonded joints for use in a marine environment where fatigue, temperature effects and durability will all be of importance.

3.2 Background

The penetration of grp composites into offshore applications is necessarily cautious and slow[1] and it is reasonable that preliminary applications should focus on low pressure piping[2] and non-structural fire/blast panels[3]. In the panel application, the configurations are often such that only a low strength grout or the use of base resin is required for joining, particularly if the blast resistance requirement is relatively modest.[4] Whilst the piping application can currently involve the use of an adhesive at joints, this is often supplemented by mechanical fastening[5]. There are applications where polymer composite materials can readily be shown to have significant advantages, so that there is a powerful driving force for regulatory changes to ensure the acceptance of these materials. Further research and development work is required to support proposals to change regulations concerning fire and blast[6] etc. The scientific and economic impediments are not as restrictive as the international regulations. These regulations are important to protect life at sea.

Similar patterns emerge in naval applications where larger grp vessels such as mine counter measure vessels (MCMV) largely employ hand lay-up methods, both for the hull and stiffeners, using base resin adhesion (often supported by a flexible acrylic adhesive) with glass fibre lay-up techniques for large connections, as well as the many minor attachments. In the UK, a single skin construction was favoured, using foam-cored, fibre-reinforced top hat stiffeners. A toughened resin system improves the performance of the foam cored reinforcement interfaces to a level where the bondline has higher shear properties than the substrate[7]. Although the Royal Navy led in adopting composite construction for MCMVs, which now accounts for over 23 ship years and has been followed by at least 15 other nations, consensus has not emerged on an optimum hull configuration[8]. The trends in advanced ship technology world-wide are to make greater use of prefabricated components and structural sandwich technology in ship designs which then require a larger proportion of flat panel components[9,10]. These marine structures are designed to take advantage of advanced production techniques and the final fabricated structure relies heavily on the performance of bonded connections which carry significant loads[11]. Extensions of this composite technology are also proposed for the fabrication of the superstructure of larger warships and commercial vessels[12,13].

Developments in thermosetting resins and material reinforcement technologies have resulted in a new generation of continuously laminated composite pultrusions. Pultrusion is a continuous process in which a thermosetting polymer

and reinforcement fibres are moulded into a profile by drawing the glass fibres through a resin bath and die. Due to their enhanced performance, together with flexibility and impact strength, pultrusions have been incorporated in many successful structural applications[14]. Specific variants have been developed which have a good resistance to fire together with low fume emissions which, with other attributes, make them ideal for applications in the marine environment. These other attributes include:

- resistance to degradation
- good stiffness-to-mass ratio,
- low thermal conductivity

In land based applications, the use of preformed structural grp components has proceeded much faster than in the marine/offshore area. Large scale fabrications based on pultruded sections and structural sandwich panels are becoming quite common. These range from applications such as footbridges[15] and motorway gantry signs to entire, significantly-sized buildings. In many of these structures adhesive bonding provides the only high integrity connection between major components to permit relatively high design loads and load transfer from component to component.

Pultruded grp sections are now widely available which, together with mass produced grp panels, form the building blocks for a wide range of fabricated grp applications. The use of pultrusions as a structural core is regarded as both economic and structurally efficient[16]. The potential of such structures in the marine and offshore industries is considerable; however, the overall performance depends on a bond line between the skin panels, the reliability of which, particularly under impact loading, is questionable. On the other hand, sandwich construction comprising grp skins with a low density core material offers an alternative to conventional panel construction. There are many marine structures in which the stiffness-to-mass ratio is an important design issue. One of the fields where sandwich construction is thought to be most relevant is in the fabrication of topside components for offshore drilling and production rigs. These applications include decks, bulkheads, helidecks and accommodation modules. The potential of hybrid sandwich structures for the construction of temporary safe havens consisting of fire and blast resistant panelling demands serious consideration. Sandwich construction for offshore applications needs to fulfil weight, strength and fire resistance criteria to achieve such objectives.

Traditional marine construction uses stiffened steel plate grillage to resist both global axial bending and shear loads and local out-of-plane static and dynamic

loading. These generally have lower stiffness in the transverse than longitudinal direction and uneven stress distributions in bending. Thus stress concentrations are present that may give rise to relatively poor fatigue lives under cyclic loading. Sandwich panels offer a substitute for such traditional stiffened construction. Various types of sandwich panels may be designed from simple arrangements having two thin stiff faces of dense material separated by a thick, low density, low strength continuous core material, through cores made up of symmetrical structural sections, to more complicated honeycomb or corrugated cores.

The increasing utilisation of polymer matrix composite materials (usually glass reinforced) in marine/offshore structures leads naturally to an increasing requirement for the use of structural adhesives as an alternative to mechanical fastening. The physical nature of fibre/matrix composites does induce problems that are not encountered with metals. The behaviour of a joint is dependent on the composite stiffness, strength, low inter-laminar shear and through-thickness tensile strength[17] and these in turn are influenced by the fibre type and array, fibre surface preparation[18], resin and the fibre volume fraction and void content[19]. The strength of an adhesively bonded joint is dependent on the geometry and adhesive type. A bolted joint is also dependent on the joint type, geometry, bolt size, washer size, clamping force, hole size and tolerance.

Many applications can benefit from adhesive technology as a joining process. The major benefits of adhesive bonding are the generally-low stress levels associated with large areas of contact, the compatibility of the adhesive with the adherends in terms of similar properties and ease of use. The major disadvantages of mechanical fastening for composite materials are those associated with crushing of the composite under high point loading, local transmission of heat in a fire situation, reliability of a system involving a large number of components and the requirement to pre-drill holes for fasteners, thus some of the material of the component part has to be removed; this causes higher stresses and areas of concentration within the vicinity of the bolt, corrosion of the (normally) metallic fasteners and the inspection/quality assurance difficulties. A mechanical connection does tend to be bulky and may incur a weight penalty. The advantages of the mechanical joints over the adhesively bonded joints include the repeated assembly, absence of environmental effects particular to polymers (such as inhomogeneous swelling in aqueous environments) ease of inspection and no specific surface preparation of the components to be joined. Adhesive bonding also offers resistance to shock and thermal cycling plus increased fatigue performance and inhibited heat transfer.

Although it is well established that bonded joints can show higher efficiencies than mechanical joints[20], mechanical joints find application where bonding is impractical, uneconomical or where parts have to be removed or replaced. In addition a mechanical joint may be generally preferred for on-site assembly.

3.2.1 Grp Sandwich Construction

If it is necessary to increase the stiffness of the overall cross section of the composite, a sandwich construction may be used, consisting of composite faces bonded to low density core or discrete elements such as pultruded sections. The core need not be plastic itself, steel structural sections have been successfully used[21]. The face plate (skin) would generally support the bending moments and axial forces within the composites and the core would take the majority of the shear. Thus the integrity of the connection between the core and the face in the sandwich construction is of vital importance if the potential benefits of the sandwich are to be utilised. If the adhesion between the core and the face are poor then the two faces will act as two separate beams. Generally adhesive bonding is the only practical solution for fabricating a grp sandwich unless the foam core has good adhesion properties itself. Plastic sandwich construction using a foam core is frequently used in yacht production. Articulated refrigeration trailers commonly utilise bonded sandwich construction for the lightweight, structural and thermal properties.[22]

3.2.2 Adhesive Selection

In choosing to use structural adhesive bonding for sandwich construction the following factors must be taken into account:

1. the nature of the adherends.
2. detailed joint design, including fit-up.
3. mechanical properties required.
4. processing/fabrication requirements (surface preparation, dispensing, clamping and curing).
5. loading and environmental conditions.

After consideration of these factors it is then possible to select a suitable structural adhesive.

There are four main types of adhesives suitable for bonding composite materials. These are epoxies (with or without additional toughening mechanisms), acrylics (which may be toughened), polyurethanes and phenolics. In addition there is a

number of hybrid products available eg. epoxy/acrylic mixture. A brief summary of each type of adhesive is given below:

Epoxies

This adhesive system can involve one of a number of reactive hardeners as either a single part hot curing adhesive paste or a two-part cold or warm-cure paste. In the two part form the resin and hardener are mixed to activate polymerisation. The single part hot cure generally requires a minimum of 100°C temperature rise to initiate a reaction. Thus the single part adhesives are not particularly appropriate for bonding of composite materials. Epoxy adhesives may contain fillers of various types of particulate materials such as inorganics, metals and elastomers. These fillers are designed to impart strength or increase fire resistance or toughness. In general the epoxy type adhesives produce the strongest bonds and exhibit good durability. The two-part epoxy adhesives are good candidates for bonding of composite materials.

Acrylics

The major structural application of acrylic adhesives is in the form of a toughened two component product for use in relatively thin films. The two parts, resin and initiator, are applied separately to the two adherend surfaces, contact then initiates polymerisation which is often completed within minutes, although full strength can be longer. These adhesives have good gap filling properties and the incorporation of dispersed elastomeric fillers imparts good toughness such that these acrylics compare well with toughened epoxies, although generally of lower strength.

There are alternate forms of acrylic adhesives with special characteristics such as fast curing cyanoacrylates and anaerobic locking compounds. Neither of these compounds impart high enough strength to be considered as structural adhesives.

Polyurethanes

These are generally low strength, low modulus adhesives with short curing times at ambient temperatures and good gap filling properties. Bonded joints are however susceptible to environmental attack by water, particularly when at least one adherend is metallic[23]. There are niche applications for these adhesives using large areas of low strength, low modulus materials but are not suitable for structural applications alone.

Phenolics

This group of adhesives provides good resistance to environmental attack but in general are difficult to use and require complex processing. They are more suited to strictly controlled environments than is normal in a marine/offshore fabrication environment. Thus, their usefulness is limited for marine applications.

Where structural joints are required then possibly only the untoughened epoxy and acrylic formulations may offer a solution. However, untoughened adhesives may also be brittle and to overcome this a modified toughened formulation may be required. (A toughened adhesive is one which incorporates a microscopic rubbery or rigid phase dispersed throughout the resin matrix providing internal crack arresters which will inhibit crack growth thus reducing brittleness and increasing impact resistance). Currently the epoxy and the acrylic based toughened adhesives are used for general grp application and have proven over the years to be very versatile.

3.2.3 Health and Safety

Generally all the adhesives in this study are safe to handle provided the health and safety guidelines recommended by the manufacturers are followed. The main hazard with epoxy resins is skin irritation as with the majority of other high performance types of adhesives. The degree of resistance to the effect of adhesive compositions on skin varies amongst the population. Initially most people are resistant to this effect on skin and irritation may only occur after prolonged contact. Some individuals are, however, particularly sensitive to adhesives and skin irritation may occur at early stages of handling. Once sensitisation has occurred it is necessary to remove the operative from the area for a prolonged period. Some specialist compositions may have a more serious, corrosive effect on the skin, causing burns. The container labels must display the appropriate hazard warning symbols and risk and safety phrases. In addition to skin irritation and sensitisation, adhesive formulations generally can act as eye irritants and some formulations have ingredients which cause headaches and nausea when used in enclosed areas. Some also have a strong and unpleasant odour.

Generally, fully cured epoxy resin based systems are non-toxic and do not irritate the skin. However, post cure treatments such as grinding can cause hazards from the ensuing dust and fumes. If these or similar processes are used, adequate extraction and ventilation systems should be provided. If precautions are followed, as specified in the Health and Safety data sheets from the manufacturers, the adhesives will generally be safe to use. It is important that all personnel using

adhesives should read and follow the instructions provided, since simple prevention is better than cure. To prevent the product from coming into contact with the skin the operator should wear disposable plastic gloves and avoid contaminating door handles and work surfaces etc. by removing the gloves before touching these areas. The plastic gloves should be discarded at appropriate intervals as contamination may build up. To guard against accidental contact with the skin when removing the gloves a suitable barrier cream should be applied to the hands prior to commencing each work session. This should also be applied to the wrist area where contaminated gloves from protective overalls may allow the product to contact the skin. At the end of each work session hands should be washed in hot soapy water. If there is any danger of the product coming onto contact with the eyes or face such as splashing then a protective mask should be worn. There should also be adequate ventilation at all times and a local exhaust in appropriate cases might be necessary. Extra care should also be taken in warm weather or when hot cure operations are in use.

3.2.4 Bonded Joint Design

Composites are not homogeneous through their thickness as many polymer thermosetting composites have a gel coat; resin-rich surface layers which are brittle and when overloaded are liable to display brittle fracture. To some degree this can be compensated by an appropriate choice of adhesive[24]. Thus the general review of bonded joint stress analysis in the previous section is not completely applicable. Special consideration must be given to the joint design due to the nature of the adherends. In joining composite structures, issues which require to be addressed are:

(i) the micro-mechanics level, at the fibre/matrix interface
(ii) the macro-mechanics level, at the interfaces between layers, as characterised by the free edge problem
(iii) the structural level, at the interfaces between two or more separate components as in the conventional joint.

Grp structures are particularly sensitive to failure at bonded connections in which the weakness arises from:

- the absence of load bearing fibres across the bond interface especially if the adhesive material used is the base resin
- stress concentrations associated with the joint geometry[25].

When designing joints special care must be taken to ensure efficient load transfer through the joint by reducing stress concentrations as much as possible. Bonded joints perform best in compression and then shear and are poorest in peel and cleavage. Peel loads can be encountered when using a stiff toughened adhesive which will, although there maybe a large total bond area, only load a very small proportion of the joint so that local stresses are very high and fracture occurs at low loads. A toughened ductile adhesive yields extensively prior to failure, thus allowing the load to be carried extensively over a large area. Joints should be designed to be in compression and/or shear. The essence of the effective use of a joint has been described as design for bonding and not simply to substitute it for other means of jointing. Care should be taken that stress concentrations are minimised and that loads be carried over as large an area as possible.

There are four main modes by which adhesively bonded composite joints can fail. These are:

(a) a failure of the adherend outwith the bonded section. This would result in the strongest joint, in that the load level is 100% of the strength of the adherend
(b) a failure of the adhesive. This is an adhesive failure of the bond between the adherend and the adhesive in shear.
(c) a mode associated with the failure of the adhesive under peel or cleavage. This is due to a tensile stress which develops its maximum value near the free edge of the joint. This stress is developed in association with the shear stress and can be particularly severe in thick lap joints.
(d) a failure by delamination of the fibrous composite adherends adjacent to the bonded section. The low inter-laminar tensile strength of composite laminates limits the practical thickness of the adherends. The inner laminate of the adherend can split locally due to peel stresses, thus destroying the shear transfer capacity between the inner and outer plies. This overloads the outer filaments which break in tension and failure progresses through the adherend thickness.

Butt connections are commonly required between prefabricated hull/panel units and also may be required for repair purposes. Panel to panel connections of grp sandwich or sheet panels is an important consideration. The two principal loading mechanisms for such connections are lateral bending and tension. Both of these are severe types of loading for adhesive connections. Bending loads will produce both tensile and cleavage stresses at the joint as well as shear stresses. Often, the base resin and/or bolts are used for joining using simple lap joints. Where the base resin is used alone, a stepped joint design is required and is produced by staggering single-ply edges during lay-up. A scarf design of this type can produce an efficiency of 70% and a stepped joint design 90% efficiency[26]. The most

effective connection appears to be a step joint[26] which are produced by staggering ply edges during layup, or in the case of repairs, by peeling back plies from the edge of the laminate. The best results being obtained where each step is of a single ply thickness. This method of joining can obtain 90% joint efficiency (UTS joint / UTS parent composite material). This method of joining is time consuming and therefore costly in man-hours. In this research various joint configuration for butt joints have been considered. The object of this section of work was to investigate the various methods of joining two grp panels, either sandwich or sheet, by adhesive bonding to give a simple, efficient and effective practical connection for a marine application and of high structural efficiency. Many joint configurations are possible but those which require minimum machining and are straightforward to fabricate are preferable. Several common joint geometries for composite panels are shown in figure 3.1. The problem of predicting the strength of adhesively bonded joints which maybe used in the butt joining of materials has been the subject of research for more than two decades[27]. The simplest joints are of the single lap or single strap types. Very high complex bending stresses are encountered in these simple joints and the ultimate strength is severely reduced. Double strap joints do not exhibit the same degree of bending stress as the single lap joints but may not be acceptable for reasons of external appearance. It has long been recognised that various failure processes, such as tensile failure of the adherends, cleavage (peel) or shear failure of the adhesive and delamination of the composite adherends compete when strap joints are loaded in tension[28]. These failure processes and the loading carrying capacity of strap joints have also been compared[29] with single lap, stepped lap and scarf joints each with and without additional external straps or doublers. Higher strengths are achievable using multiple step lap joint designs and scarf joints with very low scarf angles but because of practical machining limitations these joints are not considered in this study. The precision required for machining laminate edges is sufficiently significant to render such designs commercially unviable for large marine applications. In addition the extensive machining required is likely to impose environmental constraints. The overall aim has been to maximise the efficiency of the joint in terms of the basic tensile strength of the adherend. The major design requirement in improving joint capacity is to minimise peel stresses in thin adherends and the parallel cleavage stresses in the thick adherend situation, consequently the relative stiffness of any doubler or strap plays an important role in defining overall joint strength. Whilst design optimisation is able to overcome most problems associated with the joining of thin adherends[30] problems of low joint strength are more acute for thick, heavily loaded joints. However, the principle of attempting to balance adherend stiffness still applies[30]. Many forms of lap joints contain adherends which are not parallel sided, but have a variety of forms in an attempt to reduce the high

stress/strain concentrations which occur at the ends of the overlaps. Practical details to reduce the maximum stress and strain in the adhesive are[31]:

(a) The cover plate adherend is tapered.
(b) The adhesive layer is thickened locally.
(c) A spew fillet is incorporated at the end of the adherend.

Adams and Wake[32] showed that by reverse tapering the steel adherend of a steel composite simple lap joint and producing a spew fillet of approximately 30° an increase in joint strength of more than three fold was achieved. In this case the through thickness stresses were sufficiently reduced to prevent failure initiating within the composite and failure occurred by cracking through the adhesive layer. Thamm[33] has shown that the adherends have to tapered to a fine edge if significant benefit is to be achieved and this is usually impracticable. Where peel is encountered with lap joints the best positive restraint of the joint end is by riveting, bolting or spot welding.

Many diverse joint geometries and analysis techniques have been published both for joining of metals and composites of varying resin fibre mixtures. The simple lap shear joint has been studied extensively and details of the more established theories are given in section 2.2.1. The study on butt connections in this section is not a fully inclusive study but is intended to be a practical experimental study of simple and economic techniques for joining one specific type of thick polymer composite material with intended use for panel/panel butt connections. It utilises some of the techniques documented in the literature and produces a practical solution of joining panels for the intended application.

3.2.5 Thermal Performance

In 1988, the destruction of the Piper Alpha platform resulted in the loss of 167 lives. The events that happened were described in the report made by Hon. Lord Cullen following the Piper Alpha Public Enquiry. This report made recommendations as to improved safety on offshore installations. Composites offer the offshore industry significant savings in both platform topside weights as well as installation and maintenance costs. Although organic matrix resins are intrinsically combustible, it became apparent that thick polymer based composites possessed desirable properties in fire. It was observed that the low conductivity of these materials (about 200 times less than steel) was advantageous in the prevention of fire spreading and thick section composites with high woven glass reinforcements show very good integrity in fire. Furthermore, one of the key features that made composites attractive was the elastic blast response of the

composite structures. The elastic response meant that the chances of impairing the fire resistance of a structure, due to plastic deformation of the structure under blast loading was removed. The problems posed by fire / blast barriers are the thermal resistance of both the grp layers and the adhesive if such structures are to meet the demanding fire resistant test specifications relating to hydrocarbon fires up to 1050°C[34]. As with bonded joints of metal adherends, the adhesives used to bond composites are polymeric materials and as such are subject to time dependent behaviour which can be greatly accelerated by high operating temperatures, increased stresses or the absorption of plasticisers such as moisture. Reduced crosslinking of a polymer also results in excessive time dependence. Bonded composite structures are a dual viscoelastic problem due to the matrix of most composites being polymeric and are subject to viscoelastic behaviour. Creep of these materials can be substantial, particularly when subject to high loads, elevated temperatures or moisture. The time/temperature superposition principle has been successfully applied to permit a prediction of a response 'master' curve which may be valid over many decades of time[35].

3.2.6 Fatigue

Fatigue can be described as a process which causes damage in materials and structures under fluctuating loads, of magnitude much less than the static failure load. The accumulated damage may result in a gradual and significant decrease of mechanical properties such as strength, stiffness and finally in complete failure. In many cases crack growth as a result of fatigue loading is the dominant failure mechanism.

All marine structures are subjected to varying loads under normal working conditions. Cyclic loads tending to cause fatigue failure are as a result of wave action or of machinery or propeller induced vibrations. Underwater vehicles may experience a sufficient number of diving and resurfacing cycles to cause low cycle compressive fatigue. Designing against fatigue failure and prediction of fatigue life is difficult and complex due to many influencing parameters. The fatigue behaviour will be determined by microstructure and material properties, dimensions and geometries, loading conditions and history, environment and by the mutual influence of these parameters. To determine the influence of these parameters laboratory tests on small standard specimens and larger scale structural components are required.

The mechanism of fatigue failure in composite materials is quite different from the mechanisms in steel and depends on the properties of the matrix and reinforcement as well as on the interaction between the two. In reinforced plastics

crack propagation processes are complex due to their anisotropic and inhomogeneous nature. A noticeable difference from the fatigue behaviour of metals is the gradual and general degradation of the composite material which starts almost immediately within the first few cycles contrary to the predominantly single cracks in metals. In woven roving laminated composites, fatigue failure generally starts with fibre debonding followed by resin cracking which appears as a characteristic whitening of the laminate[36]. Cracks then tend to propagate parallel to the fibres in a cumulative manner until the laminate is weakened to the point that fracture occurs involving fibre breakage[37]. The debonding and resin cracking may itself result in an increased sensitivity to the environment.

Composite fatigue data usually refer to the laminate. However in structures the risk of fatigue failure is commonly at the locations of high stress concentrations or hot spots associated with notches connections etc. In bonded structural connections the weakness is caused by the absence of load bearing fibres across the interface and by low interlaminar tensile and shear properties in combination with joint geometry. In many cases the occurrence of loads perpendicular to the plane of the laminar aggravates the problem.

3.2.7 Failure Theories for Finite Element Analysis

Numerous failure theories have been proposed for fibre reinforced composites but very few apply to joints of inhomogeneous materials and even less to composite joints. For homogeneous, isotropic, materials such as metals, which are often considered to have failed at the onset of plastic deformation, two criteria which agree most closely with experimental results are the maximum shear stress theory (Tresca Yield criterion) and the maximum shear strain energy theory (von Mises criterion). For fracture of brittle materials the most popular criteria are the maximum normal stress theory where the maximum normal stress reaches the tensile fracture stress of the material. For fibre reinforced composites, many fracture failure criteria have been devised. The most popular of these are based on a maximum stress or strain criteria or of the interactive type. For composite materials on a simple level the maximum stress and strains are compared with allowable values. But there is assumed to be no interaction between various stress strain components. For composites, the Tsai-Hill[38] failure criterion allows for component interaction as does the Tsai-Wu method[39]. These failure criteria are based on the assumption that composite lamina may be treated as being anisotropic yet homogeneous. The problem with these criteria for laminated composites is that they are based on a single ply basis and the assumption that the behaviour of a single unidirectional ply within the laminate is the same as that of an isolated ply. Clearly, in a composite, this assumption breaks down as

adjacent plies provide constraints and thus modify the behaviour. These theories do not account for interlaminar shear strengths or tensile strengths, and in a bonded joint, these may be areas that contribute to failure. One of the most frequently encountered problems in composite laminates is interface cracking known as delamination. Delamination in layered composites may occur due to a variety of reasons, such as manufacturing defects, impacts or high stress concentrations at geometric or material discontinuities. Through-thickness failure is often a limiting factor for composite structures and interlaminar stresses are one of the most important controlling parameters regardless of the nature of the loading. However, due to the anisotropy and inhomogenity of composite materials, a universally accepted failure theory has not been established. Chandler et al[40] proposed that a simple failure criterion could be devised on the basis that fibre failure occurs when the strain or stress in the fibre reaches a critical value. Fracture in the matrix can be considered in terms of suitable isotropic failure criterion. Matrix tensile failure normal to the fibre axis is liable to be governed by the stress concentrating effects of the fibre and should be considered. This failure criterion appears the most appropriate for this study since the composite butt joints are layers of woven rovings and resin.

3.3 Experimental Programme

3.3.1 Testpiece Preparation

Owing to the limited volume of available data on adhesively bonded composite joints and the associated adhesive performance, there is a strong need to use mechanical testing. As no standard tests relate directly to the specific applications, it has been important to develop suitable experimental tests. The selection of an adhesive should be based on thorough consideration of material compatibility, stress regime, joint geometry and fabrication methods. A series of small scale tests, see figure 2.6, has therefore been used to review a number of suitable adhesives for use in bonding grp. The adherend specimens were produced from marine grade grp panels supplied by Vosper Thornycroft U.K. Ltd.. These grp panels were formed from isothalic polyester resin containing 55% woven roving E glass and manufactured to MoD standards. The adherend materials were machined to size and the initial bonding process involved the stages as described in section 2.3.1.

It should be noted that, with some formulations of acrylics, the two components are applied to separate adherends and then clamped together thus removing the need for manual mixing. The bondline thickness varies across the rear face of hand laid grp due to the inherent roughness.

3.3.2 Adhesive Selection

Six candidate, cold cure, structural adhesives were reviewed in the preliminary study. These were

(a) Redux 410, a two part modified epoxy.
(b) E32, a two part toughened epoxy.
(c) ITW, a toughened acrylic specified for marine type applications.
(d) F246, a toughened fast curing acrylic.
(e) XB5093, a polyurethane.
(f) VOX, a modified acrylic which has properties common to both epoxies and acrylics.

Although hot-cure adhesives generally give higher mechanical performance characteristics compared to cold cure adhesives, cold or warm cure adhesives must be used on grp adherends as the adherend materials have a low glass transition temperature (approximately 70°C) and will degrade at hot cure temperatures (which may vary between 120°C and 200°C for a typical hot cure adhesive). Each adhesive was tested for resistance to tensile, shear, cleavage

and impact loading on grp adherends, as shown in section 2.3.1. All of the spew fillets were removed. Static load tests were performed on an Instron tensile test machine at a test speed of 0.5mm/min while impact tests used an Izod impact testing machine adapted to measure shear impact resistance test. Load to failure and energy absorbed were recorded. The results of which are shown in table 3.1.

3.3.3 Selected Adhesive Performance on Pultruded Material

To assess the bond strength of a Redux 410 grp/pultruded joint, a further series of small scale tests was formulated to determine tensile, shear, cleavage and impact performance based on the test specimens shown in section 2.3.1, figure 2.6. All the spew fillets were removed. Static load tests were performed on an Instron tensile test machine at a test speed of 0.5mm/min while impact tests used an Izod impact testing machine adapted to measure shear impact resistance. Load to failure and energy absorbed were recorded. The results of the mechanical tests are shown in table 3.2.

3.3.4 Revised Adhesive Performance

During the course of this work, Redux 420 superseded Redux 410 which contained strontium chromate to act as a corrosion inhibitor and may also be a possible carcinogen. Redux 420 does not contain this chemical and is reported to have equivalent mechanical properties. Mechanical testing of Redux 420 was therefore performed using similar grp test specimens to those utilised in the 'selection' section, 3.3.2, with the spew fillet removed. The results of these tests are given in table 3.3.

3.3.5 Pultrusion Surface Treatment

As the research progressed, it became more apparent that, provided a good quality structural adhesive is used, the performance of a bonded grp/pultrusion joint depended largely upon the inter-laminar strength of the pultruded material and not upon the mechanical performance of the adhesive layer. Further tests were undertaken to establish if some form of mechanical surface roughening of the pultrusion material would improve the adhesive joint performance. Ten pultruded lap shear specimens, see figure 2.6, bonded with Redux 420 were prepared using five different roughening treatments as shown in table 3.4. The results of these treatments are also shown in table 3.4.

3.3.6 Thermal Performance

Thermal performance data relating to specific adhesives is of two types, one relating to the failure strength of a joint as a function of temperature and the other to the ability to sustain load as a function of time (creep) at a constant temperature. The former requires the joint to be held prior to loading at a temperature only for a period sufficient for temperature equalisation. Most existing data refers to metal joints and records the effect on both modulus and strength of the adhesive in modifying the strength of the joint. Only at elevated temperatures, near to the limit of use of organic adhesives, do changes in the modulus of the adherend affect joint strength. With grp adherends, however, changes in stiffness of adherends below these temperatures make the joint more sensitive to temperature. In this study therefore the effects of temperature on the failure strength of grp adherends and the adhesives were measured separately.

3.3.6.1 Adhesive Joint High Temperature Performance

In the first stage, steel lap shear specimens, see figure 2.6, were bonded using the fabrication procedure described in section 2.3.1 and with the spew fillet removed. Three types of adhesive were chosen for this part of the study:

(i) The selected adhesive (Redux 410).

(ii) An inorganic ceramic paste adhesive (Autostic) specifically made for high temperature applications. This adhesive may only have a role at high temperatures due to its very low strength at ambient temperatures when compared to organic adhesives.

(iii) A reference hot-cured epoxy (Araldite 2007) with good thermal characteristics (Tg ~ 120 °C).

The purpose of this study was to review the thermal performance of the selected adhesive in comparison with two others known to have good thermal performance. The tests were performed on a Lloyd 10000L tensile testing machine at a constant crosshead speed of 2mm/min. This machine incorporated a thermal cabinet capable of rapidly varying the temperature of the specimens under test from -70°C to 250°C, using liquid nitrogen or a fan assisted oven. Test temperatures between 60°C and 140°C were chosen so as to include the glass transition temperatures of the epoxy adhesives while being also in the range of the rear face temperature required to achieve hydrocarbon fire ratings[34]. The failure loads for the three adhesives are shown in figure 3.2.

3.3.6.2 Grp Thermal Performance

In the second stage, tests were carried out on grp tensile test specimens as defined in figure 2.8. These specimens were machined to size from larger grp panels with the grp fibre axis orientated parallel and perpendicular to the axis of the specimens. The results of elevated temperature tests are shown in figure 3.3 when tested at a loading rate of 2mm/min.

3.3.6.3 Adhesive Joint Low Temperature Performance

An important factor which must also be considered for adhesive performance in a marine environment is the subzero temperature performance. Third stage tests were therefore conducted with the three adhesives using steel adherends at temperatures down to -30°C. Similar adhesives and fabricating techniques were used as described in section 3.3.6.1. The tests were performed on a Lloyd 10000L materials testing machine at 2mm/min. Results of these experiments are shown in figure 3.4.

3.3.6.4 Thermal Creep Performance

To determine the thermal creep performance of 'selected' adhesively bonded specimens, experiments were conducted to investigate the thermal creep performance of grp/steel and grp/grp bonded shear specimens, see figure 2.6. The samples were bonded with Redux 410 initially and, as the tests proceeded, equivalent experiments were performed using Redux 420 (the updated version of Redux 410). The specimens were designed to ensure that the bondline was central to the test piece and thus were predominantly loaded in shear (figure 2.6). To fabricate the grp/grp connections the central bond was made with Redux 420/410 with no spew fillet and the connection between the steel and grp faces bonded with Araldite 2004. 2004 is a two part epoxy adhesive with good thermal stability and strength[41]. The bonding procedures in section 2.3.1 were followed. The specimens were loaded in tensile creep testing machines under temperature control, with two LVDTs per specimen to monitor the creep rate. Initial experiments involved applying the load to the specimens when it was thought that the whole specimen had stabilised at the required temperature. However, it was found that if the length of this stabilisation time was increased the specimen could sustain a higher initial applied load. Thus subsequent experiments incorporated a 24 hour 'soaking' time at the required temperature before load application. Three particular types of experiment were performed:

1) grp/steel connection at 100°C (Redux 410, Redux 420)

2) grp/steel connection at 150°C (Redux 420)

3) grp/grp connection at 100°C (Redux 420)

The results of these experiments are shown in figure 3.5 which gives the time to failure of specimens at specific constant loads and temperatures.

3.3.6.5 Post Cure Effect

As mentioned above, it was noted that the creep specimens which were allowed to equalise their temperature over a longer time tended to be able to maintain a higher initial load. One explanation of this is that post-curing of the adhesive is occurring. The manufacturer states that the adhesive Redux 420 can be cured at 120°C for 1 hour. However, the adhesive was not cured according to this schedule since the grp adherends had a glass transition temperature of only 70° C. To investigate the apparent post-curing effect, similar creep (see figure 2.6) specimens using both grp and steel adherends were fabricated and tested for their static strength after exposure for times of up to six hours, at a constant temperature of either 100°C or 150°C. A Lloyd tensile testing machine was used with a thermal cabinet to maintain the constant temperature during testing at a constant test speed of 0.5mm/min. The results from these experiments are shown in figure 3.6.

3.3.7 Adhesive Handling Characteristics

3.3.7.1 Manual Mixing

To quantify the effect that manual mixing has on the static strength, four independent batches of three steel lap shear specimens, see figure 2.6, were bonded with Redux 410, with spew fillets removed, as described in section 2.3.1 and tested to failure. The testing was performed on a Instron tensile testing machine at a constant crosshead speed of 0.5mm/min. An indication of the consistency attainable through manual mixing is given by the uniformity of the ultimate static strength. The results shown in figure 3.7

3.3.7.2 Pot Life

Experiments were performed to investigate the effect of post pot life application of the adhesive to the adherends. For ease of manufacture, steel lap shear specimens, see figure 2.6, were bonded with Redux 410 following the procedures

listed in section 2.3.1. The specimens were then tested on an Instron tensile testing machine at a constant crosshead speed of 0.5mm/min The elapsed time was up to five hours before application of the adhesive to the substrate. The results of the loss in static strength are shown in table 3.5.

3.3.7.3 Cure Schedule

The 'selected' adhesive, Redux 410, requires seven days to attain a full cure at ambient temperature. Experiments were performed to examine the static strength prior to full cure. Steel lap shear specimens were fabricated according to methods listed in section 2.3.1 and tested over a seven day period, at daily intervals, on an Instron tensile testing machine at a crosshead sped of 0.5mm/min. The results of these experiments are shown in figure 3.8.

3.3.8. Bonded Butt Joint Performance

Since the initial aim of this section of work was to maximise the strength of a grp butt joint the performance of each joint is quoted as a percentage of the parent material performance. A series of grp butt joint configurations as described in table 3.6 were tested in tension and three point bending, each configuration forming a progressive development. Standard fabrication techniques were employed which are described in section 2.3.1. All the tests were performed on an Instron tensile testing machine. The results are shown in table 3.6. The most encouraging result was obtained using a hybrid joint configuration of tapered steel straps and grp as shown in figure 3.9.

3.3.9 Fatigue Performance

Two test programmes were formulated to investigate fatigue performance of bonded grp/ pultruded constructions: see figure 3.10

(i) A square pultruded stiffener bonded onto a grp face plate with the selected candidate adhesive, fatigue testing in transverse, positive, three point bending (unstressed attachment).

(ii) A square pultruded stiffener bonded to a grp face plate using the selected adhesive, testing by stressing the stiffener in three point bending (stressed attachment).

The specimens were fabricated using Redux 410 adhesive following standard preparation procedures detailed in section 2.3.1 with the spew fillet left intact. The

fatigue testing was performed on Dartec 100kN servo hydraulic frames in load control at a frequency of 2Hz. The number of cycles to failure were recorded for each fatigue loading regime and the results are shown in figure 3.11.

3.3.10 Bulk Adhesive Data for Finite Element Analysis

Tensile test samples were cast from the adhesive (Redux 410) used in the experimental models. The method used to cast bulk adhesive samples is described in section 2.3.2. Properties determined in this way are particular to the bulk adhesive and they were obtained under a uniaxial state of stress without influence from the adherends. The bulk specimen geometries are shown in figure 2.8. These specimens were tested on a Lloyd 10000L tensile test machine at a displacement rate of 0.2mm/min, to reduce viscoelastic effects. Deformations of the specimens were recorded using an LVDT attached to the surface of the specimen and with a strain gauge rosette. From this type of test Young's modulus and Poisson's ratio may be derived while from linear elastic relationships, shear modulus and bulk modulus may be deduced. The results from these experiments on Redux 410 bulk samples are shown in table 3.7.

3.4 Results

3.4.1 Adhesive Selection

Table 3.1 gives the comparative results for the six adhesives in this test series. Although all candidates performed well, Redux 410 was established as the selected adhesive for the rest of the experimental programme because of the very good overall mechanical properties exhibited when bonded to the polyester grp adherends. This epoxy showed very good performance in shear, tensile and cleavage loading. Surprisingly the other epoxy tested did not perform nearly as well. The acrylics showed the next best performances in terms of static strength on these adherends. The poorest performance was shown by the polyurethane adhesive. This result might be expected as the polyurethane adhesive is generally not recommended for thick section structural applications.

3.4.2 Selected Adhesive Performance on Pultruded Material

The pultruded material generally had a thin outer resin skin. This outer skin has been shown to be the weak link in the performance of the bonded pultrusion joint. Under all load conditions failure initiated within the pultrusion material at the interface between the outer resin layer and the first layer of reinforcement. The performance of the selected adhesive was not the issue but the tested strengths have been found to be comparable with the grp joints, see table 3.2. If increased performance is required modification to the pultrusion material will be required to increase the through thickness properties.

3.4.3 Revised Adhesive Performance

Table 3.3 shows Redux 420 to have equivalent mechanical properties to Redux 410, within possible experimental error. The shear strength of Redux 420 is approximately 12% less while the tensile strength increased by approximately 23% compared to Redux 410.

3.4.4 Pultrusion Surface Treatment

Ten lap shear specimens bonded with Redux 420 were prepared using five different mechanical roughening treatments, as shown in table 3.4, and tested to destruction. The results of nine of the ten tests show a material failure within the pultrusion substrate and the tenth was an adhesive cohesive failure. This confirms the earlier observations in section 3.4.2. The effect of surface preparation on adhesive performance is not an issue, whereas the pultrusion material controls joint performance.

3.4.5 Thermal Performance

3.4.5.1 Adhesive Joint High Temperature Performance

The purpose of this study was to review the thermal performance of the selected adhesive Redux 410 in comparison with two others known to have good thermal performance. In figure 3.2, both organic polymer adhesives showed typical polymer characteristics above their glass transition temperatures i.e. there was a significant decrease in failure load at temperatures above their Tg, while the ceramic paste adhesive showed no temperature dependence on a low failure load over the test temperature range.

3.4.5.2 Grp Thermal Performance

The grp adherends showed a similar temperature sensitivity in this range of test temperatures (see figure 3.3). Their failure stress and modulus of elasticity decreased as the temperature increased. The Young's modulus showed a decrease of approximately one third in value over a temperature range from ambient to 140°C. Similarly the ultimate failure stress decreased by approximately one third.

3.4.5.3 Adhesive Joint Low Temperature Performance

The results from these tests (see figure 3.4) indicate, for the organic polymer type adhesives, an increase in ultimate shear failure load at sub zero temperatures. At ambient temperatures Redux 410 had an average failure load of 9.5 kN with steel adherends. The failure load increased by 76% at -30°C compared to ambient conditions. Araldite 2007 showed a smaller increase in failure load over a similar temperature range of 13%. At ambient temperature Araldite 2007 average failure load is 20kN. The inorganic adhesive was unaffected at these temperatures.

3.4.5.4 Thermal Creep Performance

The test results shown in figure 3.5 clearly indicate the thermal and creep resistance of the epoxy adhesive as well as the polyester resin above the glass transition temperatures for these materials. These results indicate the ability of this adhesive Redux 420 to resist some degree of loading at high temperatures. Redux 420 shows a higher resistance to creep than Redux 410 at 100°C.

3.4.5.5 Post Cure Effect

The results from these ambient temperature experiments (figure 3.6) are inconclusive. There is a complex effect of a post cure cycle for this type of adhesive. The data may indicate a one hour post cure for bonded grp/steel adherends at 100°C and 150°C may be of benefit. A longer post cure appears to be detrimental to adhesive joint strength. Bonded joints with grp/grp adherends post cured at 100°C reached their maximum joint strength after 2 hours.

3.4.6 Adhesive Handling Characteristics

4.4.6.1 Manual Mixing

The "selected" adhesive is a two-part cold or warm cure adhesive. The inherent problems with this type of adhesive are the entrapment of air during mixing, causing voids in the bonded joint, and the limited pot life of a two part adhesive. Both of these characteristics may cause reliability problems if not carefully controlled. These problems may be significantly greater in a production environment. Previous work at Glasgow University[42] indicated how some production problems may be overcome. It was demonstrated that automatic mixing can increase joint strength by approximately 14% due to uniform mixing of the adhesive and fewer air voids. The results shown in figure 3.7 are very promising for manual mixing, displaying a standard deviation in the average failure load, for identical samples, of 0.62kN and variance of 0.38kN, indicating that manual mixing can give consistent results.

3.4.6.2 Pot Life

Once the two-part adhesives have been mixed in the correct ratios, the manufacturers' recommend adhesive application to the substrate within an hour of mixing. This time is very much dependent on the quantity of adhesive mixed and the type of container in which it has been mixed. The results of the loss in static strength are shown in table 3.5 for variable pot life durations. The reduction in static strength of 9% is surprisingly low after 5 hours delay but the mixed adhesive became very viscous and the wetability of the substrate was reduced. (The cylindrical plastic container size had a base area of 7800mm^2 by 80 mm depth. The mixed adhesive was 7800mm^2 by 20mm in volume.)

3.4.6.3 Cure Schedule

The results of these experiments are shown in figure 3.8 and indicate that 77% of the ultimate strength is attained after only two days ambient curing.

3.4.7. Bonded Butt Joint Performance

The most encouraging result was obtained using a hybrid joint configuration of tapered steel straps and grp shown in figure 3.9. This attained 71% of the strength of the parent material under tensile loading, see table 3.6. The adhesive used in this joint was Araldite 2005 since it is compatible both with the grp and steel strapping and has good mechanical properties[43]. There are essentially three modes of failure displayed by the joints:

1. adhesive failure
2. delamination of the laminate between the resin rich layer and the first ply
3. interply delamination in the parent grp adherend.

The greatest joint strengths were associated with the interply delamination failure mode. This was demonstrated as the failure mode of the tapered steel strap joint indicating that this joint geometry minimises the peel stresses at the end of the overlap.

3.4.8 Fatigue Performance

Both types of loading produce cleavage stresses in the bond. This is the most severe form of loading for an adhesively bonded connection. In the stressed attachment test geometry the adhesive joints are also loaded in tension. The two sets of results are shown in figure 3.11. Failure initiation of the specimens, in both cases, occurred through the outer layer of the pultrusion material. Supporting stress analyses of these fatigue specimens using finite element methods were undertaken with the Abaqus package. (See section 3.5). The stressed attachment had a shorter fatigue life compared to the standard attachment at a given stress range. Both loadings showed a typical S - N curve for fatigue loading with a slope of 8.07 for the unstressed attachment and 5.45 for the stressed attachment.

3.4.9 Bulk Adhesive Data for Finite Element Analysis

The data collected on bulk adhesive specimens of Redux 410 are listed in table 3.7. As expected the cold cure adhesive had a lower modulus than a typical hot cure epoxy adhesive, see table 2.4.

3.5 Finite Element Stress Analysis

3.5.1 Bonded Butt Joint Performance

It is difficult to use simple analytical techniques to determine detailed behavioural characteristics of bonded butt joints, especially localised loading at the edge of the bonds between the grp sections. Finite element stress analysis was used to overcome this difficulty to model the configuration of a bonded butt joint. Various finite element (f.e.) analysis packages are available but Abaqus[44] was used in this case together with a pre-processor (Patran)[45]. A three-dimensional model of a recessed double strapped joint, see figure 3.9a was originally created with three-dimensional 20-noded solid elements, as shown in figure 3.12. The adhesive, assumed to be 0.5mm thick, was modelled by one layer of elements through the thickness although, in reality, the adhesive thickness may vary significantly due to the inherent roughness of hand-laid grp panels. Ideally, to achieve a complete stress distribution throughout the adhesive, a fine mesh in this area is required. However, as the model is composed of 20-noded solid elements, to try to model the orthotropic nature of the adherends, to increase the mesh density of the adhesive would make the model too large to run. A second f.e. model using similar modelling techniques as the previous versions, shown in figure 3.13, was created for the butt joint geometry which performed best in the experimental programme, see figure 3.9b. This specimen was the tapered steel strapped butt grp joint. Both models were subjected to three point static bending, a nominal displacement of 5mm was applied to both models, and in-plane tensile loading across the joint. In both cases, the experimental tensile failure load was applied to the tension models. Graphical results for both loading modes and joint types are presented in figures 3.14-3.19.

The analyses assumed plane strain, linear elastic material properties for the adhesive and the steel and orthotropic properties for the grp adherends with the material directional properties orientated parallel to the global axis of the specimens. The properties are given in table 3.8. This type of analysis requires material data input for all materials of the model. Only limited data are available from adhesive manufacturers and much of this has been obtained from tests on bonded joints where the adhesive performance is influenced by the existence of the adherends. Furthermore, only average values are obtained from such experiments, despite the fact that it is known that the stress and strain fields in the joint are highly non-uniform. Thus, it is necessary to obtain intrinsic bulk adhesive properties experimentally for input to f.e. analysis, as obtained in section 3.4.9.

3.5.2 Fatigue Specimens

Finite element stress analyses of the fatigue specimens were also performed. The specimens were modelled by three-dimensional 20-noded solid elements and the adhesive was assumed to be 0.5mm thick and was modelled by one layer of elements through the thickness. Material data for the pultrusion profile was taken to be similar to the grp orthotropic properties, with the material directional properties orientated parallel to the global axis of the specimens, see table 3.8. A three-dimensional model was produced for both the stressed attachment and unstressed attachment tested in three point bending. A nominal load of 1000N was applied in both cases.

Figure 3.20 and 3.21 show a plot of s11 and s22 respectively within a section of the unstressed attachment specimen loaded in three point bending. The normal stress distribution in the 1- direction indicates that peak stresses occur at the edge of the stiffener, in the parent grp material where the stress concentration factor (SCF) was calculated to be 1.052, see figure 3.22. The large compressive stresses, see figure 3.20, on the top surface of the parent grp plate correspond to the cracking and whitening of the grp surface layers, as observed in the unstressed experiment model. The surface layer of the pultrusion material does not appear to be under significant stress levels, see figure 3.21 but, as shown experimentally earlier, this area is a weakness in a bonded pultrusion joint and this level of stress may possibly be sufficient to initiate a fatigue failure.

Directly stressing of the attachment resulted in a lower stress concentration factor in the parent grp plate material (approximately 1.028) at the equivalent position of the SCF in the unstressed attachment, see figure 3.22, and the level of the compressive stresses on the upper surface of the grp material was also lower, see figure 3.23. The pultrusion material surface layers were generally under a higher level of stress than in the unstressed attachment (see figure 3.24).

3.6 Discussion

3.6.1 Adhesive Selection

Apart from considering the general strengths and weaknesses of adhesives as polymers, an important task is to select the appropriate adhesive type for a specific application. This selection must be based on adhesive performance, application and processing parameters. When considering a joint between grp adherends there are three basic adhesive types (epoxies, acrylics and polyurethane) which are suitable and were selected for study in this work. The performance of these adhesives should be considered relative to the grp base resin. A typical isothalic polyester resin has a Young's modulus value of 3.6GPa and tensile failure strain of 2.0%[46]. Joints made from this type of resin rely on a large bond area for their strength and thus it would not be possible to bond pultruded stiffeners or other connections which require relatively small bonded areas.

The adhesives were graded according to their mechanical performance in small scale tests, see table 3.1. From this study, Redux 410, a modified, toughened, two-part epoxy, showed the best mechanical properties and the polyurethane type performed least well. Polyurethane adhesives show a high sensitivity to water attack[23] and possess only low modulus and stiffness characteristics. They are thus generally unsuitable for structural marine applications but find successful application in the automotive construction industry. The benefits of very good gap filling and the properties of the thick and viscoelastic bondlines is the main reason for this. In bus assembly polyurethane has gained great importance and is used widely in various applications[47].

Surprisingly, the two-part cold cure-epoxy adhesive, E32, when tested in this manner gave a significantly lower performance in shear, tension and cleavage compared to the other epoxy. In certain loading conditions, even the acrylics performed better. The greater difference in the two epoxies is shown in their tensile strength. Other recent work[48] on steel/grp adherend combination showed E32 to have similar strength properties to other two part cold curing epoxy adhesives. Redux 420 and Redux 410 are marketed as "modified" toughened epoxies which are extremely tough and resilient[49] with good shear and peel strength, and their formulation proves more suitable for bonding these type of thick, stiff adherends, see table 3.1. Examining the acrylic adhesive results shows that their strength characteristics to be all generally comparable. The ITW acrylic shows a high tensile strength, while VOX500 demonstrates the highest strength in tension. Permabond F246 results in the highest average shear strength tested on these adherends. The acrylic range of adhesives can be very

diverse, e.g., anaerobic, cyanacrylates, methylmethacrylates and toughened acrylics and thus have a wide range of properties, strengths and cure times. They are generally more ductile than the epoxy-based adhesives and have lower strength. They may have greater potential on thinner more flexible adherends, where peel stresses may be an issue. Acrylic adhesives have been extensively and successfully used in the automobile industry and are claimed to be suitable for bonding oily steel surfaces[50]. Thus based on the above results, Redux 410 was the adhesive selected for use in this work. This choice was based on its mechanical strength characteristics on these adherends. The other adhesives were rejected and would appear to be more suitable for use on thinner more flexible adherends and have been successfully used for these type of applications as discussed above.

The choice of suitable mechanical testing techniques and the understanding of failure surfaces present a challenging area. The understanding of the failure mechanisms in load bearing joints depends on the proper selection of test specimens[51]. The type of test specimens used in this work graded the adhesive performance according to its shear, tensile, cleavage and impact strength. The tensile and cleavage specimens were backed by steel to facilitate testing of the bonds. This increased the effective stiffness of the grp adherend. It was felt that since the tests to select an appropriate adhesive were for bonding thick grp adherends (9mm or greater) this increased stiffness of the adherend would not invalidate the results. It must be noted that this adhesive selection was based on small scale testing of polyester-based grp thick adherends only and, if a different type of adherend or even a different type of grp resin system is used, then other adhesives may prove more effective.

The type of failure occurring when using the selected adhesive, Redux 410, under these test conditions, whether under shear, or impact is in the grp adherend itself. In shear loading, the failure occurs at the resin/fibre interface. Under impact loading, it was within the first ply layer. In cleavage and tensile loading the failure was by loss of adhesion at the interface between the adhesive and grp.

3.6.2 Health and Safety Issues

Generally all the adhesives in this study are safe to handle, provided the health and safety guidelines recommended by the manufacturers are followed. Unfortunately, the initial prime candidate adhesive, Redux 410, was an adhesive of higher risk category. The Redux 410 hardener is corrosive and will cause skin irritation to sensitive skin. Thus, particular care must be taken in observing the manufacturer's precautions concerning measures to be taken to prevent the

uncured material from coming into contact with the skin. Also, Redux 410 resin contains strontium chromate and, as from the beginning of 1991, all such products carry the phrase "May cause cancer" in their labelling. It should be noted, however, that the health and safety precautions required for structural adhesives are, in general, no more stringent than for basic grp production and may be even less hazardous.

Adhesive manufacturers are constantly updating their product range and becoming increasing aware of health and safety concerns. Within the duration of this project, Redux 410 was superseded by Redux 420. Tests showed this adhesive to have generally equivalent mechanical properties to Redux 410 (see table 3.3). Redux 420 is safer to handle than Redux 410, having the strontium chromate removed. Redux 420 is labelled as a corrosive and standard precautions, as with handling most resins, need to be adhered to.

3.6.3 Adhesive Performance

3.6.3.1 Thermal Performance

The application of adhesive technology in grp fire and blast panels and structural components would indicate bonding as an ideal solution. However, all organic adhesives lack high strength at elevated temperatures, so some effort is required to assess the effect of heat on these joints from accidental fire. A rise in temperature has two primary effects on organic polymer adhesives[52]. Firstly, their shear and tensile strength properties reduce, slowly initially and then more rapidly in the region of their Tg (glass transition temperature) with properties remaining very low up to the temperature where the material will char. Secondly, over the same temperature range their natural tendency to creep increases rapidly in a similar fashion, see figure 3.5. At lower temperatures, the converse appears to be true, although the ductility of the material may gradually reduce[52]. These phenomena are illustrated in figures 3.2 and 3.4. Autostic is an exception to these rules, being an inorganic adhesive. This particular adhesive has a relatively low strength but maintains this strength throughout the test temperature range. The manufacturers claim it will perform up to 1100°C. Incorporated in this test temperature range are both the glass transition temperature for Redux 410 and Araldite 2007 (70°C and 120°C respectively). Both of these adhesives showed typical polymer characteristics above these temperatures i.e. there is a significant decrease in failure load at temperatures above their Tg. Temperature changes in adhesively bonded joints cause a wide variety of different stress states for several reasons. This may include shrinkage stresses during cure, thermal mismatch of the adherends and, not least, the fact that, the adhesive has different stress/strain behaviour at different temperatures[53]. An adhesive

designed for use at ambient temperatures might be strong but brittle at -100°C and have low strength and high ductility at 100°C[53]. To illustrate this, figures 3.25 and 3.26 show the two organic adhesives' load-displacement curves when used with steel lap shear joints over a range of temperatures. Figure 3.26 shows the adhesives loaded in the subzero temperature range. The hot cure epoxy 2007 exhibits a general increase in strength, compared to ambient conditions of approximately 13%, although over this test range there is not a significant increase in strength but there is a small increase in modulus. Redux 410, the two part cold cure adhesive, shows an increase in joint strength of 76% compared to ambient conditions, reduction in plasticity and correspondingly a decrease in extension to failure. The general trend shown by this adhesive is to increase in strength, reduce plasticity and extension to failure as the temperature decreases in the sub zero temperature range. Work by Al-Hamden[54] on steel lap joints bonded with Ciba Geigy 2004 over a temperature range -60°C to 200°C showed that the joints were strongest in the 0°C to 70°C range. Although, at lower temperatures the adhesive became brittle, as seen in this work, and led ultimately to a reduction in strength and increased scatter in results.

At higher temperatures, both organic adhesives showed distinct temperature dependency of adhesive properties, especially above the glass transition temperature. Figure 3.25 shows that, at elevated temperatures, Redux 410 exhibited no distinct yield point, unlike at lower temperatures where there is a distinct yield point and considerable plasticity. Redux 410 exhibited a brittle type failure at high temperatures possibly to increased crosslinking from post cure effects. Araldite 2007 at low temperatures behaved as a brittle material and at higher temperatures (between 60°C and 80°C) demonstrated an upper and lower yield point but little plasticity and extension to failure. At 100°C the type of failure changed, showing a yield point and increased plasticity. Above 120°C (approximately the glass transition temperature), the strength was much reduced. Here, the adhesive softened and could not sustain the load, leading to failure by total plastic yielding of the joint. Redux 410 showed the same characteristics of a significant loss of strength post Tg (approximately 70°C). Wake[55] demonstrated the temperature limitations of an Araldite adhesive above 120°C and recommended that they have very little application above this temperature. However, with the advent of so called high temperature adhesives, with elevated Tg, potential service range have been considerably extended.

It can be seen from tests on the organic adhesives that there are significant differences between them at high and low temperatures but at low temperatures all of them tended to become increasingly brittle. Kinloch[56] explains that the change in behaviour with temperature is due to the crack tip micro mechanisms.

In toughened structural adhesives, this is complex since the effect of toughening additives is to invoke crack tip micro mechanisms which increase the extent of energy dissipation and which are dependent on temperature, test rate and joint geometry. At low temperatures Araldite 2007 demonstrates brittle characteristics. This is associated with an adhesive with a high yield stress and hence minimum crack tip plasticity occurs, which results in a relatively sharp crack. The yield stress of this material remains relatively high until close to the glass transition temperature, so that the crack tip remains relatively sharp. Above this temperature, the adhesive softens and cannot sustain the load, leading to failure by total plastic yielding of the joint. Optimal results will be obtained in the temperature range for which the adhesive has been designed, where it has acceptable strength and strain to failure[53].

The grp adherends showed a similar temperature / strength sensitivity in this range of temperatures (see figure 3.3). Their failure stress and modulus of elasticity decreased as the temperature rises. This temperature response is similar to that found by Smith[57]. The mechanical properties of polymer matrices and reinforcements are affected quite differently by an increase in temperature. Under compressive, flexural, shear and transverse tensile loads, temperature dependence of the mechanical properties is dominated by matrix behaviour. Smith[57] found that the performance of phenolic grp is superior, with vinyl ester showing some advantage over polyester. However, it must be remembered that in the case of fire, marine grade polyester woven roving may not have the best temperature performance, but its thermal conductivity is low[58] (0.3 W/m°C compared to steel 46 W/m°C) and thus fire/temperature damage may be localised.

The second effect is the load/time related creep performance of adhesives which is particularly important at elevated temperatures. Therefore, a number of tests was undertaken to examine adhesively bonded grp/steel and grp/grp connections of Redux type adhesives at temperatures in the range 100°C to 200°C. The joints were designed to avoid delamination of the grp laminate by maintaining the load line centred through the adhesive. Such geometries were used successfully previously at Glasgow[59].

In addition to time to failure, deflection was also measured against time for most load cases of the Redux 410 bonded grp/steel joints maintained at 100°C. Linear transducers with a data acquisition logging system for creep deflection measurement were used. Creep deflection measured the shear deformation of the adhesive line with a nominal thickness of 0.5mm and overlap length of 15mm. Figure 3.27 and figure 3.28 illustrate the creep deflection curves based on a log

and linear scale time scale respectively. In figure 3.27, the specimens sustaining a high load level 350N, the time to failure was relatively short, approximately 60 minutes and the creep rate continued to accelerate until the joint finally failed. Where the load level is lower (150N - 250N), after the initial load application the specimens continue to creep at a slow but almost constant logarithmic rate, the rate of creep accelerates before final failure. Similar trends were found by Allen and Shanahan[60]. They suggest that under given conditions but varying loads, the creep becomes catastrophic i.e. accelerated creep rate and leading to stress rupture after the strain reaches a certain value independent both of time and load. Allen and Shanahan[60,61] studied the tensile creep of lap shear joints at temperatures in the neighbourhood of the Tg and below. They found that the actual creep under load was preceded by a delay or induction period which was temperature and load dependent. Following this delay period, steady state creep took place which was logarithmic with time. Finally, the steady state creep gave way to an accelerated creep terminating in stress rupture. Examination of figure 3.27 shows that a delay period does not appear to be detected. Examination of the plots of adhesive creep deflection versus linear time, (figure 3.28) shows that there are three regions which can be identified on the creep curves. In the first, the initial extension on loading is followed by a period of creep at decreasing rate. In the 150N load case the duration of this period is short extending to perhaps 20% (approximately 100 minutes) into the tests and could correspond to the delay time described by Allen and Shanahan[60,61]. These authors inferred that during the delay period some elongation of the adhesive may take place but their equipment was not sensitive enough to measure this. The equipment used in this work can measure to 1 micron displacement and indicates that, in this first region, creep elongations do not exceed 20 microns, which would not be registered by the experiments described in the above reference. This phenomenon was noticed by Small et al[62] in similar creep experiments on steel adherends. Of course, in this experimental example we have a duo-viscoelastic problem and creep in the grp itself may mask the delay period of the bonded joint. Furthermore, Allen and Shanahan[60,61] report that close to the glass transition temperature the delay period is less perceptible but maybe due to lack of resolution in time measurement. This may also be a problem in this study. Thus, investigation of a delay period in a grp bonded joint warrants further detailed investigation.

The second region of creep is characterised by a linear relationship between elongation and time and extends up to 450 minutes of the joint lifetime in the 150N load case. The point at which the third region begins can vary widely for a given load[62]. In this region the elongation increases rapidly until the joint ruptures. For the 150N load case this occurs at approximately 450 minutes and final failure occurs approximately 100 minutes later.

Throughout the creep experiments there appears to be a very large scatter in results which affects reproducibility. Small et al[62] found that although their creep specimens were subjected to identical load and environmental conditions, they had a large difference in times and rates of acceleration to rupture. They related this to such factors as variation in bondline quality, fillet condition and adhesive thickness. In this study, the bondline thickness and grp roughness is inherently variable and may explain the large scatter in some results.

The failure of the grp/steel bonded joints was observed to be by creep shear failure of the adhesive at the steel interface, see figure 3.29 and this is similar to the failure mechanism found by Hashim[63].

The performance of grp/steel joints using Redux type adhesive was examined at temperatures of 100°C and 150°C. The test results shown in figure 3.5 clearly indicate the thermal and creep resistance of the epoxy adhesive as well as the polyester resin above the glass transition temperatures for these materials. These results indicate the ability of this adhesive Redux 420 to resist some degree of loading at high temperatures. Redux 420 shows a higher resistance to creep than Redux 410 at the equivalent temperature. A grp/steel connection appears to be much less susceptible to creep than a bonded grp/grp connection and may be related to the stiffness of the adherend i.e. shear stress in the adhesive . The creep results of previous work[59] demonstrated that steel/steel joints are more resistant to creep than steel/grp. At higher temperatures, the creep resistance of a bonded grp/steel connection is reduced. The creep data illustrates that even at high temperatures (150°C) and low nominal loads, the grp/steel connections show a degree of resistance. At 150°C, Redux 420 at a low nominal load can sustain joint integrity for sixty hours. In comparison, the Redux 420 system has a lower resistance to creep than the 2004 (a cold cure epoxy system from Ciba Geigy) by three order of magnitude[64]. The 2004 system is specifically designed for good temperature resistance while it may not show as good as ambient temperature mechanical properties. Ideally, these loaded joints, which may be subjected to high temperatures for a sustained period of time should be designed such that a fail safe geometry is employed. Thus, if the joint fails, catastrophic failure of the structure will not follow. The use of adhesives in fire and blast panels has been shown to be effective[65] if these panels are designed such that the adhesive structural connection is at the rear face of the panel which is thermally insulated. It has been demonstrated that there is no observable creep during an H60 fire test on these panels. Obviously, unprotected structural adhesive joints in a hydrocarbon fire situation would be unacceptable, especially at high loads.

3.6.4 Production Environment

The small scale bonding process used throughout this project involved relatively straightforward manufacturing and safety procedures. In a full scale production environment, automated jigs, adhesive mixing and dispensing equipment would be required to take full advantage of adhesive technology. Certain knowledge of adhesive characteristics would be required in this situation. One important characteristic is the "handling time". This is the time in which the adhesive construction can be removed from the jig but has not yet fully cured. A full cure schedule for Redux 410 at ambient temperatures is seven days. This would be unsatisfactory for high production rates if full strength is required in shorter periods. However, a set of small-scale tests showed that after curing for only one day, joints attained 77% of their full ultimate strength and thus are sufficiently cured to handle in most applications, see figure 3.8. Another characteristic to consider is the "pot life". This is the length of time the mixed adhesive is useful before partial curing of the adhesive occurs. The pot life of an adhesive is very much dependent on the amount of adhesive mixed and the shape of the container it is mixed or held in. This is because the cure process involves an exothermic reaction. A large mass of adhesive in a container with a low relative surface area will cure rapidly. If the curing process has commenced (i.e. post normal pot life) and this adhesive is then applied to a joint, a reduced fully cured bond strength is achieved, as shown in table 3.5. Thus, careful consideration must be given to the amount of adhesive required and when it is required. Automated dispensing and mixing overcomes this problem as the adhesive is mixed only when required at the point of dispensing. Although automatic mixing gives the best results[42], adequate values are attainable with manual mixing (see figure 3.7) of small volumes.

3.6.5. Structural Performance

Butt joints of single skin panels and sandwich panels are required to make use of prefabricated units. Simple methods which are cheap and effective are required to join grp elements. This study looked at methods of bonding two thick grp panels in a butt form of joint. The simple lap shear joint, which is the weakest joint tested, showed only 10% efficiency in tension, see table 3.6. The unsupported lap joint can never be as strong as the members being bonded together due to the large stress concentration from the eccentricity of load path. Nevertheless with an adequate length to thickness ratio (50:1 to 100:1) the gentle transverse deflections under tensile load can relieve the eccentricity in load path[17]. Thicker laminates for lap shear joints will require the ends of the adherend to be tapered to prevent premature failure by induced peeling or cleavage stresses before the

full potential of the shear strength of the adhesive can be developed. For laminates of greater thickness than those suitable for a single lap joint, two bond surfaces are required to transfer the strength of the adherends[17]. The failure mode of a composite joint is affected by the thickness of the adherends being bonded. Consequently, seemingly similar adhesively bonded joints will fail by quite different modes at quite different structural efficiencies, primarily as a function of the thickness of the joint[17]. Unfortunately, the simpler, cheaper configurations such as the lap shear joint cannot sustain the higher load levels of the more elaborate systems, no matter how much quality workmanship is employed.

There are essentially three failure modes demonstrated in the tension experiments here using two bond surfaces. The first is an adhesion failure of the adhesive in the recessed lap joint. This gives a low joint efficiency of 18%. Failure starts at the interface between the parent material and the adhesive next to the strap, see figure 3.30. The second mode is delamination of the laminate between the resin rich surface layer and the first ply of glass, see figure 3.31. This consistently results in joint efficiencies of between forty and the low fifties percent. The higher efficiency is associated with interply delamination of the laminate and depending upon the design of the straps, gives efficiencies of between 52% and 72%, see figures 3.32 and 3.33. Using separate tapered (2.5°) steel strapping plates, the maximum thickness at the midpoint is 2.65mm and at the end of the taper is 0.5mm with the cold cure epoxy Araldite 2005 (see table 3.6) a tensile strength of 71% of the parent material was obtained. This arrangement gives a 40% improvement in joint efficiency when compared to rectangular steel straps of the same maximum thickness. The results of numerical predictions between grp and metals of single lap joints by Hildebrand[66] suggest that with a careful joint end design the strength of the joints can be increased by 90% to 150%. Other work demonstrated that taper strap butt or scarf joints are suitable for joining thick composites giving good structural characteristics, simple to make, easy to inspect before bonding to assure a good fit and this in turn will keep costs down[67]. However the edge machining is hazardous and the resulting edge preparation is fragile and not necessarily suitable for offshore fabrications.

3.6.5.1 Butt Joint Numerical Analysis

The motivation to perform numerical analysis in this work was to assist in the design of a bonded butt joint in grp panels. This numerical analysis was also undertaken to compliment the experimental programme and assist in explanation of some experimental observations.

Two f.e. models were developed, see figures 3.12 and 3.13, to be analysed in both pure tension and three point bending separately:

a) a recessed strapped joint, see figure 3.9a, and
b) a tapered steel strapped joint, see figure 3.9b.

3.6.5.1.1 Tensile Results

Figure 3.14 shows the stress distribution of the recessed strapped bonded joint in tension. Peak stresses occur at the butt connection i.e. the centre of the joint and at the corner of the recesses of the parent material, see figure 3.14a, which are not significant in the failure of the joint. This geometry of joint produces high stresses transverse to the load direction within the adhesive, see figure 3.14b and high shear stresses, see figure 3.14c, due to a bending moment set up in the straps. It is here, in the adhesive where failure initiates (as seen in the experimental programme shown in figure 3.30). Failure occurred at the interface of the adhesive and the grp butt face first. The failure occurs on the free adherend interface and propagates along the interface. Figure 3.15 is a plot of the shear and cleavage stress variation in the adhesive at the interface denoted as A in figures 3.14b and 3.14c. These plots illustrate that there are higher stresses in the adhesive at the free adherend interface (line L in the plots).

Figure 3.16 shows the stress distribution for the steel tapered strap joint. It is clear that there is a limited region of high cleavage stresses in the adhesive layer at the very tip of the taper. However, even if this promotes local failure, it is unlikely to propagate[29]. The more significant zone is the area of high cleavage stresses in the laminate below the toe of the taper. It is here that the global failure initiates as cleavage delamination of the laminate between the first and second ply. The area of damage then propagates along to the free end of the laminate at the centre of the butt joint, allowing the core laminate to be withdrawn from between the steel straps (figure 3.33). The cleavage stresses in this area of failure initiation are of the correct magnitude for tensile delamination failure of the composite system[68] being of the order of 15N/mm^2, see figure 3.17. The failure stresses in the resin perpendicular to the plies are generally very much lower than the base resin itself due to the stress concentration effects of the fibres. The distribution of cleavage stresses through the thickness of the laminate, at the toe of the tapered strap, exhibit a maximum at approximately 15% of the thickness, which correlates well with the failure mode. Failure propagates due to the high shear stresses, see figure 3.17, causing interlaminar shear failure. The magnitude of the shear stresses are 18N/mm^2 and Smith[69] reported interlaminar shear strength values for 55% woven roving polyester laminates to be of this magnitude. This form of

joint develops the full potential of the adhesive and failure is observed to initiate between the weaker grp interlaminar layers. The parallel-sided steel strap joint is much less efficient, invoking significantly higher cleavage stresses in the area of the adhesive and the resin rich surface layer. Consequently, the failure load is reduced compared to the steel tapered strap design. Figure 3.32 also shows the steel strap H section. The ethos behind its use is that it would allow butt joint components to be mass produced and such sections will also improve joint stability during the period of adhesive cure. Ultimately, such sections need not be fabricated from steel. A pultruded composite section, with properties designed to maximise joint efficiency, could be produced.

3.6.5.1.2 Three Point Bending Results

In bending, the underside of the joint is loaded in tension while the top face is under compression. Adhesives perform exceptionally well in compression; thus, in both cases failure will initiate on the underside and a similar type of failure mode as displayed in the tension experiments might be expected.

Figure 3.18 shows the stresses (s11 & s22) in the tapered strap joint due to bending i.e. the joint in compression and tension on opposite sides. Increased cleavage stresses occur under the tip of the steel strapping in the grp on the tension loaded side and these stresses are sufficient to cause interlaminar failure, as seen in the experimental model. This mode of failure is similar to that seen in the tensile experimental testpiece.

Figure 3.19 is a view of the stress distribution (s22) in the corner detail, including the adhesive, of the recessed strapped joint. The stress levels developed within the adhesive in this area is sufficient to cause failure of the adhesive and thus failure of the joint. This is demonstrated in the experiment and is a similar mode of failure to the tensile specimen.

The grp material was modelled as an orthotropic solid material, its composite layer behaviour and, probably the most important effect, the interlaminar strength between the adjacent plies of woven glass within the composite was not taken into account. Furthermore, there is a resin rich area on the composite surface which is more brittle and should also ideally be accounted for. The extent and reliability of strength values for grp is to some extent poor. The tensile and compressive strengths of the laminates are often well known, but measurement of the interlaminar shear and tensile strength is a difficult task. Both of these parameters have a major influence on the strength of grp joints and therefore failure prediction. Modelling of these details would involve a very complicated

model. However, the simpler models used in this study provide a more than adequate estimate of the stress levels within both joints for this research purpose. If further research were to be undertaken finite element sub models can could produced to model fibre orientation and lay-up around the critical areas.

Research by Hart Smith[17,27,28,29,30] laid down the basic principles for bonding composite sections for the aircraft industry. He recommended that the uniform double lap joint is limited to joining about 3mm - 4.5mm of material. The use of tapered straps might increase the material thickness as high as 6.35mm without a significant increase in machining. The tapered strap joint employs thickening of the splice plate in the middle to achieve simultaneously the alleviation of peel stresses and an increase in shear strength of the adhesive joint. In his work, Hart Smith[17] recommended that, for joining composite sections of 6.35mm thickness, or more, only the stepped lap joint or the scarf joint should be considered. The more sophisticated joints tend to increase joint strength. Unfortunately, the level of machining required for this type of joint for large scale applications is too great. The section thickness considered here are between 9mm and 15mm and thus relatively simple connections for joining thick composites have been shown to be effective, which does not follow the established theory. In thicker section composite 'simple' joints the failures are initiated by high peel stresses which may cause failure in the adhesive or in the composite itself. This is well established knowledge. Hart Smith[70] proposed that these joints are, consequently, relative weak compared to the parent material. Higher strengths are attained using more complex joints which will fail in the adhesive due to high shear stresses. However, this study has used a 'simple' steel tapered strap composite joint and appropriate adhesive and to attain a strength of 71% of the parent material, which is a strong connection. Furthermore, it was shown that the adhesive strength is not an issue in the failure of such composite connections. The joint efficiency in a double lap joint design is very sensitive to the induced cleavage stress at the ends of the straps. If the full strength of the parent material is required using a simple connection, the parent grp material could be modified. There are now woven fabric reinforcements on the market[71] which are basically three-dimensional structures and thus will offer improved resistance to peel and cleavage stresses or alternatively use advanced composites e.g. epoxy based grp. The bonded tapered steel strap joint which is 71% efficient compares very favourably in strength with the conventional joint designs where the base resin and staggered plies are used[26] but which are more time consuming and costly to manufacture.

3.6.6 Fatigue

Fatigue performance of adhesively bonded structures can be very important in some applications in a marine environment. This study has examined the performance of a sandwich structure and its components of adhesively bonded grp and pultruded profiles. Using adhesive bonding as the joining technique not only allows the joining of dissimilar non-metallic materials like grp and pultrusions but also reduces the probability of high stress concentrations and which may encourage good fatigue performance.

On numerous occasions throughout this study, the cause of bonded specimen failure in monotonic loading has been through delamination of the surface layers of the pultrusion material. This would indicate that the adhesive/pultrusion interface is a possible site for failure initiation in fatigue. The experimental models displayed two forms of failure, depending on the type of loading. The stressed attachment generally only failed in the pultrusion material at the weak top surface layer, see figure 3.34. In only one case the failure occurred at the resin rich surface layer of the grp laminate material. The finite element stress analysis demonstrates consistently higher levels of stresses (s11, s22, s12) in the pultrusion material of the stressed attachment compared to the unstressed attachment at an equivalent load level, (see figures 3.20 to 3.24). Correspondingly, the level of the compressive stresses on the top surfaces of the parent material were less in the stressed attachment, and no micro cracking occurred there. Total failure of the stressed attachment occurred when the pultrusion stiffener parted from the parent material due to the interlaminar failure of the pultrusion.

In the unstressed attachment, failure initiated and propagated from the surface of the pultrusion material, see figure 3.35. A large area of whitening was seen around the load point on the compression surface due to fibre debonding and resin cracking. This is a common type of fatigue failure demonstrated in composite materials[36]. Studies have shown that axial cycling which involves compression leads to a significant deterioration of fatigue life[72]. This verifies why fatigue failure in flexural fatigue loading is initiated on the compression surface of the parent grp plate. It is here that cracking can occur through the grp layers. Ultimate failure occurs when the specimen loses stiffness due to the parent grp cracking transversely through the thickness of the material to meet the crack propagating through the pultrusion and adhesive. Dharan's[73] studies of flexural fatigue on unidirectionally orientated carbon fibre reinforced polyester demonstrated similar failure patterns. The initiation of a crack on the compression surface appeared to be due to a fibre buckling instability. This was usually

followed by delamination under the initiation zone, formation and propagation of a transverse crack and delamination propagation parallel to the fibres. Failure of the unstressed specimens may include total separation of the pultrusion attachment.

The fatigue life of the stressed attachment was significantly less than that of the unstressed attachment, as shown in figure 3.11. In both load cases, failure is determined by the level of stress at the outer free edge of the pultrusion surface layer. In the stressed attachment, the stresses at the edge of the stiffener are tensile whereas in the unstressed attachment are compressive at the equivalent load level. It is this that is believed to explain the difference in fatigue life. A recent study[74] indicated the criticality of lay-up of the surface layers when composite bonded cracked lap shear specimens were tested under fatigue loading. It was discovered that if the top surface fibre layer was orientated at 90° to the applied load, the strength was so low that ply cracks developed at levels of stress below that required to create the threshold strain energy release rate in the adhesive. Whereas, with a 45° fibre orientation ply lay-up at the bond surface, the resulting minimum average cyclic stress was significantly greater than that for the 90° fibre orientation interface plies which allowed no damage in fatigue. Failure of a 0° and 45° fibre orientation of ply at the bond interface resulted in fatigue damage initiation with cyclic debonding in the adhesive. 90° plies resulted in a fatigue failure initiation with transverse cracking of the 90° ply of the strap in the adherend. Thus, the stacking sequence of plies at the bond surface is important, especially if the plies are at 90° to the principal stress as may be found at the pultrusion material surface layer of the experimental models. To improve the fatigue performance of the bonded pultrusion models, the lay up of the pultrusion material surface layer would need to be reconsidered and altered. Where pultrusion materials have been bonded for structural applications, the pultrusion profile has been specifically designed for the purpose[15] and not like in this case where a standard profile has been used.

The fatigue performance of the bonded components were compared to marine grade woven roving polyester laminates tested in fully reversed loading[72] as shown in figure 3.11. The stressed attachment, where the failure mode is predominantly a pultrusion surface failure, was shown to have a poorer fatigue life than the polyester marine grade woven roving grp at a given stress range. In the unstressed attachment, where the failure involves the parent plate as well as the pultrusion, the slope of the SN curve was calculated to be the same as that of the woven roving laminate, approximately 8.07. In metals, from fracture mechanics theory of fatigue, it is known that if the crack initiation phase is negligible the slope parameter of the SN curve is identical to the crack growth power law. This

parameter depends mainly on the material property and hence all SN curves for a given material should be essentially parallel.

Most experimental data for crack growth in structural steels has an exponent of curve gradient as m = 3[ref.76]. In the experimental models here, the calculated gradients, using regression analysis, were 8.067 and 5.45 for the unstressed and stressed attachments respectively and for the woven roving grp 8.074. These values are high compared to fatigue crack growth in steel. Other workers have found similar steep gradients for composites, bulk adhesives and bonded joints. In a glass cloth polyester laminate the fatigue crack growth rate gradient in the form of Paris Law was calculated as 6 and for a chopped strand glass polyester laminate, a gradient of 13[ref.77]. Luckyram and Vardy[78] calculated, for a cold cure adhesive, a Paris power law gradient of approximately 4. The gradient calculated, for a bonded composite cracked lap shear joint was found to be in the range of 4 to 4.5[ref.79] for the modified Paris law equation incorporating the strain energy release rate parameter. The relatively steep slopes shown in the experimental data here, 8.067 and 5.45 mean that small changes in applied loads, and hence stress range, cause a large change in the fatigue life. Thus, the failure propagation rate in these components is more sensitive to errors in design load than in typical crack growth rate in metallic welded structures. Because of this sensitivity the design of bonded composite components for a relatively short finite life may be unacceptable with regard to reliability. An effective infinite life (say $>10^8$) may be a viable alternative. Then the crack growth threshold value may be a important material property. In figure 3.11, a stress range of 100N/mm^2 in the unstressed attachment and in the stressed attachment a stress range of 20 N/mm^2 both gave a life in excess of 10^7 cycles. More work would be required to establish if this is the threshold stress level where no fatigue cracks will propagate.

There has been over 20 years of ship experience for large grp structures in which localised fatigue damage must have occurred at hatch corners etc. but in which there has been no recorded instance of through thickness fatigue cracks. Smith[80] thus postulates that the SN curves, see figure 3.11, are an unrealistic indication of fatigue life for large grp structures containing localised stress concentrations. A more realistic danger is that of interlaminar failure and debonding. This is demonstrated in the experimental model where a much reduced fatigue life occurs when the failure mode is predominantly interlaminar surface failure in the stressed attachment. In the unstressed attachment, where the failure mode takes the form of a diffuse path of resin cracking and fibre debonding in the grp plate, this may initially lead to a local reduction in the modulus of elasticity in the

damage zone and hence it is likely to reduce any stress concentration thereby inhibiting damage propagation and increasing fatigue life.

The type of specimens selected were intended to model the behaviour of single skin panels or sandwich panels fabricated from grp skins and discrete pultruded cores bonded by adhesives. These experiments have highlighted the pultrusion surface to be an area of weakness under flexural fatigue loading. For sandwich construction to perform efficiently the integrity of the connection between the core and the face plates is of vital importance. If the 'connection' between the core and the face is poor then the two faces will act as two separate beams and the structural benefits of the sandwich construction are lost. Thus it may be necessary to improve the through thickness properties of the pultrusion outer surface layers to improve performance for the use of such structural elements in bonded sandwich panels.

Detailed differences in the stress distributions in the composite models, as given by the finite element stress analysis, can aid understanding of the failure mechanisms. The most noticeable difference in the failure modes of the two experimental models is that resin stress whitening occurs at and adjacent to the load point of the unstressed attachment due to fibre/resin debonding, as shown in figure 3.35. The fibres then demonstrate buckling instability. This buckling failure occurs approximately 10 mm from the load point. This is difficult to measure due to the ill-defined region of the crack. The results of the finite element stress analysis indicate that the effect of a combination of tensile stresses, transverse to the fibre direction and shear stresses, is literally to cause fibre debonding and this leads to fibre buckling failure due to compressive stresses parallel to the fibre direction and ultimate failure. Figure 3.36 plots the variation of stresses across the plate surface and at the first ply level. The tensile, shear and increased compressive stress levels occur only in the unstressed attachment adjacent to the load point where fatigue damage of the grp plate occurs. This type of compressive failure in composite materials is commonly referred to as a 'kink band'[81]. A shear failure of the matrix on a 45° plane then precedes the fibre instability leading to a collapse of the form shown in figure 3.35. When the failure path enters the underside section of the plate, where tensile stresses become predominant in bending, the failure mode of the fibres changes to a tensile failure and, finally, ultimate failure of the grp plate occurs.

Fatigue failure of the stressed attachment is due to failure of the pultrusion material. The predominant stress to cause failure is the transverse tensile stress, s22, at the edge of the pultrusion material. Figure 3.37 is a plot of stresses within the pultrusion material, for both load cases, at the top surface and the middle

surface. These plots demonstrate that the cleavage stresses, s22, are greater in the stressed attachment at both positions in the pultruded material at the free edge area. The through thickness strength of the pultrusion material is low and thus this is the dominant mechanism to cause failure. Figure 3.34 show the fatigue failure surfaces of a stressed attachment showing a pultrusion surface failure as indicated by the remaining pultrusion material on the adhesive surface.

The variation of the maximum bending tensile stress is plotted in figure 3.22 for the two modes of loading. The calculated stress concentration factor, SCF, of the stressed attachment is 1.028 and for the unstressed attachment is 1.052. In metallic structures, where the most influential factor deciding the fatigue strength are values of SCF and hot spot stress, a high stress concentration at a weld toe is a major problem, leading to lowered fatigue life. The fatigue crack growth depends on the stress conditions at the crack tip and cracks grow when opened by tensile stresses. It is still a matter of discussion whether a compressive stress should be considered to contribute to the fatigue damage in metals whereas, in composites, the compressive fatigue life of a component is less than the tensile life[70]. Thus, although the unstressed attachment demonstrated a higher SCF than the stressed attachment, the fatigue life is greater by approximately four orders of magnitude at a given stress range as this is not the dominant fatigue damage mechanism. In fact, Smith[80] found that although on a rounded hatch corner where the SCF was calculated as 1.9, the experimental fatigue performance did not vary significantly, in tensile/compressive fatigue loading, to a sharp hatch corner where the SCF is theoretically assumed to be infinite. Damage to both corners was similar and there was no loss of overall stiffness. It is proposed that in grp the fatigue damage may lead to a local reduction in elastic moduli in the damage zone and thus possibly reduce the stress concentration thereby inhibiting damage propagation.

The maximum level of stresses in the adhesive occurred at the interface to the grp and are shown in figure 3.38. Again, the cleavage stresses are the greatest in both load cases and are the greater in the stressed model. Generally, failure will not occur here as the adhesive has a much greater tensile failure strain (>5%) than the polyester resin. A typical isothalic polyester resin has a Young's modulus of 3.5GPa and tensile failure strain of 2.0%[46].

In conclusion, the candidate two part cold curing epoxy adhesive studied produces more than adequate mechanical strength when bonded to connections between polyester laminates and polyester pultrusions. It is possible to design butt connections between panels which will be up to 70% efficient without extensive hazardous machining of the laminates. In most cases for both bonded

laminate connections and bonded attachments, joint strength is controlled by the interlaminar properties of the composite components rather than the adhesive properties. Under fatigue conditions, failure is generally in the polyester pultrusion laminate. The results of this section of work demonstrate that adhesive bonding technology is suitable for applications in the offshore sector. It was demonstrated that it is possible to fabricate an adhesively bonded butt type joint of thick adherends with the appropriate adhesive selection which is simple to fabricate, efficient and effective. These joints are comparable in strength to the very much more complex joints fabricated from the base resin and plies. In these high strength bonded joints, the integrity of the adhesive is not an issue and failure generally initiates in the grp. These bonded joints should be cheaper to fabricate as they are less labour intensive. The adherend surface to be bonded requires little surface preparation; mechanically roughened or peel plies are ideal to produce adequate joint strengths. The bonded joints have been shown to withstand natural climatic temperature (-30°C to 30°C) effects without a significant change in properties and, where suitably protected, can withstand a fire situation showing a degree of resistance to creep. In all cases, the selection of the appropriate adhesive and test method for the end application is important. Processing the adhesive joints requires low grade skill as they can be manually mixed or dispensed via a mixer thus removing the problem of pot life. Although for the selected adhesive it appears to be for up to six times the manufacturer's recommended life. For cold curing adhesives, thought must be given to the fabrication times to allow for full cure or at least a handling time before moving the joint. It is felt that further work is necessary to establish if the cold cure adhesive will cure in a cold and wet environment (less than 5°C) found offshore or if this will ultimately limit their use without the use of environmental enclosures and heat input.

The results of this work should, to a degree, allay many previous uncertainties regarding adhesive bonding of composites of types, sections and sizes suitable for marine structures. The results of the work are incorporated into a draft summary design guidance which is presented in the following section.

3.7 Summary Outline Design Guidance

As a result of the studies reported here and the results of previous work it is possible to suggest some outline design guidance applicable to the use of structural adhesives in the bonding of grp for marine applications.

This outline design guidance is as follows:

(i) When the adherends are polyester laminates or pultrusions and in connections where the predominant loading is shear and tension, the static performance of readily available structural adhesives is greater than the interlaminar strength of the adherends. This is more noticeable in the pultruded sections due to manufacturing process limitations.

(ii) In stiffened panel construction, fabricated from grp and pultruded sections, in transverse bending the SCF's are less than 1.1. A non-stressed attachment has a superior fatigue performance than a stressed attachment by a factor on life of 10^3. This may be favourable when compared with other methods of joining these adherends.

(iii) The interlaminar strength of pultrusions is a critical point in the use of bonded stiffened composite construction.

(iv) Surface preparation of both laminates and pultrusions need not be more sophisticated than abrasion. There may be more care required in the roughening of pultruded surfaces due to the thin resin layer.

(v) Manual mixing of two part adhesives is adequate, however metered or instantaneous 'spiral' mixing can produce a 10% increase in strength[42]. The mixing method will be influenced by the construction to be bonded.

(vi) Manufacturers' recommended handling times can be exceeded with only small losses of joint strength. The limitation is the dispensing of the adhesive, wetability of surfaces and the mass of adhesive mixed.

(vii) High grp/adhesive joint strengths can be obtained using relatively simple joint configurations

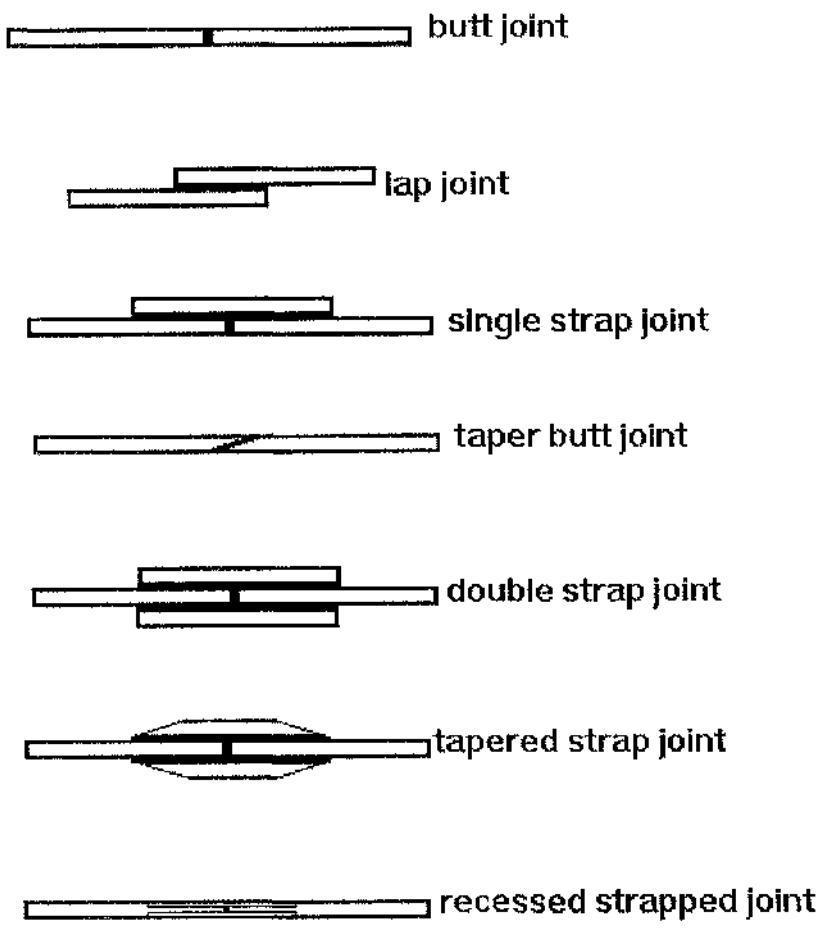

Figure 3.1 Several common joint geometries for composite panels

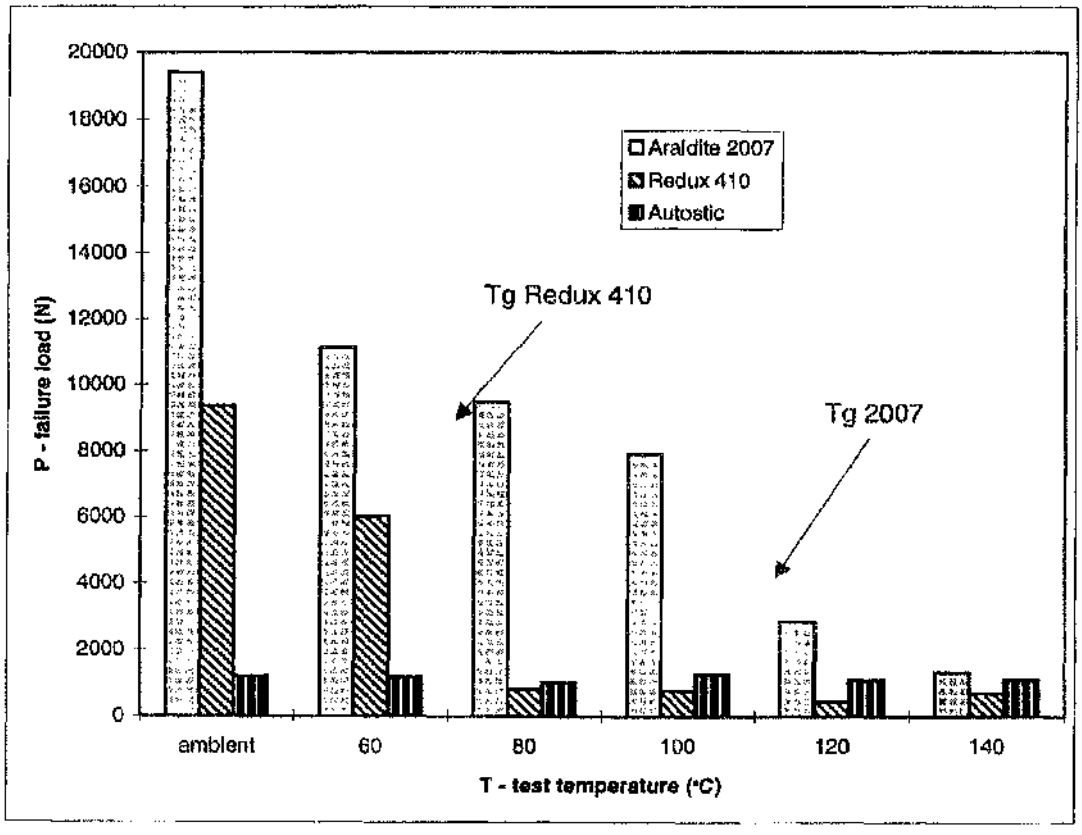

Figure 3.2 Shear failure strength of three adhesives tested at elevated temperatures on steel adherends (XSA15x25mm)

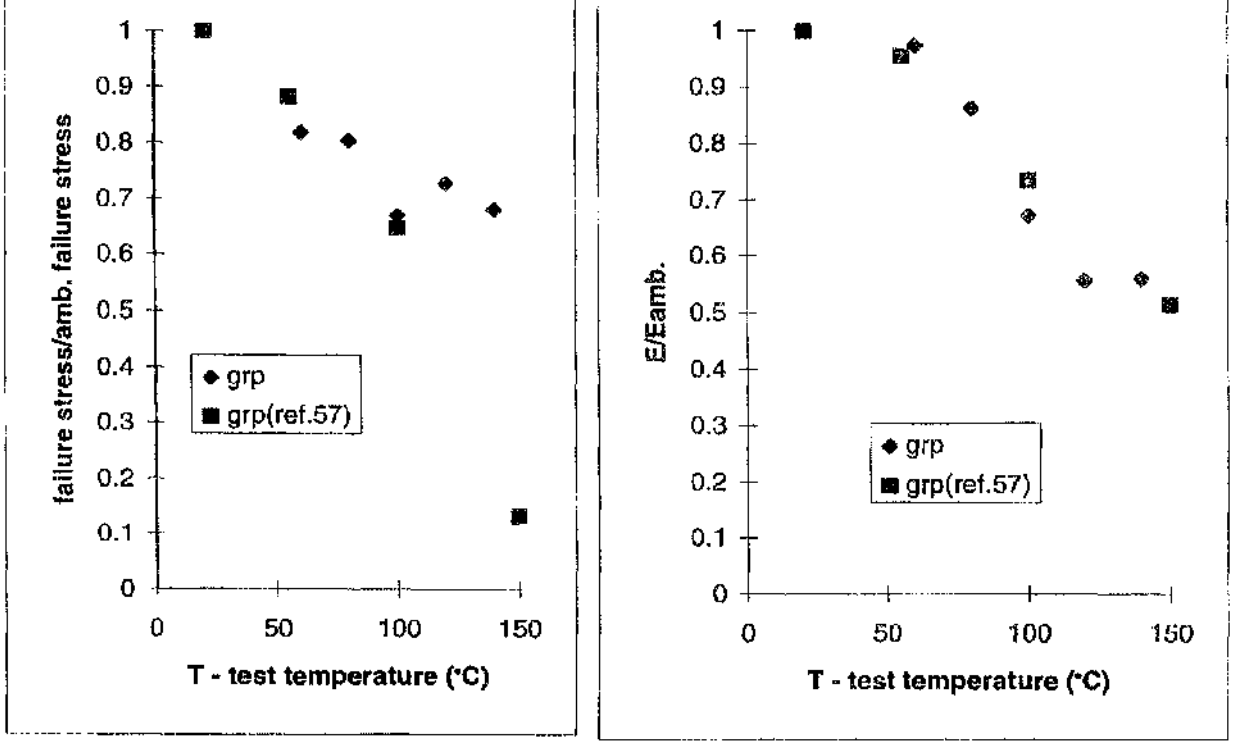

Figure 3.3 Grp thermal performance at elevated temperatures

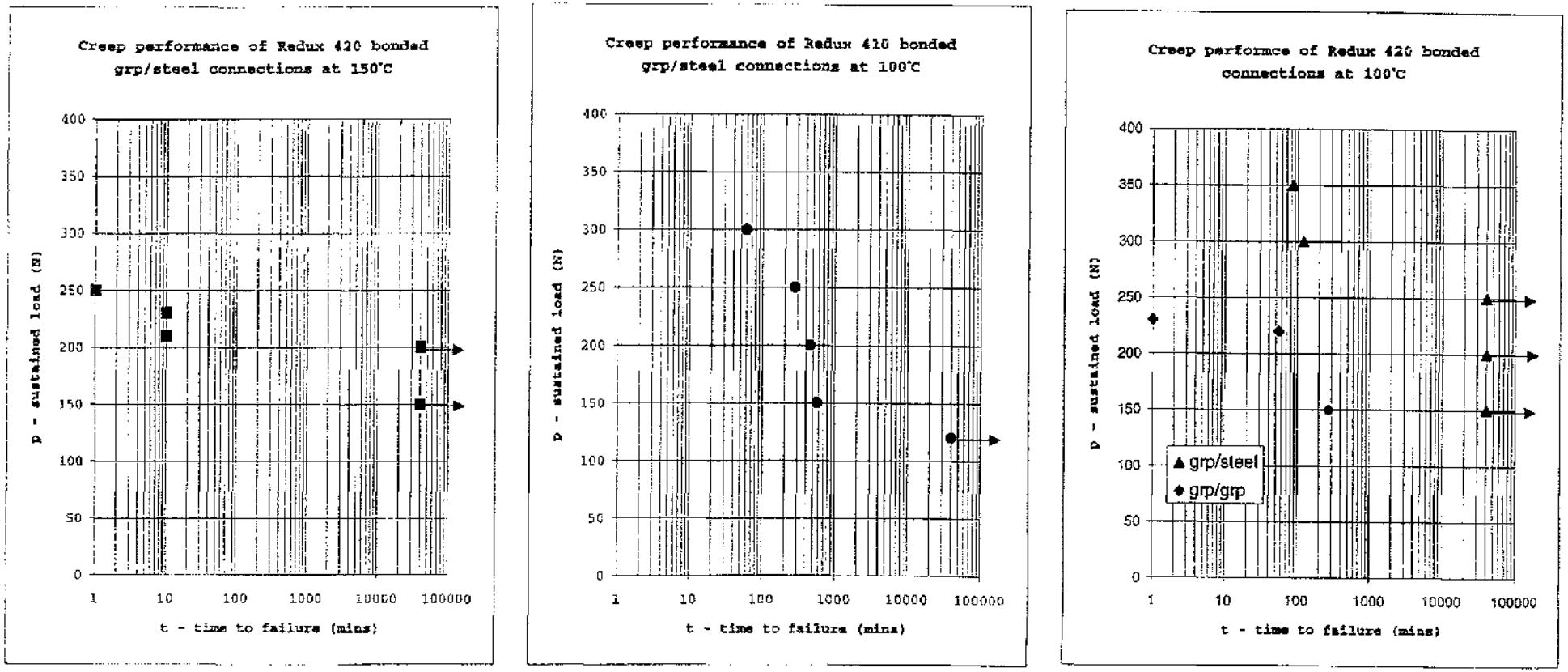

Figure 3.5 Thermal creep performance of adhesively bonded tensile shear connections (XSA15x25mm)

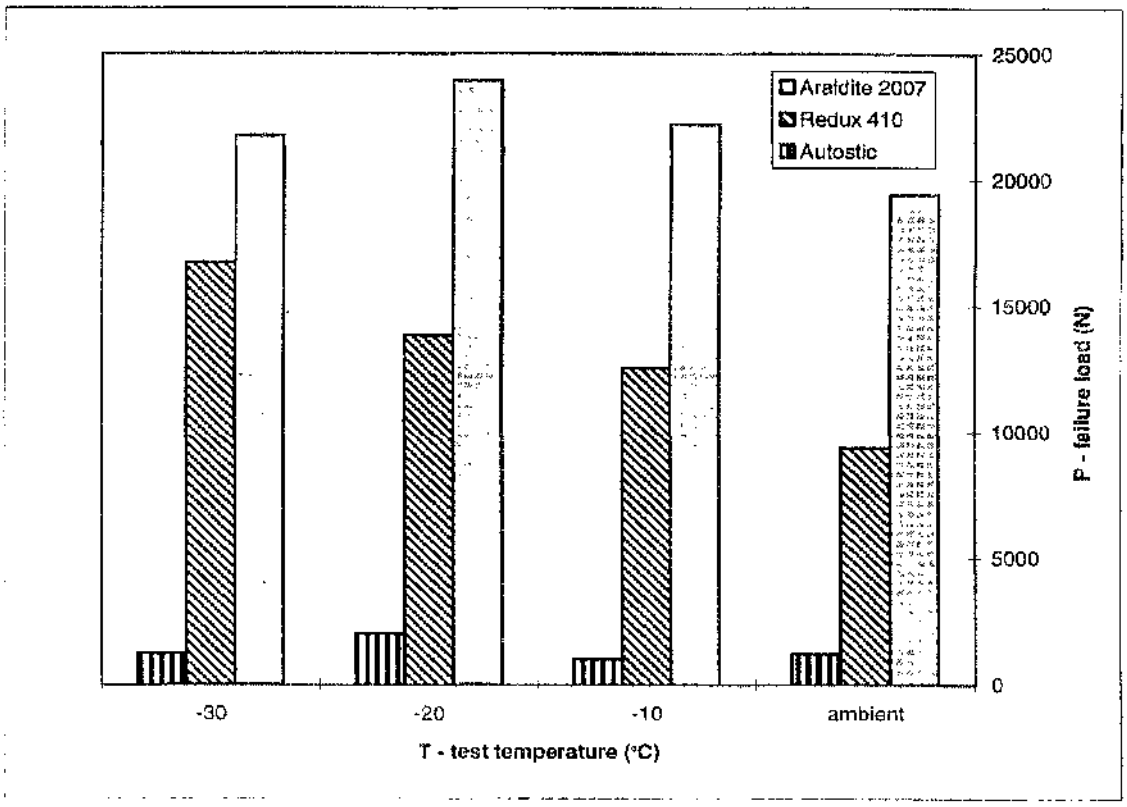

Figure 3.4 Shear failure strength of three adhesives tested at subzero temperatures on steel adherends (XSA15x25mm)

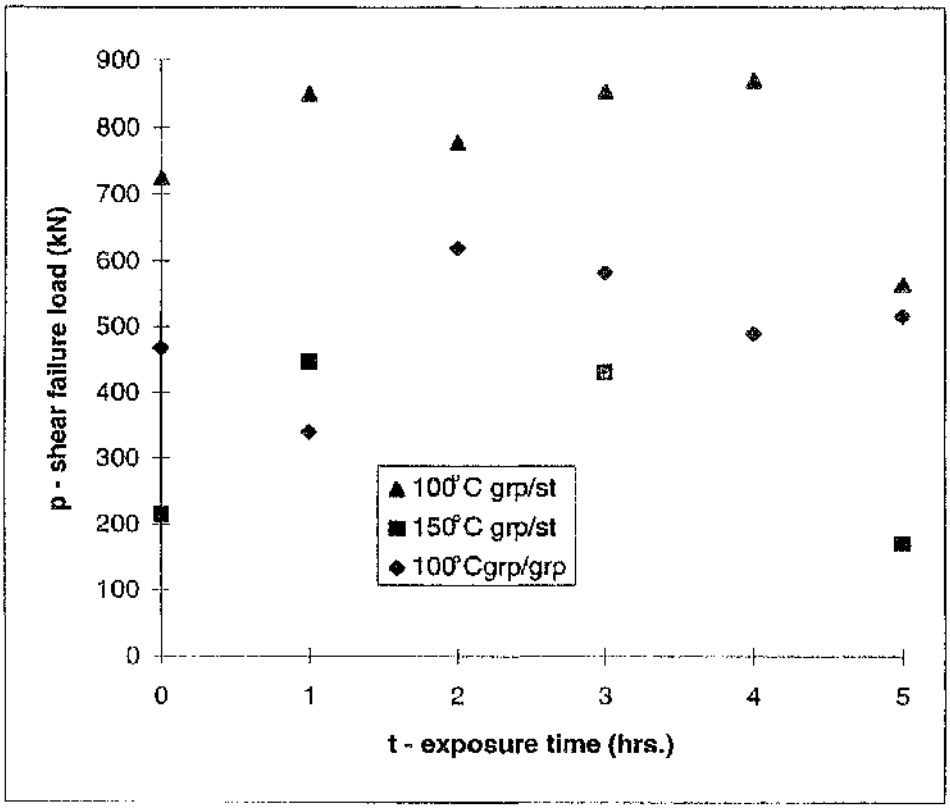

Figure 3.6 Post cure effect on Redux 420 bonded tensile shear connections (XSA15x25mm)

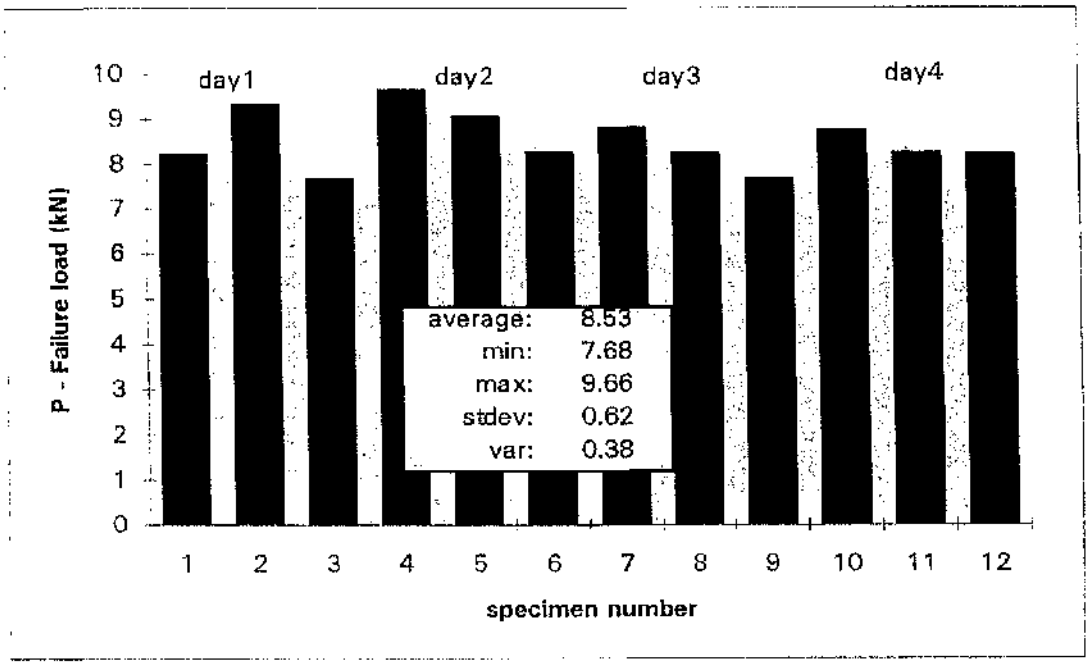

Figure 3.7 Variation in static strength due to manual mixing of Redux 410 bonded steel shot blast lap shear specimens (XSA15x25mm)

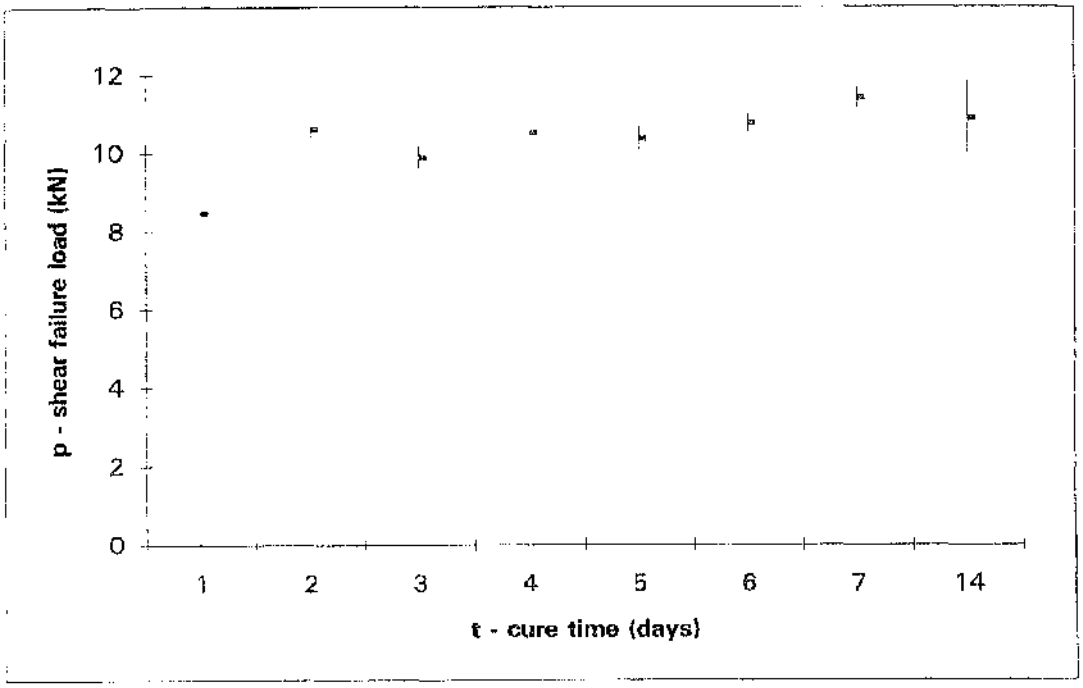

Figure 3.8 Cure schedule at ambient temperatures for Redux 410 bonded steel lap shear joint (XSA15x25mm)

(original in colour)

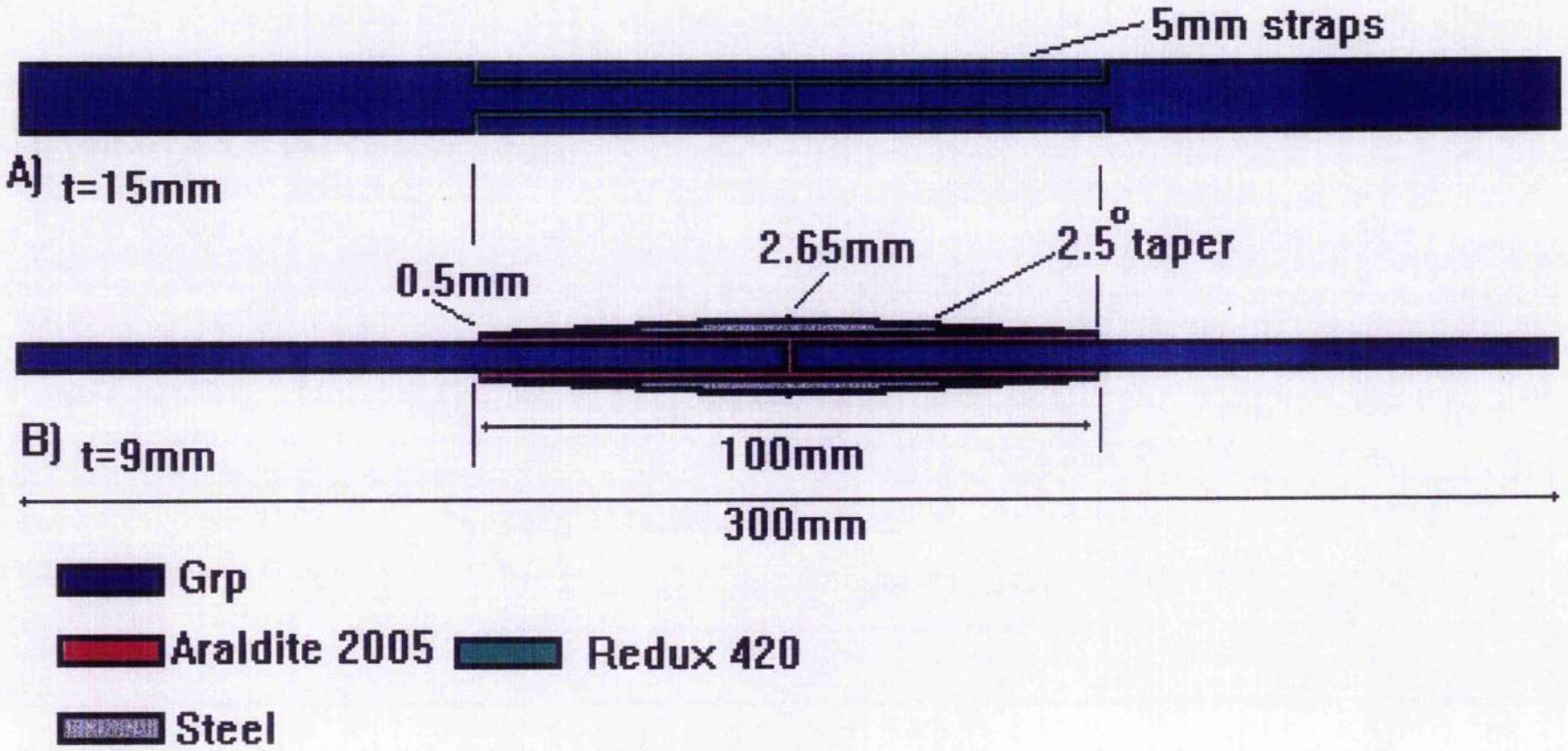

Figure 3.9 A)Recessed strap joint
B)Best experimental butt joint: Bonded hybrid joint of tapered steel straps and 9mm grp adherends

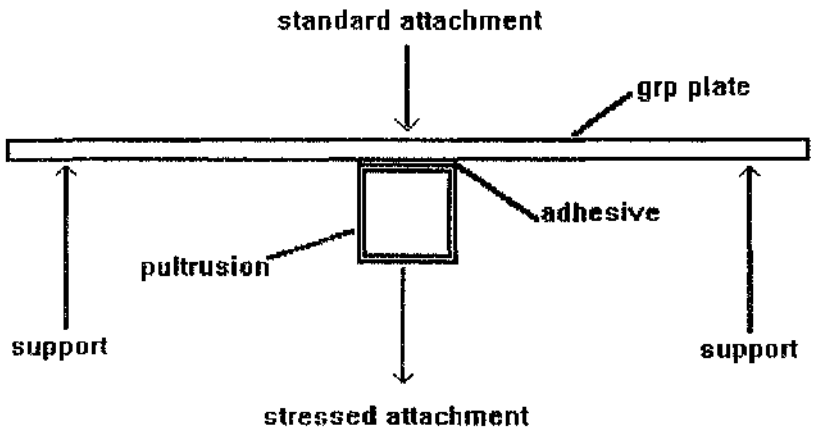

span=200mm	pultrusion thickness=2.5mm
length=300mm	pultrusion dimension=37.5mm x 37.5mm
width=75mm	grp thickness=9mm

Figure 3.10 Redux 410 adhesively bonded pultruded stiffener/grp plate connection used for fatigue testing in transverse bending

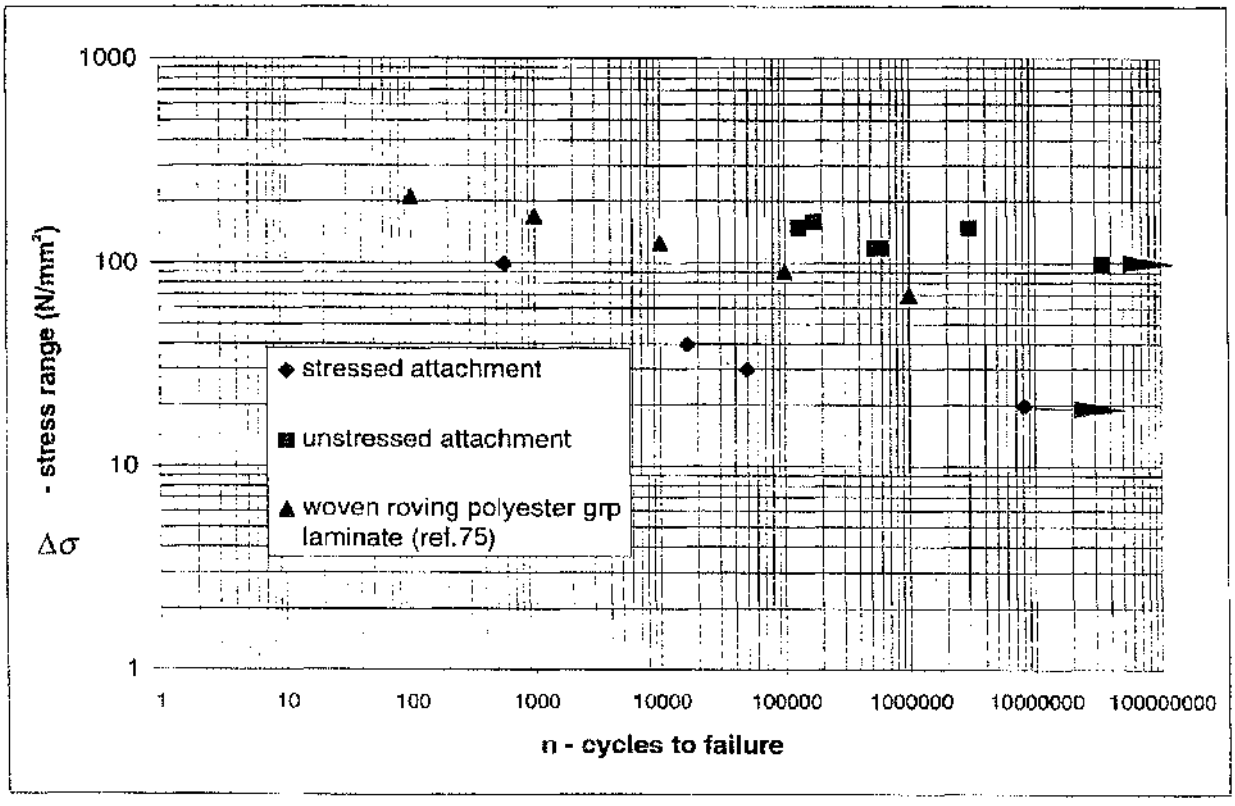

Figure 3.11 Fatigue performance of composite/pultrusion Redux 410 bonded attachments in bending (R=0.2) and marine grade woven roving polyester laminate

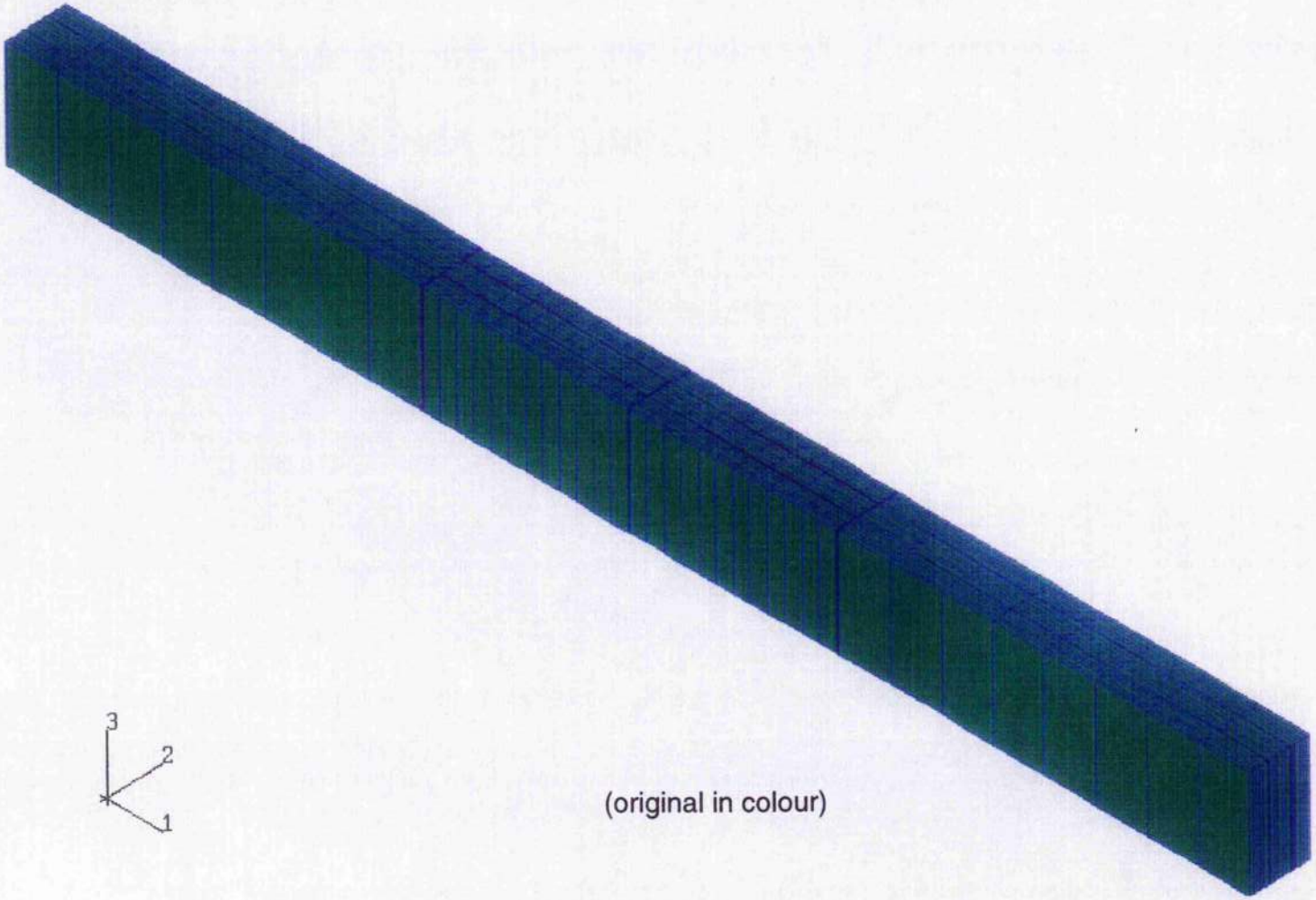

(original in colour)

Figure 3.12 Three dimensional 20 noded solid element model of a recessed strapped joint.

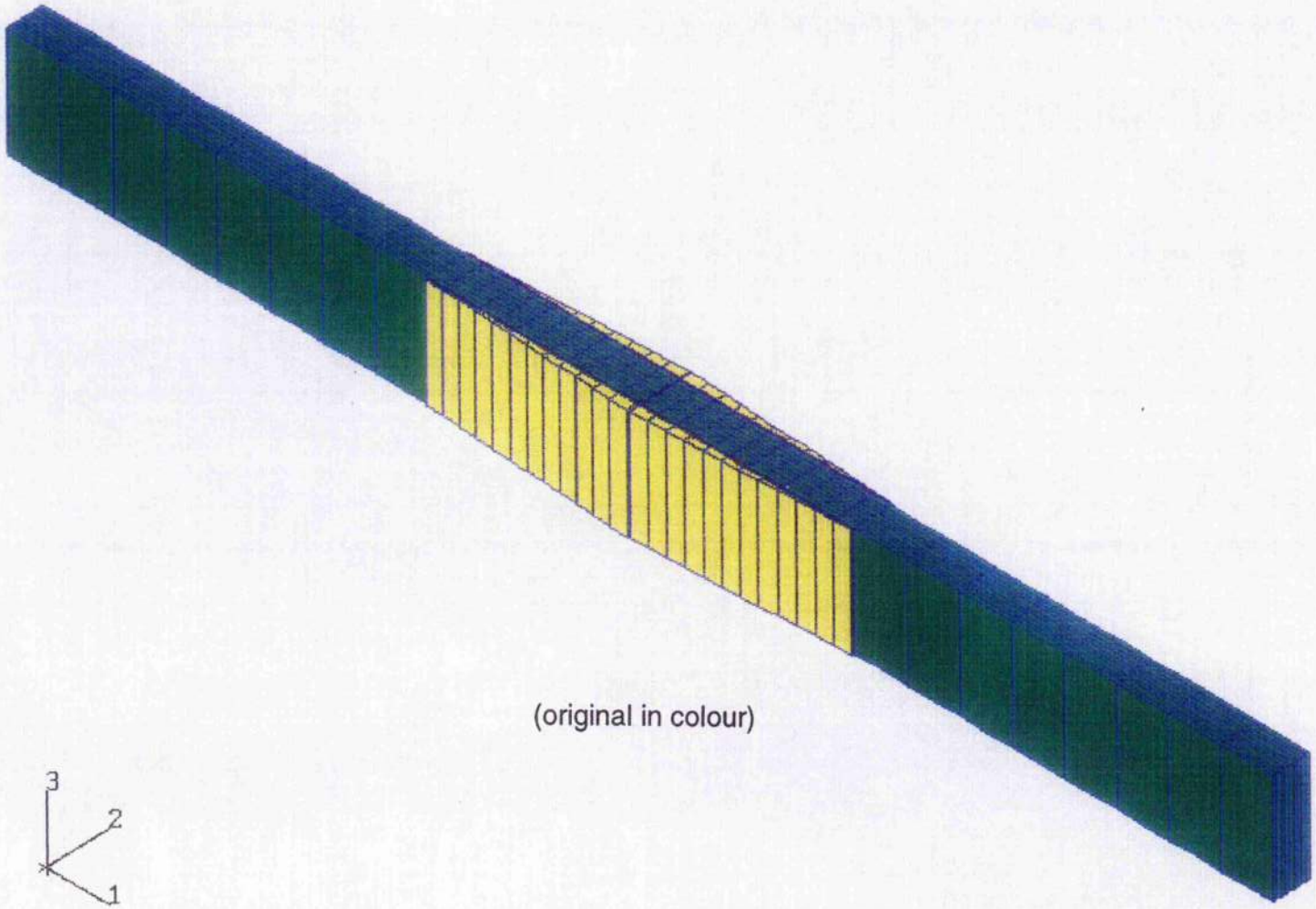

(original in colour)

Figure 3.13 Three dimensional 20 noded solid element model of a steel tapered strapped joint

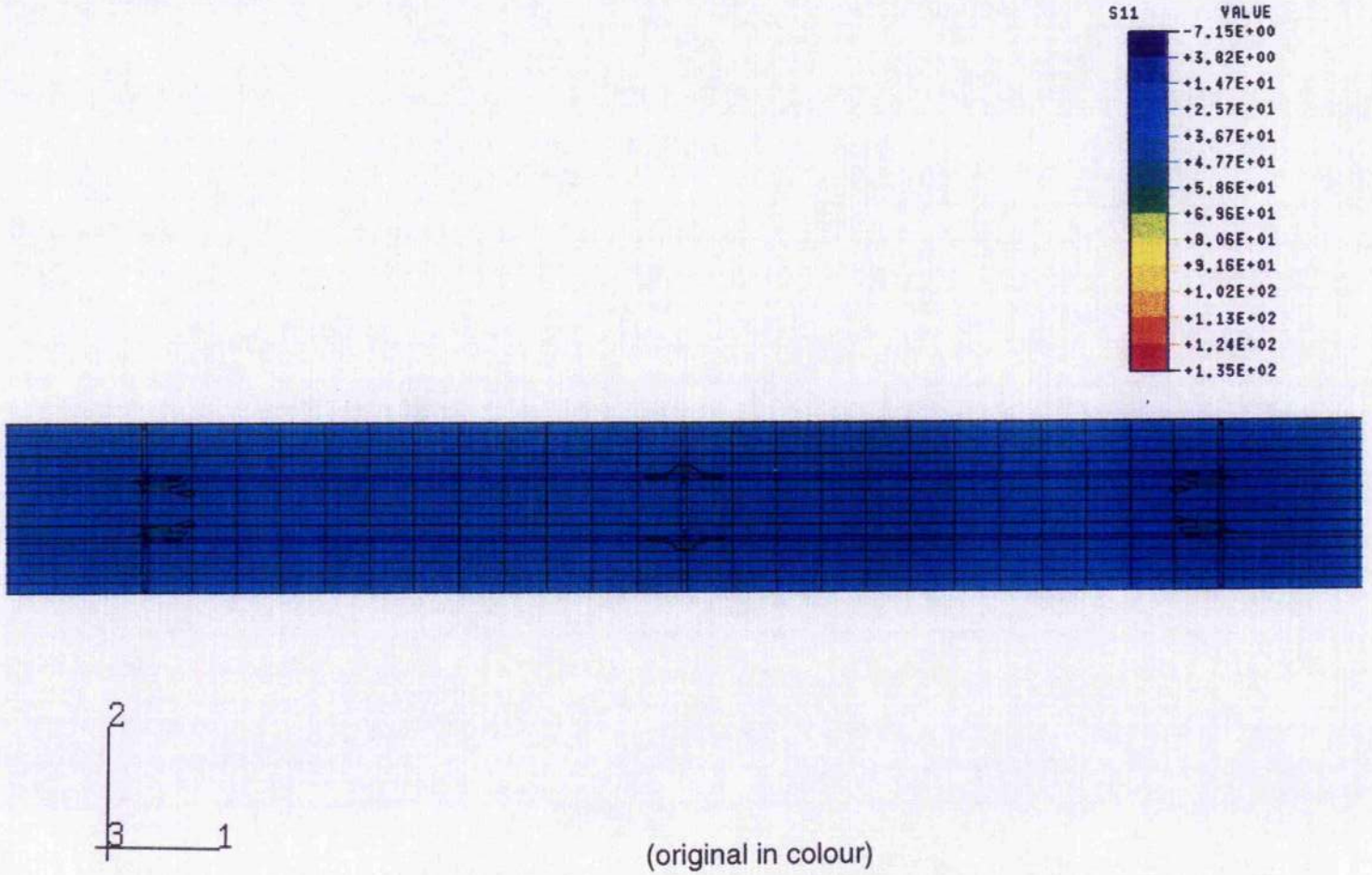

(original in colour)

Figure 3.14 Finite element stress analysis results for the recessed strap joint (tension)
a) S11

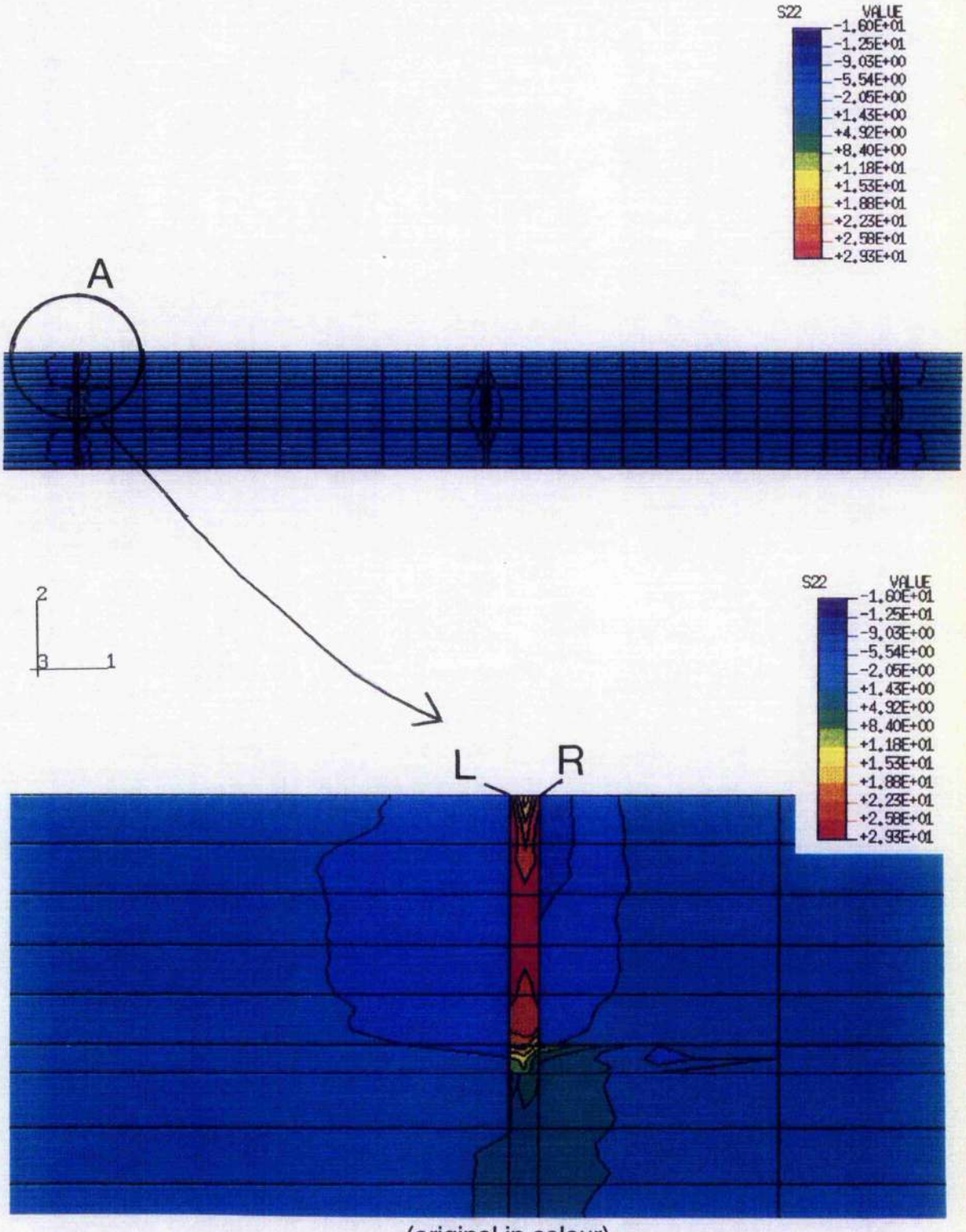

(original in colour)

Figure 3.14 Finite element stress analysis results for the recessed strap joint (tension)
b) S22

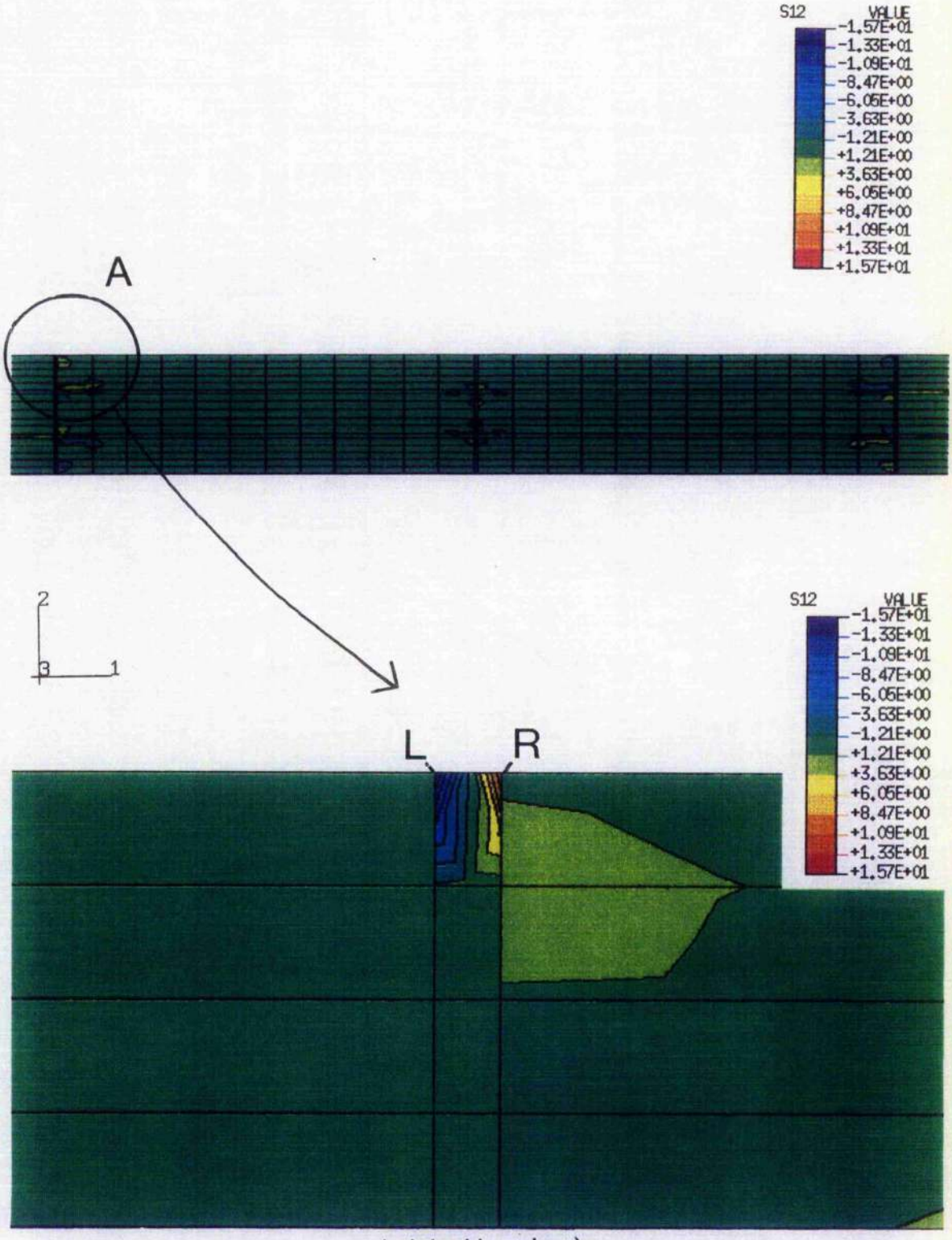

(original in colour)

Figure 3.14 Finite element stress analysis results for the recessed strap joint (tension)

c) S12

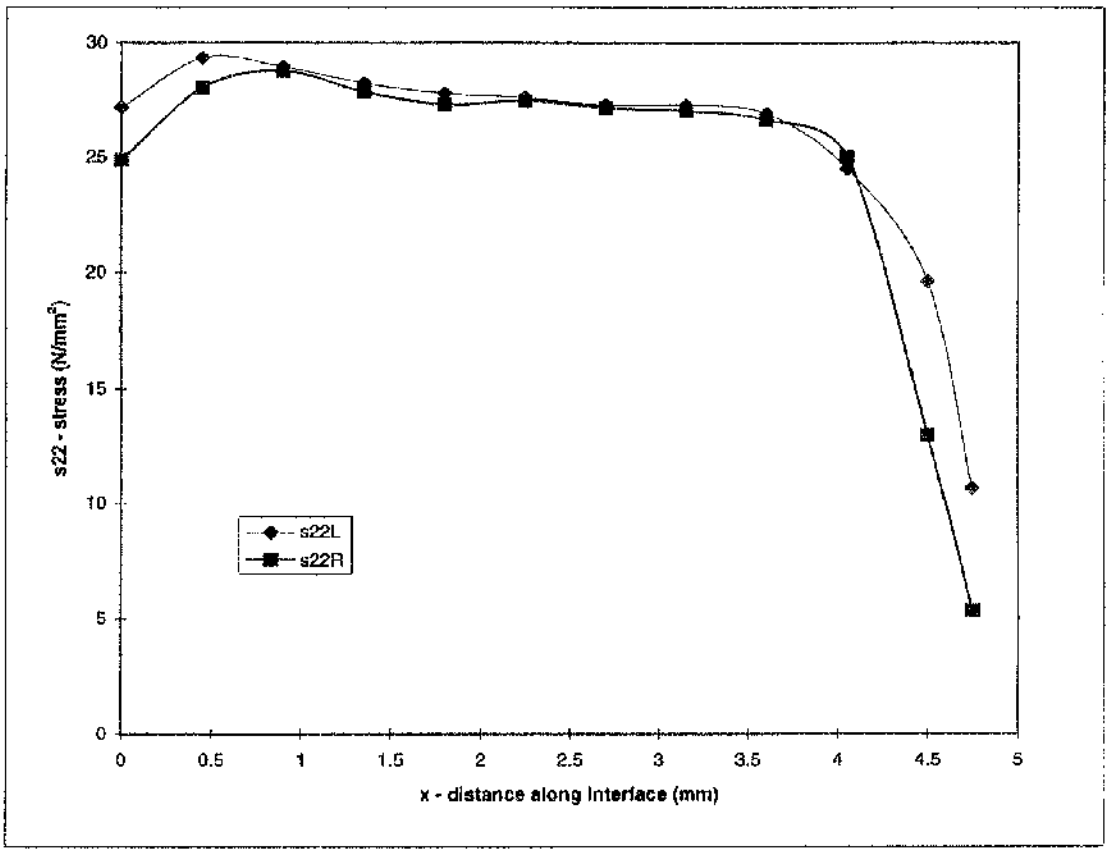

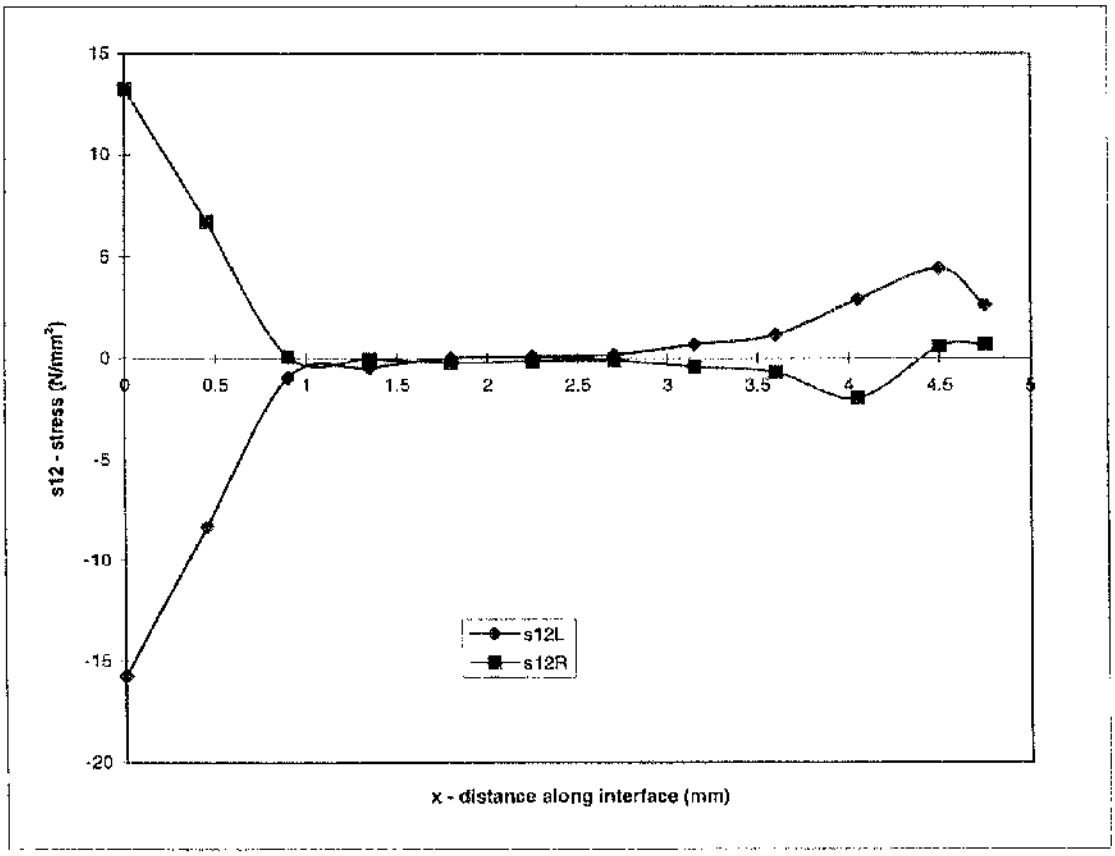

Figure 3.15 Adhesive stress (s12, s22) at the grp/adhesive interface at the position indicated in figure 3.14 of the recessed strap joint (tension)

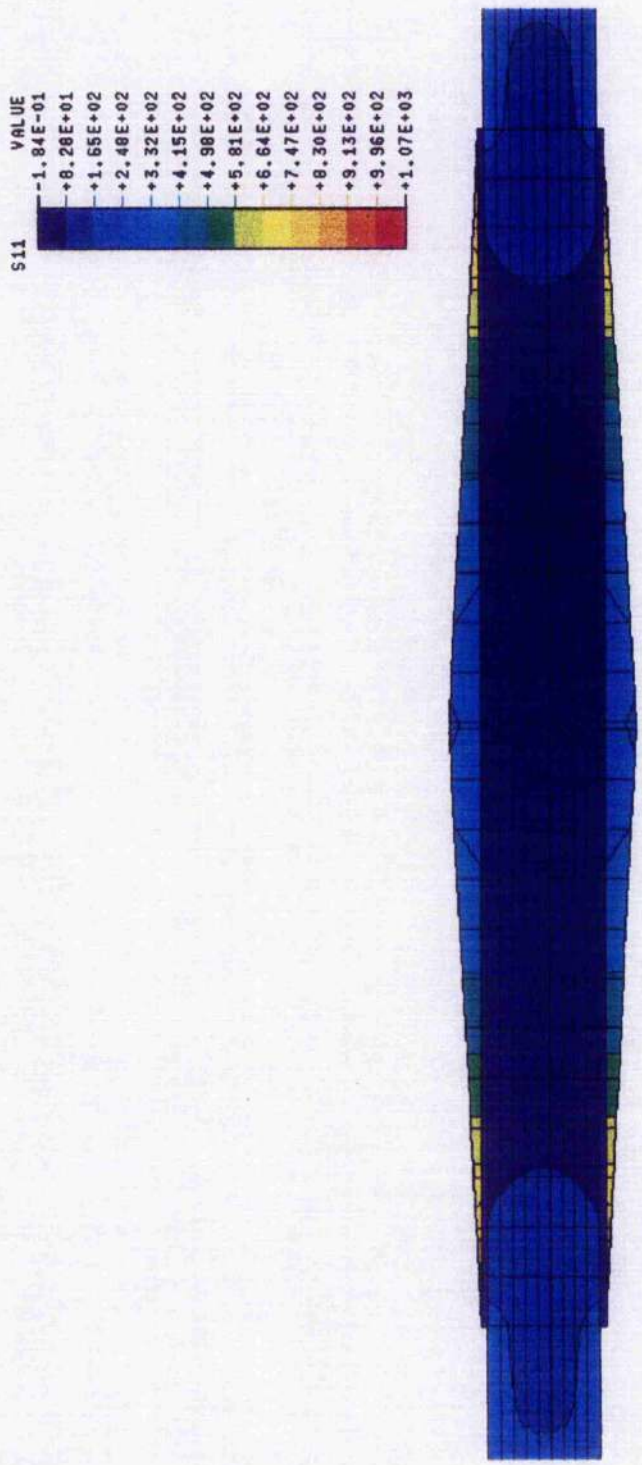

(original in colour)

Figure 3.16 Finite element stress analysis results for the steel tapered strap joint (tension)

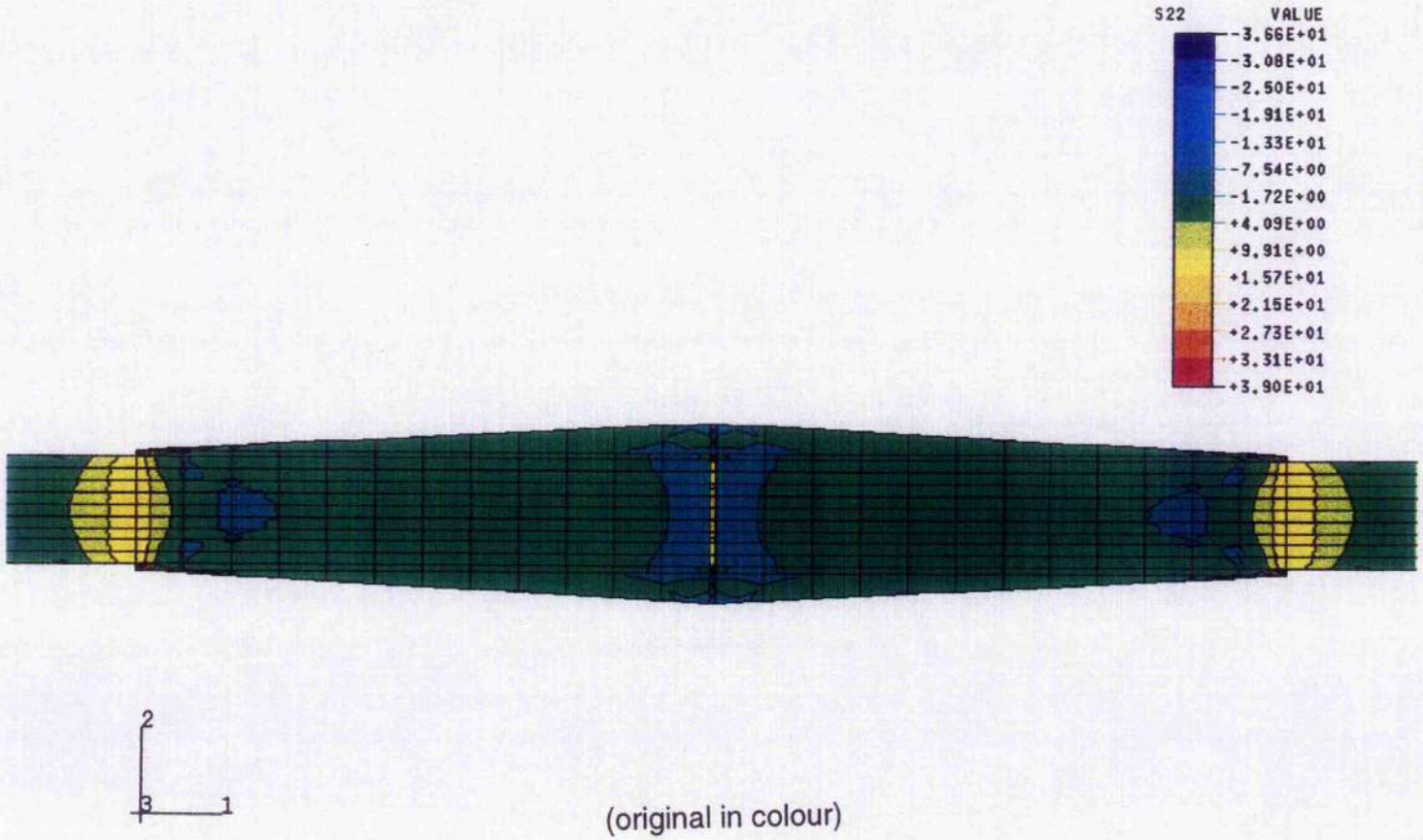

(original in colour)

Figure 3.16 Finite element stress analysis results for the steel tapered strap joint (tension) cont.

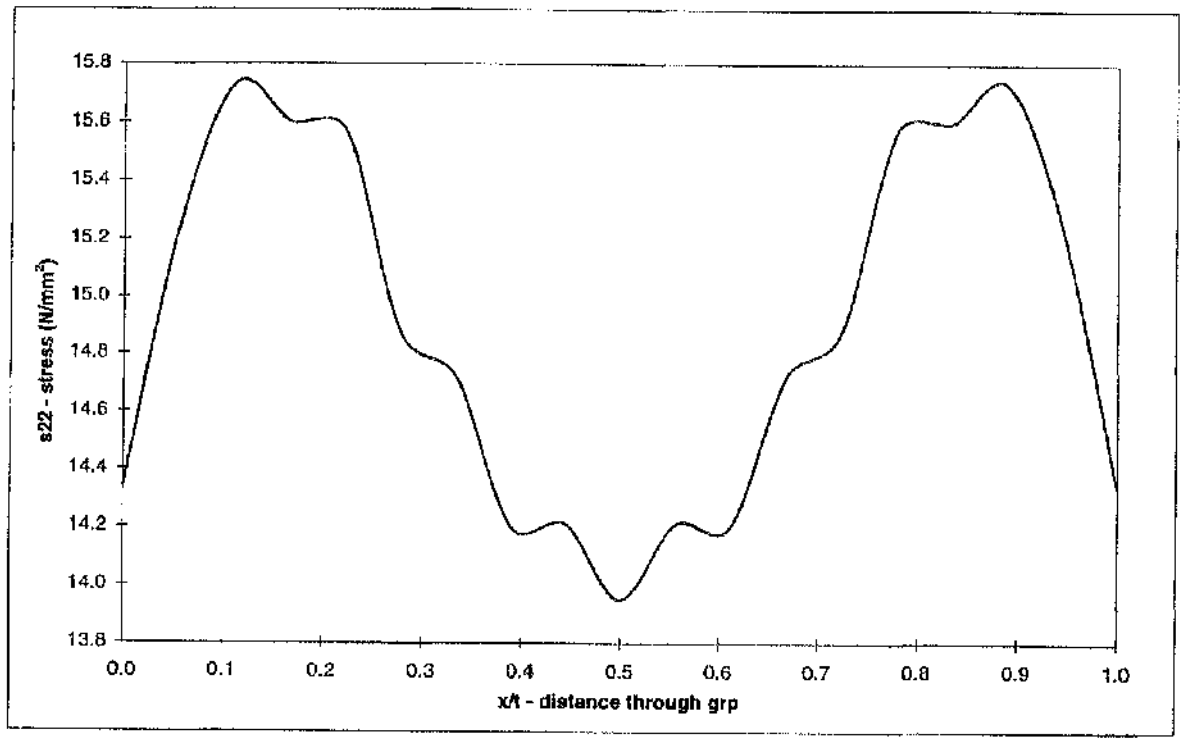

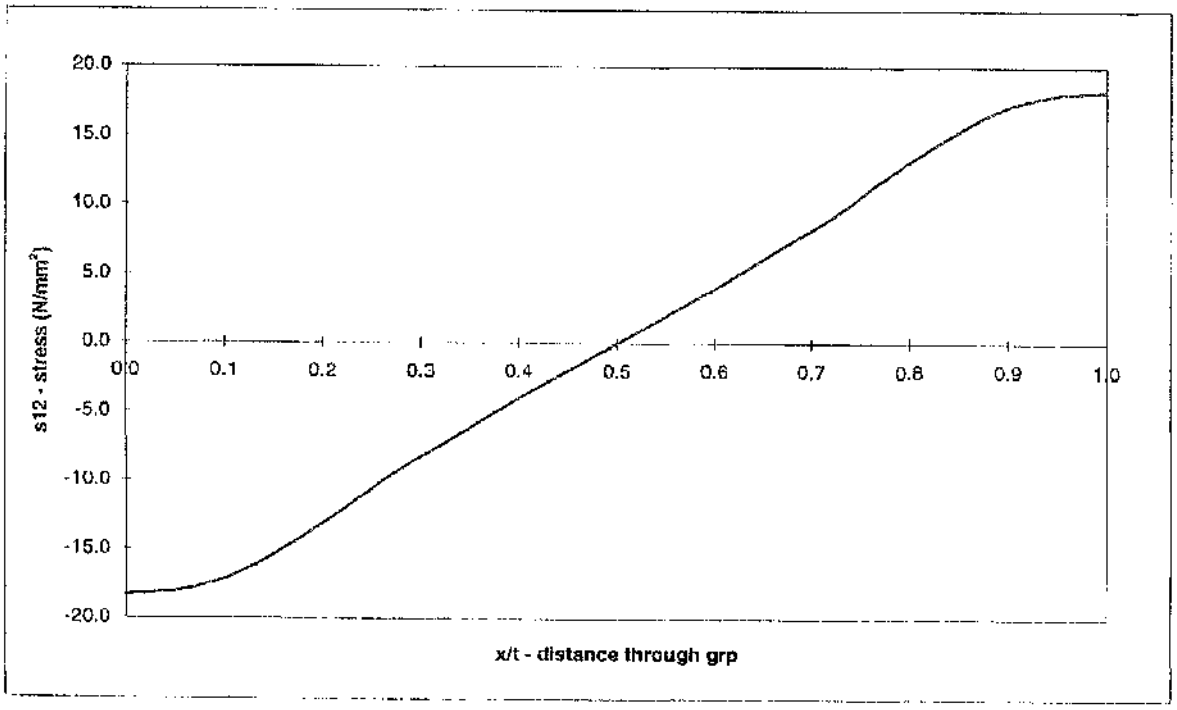

Figure 3.17 Detailed stress distribution (s12, s22) through the grp at the tip of the tapered strap (tension)

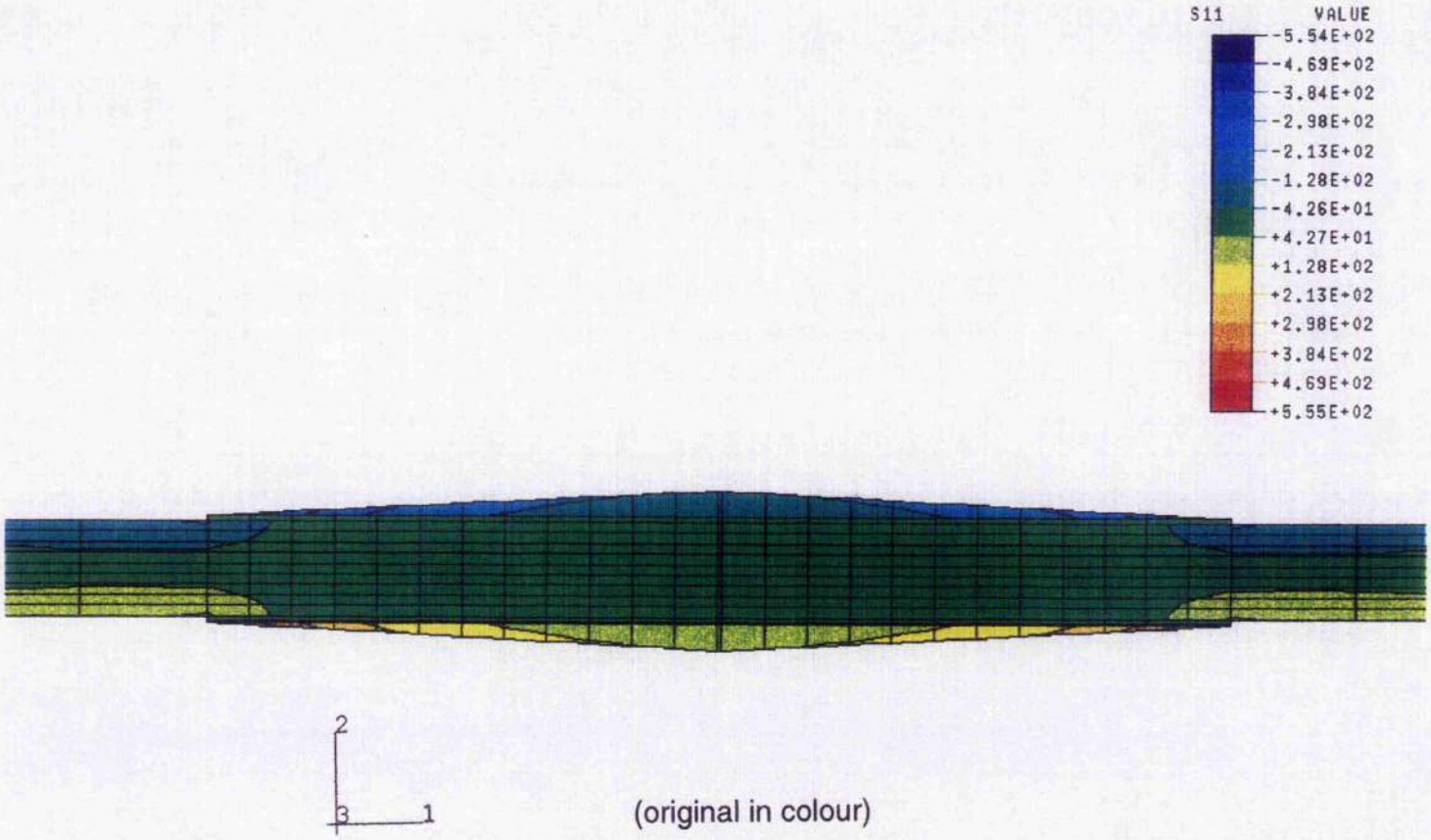

(original in colour)

Figure 3.18 Finite element stress analysis results for the steel tapered strap joint (three point bend)

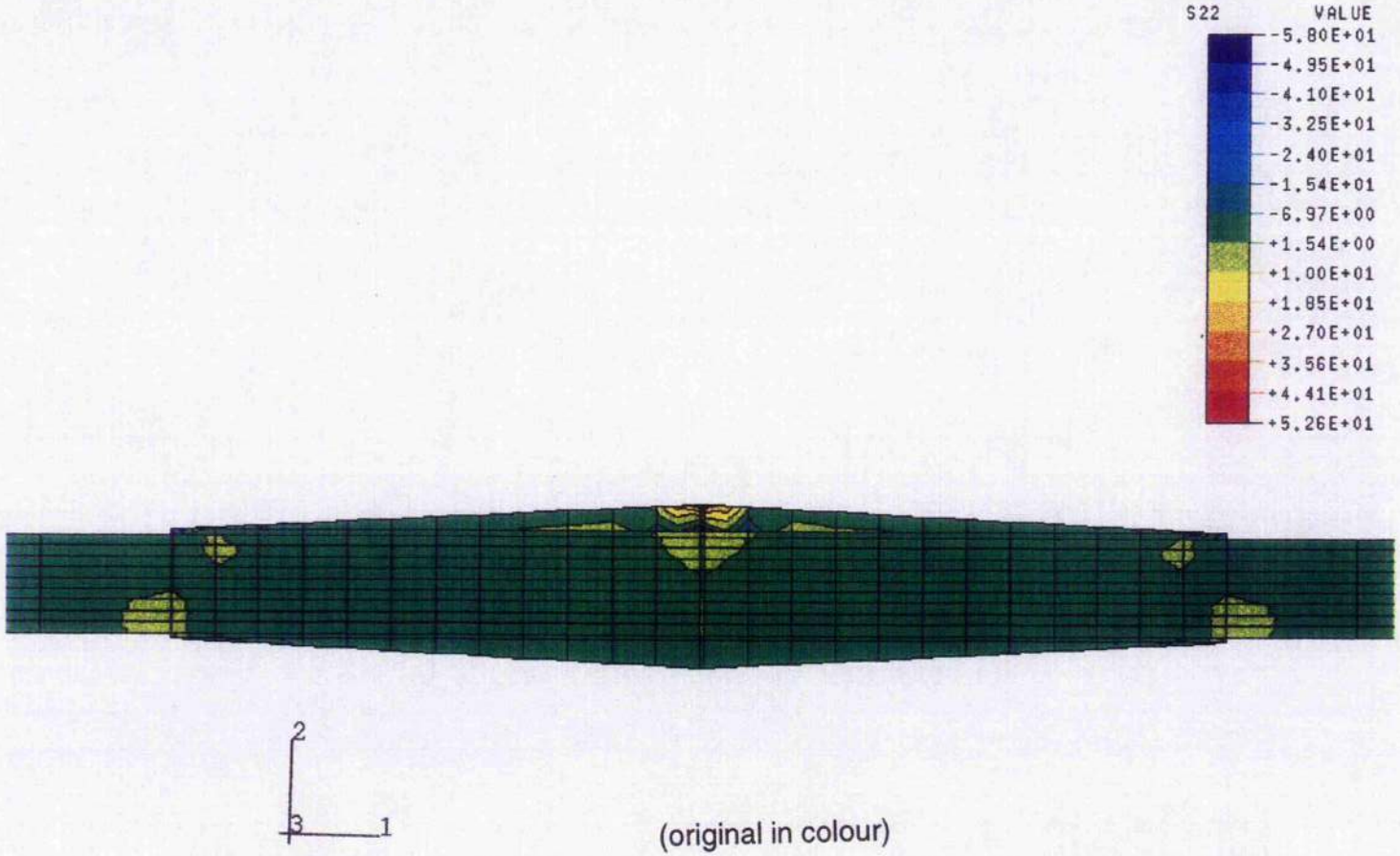

(original in colour)

Figure 3.18 Finite element stress analysis results for the steel tapered strap joint (three point bend) cont.

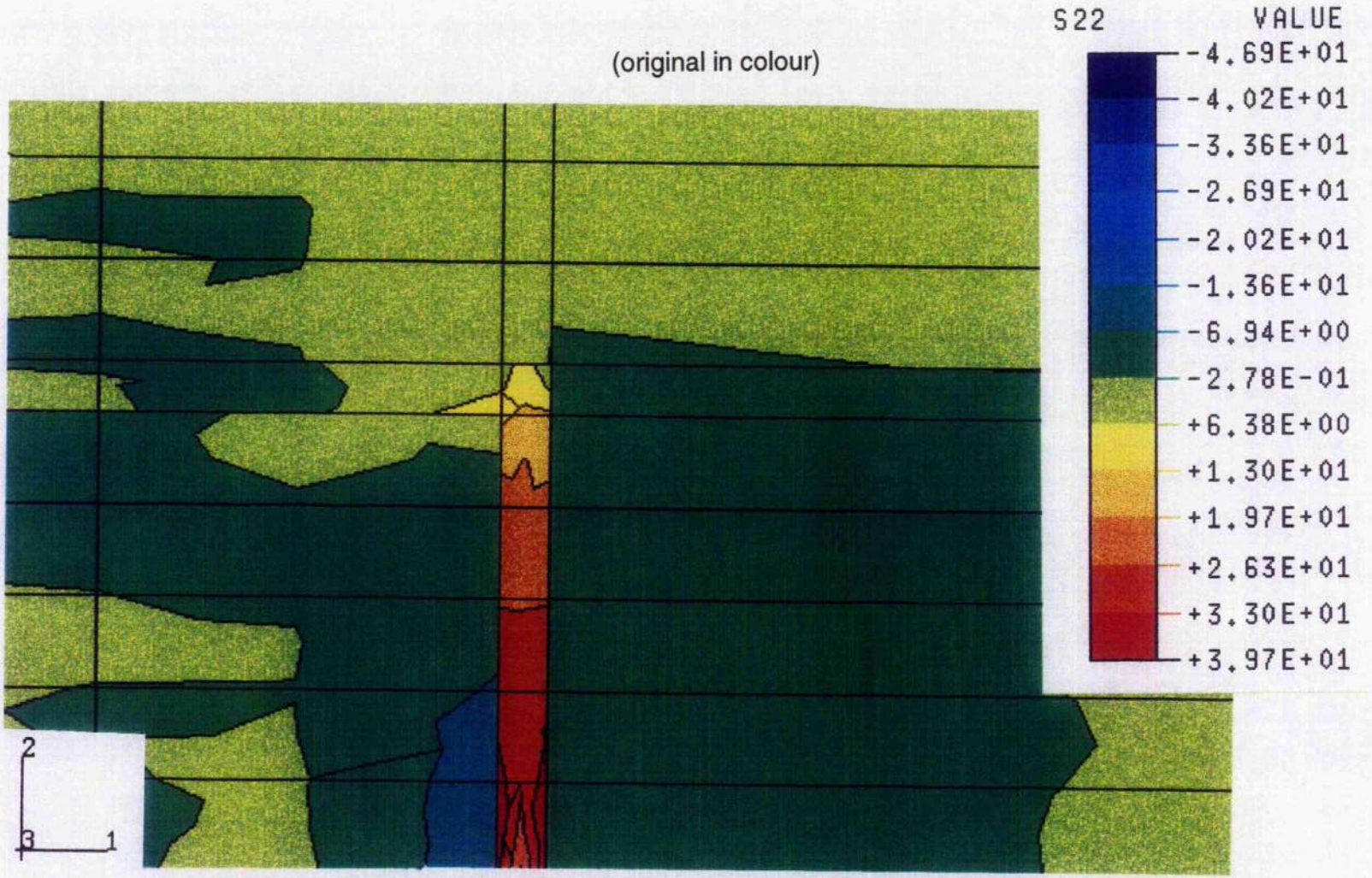

Figure 3.19 Detailed stress distribution (s22) of the recessed strap joint in the adhesive at the end of the straps (three point bend)

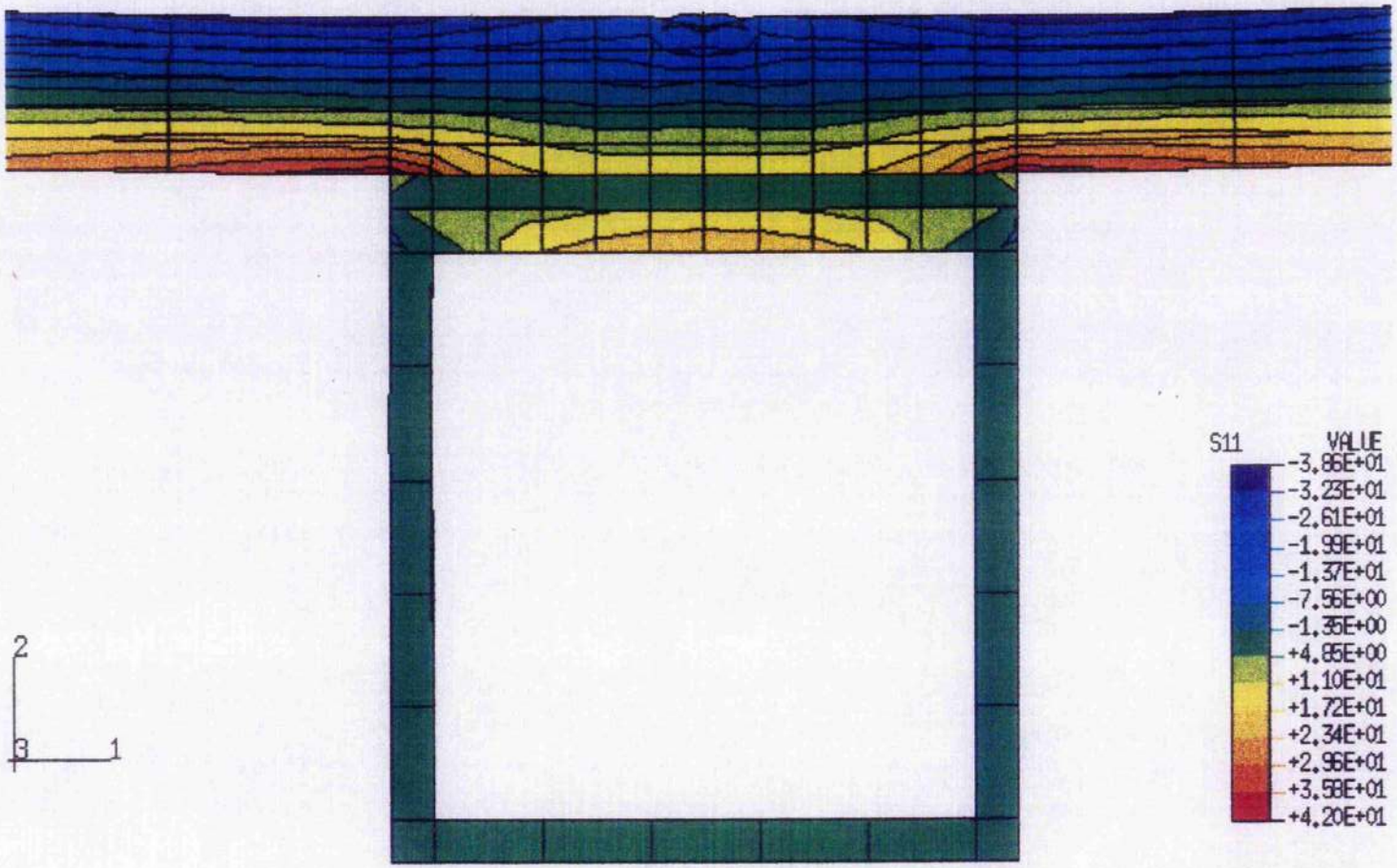

(original in colour)

Figure 3.20 Finite element stress analysis results (s11) for the unstressed attachment fatigue specimen

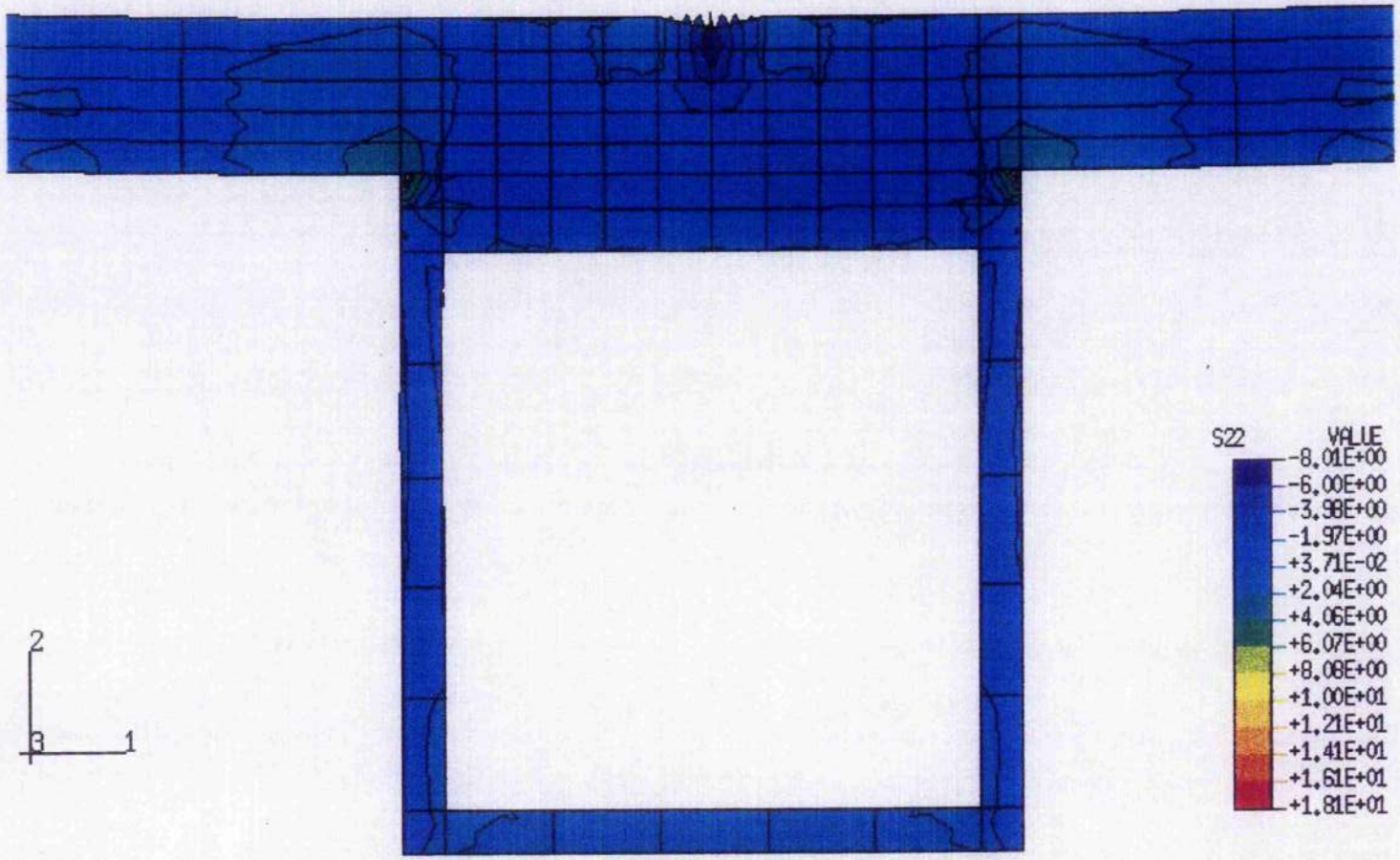

(original in colour)

Figure 3.21 Finite element stress analysis results (s22) for the unstressed attachment fatigue specimen

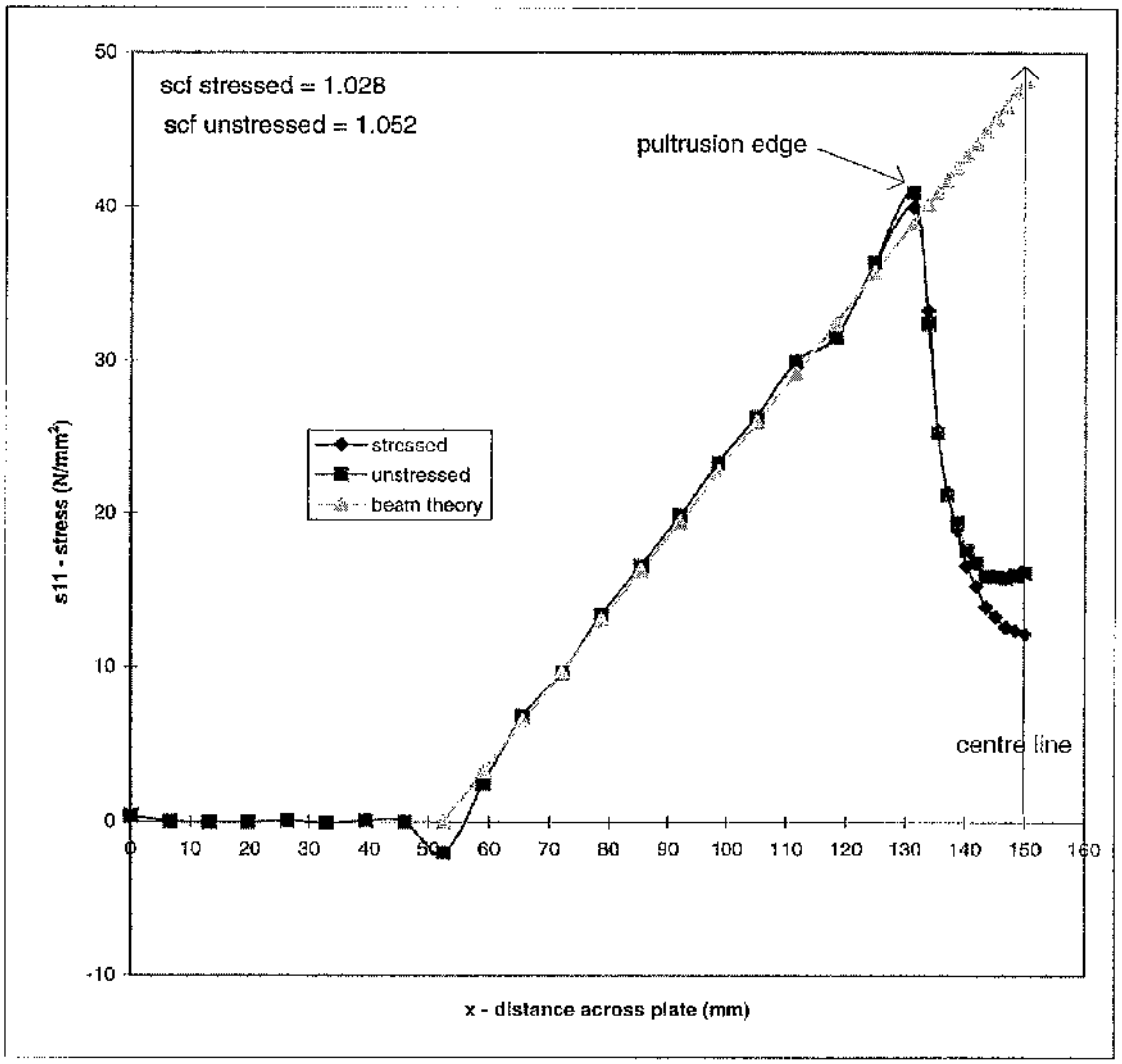

Figure 3.22 Maximum bending stress distribution in the grp plate of the fatigue specimens

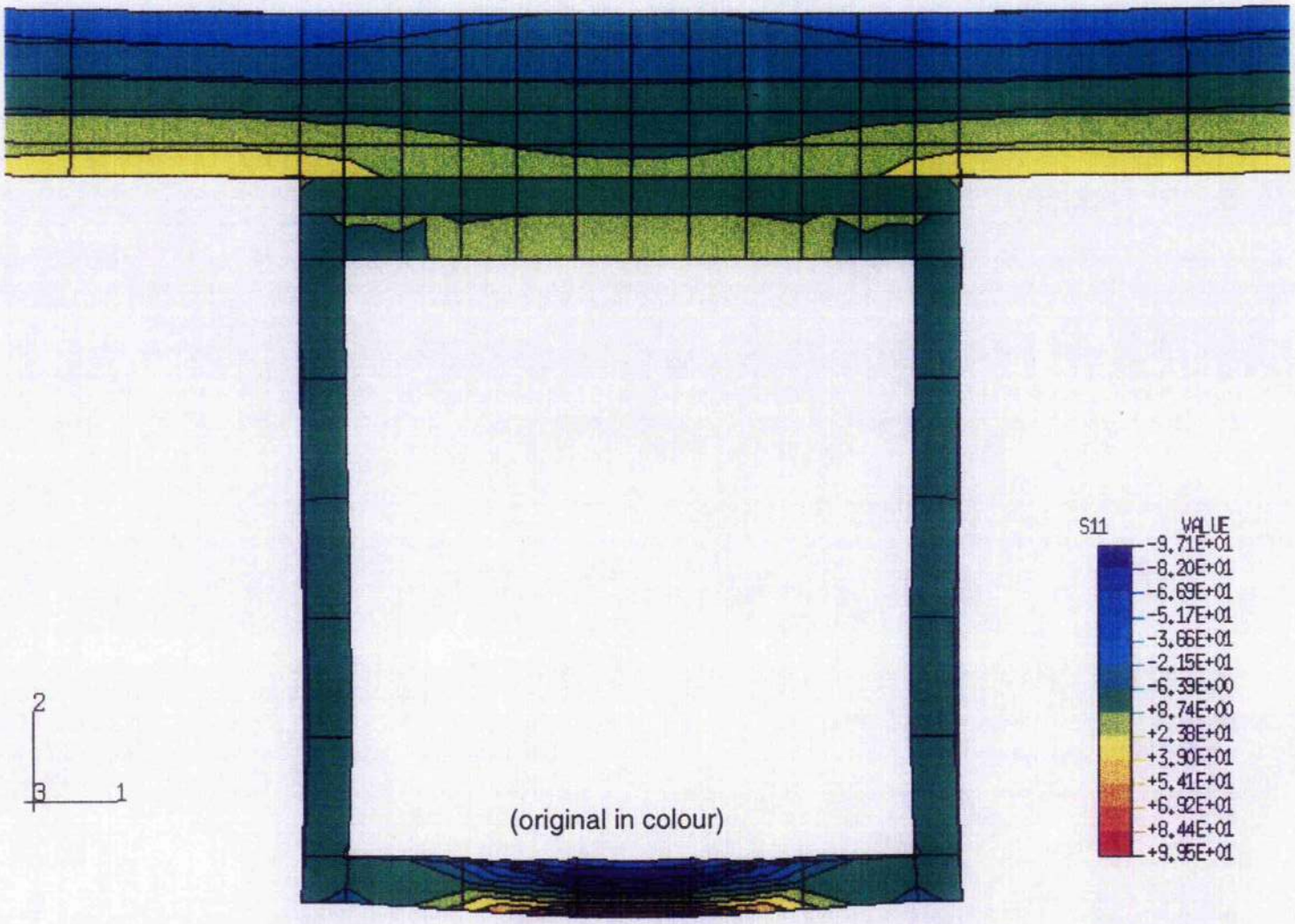

Figure 3.23 Finite element stress analysis results (s11) for the stressed attachment fatigue specimen

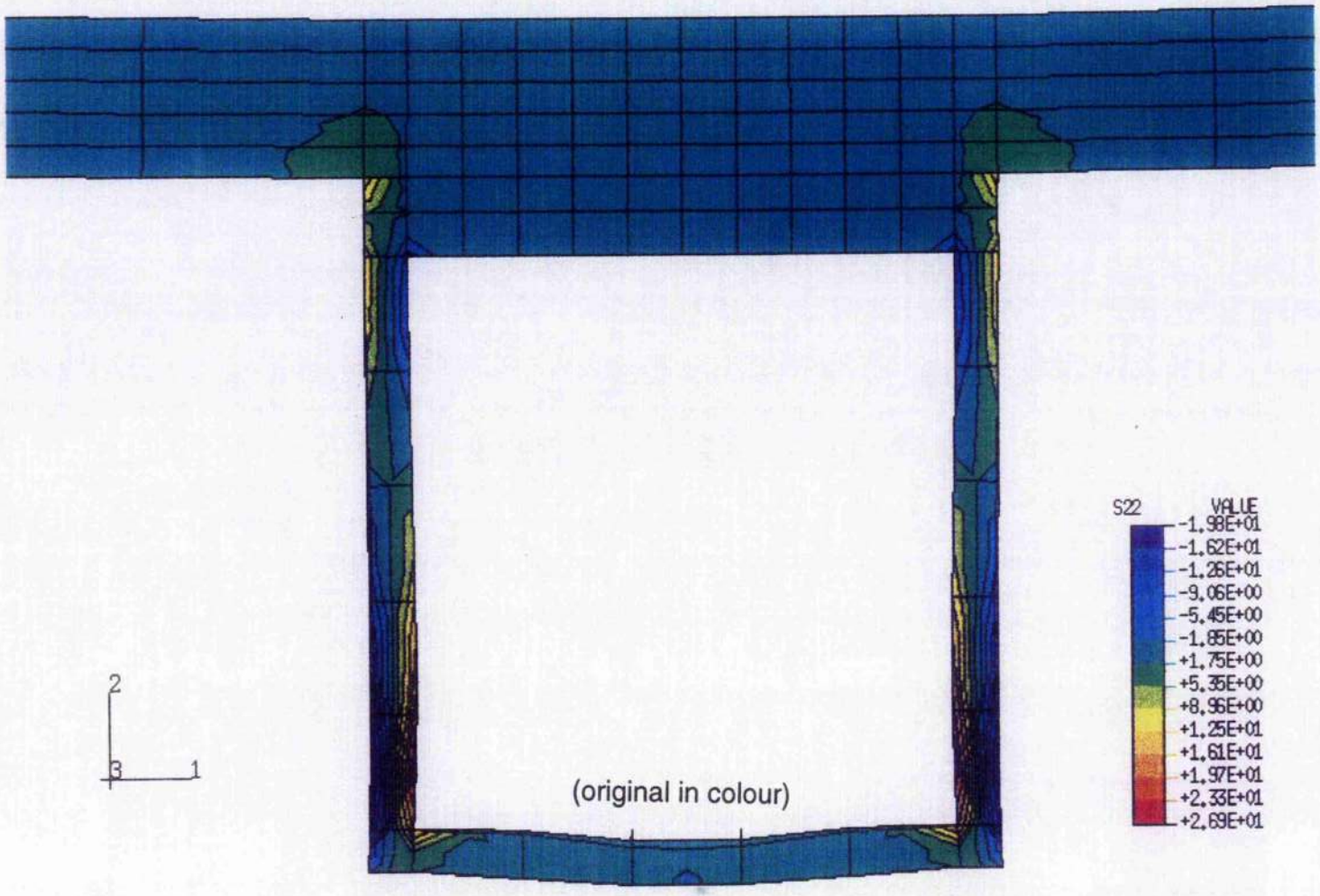

Figure 3.24 Finite element stress analysis results (s22) for the stressed attachment fatigue specimen

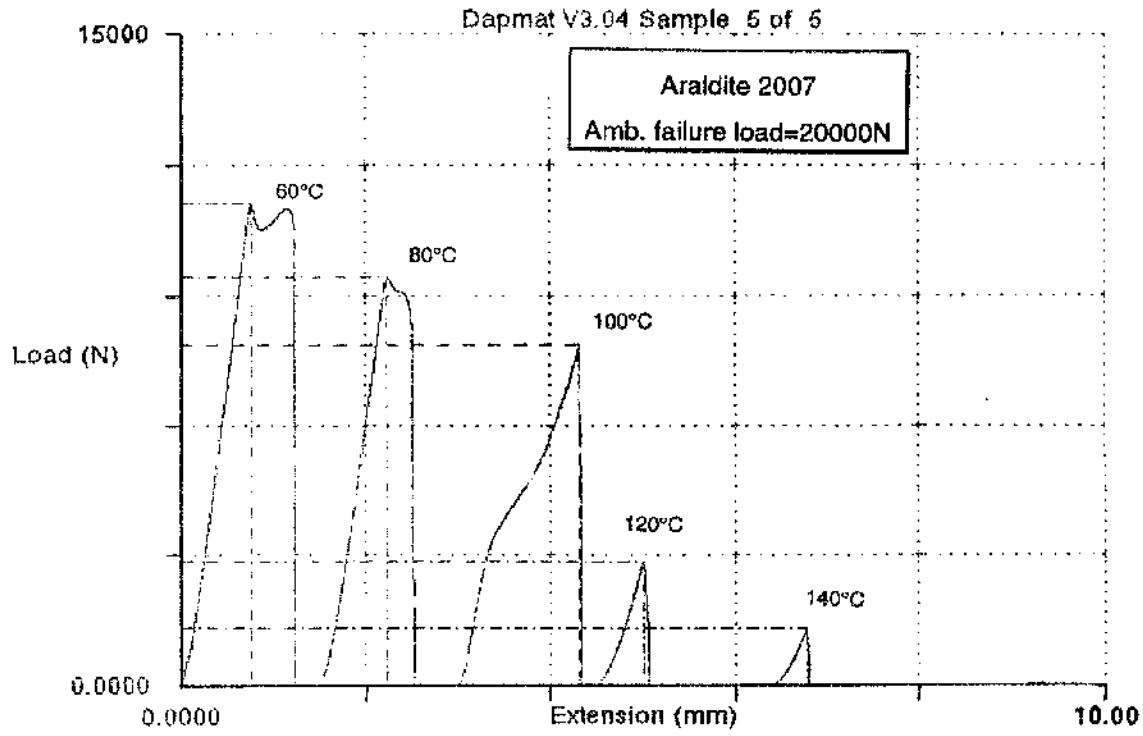

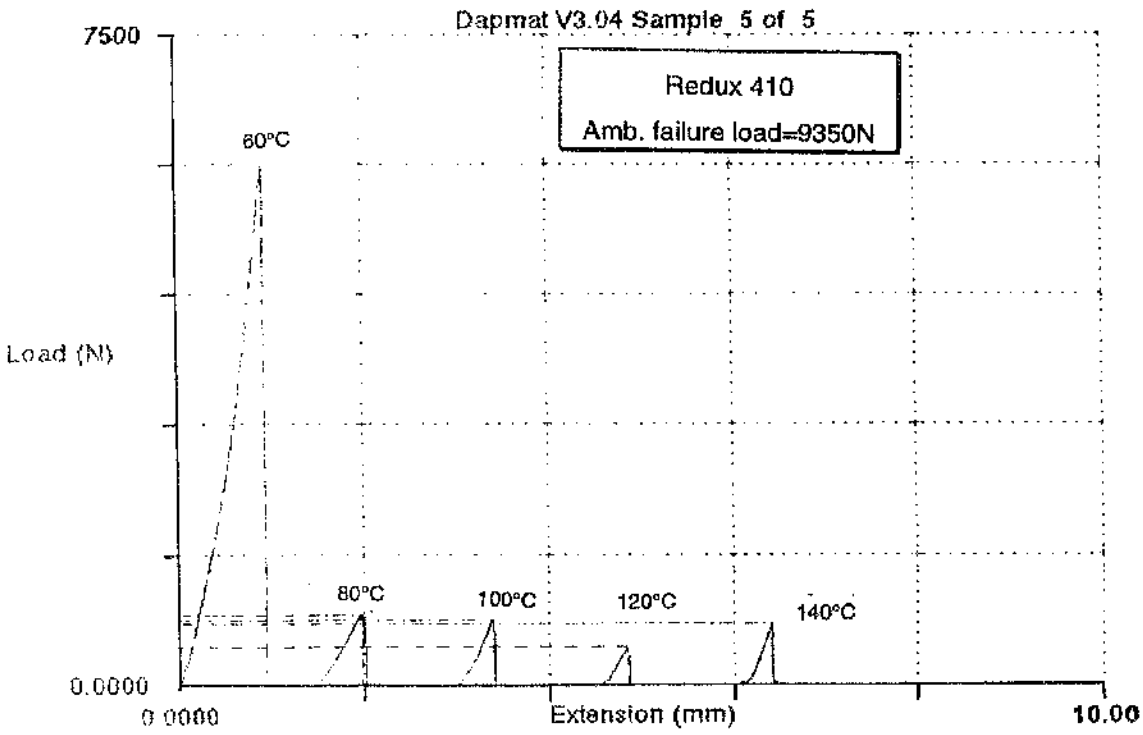

Figure 3.25 Experimental load - displacement curves obtained for Redux 410 and Araldite 2007 bonded steel lap shear joints at elevated temperatures (XSA 15x25mm)

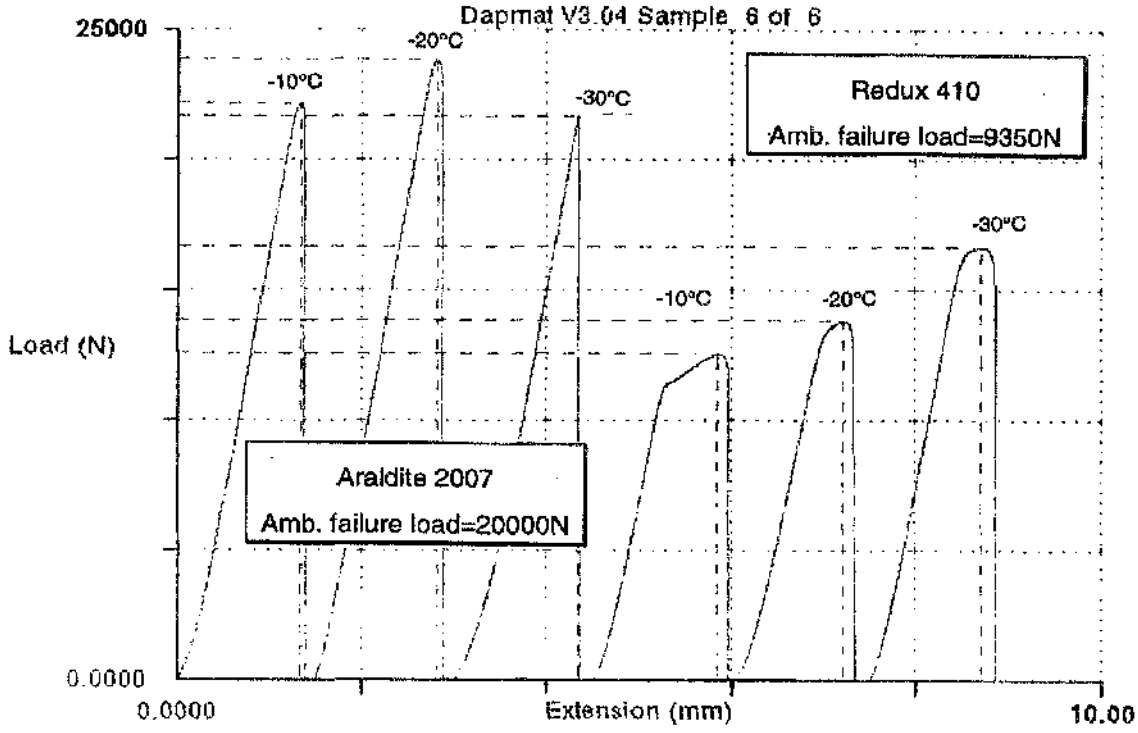

Figure 3.26 Experimental load - displacement curves obtained for Redux 410 and Araldite 2007 bonded steel lap shear joints at sub zero temperatures (XSA 15x25mm)

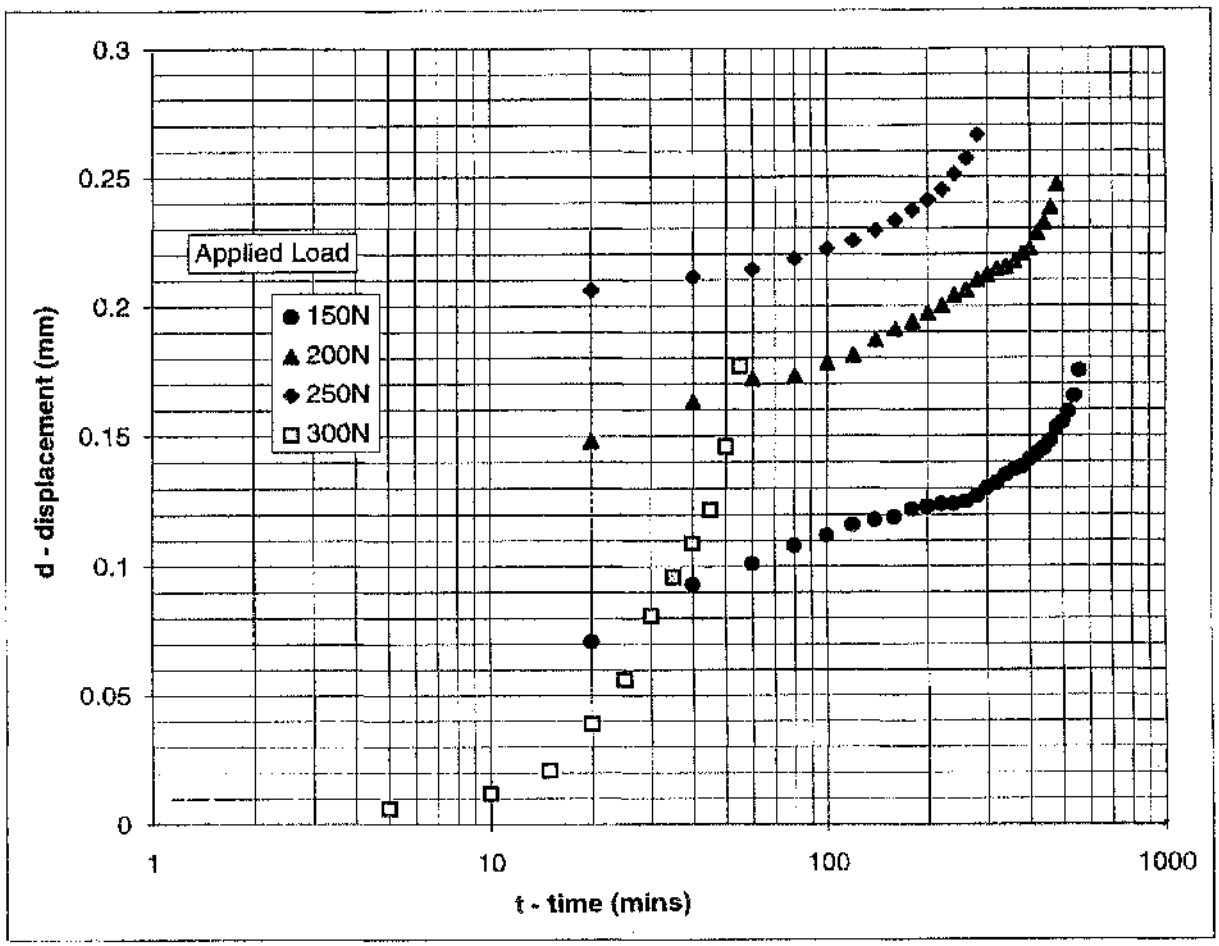

Figure 3.27 Creep curves for Redux 410 bonded grp/steel tensile shear specimens sustaining various loads at 100°C displayed on a log time graph (XSA 15x25mm)

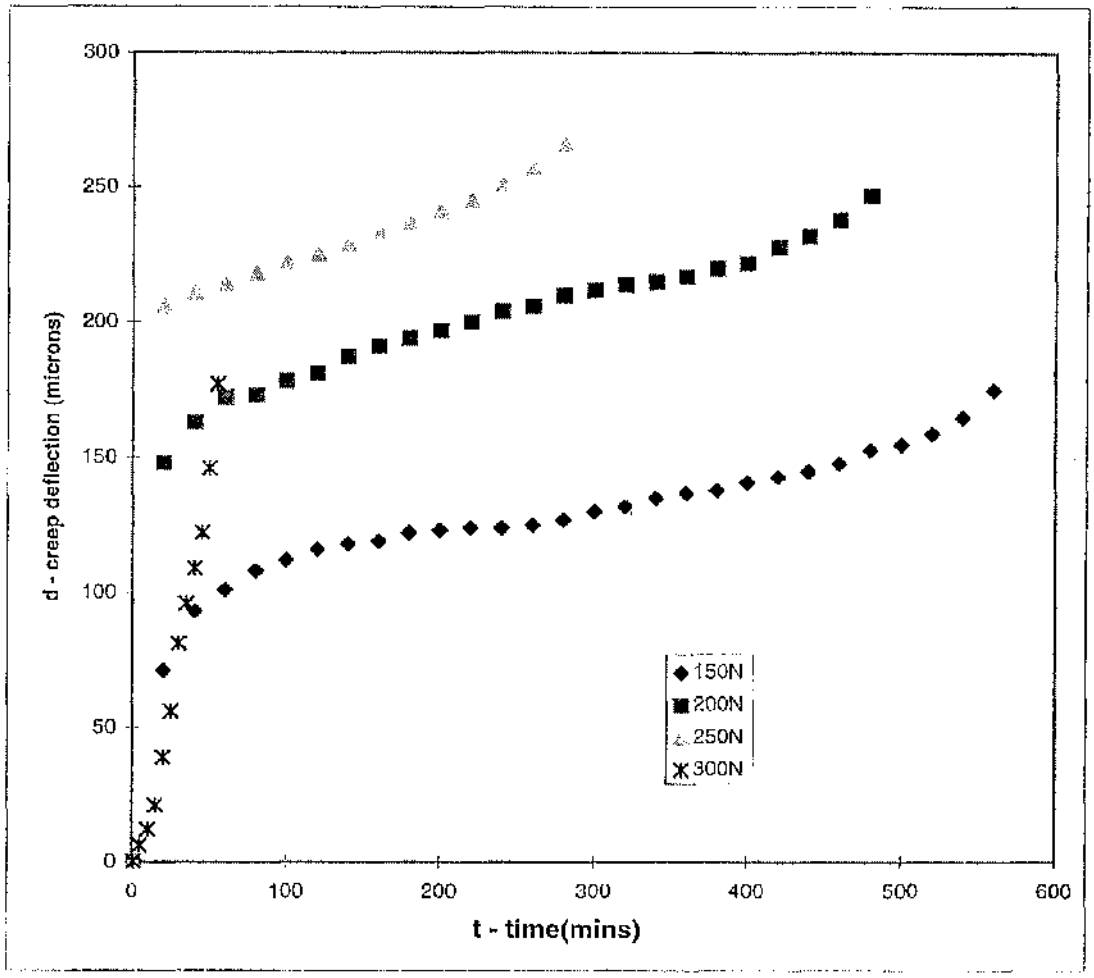

Figure 3.28 Creep curves for Redux 410 bonded grp/steel tensile shear specimens sustaining various loads at 100°C displayed on a linear time graph (XSA 15x25mm)

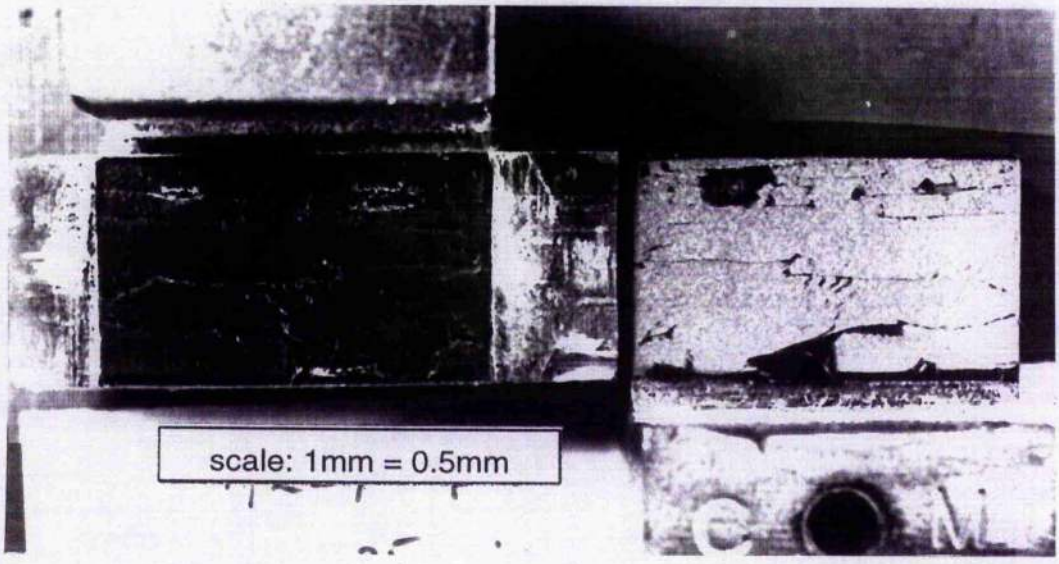

Figure 3.29 Failure surface of a Redux 410 bonded grp/steel tensile shear specimen

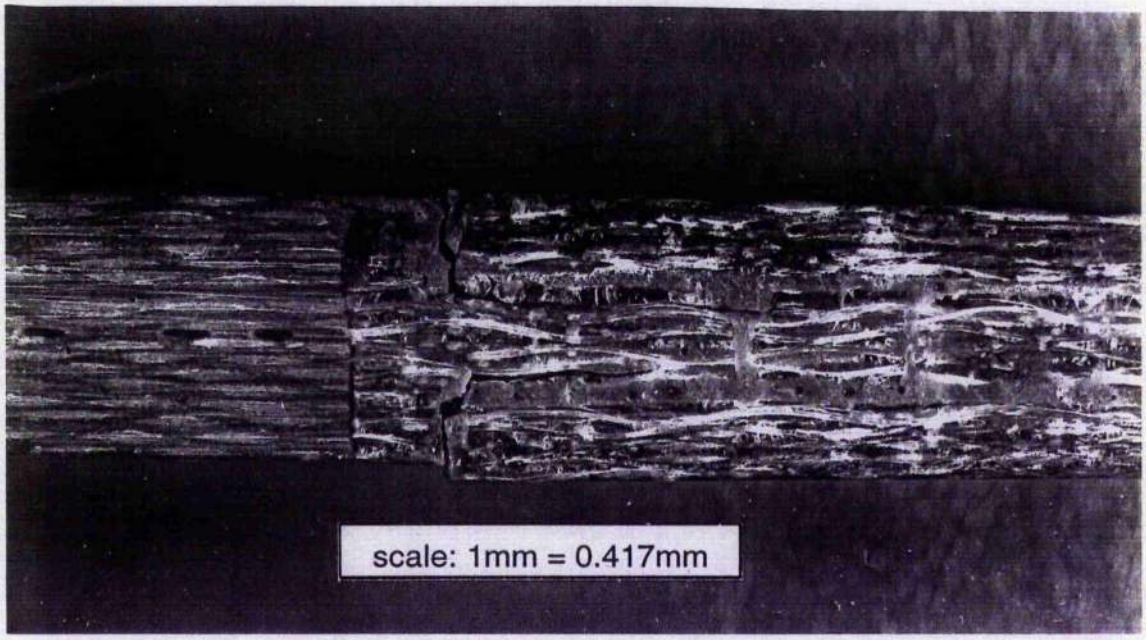

Figure 3.30 Recessed strap joint tested in tension demonstrating an adhesive failure

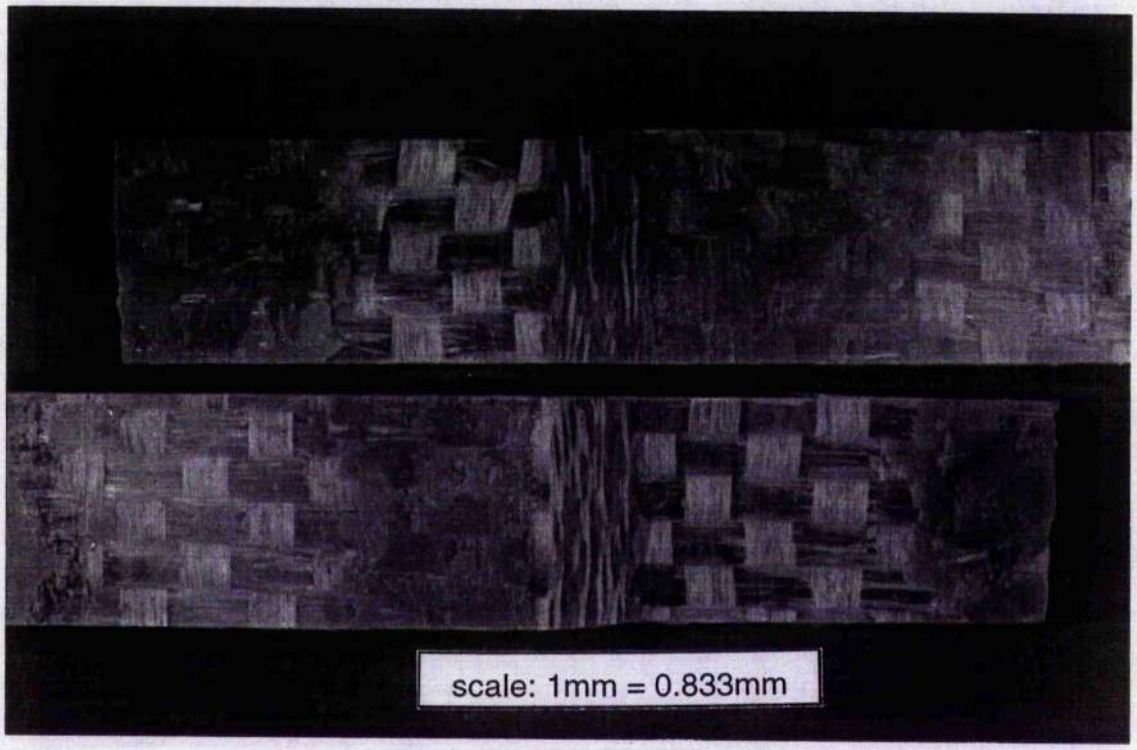

Figure 3.31 Double strap grp joint tested in tension demonstrating a resin type failure

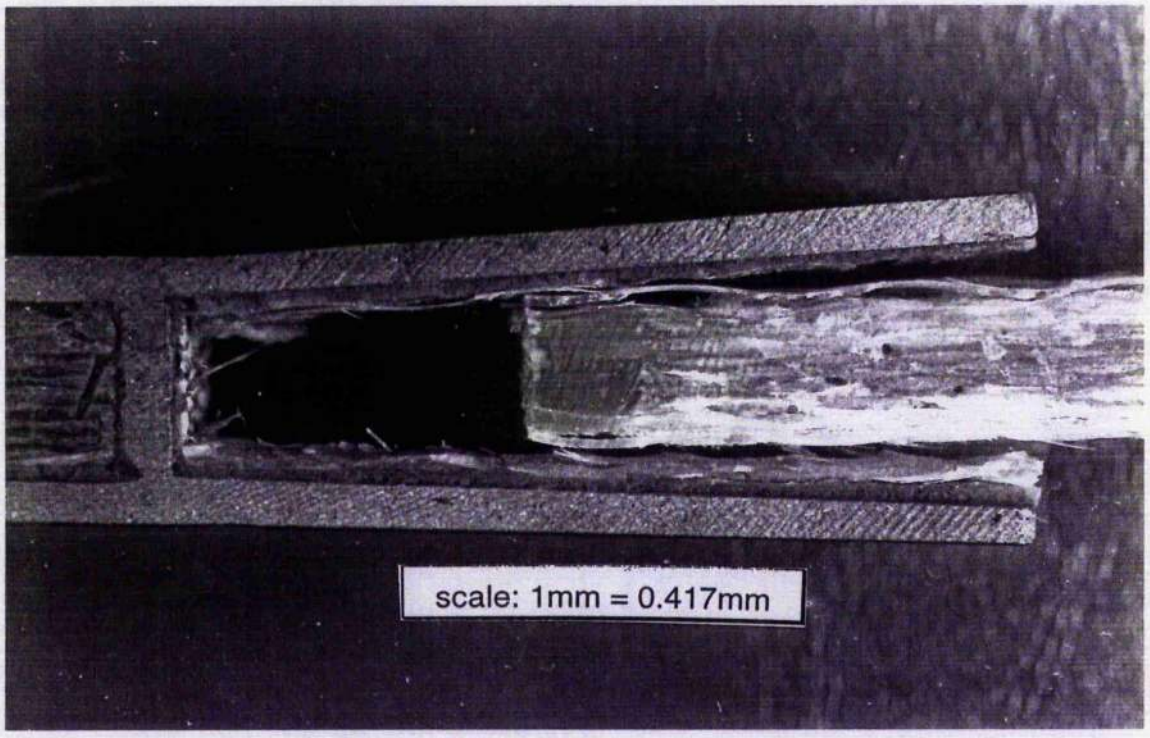

Figure 3.32 H - section steel strap joint demonstrating an interply delamination failure

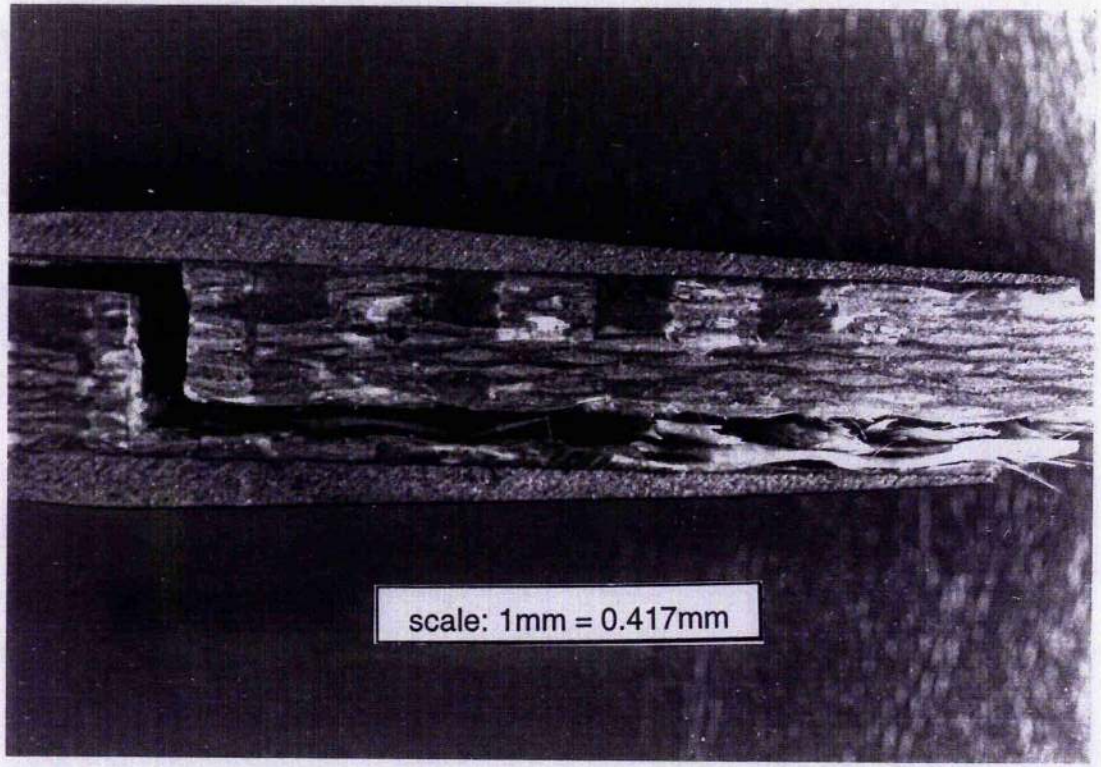

Figure 3.33 Steel tapered strap joint demonstrating an interply delamination failure

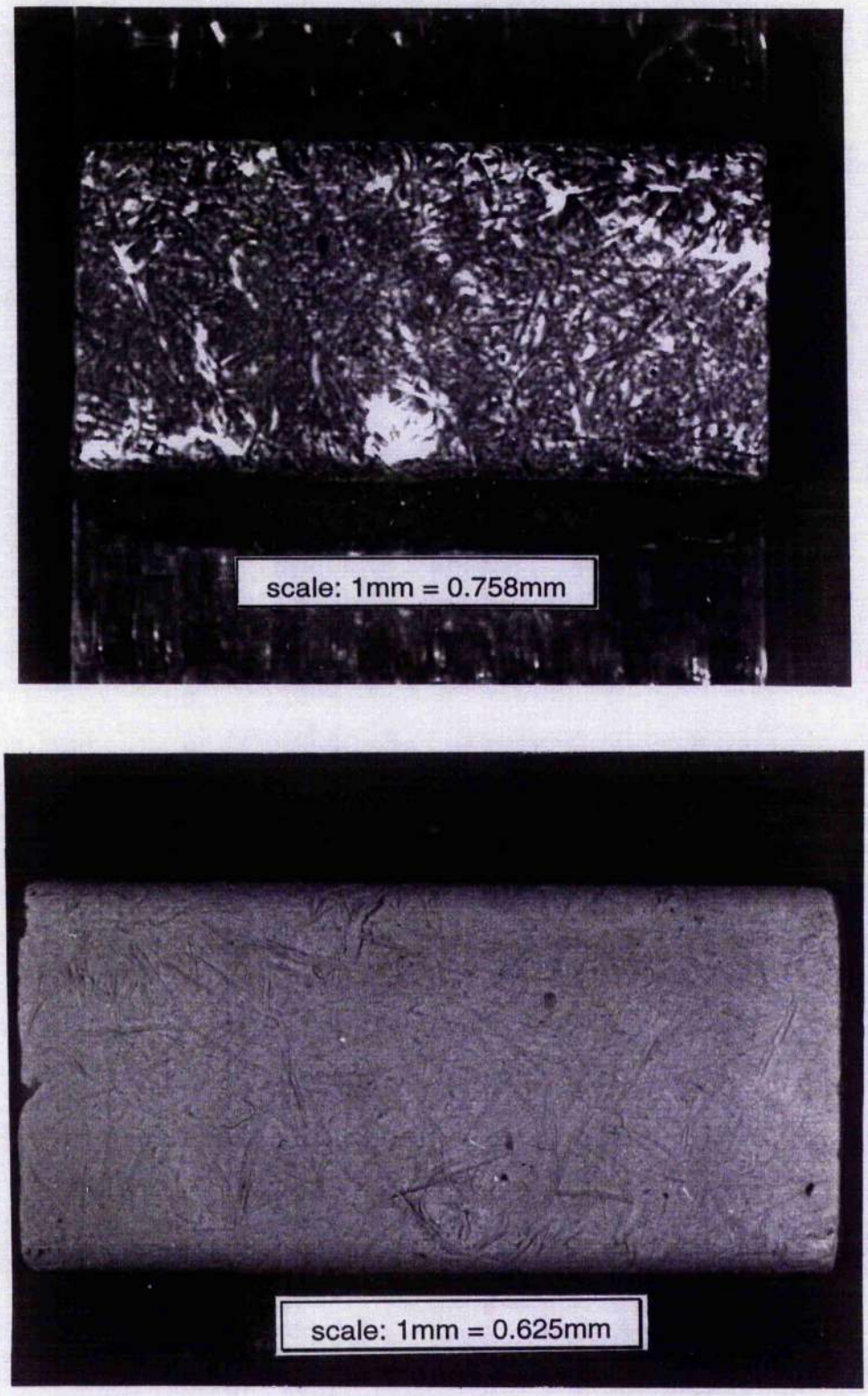

Figure 3.34 Fatigue failure surfaces in the pultrusion of the stressed attachment

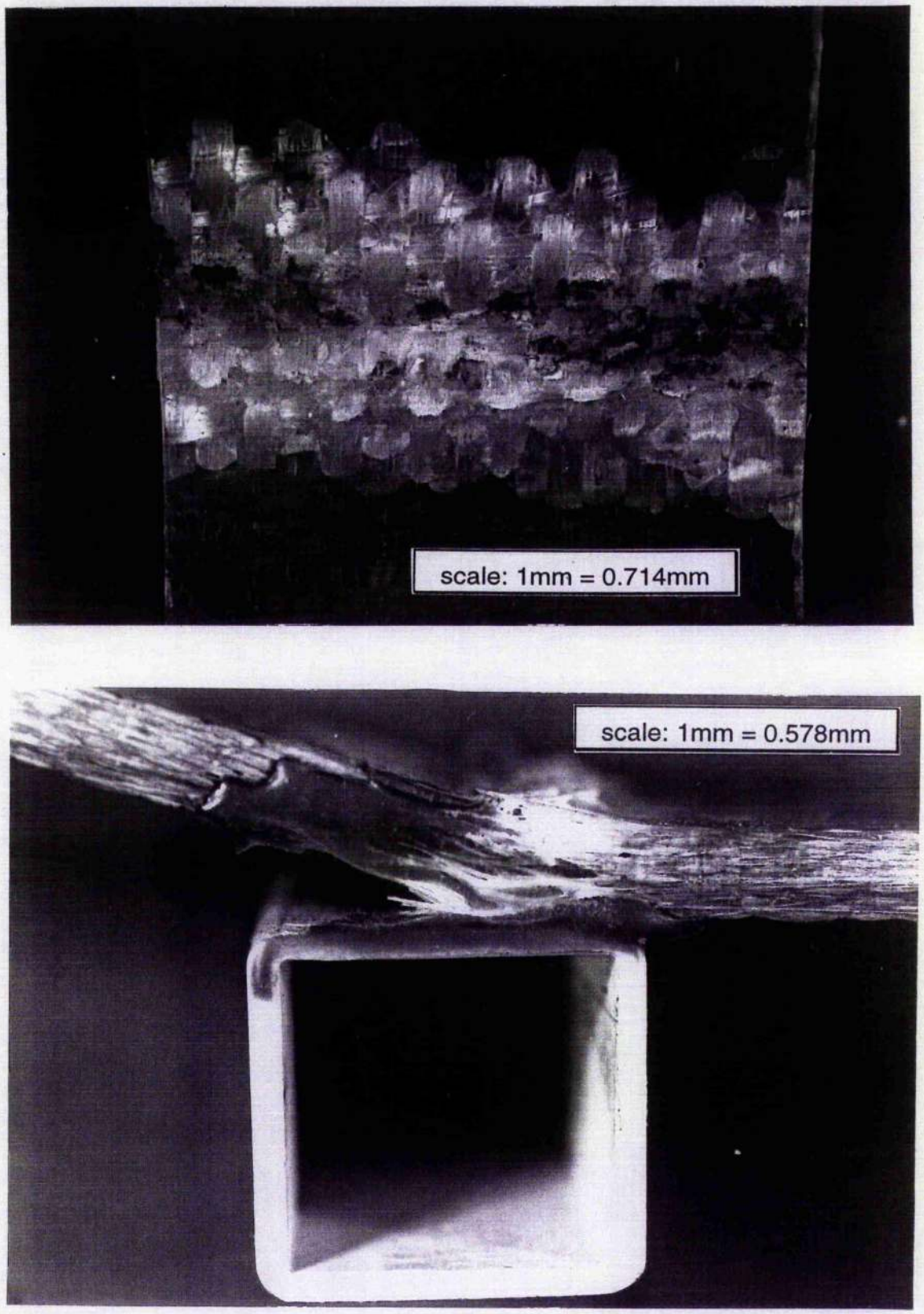

Figure 3.35 Fatigue failure surfaces of the unstressed attachment

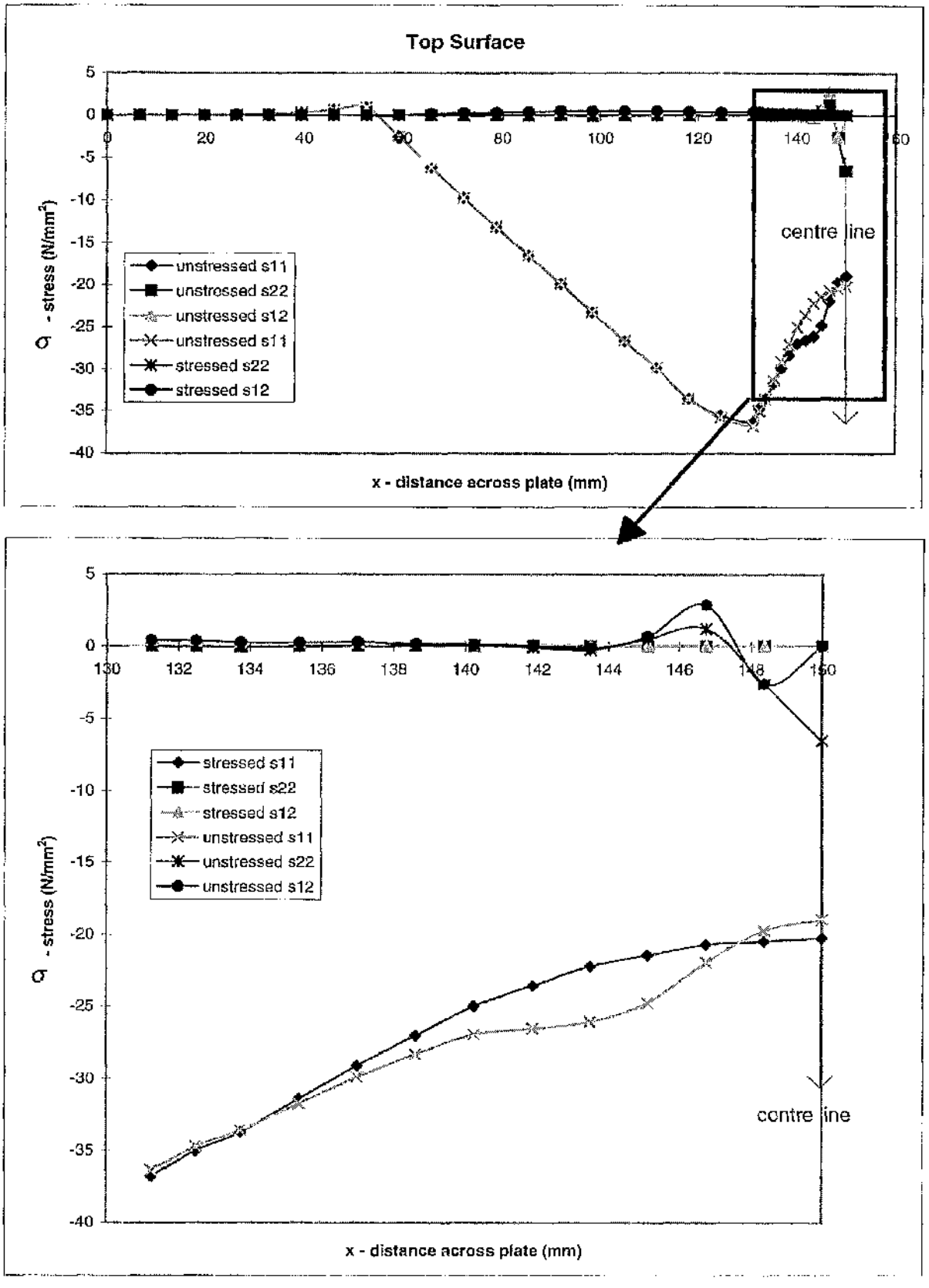

Figure 3.36 Detailed variation of stresses across the plate top surface and at the first ply level of the unstressed fatigue specimen

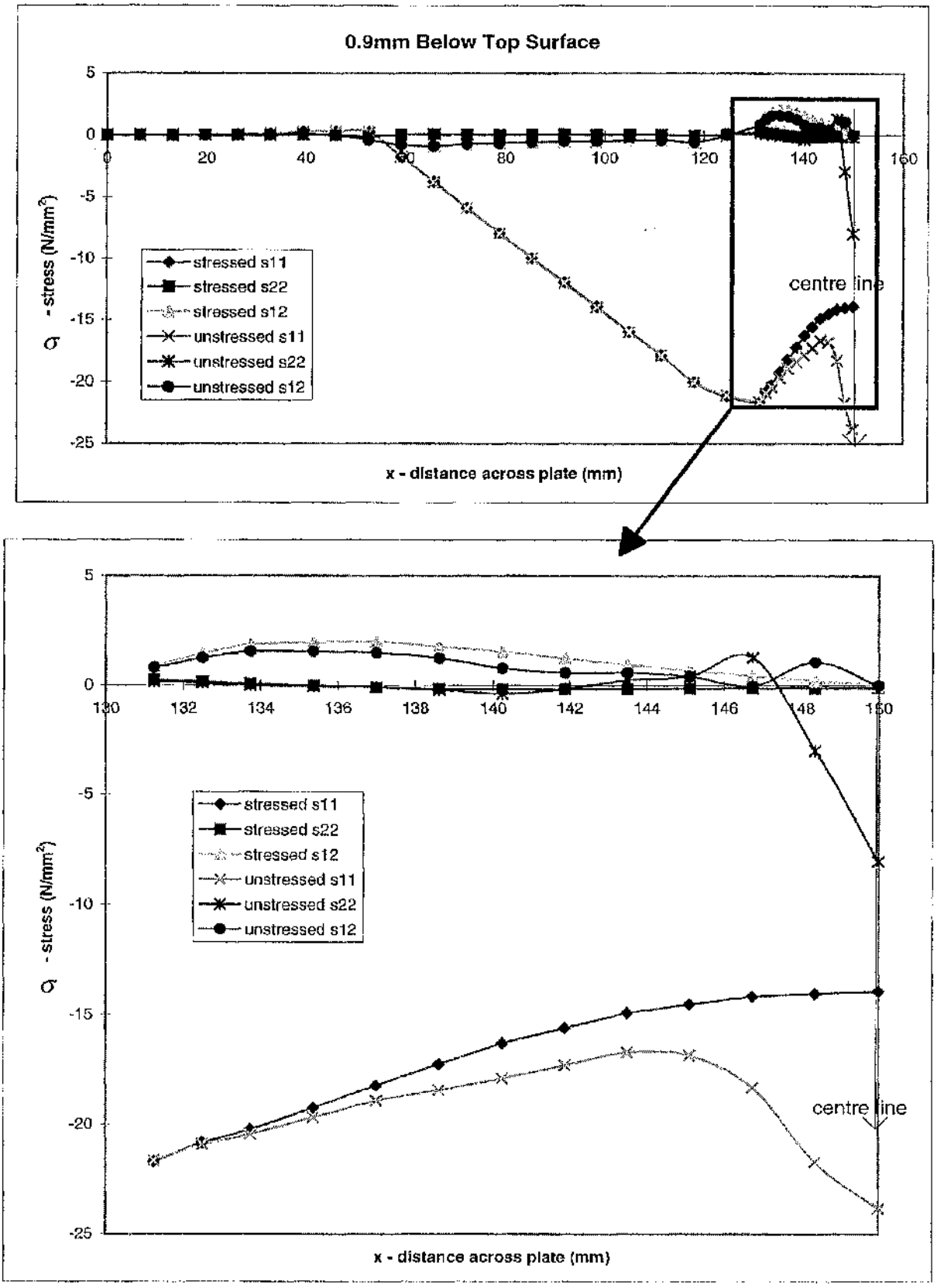

Figure 3.36 Detailed variation of stresses across the plate top surface and at the first ply level of the unstressed fatigue specimen cont.

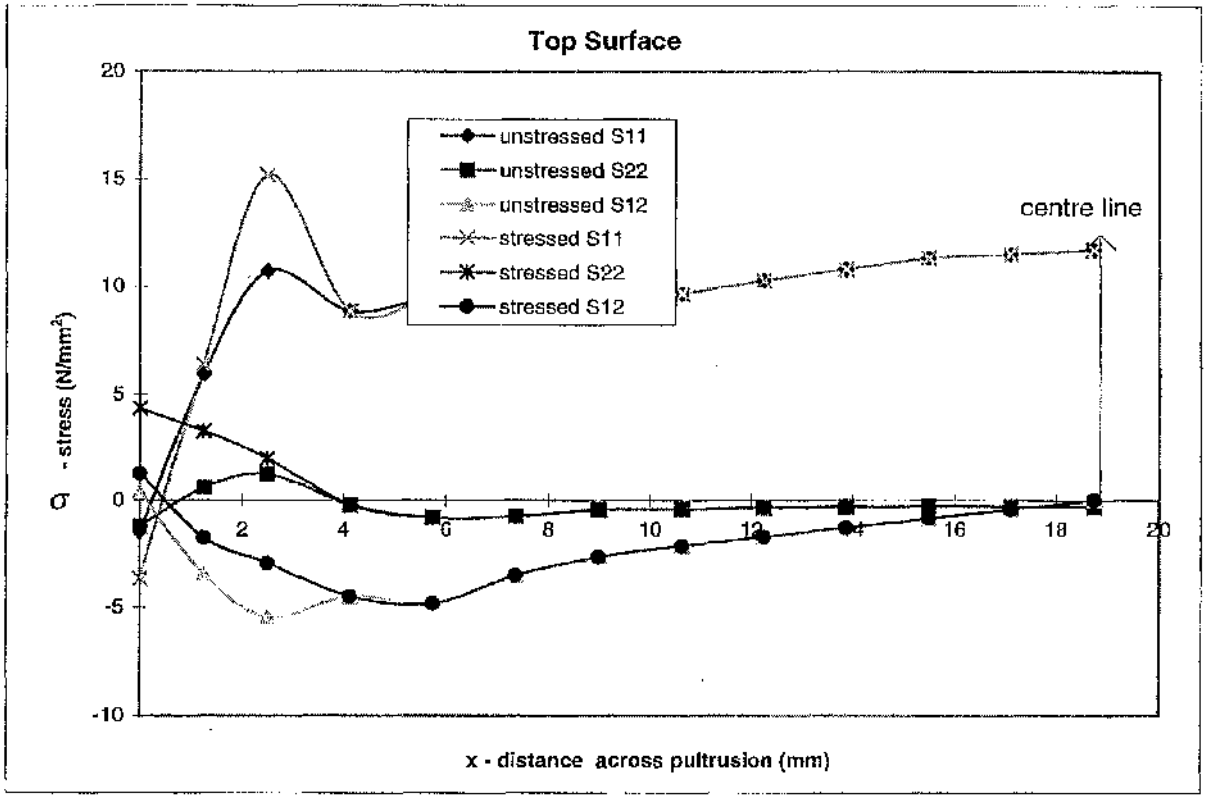

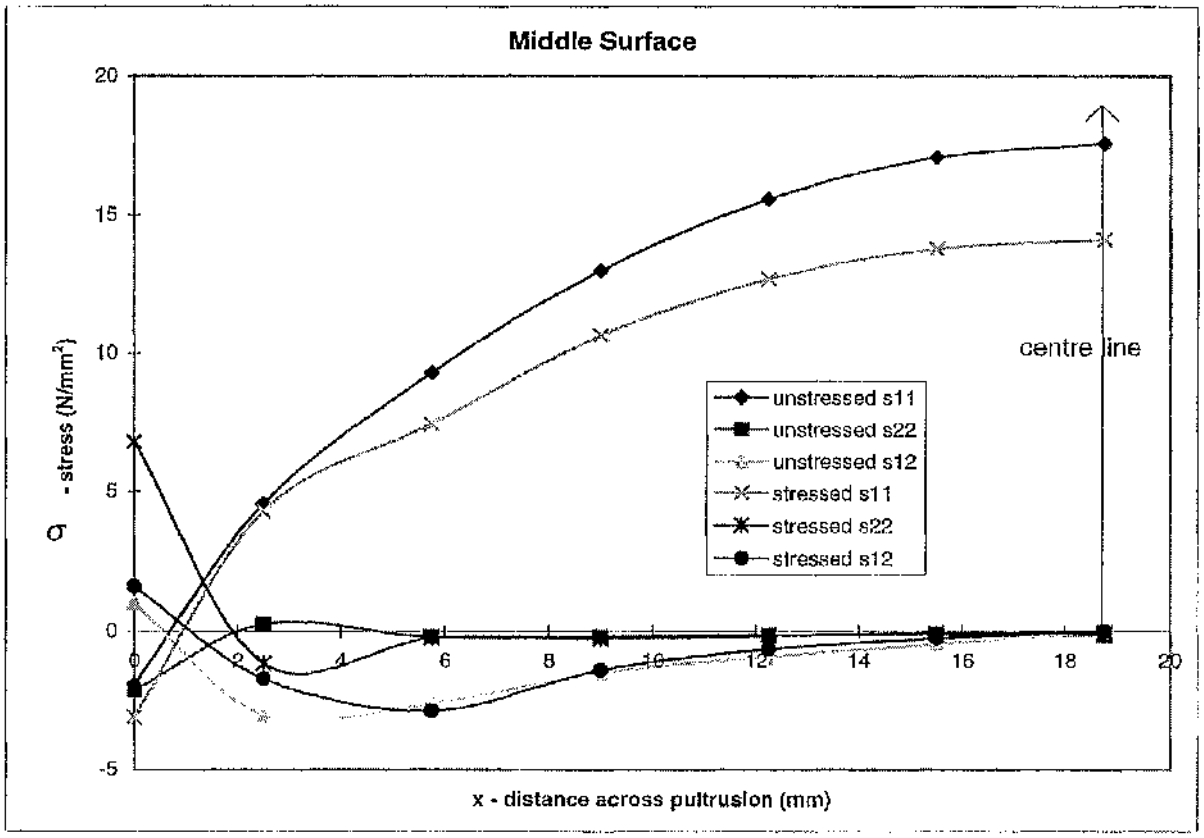

Figure 3.37 Detailed variation of stresses across the top surface and the middle area of the pultrusion material of the stressed fatigue specimen

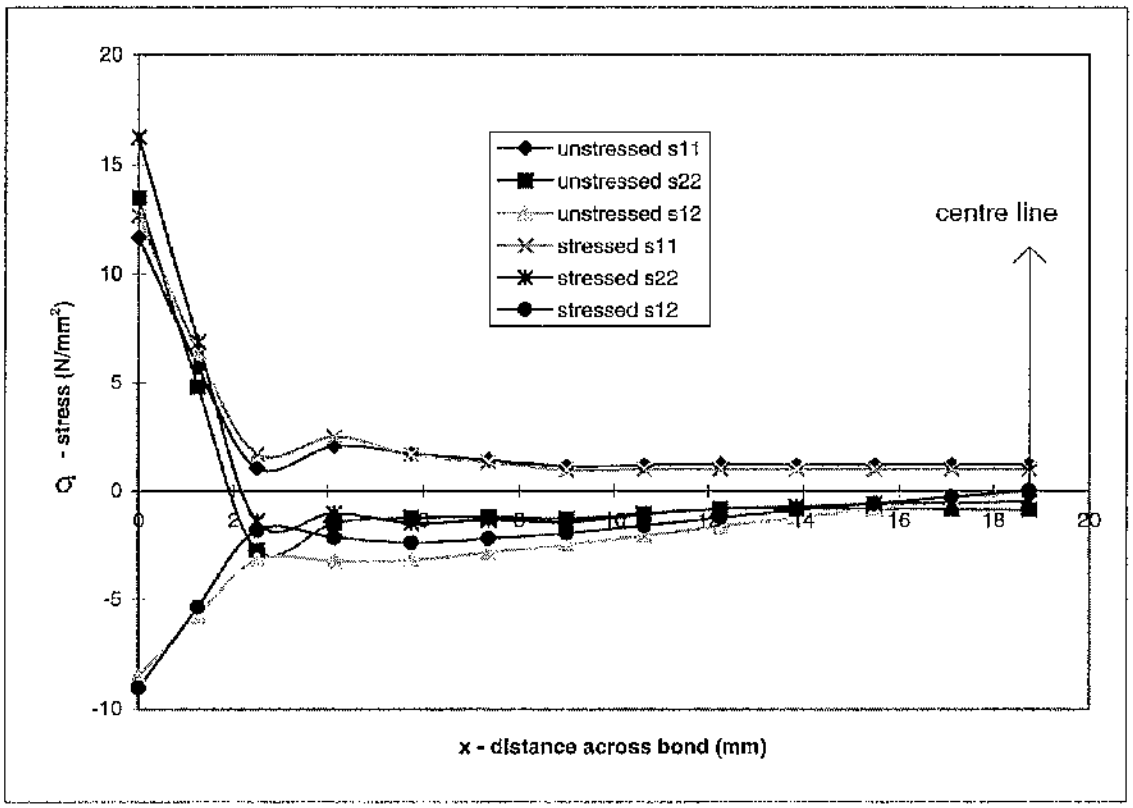

Figure 3.38 Detailed variation of stresses at the adhesive/grp interface in the adhesive

Adhesive Name	Adhesive Type	Manufacturer	Lap shear kN	Tensile kN	Cleavage kN	Impact* J/cm2
Redux 410	epoxy	Ciba Geigy	5.14	10.00	1.70	6.72
			5.10	9.88	5.10	6.72
XB 5093	polyurethane	Ciba Geigy	0.71	3.40	1.63	6.29
			0.60	4.25	1.68	6.29
ITW5500	acrylic	ITW	3.16	5.40	3.15	6.51
			3.17	5.98	3.15	6.29
VOX500	acrylic/epoxy	Permabond	1.96	7.10	3.12	6.72
			1.80	3.87	x	6.83
F246	acrylic	Permabond	3.22	1.83	2.46	7.38
			5.13	3.82	1.87	8.68
E32	epoxy	Permabond	3.17	4.39	1.64	8.24
			2.46	5.99	2.25	6.51
XSA mm			15x25	25x25	25x25	25x25

*Impact values are for comparison only

Table 3.1 Performance of cold cure adhesives on grp polyester shot blast adherends

Adhesive Type	Lap shear kN	Tensile kN	Cleavage kN	Impact* J/cm2
Redux410	5.47	8.60	3.39	8.03
	5.32	10.50	3.92	7.59
XSA mm	15x25	25x25	25x25	25x25

*Impact values are for comparison only

Table 3.2 Performance of Redux 410 on grp/pultrusion polyester shot blast adherends

Adhesive Name	Manufacturer	Shear kN	Tensile kN	Cleavage kN	Impact* J/cm2
Redux 410	Ciba Geigy	5.14	10	4.16	6.72
		5.1	9.88	5.1	6.72
Redux 420	Ciba Geigy	4.35	11.6	4.7	6.51
		4.7	12.86	3.03	6.79
XSA mm		15x25	25x25	25x25	25x25

*Impact values are for comparison only

Table 3.3 Performance of Redux 420 on grp polyester shot blast adherends

Specimen number	Surface preparation	Failure load (kN)	Failure type
1	as received	3.31	in pultrusion
2	as received	2.35	in adhesive
3	shot blast	3.49	in pultrusion
4	shot blast	3.12	in pultrusion
5	abrasion (trans.)	3.56	in pultrusion
6	abrasion (trans.)	3.32	in pultrusion
7	abrasion (long.)	3.94	in pultrusion
8	abrasion (long.)	4.05	in pultrusion

Table 3.4 Lap shear strength of Redux 420 bonded polyester pultrusion joints using various surface roughening techniques (XSA 15x25mm)

time after mixing hrs.	shear failure load kN
0	9.34
0	9.66
1*	9.27
1*	9.39
2	9.51
2	9.06
3	8.9
3	9.13
4	9.13
4	8.76
5	8.66
5	8.59

*Manufacturer's recommended maximum

Table 3.5 Influence of pot life on shear strength of Redux 410 bonded steel adherends (XSA 15x25mm)

Joint Type	Adhesive	Tension (kN)	% performance	Failure Type	Bending (kN)	Failure Type
parent material 16mm	xx	89	100	xx	8.59	xx
parent material 9mm	xx	53.5	100	xx	xx	xx
grp recessed strapped 16mm	Redux410 NA	16	18	adhesive	3.19	adhesive
lap shear 16mm	Redux410 NA	9.05	10.2	resin surface	1.29	adhesive
grp strapped 9mm	Redux410 NA	28.6	53.5	resin surface	xx	xx
grp scarfed 9mm	Redux410 NA	28.8	53.8	resin surface	xx	xx
steel strapped 5mm	A2005	21.9	40.9	resin surface	xx	xx
steel strapped 5mm	Redux410 NA	26.05	48.8	resin surface	xx	xx
steel strapped 2.65mm	A2005	27.85	52.3	resin surface	xx	xx
steel strapped 2.65mm	Redux410 NA	27.55	51.7	resin surface	xx	xx
steel tapered strapped	A2005	38.4	71.8	ply failure	2.35	ply failure
steel 'H' section	A2005	28.45	53.2	ply failure	xx	xx
steel 'H' section scarfed	A2005	29.45	55	ply failure	2.45	resin surface

Table 3.6 Experimental butt joints tensile and bending performance (bond overlap length = 100mm, total length = 300mm, width = 25mm)

modulus of elas. (N/mm^2)	Poisson's ratio	sample width (mm)	sample thick' (mm)
1444	0.41	12.51	3.38

Table 3.7 Redux 410 experimental bulk properties

Steel	Adhesive	grp/pultrusion[82]
E=210000	E=1400	E1=14700
v=0.33	v=0.41	E2=3600
		E3=13100
		v12=0.123
		v13=0.139
		v23=0.36
		G12=3090
		G13=3090
		G23=1325

Table 3.8 Material data input for finite element analysis

4.0 Section C:

Steel Corrugated Core Sandwich Construction

4.1 Introduction

The advent of modern structural adhesives which have relatively high strength, stiffness and toughness has now allowed designers to fabricate heavy grade steel constructions which were not possible before. The previous section covered the adhesive performance, selection and characteristics with view for use on grp structural panels in a marine environment. In the following section, the review of adhesive performance is taken a stage further and the overall structural performance of a novel form of adhesively bonded construction is investigated. The main objectives of the work were:

(i) to fabricate steel corrugated core sandwich construction using adhesive technology

(ii) to investigate the performance characteristics of a corrugated core sandwich construction

(iii) to investigate the possible failure mechanisms

(iv) to compare the performance of a specific geometry of adhesively bonded sandwich construction to a similar design which had been fabricated using laser welding.

4.2 Background

The simplest type of sandwich construction consists of two thin, stiff, strong sheets of dense material separated by a thick layer of low density material which may be much less stiff and less strong. The core has several important tasks. It must be stiff and strong enough in the direction perpendicular to the faces to ensure that they remain the correct distance apart. It must be stiff enough in shear to ensure that when the panel bends the faces do not slide over each other. If these requirements are not met, the faces will behave as separate beams and the sandwich effect is lost. The core must also be stiff/strong enough to keep the faces flat, otherwise a face may buckle locally under the influence of compressive stress in its own plane. If the core is stiff enough it may make a significant contribution to the bending stiffness of the panel. This contribution is small in the case of the low density cores which are usually employed and thus may often be ignored leading to simplification in analysis.

The combination of materials used for the construction of sandwich panels will depend on the intended application. Structural panels for aircraft applications usually employ metal faces with a metal honeycomb or corrugated core. Sandwich construction is favoured for most applications as it is relatively resistant to buckling deformations at working loads, unlike skin and stringer construction.

Panels for the building industry tend to be for non-structural applications used to carry low loads over fairly long spans or for aesthetic appeal on the facade of buildings or as insulation materials[1]. Owing to the nature of their use, the panels must be light but are also required to be relatively cheap. New materials and new combinations of old materials are constantly being proposed and used.

There are many areas of marine construction in which the stiffness to mass ratio is an important design issue. One of the fields where sandwich construction is thought to be most relevant is in the fabrication of topside components in offshore drilling and production rigs. These applications include decks, bulkheads, helidecks and accommodation modules. The potential of hybrid sandwich structures for the construction of 'safe havens' consisting of fire and blast resistant panelling demands serious consideration. This is especially so in the light of the Piper Alpha disaster[2].

Traditional ship construction uses stiffened plate grillages to resist both global axial bending and shear loads, as well as local out-of-plane static and dynamic loading. These grillages generally have lower stiffness in the transverse than

longitudinal direction and uneven stress distributions in bending. Thus stress concentrations are present that may give rise to relatively poor fatigue lives. However, the design of such stiffened panels is usually dominated by either longitudinal stress, panel buckling or bending criteria and therefore the plate components may not be fully stressed because of their proximity to the neutral axis in bending. Traditional construction using solid steel plates is structurally inefficient, for example, 50% of the weight of a solid plate provides just 12% of its stiffness[3]. Sandwich construction works on the principle of using weight only where it is needed. Placing steel skins on the faces of a low density core enables maximum advantage to be taken of the high Young's modulus of steel. Sandwich panels offer a substitute for traditional stiffened plating which, with careful consideration of face and core parameters, may perform better than stiffened plates. Such construction utilises the plate material more efficiently, thus obtaining greater bending stiffness for lower weight[4,5]. Various types of sandwich panels may be designed, from simple arrangements having two thin, stiff faces of dense material separated by a thick, low density, low strength continuous core material, or more complicated honeycomb or corrugated cores. The corrugated core is highly orthotropic having a much greater stiffness in the direction parallel to the corrugation compared to the direction transverse to the corrugations. Alternatively, a two-way corrugated construction could be used forming an egg-box construction. This would be less orthotropic and simulate a cellular core[6]. The possible combinations of face and core materials are infinite but the current work has focused on all steel corrugated core sandwich construction for marine applications (see figure 4.1).

The aircraft industry has incorporated lightweight, adhesively bonded sandwich elements into aircraft structures for approximately fifty years. Until recently, the use of heavier grade steel sandwich construction for marine application has been dismissed because of difficulties of fabrication with 'thin' cores. With a cofferdam construction, it is possible for welders to work between the two skins. The major problem of joining 'thin' sandwich assemblies is that there will always be one face that is only accessible externally. Research at Newcastle University[7,8], DRA Dunfermline[9] and the USA military[9] has considered the use of through-thickness laser welding to join steel corrugated core sandwiches. There are, however, distinct practical disadvantages in this form of assembly, not least the need for easily accessible portable high powered lasers. Other disadvantages include a significant volume of crevices formed between adjacent but intimately connected elements, which can promote crevice corrosion, and also the relatively high proportion of brittle heat affected zone material in the finished welds. The highly localised nature of a joint formed by a laser weld may produce high stress concentrations and thus lead to a poor fatigue life. Alternatively, research of

Manchester University[10,11,12,13] has considered the use of spot welding as a possible practical fabrication technique for corrugated core sandwich panels for offshore applications. However it was concluded that[13,14] their fatigue performance of the sandwich construction may be limited due to the poor performance of the spot welds and requires further research. Using adhesive bonding as a joining technique significantly reduces the need for costly equipment i.e. the laser, giving greater flexibility of where the fabrication is performed. Other advantages arising from the use of adhesives include the lack of high stress concentrations, crevices for corrosion, heat affected zones and distortion.

The potential advantages of adhesives over mechanical fasteners for joining have long been recognised. However, experience and general industrial acceptance of adhesives for heavy structural fabrications have been low, except in limited applications within civil engineering[15]. This slow uptake of adhesive technology is due to the lack of adequate information about reliability and understanding of the failure mechanisms of adhesive joints.

Progress in the development of corrugated sandwich panels in the past has also been hindered by the lack of understanding of their behaviour under load. Although research results are available relating to thin sandwich construction for aviation applications, very little has been found for the less common thick sandwich sections required for heavy engineering structures.

4.3 Simple Sandwich Theory

The fundamental theories of structural sandwich construction were derived during the 1940's and can be found in many texts[16,17]. On the simplest level a sandwich beam may be considered, as in figure 4.2, to be composed of two thin faces of thickness t, separated by a thick, low density core of thickness c, the overall depth of the beam, h, and the width, b. All of the materials are considered to be isotropic and are well bonded to each other. It is assumed the face material is much stiffer than the core material. The stresses and deflections in this simple model may be found using ordinary beam theory. The theory assumes that the cross sections, which are plane and perpendicular to the longitudinal axis of the unloaded beam remain so during bending. This assumption leads to the relationship between bending moment (M) and curvature (1/R):

$$\frac{M}{EI} = -\frac{1}{R}$$

where E is the Young's modulus
I is the second moment of area
and the product EI is the flexural rigidity D

The negative sign is introduced to comply with the sign convention shown in figure 4.2.

The sandwich beam is, however, a composite beam and its flexural rigidity is the sum of the flexural rigidities of the two separate parts, faces and core, measured about the centroidal axis of the entire cross-section. Thus:

$$D = E_f \frac{bt^3}{6} + E_f \frac{btd^2}{2} + E_c \frac{bc^3}{12}$$

where E_f, E_c are the moduli of elasticity of the faces and core respectively and d is the distance between the centre lines of the upper and lower faces:

$$d = \frac{h+c}{2}$$

(It is assumed for the present that the beam is narrow, so that the stresses in the y-direction can be taken as zero.)

The assumptions of the ordinary theory of bending lead to the expression for stresses in the face and core adapted to the composite nature of the cross section. Because sections remain plane and perpendicular to the longitudinal axis the strain at a point distant z below the centroidal axis is Mz/D. This strain may be multiplied by the appropriate modulus of elasticity to give the bending stresses at the level z. Therefore

$$\sigma_f = \frac{Mz}{D} E_f \qquad (\frac{c}{2} \le z \le \frac{h}{2}; \quad -\frac{h}{2} \le z \le -\frac{c}{2}),$$

$$\sigma_c = \frac{Mz}{D} E_c \qquad (-\frac{c}{2} \le z \le \frac{c}{2})$$

The maximum face and core stresses are obtained with z equal to $\pm h/2$ and $\pm c/2$ respectively

$$(\sigma_f)_{max} = \pm \frac{ME_f}{D} \frac{h}{2} \qquad (\sigma_c)_{max} = \pm \frac{ME_c}{D} \frac{c}{2}$$

The ratio of the maximum face stress to the maximum core stress is $(E_f/E_c)(h/c)$. If the ultimate strengths of the face and core materials are exactly in proportion to their moduli the faces will fail marginally before the core does, since h/c is slightly greater than unity.

Following the same assumptions for beam theory, an expression for shear stress is also obtained

$$\tau = \frac{QS}{Ib}$$

where τ is the shear stress in a homogeneous beam at depth z, below the central axis and Q is the shear force at the section under consideration

I is the second moment of area of the entire section about the centroid

b is the width at the level z_1

S is the first moment of area of that part of the section for which $z > z_1$

For a composite beam the equation must be modified to take account of the moduli of elasticity of the different elements of the cross section:

$$\tau = \frac{Q}{Db} \sum (SE)$$

D is the flexural rigidity of the entire cross section and $\sum(SE)$ represents the sum of the products of S and E of all the parts of the section for which $z > z_1$.

Very few papers have been published which deal with the bending and buckling of sandwich panels with cores which are rigid enough to make a significant contribution to the bending stiffness of the panel, yet flexible enough to permit significant shear deformations. Furthermore, there is a considerable problem of the sandwich panel with an antiplanar core, one which possesses no stiffness in the xy plane and in which the shear stress τ_{zx} , τ_{yz} are constant throughout the depth (i.e. they are independent of z). Such panels differ from ordinary homogenous plates in that the bending deformations may be enhanced by the existence of non-zero shear strains (γ_{zx}, γ_{yz}) in the core and of direct strains e_z in the core, perpendicular to the faces. The shear strain and the direct strain in the core are also directly associated with the possibility of short wavelength instability of the faces (wrinkling). Thus in an antiplanar core the modulus of elasticity in the planes parallel to the faces is zero but the shear modulus in planes perpendicular to the faces is finite. By this definition, Ec=0 and the core makes no contribution to the bending stiffness and constant shear stress, $\sigma_x = \sigma_y = \tau_{xy} = 0$.

This problem has been the subject of two main methods of analysis and has been well documented in a book by Allen[16]:

Selective method[16]
General equation method[18]

In the General method, equations are set up to define the equilibrium of the separate faces and of the core and to prescribe the necessary continuity between the faces and the core. The result is a set of differential equations which may be solved in particular cases for the transverse deformations of the panel and the flattening of the core.

The Selective method is divided into two separate parts which may be labelled as the bending problem and the wrinkling problem. In the bending problem it is convenient to assume that the core is antiplanar but infinitely stiff in the z direction. This excludes the possibility of flattening of the core and of wrinkling instability, but permits the assessment of the effect of core deformation on the deflections and stresses in the panel. In the wrinkling problem the true elastic properties of the core are taken into account but the task is simplified by permitting the middle planes of the faces to deflect in the z direction only, not in their own planes. In this way overall bending of the panel is excluded, but the phenomenon of wrinkling and of local distortion under concentrated load can be

studied. Most work on sandwich panels refers to the selective method. In bending, the core strains are neglected in the z-direction. The assumption that the core in the xy plane is weak leads to the conclusion that the core makes no contribution to the flexural rigidity of the sandwich, that the core shear stresses τ_{zx} and τ_{yz} are independent of z and that a straight line drawn in the unloaded core normal to the faces remains straight after deformation but is no longer normal to the faces. These assumptions, core weak in the xy plane and stiff in the z direction, allow the displacements of the panel to be expressed in terms of only three variables, one of which is w, the transverse displacement.

If a corrugated core panel has the corrugations running in the x direction, then the corrugated core sandwich panel is often stiff enough to make a distinct contribution to the flexural rigidity in the zx-plane but not in the yz-plane. Consequently, the assumption used in the Selective method that the flexural rigidity of the core is negligible breaks down for bending in the zx-plane and the shear stresses in that plane can no longer be assumed constant over the depth of the core. Fortunately for simplicity of the analysis, the shear stiffness of the corrugated core can usually be taken as infinite in the zx-plane. However if this type of analysis is to be applied to the corrugated core panel it is necessary to introduce additional terms to represent the strain energy associated with the zx bending and possibly the twisting of the corrugated core.

A notation may be used which permits the corrugated core sandwich to be treated as a special case of a general orthotropic sandwich. In this approach the character of the sandwich plate is defined by certain bending, twisting and shearing stiffness in the x and y directions. Differential equations may be set up in terms of these stiffnesses, or a strain energy function may be derived from them. The solution of the differential equations by the substitution of appropriate deflection functions is fairly easy in the simply supported case. This analysis is valid for orthotropic panels with very thin or thin faces of different thicknesses and materials. This work was developed by Libove and Batdorf[19] and further developed by Libove and Hubka[20] specifically for the corrugated core sandwich problem. Libove and Batdorf[19] derived three differential equations for the three unknowns displacement, w, and shear forces, Qx and Qy, . The properties of the sandwich panel are expressed in the terms of flexural, torsional and shear rigidities in terms of the dimensions and material properties of the individual components of the sandwich construction. The differential equations are:

$\frac{\partial Q_x}{\partial x}+\frac{\partial Q_y}{\partial y}+q(x,y)=0$, where q(x,y) is the lateral load per unit area at x and y

$$\left[-D_{xy}\frac{\partial^3}{\partial x\partial y^2}-\frac{D_x}{g}\left(\nu_y\frac{\partial^3}{\partial x\partial y^2}+\frac{\partial^3}{\partial x^3}\right)\right]w+\left[\frac{1}{2}\frac{D_{xy}}{D_{Qx}}\frac{\partial^2}{\partial y^2}+\frac{D_x}{gD_{Qx}}\frac{\partial^2}{\partial x^2}-1\right]Q_x+\left[\frac{1}{2}\frac{D_{xy}}{D_{Qy}}\frac{\partial^2}{\partial,\partial,}+\frac{\nu_y}{g}\frac{D_x}{D_{Qy}}\frac{\partial^2}{\partial x\partial y}\right]Q_y=0$$

$$\left[-D_{xy}\frac{\partial^3}{\partial x^2\partial y}-\frac{D_y}{g}\left(\nu_x\frac{\partial^3}{\partial x^2\partial y}+\frac{\partial^3}{\partial y^3}\right)\right]w+\left[\frac{1}{2}\frac{D_{xy}}{D_{Qx}}\frac{\partial^2}{\partial x\partial y}+\frac{\nu_x}{g}\frac{D_y}{D_{Qx}}\frac{\partial^2}{\partial x\partial y}\right]Q_x+\left[\frac{1}{2}\frac{D_{xy}}{D_{Qy}}\frac{\partial^2}{\partial x^2}+\frac{D_y}{gD_{Qy}}\frac{\partial^2}{\partial y^2}-1\right]Q_y=0$$

where $g=(1-\nu_x\nu_y)$

If the corrugations run in the x direction, it is usual to make some allowance of the core to the flexural rigidity of the sandwich in that direction. Then, even if the faces themselves are isotropic, it is expected that Dx will be greater than Dy. Because of the flexural rigidity of the core it cannot be assumed that the shear stresses in the zx plane are constant through the depth of the core. Fortunately the shear stiffness in the direction of the corrugations is usually so great it can be taken as infinite. It is therefore necessary only to consider the effect of the shear deformations in the plane perpendicular to the corrugations. Precise expressions for the stiffness of the corrugated core sandwich are given by Libove and Hubka[20]. Allen[16] gives the following approximations of their work:

$$D_x=\frac{E_f t d^2}{2}+E_c I_c \qquad D_y=\frac{\frac{E_f t d^2}{2}}{1-\frac{\nu_f^2}{1+\frac{(E_f t d^2)}{2E_c I_c}}}$$

$$D_{xy}=\frac{E_f t d^2}{2(1+\nu_f)} \qquad D_{Qy}=\frac{SdE_c}{1-\nu_c^2}\left(\frac{t_c}{d_c}\right)^3$$

$$D_{Qx}=\infty$$

$$\nu_x=\nu_f \qquad \nu_y=\nu_f\frac{D_y}{D_x}$$

where E is the Young's modulus

ν is the Poisson's ratio

subscript c refers to core, subscript f refers to face

d is the sandwich depth between the centroid of the face plates

t_c refers to core thickness

d_c is the core depth between the centroid of the flanges

I_c represents the second moment of area of the cross section of the core per unit with in the y direction

S, a coefficient, has values in the range 0.5 - 0.15 depending on the geometry of the cross section of the sandwich; reference should be made to the graphs prepared by Libove and Hubka[20].

A further extension of this work has been made by Harris and Auelmann[21] who use the strain energy expression of Libove and Batdorf[19] to study the instability of simply-supported corrugated core panels. Results are given for many combinations of edge loads. The analysis is restricted to sandwiches with very thin isotropic faces and with corrugated cores which make negligible contribution to the flexural rigidity of the panel.

Tan, Montague and Norris[10,11,12,13] verified experimentally the theoretical predictions of Libove and Batdorf[20] and showed good agreement with the theoretical predictions of deflection patterns, strains and stresses. For the simply supported case only, simple beam theory predicted the deflections to within 5% (on average), with membrane stresses and strains being within 20%. For the simply supported all round case, Libove and Batdorf's[19] theory underestimated the deflections by about 20%. The membrane stresses and strains, except ,σ_y, were also predicted to within 20%, even though the precise distribution of these strains and stresses is probably more complicated than the theory assumes. The σ_y stresses, both in theory and those measured, were very small so that a small absolute difference between the two represents a large percentage difference.

The aforementioned theories have been developed specifically for corrugated sandwich panels used in aerospace applications where the face sheets are considered to be thin or very thin and the theory has been developed accordingly. Thus, no allowance is made for the local bending stiffness of the faces about their own centroidal axes. The corrugated sandwich structures proposed in this study incorporate thicker face plates for corrosion allowances and impact tolerance and also cores whose stiffness cannot be neglected. Thus the previously developed theories may not be entirely applicable.

4.4 Parametric Study

In aerospace structures, much design analysis is carried out using finite element analysis in which details of stress distribution through the structure are examined. Such detailed methods are not particularly appropriate for the design stage of the majority of marine applications because of their complexity and design criteria are less critical. A simpler design approach may be used in which the material design is considered independently from structural design[22]. The materials design problem is concerned with the calculation and optimisation of the sandwich stiffness and strength properties. Details of the sandwich construction are then neglected in the structural design problem, which is concerned with calculating the effect of support conditions and loads on a panel of known stiffness and strength. In this research programme, a parametric study, based on simple beam theory was undertaken to determine the effects that various dimensional parameters have on the stiffness of corrugated core sandwich panels in the direction parallel to the corrugation. Figure 4.3 shows the influence of various parameters on the structural efficiency of the steel corrugated core. (The measure of structural efficiency used is the stiffness-to-area ratio as the structure is considered to be made wholly of steel of unit thickness for a unit span of one metre. The modulus is measured as the moment of inertia divided by the distance from the neutral axis to the outer surface of the face plate, I/y, per unit span of one metre). Figure 4.3 shows that core depth and web angle have the greatest influence on the efficiency of the sandwich construction, whereas the flange width and core thickness are weaker variables in the performance of corrugated cores. Figure 4.4 shows the change in modulus and the efficiency with web angle for a given core depth, plate thickness and flange size. This diagram indicates that the efficiency of the section does not significantly increase if the web angle is greater than 30 degrees, neither is there a significant change in modulus of the section. Thus a web angle of approximately 30 degrees will give an efficient structural performance. If the angle is significantly less than 30 degrees, although there is an increase in structural performance, there is a decrease in efficiency of the material used, for a given modulus.

Figure 4.5 compares the efficiency of the steel corrugated core sandwich structure to that of a single skin conventional stiffener arrangement, over a range of stiffeners spacing. This diagram indicates the improved efficiency of the sandwich construction over conventional stiffener arrangement if a correct

combination of core geometry is chosen. The envelope for the conventional stiffening is produced for a 10mm plate thickness and OBP (bulb plate) stiffener with web depth range of 120 to 430mm at spacings of 500 to 1000mm. The envelope for the sandwich constructions is based upon two 5mm face plates and a depth range from 60 to 200mm. When choosing a sandwich structure there may also be a possible space saving gain e.g. for a sandwich structure with a specified modulus/metre of 1100cm^3, depth of 200mm and efficiency of 8.5cm the equivalent conventional arrangement with modulus/metre of 1177cm^3, efficiency of 7.017cm will have a stiffener depth of 340mm. The depth of the traditional stiffening arrangement is thus 170% that of the sandwich structure. Further comparisons with other sandwich configurations, using alternative steel structural sections as the core, are shown in figure 4.6. I-Beam and channel sections proved the most efficient cores from the range of structural sections surveyed. This figure shows that the corrugated core sandwich will also be as efficient as the best alternative cores when the optimum core dimensions are used.

4.5 Experimental Work

4.5.1 Geometries

Four configurations of steel corrugated core sandwich structures were studied in a series of tests.

Model A - a half scale equivalent to that considered at Newcastle University[7].

Model B - a specimen similar to that used in work undertaken at DRA Dunfermline[9].

Model C - a heavy gauge corrugated core which is already used in industry to form a stiffened panel[23].

Model D - one sample of laser welded construction[9].

The dimensions of each sandwich geometry are shown in the table accompanying figure 4.7, which is an explanatory diagram defining the terminology.

4.5.2 Experimental Procedures

The experimental sandwich specimens were fabricated using standard techniques for hot cure single part adhesives which are described in section 2.3.1. The spew fillets were left intact.

4.5.2.1 Study of Stiffness and Ultimate Capacity

Adhesively bonded corrugated core sandwich construction provides a stiff strong lightweight structure. Because there are many variable parameters affecting the performance of such panels the mechanical behaviour is complicated and not described purely by simple beam theory in the transverse direction (i.e. across the lines of corrugation). However, it has been reported elsewhere[24] that the simple theory is adequate when applied in the longitudinal direction.

From a series of compression tests on beam elements, the characteristics of core and face plate combinations can be obtained and the effect of geometry changes such as web angle etc. may be examined. In a realistic situation a panel of corrugated material will be, in effect, simply supported and combined bending and compressive stresses will be encountered. This load configuration can be investigated in bending tests.

Models A, B, C and D were all tested under static three point bending with loading in a direction transverse to the corrugations to obtain an overall experimental stiffness value, failure mode and ultimate capacity. The positioning of loading points and supports is important. In all cases the loading points and supports were positioned at a crown position (i.e. above the apex between two adjacent webs). All the tests were performed in a 250kN Instron tensile testing machine at a constant crosshead speed of 0.5mm/min. A LVDT was positioned below the midpoint of the beam and the central deflection was recorded for each specimen. Strain gauges were also used to record strains within each sandwich construction and positioned at appropriate areas on each specimen. All these data were recorded on an Orion data logger, on disc, for further analysis after the experiments.

Models B and C were also loaded in static three point bending in a direction longitudinal to the corrugations. In addition, Models A, B and C were also axially compressed in a direction transverse to the corrugation (see figure 4.8).

4.5.2.2 Fatigue Performance

Previous work at Glasgow University on the performance of adhesive joints under fatigue loading, showed that adhesively bonded joints can perform better than the equivalent welded joints in the low stress range[25]. This superior performance as demonstrated by an adhesively bonded joint, is due mainly to the lack of high stress concentrations in the bonded joint. Limited results are available from tests carried out at Newcastle University[7] into the fatigue performance of the laser welded corrugated core sandwich. In both the Newcastle and the current studies, beams were loaded in a direction transverse to the corrugations in bending. Model A is a bonded half scale equivalent to the beam tested at Newcastle University. This model was used for the comparison of fatigue performance of bonded construction with laser welded construction. The tests were performed in a Dartec 100kN servo hydraulic test frame at a

frequency of 10Hz under constant load control. The cycles to failure for each specimen were recorded.

4.6 Results

4.6.1 Static Performance

Figure 4.9 and table 4.1 show the load versus central displacement curve obtained for each model in the elastic region and a summary of the results respectively for all static tests performed transverse to the corrugations in three point bending. Overall elastic deformation is considered to occur in the transverse direction as if it were a continuous medium. Thus it is possible to calculate an experimental beam rigidity using the simple beam theory displacement equation for three point bending from:

$$\delta = \frac{PL^3}{48EI}$$

where δ is the displacement
L is the span
P is the applied load
and EI is the rigidity

Results from limited three point bend tests performed longitudinal to the corrugated core are shown in table 4.2. These results demonstrate the high directionality of the core stiffness when compared to the previous results in table 4.1 for bending performed transverse to the corrugations. The experimental longitudinal stiffness values, table 4.2, were very much lower than the theoretically calculated longitudinal values which are shown in the table accompanying figure 4.7. For Model B, this is believed to be due to the boundary instability because only one corrugation pitch was tested. Model C experimental longitudinal experimental stiffness result is also very much lower. It is believed the length of this section of beam which was tested was too short to develop bending stresses in the beam and failure occurs due to crushing of the core under the load point.

Buckling results are shown in table 4.3. In these tests, the mode of loading forces the core to act like a large spring. The boundary conditions are important so as to ensure that the whole beam is uniformly loaded and not just the face plates extremities. It has been reported elsewhere[26] that simple support conditions are difficult to achieve in practise. A common method is to place the ends of any test specimen into V grooves which are cut into supports attached

to the loading device. However, unless the ends of the specimen are made with great care, problems of partial contact or misalignment can arise. These difficulties with loading alignment invariably lead to the onset of premature local buckling.

4.6.2 Fatigue Performance

The results from the fatigue experiments are shown in figure 4.10 in the form of a S-N diagram showing the number of cycles to failure for a given stress range. Also plotted on this diagram are the results from a laser welded construction[7]. The results clearly show for this loading regime the performance of the bonded construction is superior to a laser sandwich construction. To calculate the nominal applied stress range, the beam was considered to be continuous and, from simple beam theory, $\Delta\sigma = \frac{\Delta M Y}{I}$. The stress range can be calculated using the experimental second moment of area calculated from the static results (table 4.1). It was considered that the compliance of the adhesive in the elastic region can be ignored in the overall compliance of the beam. This assumption is often used to simplify fracture mechanics equations[27]. From the experimental results a straight line may be fitted through the data using regression analysis. For the adhesively bonded construction, the gradient of the line is 8.067 and for the laser construction the gradient is 2.7.

4.7 Numerical Analysis

4.7.1 Complete Structure

While it is possible to predict the behaviour of corrugated beam elements using simple beam theory in the longitudinal direction with reasonable accuracy, it is difficult to use such analytical techniques to determine detailed behaviour characteristics of corrugated beam elements in the transverse direction. To overcome this difficulty, finite element stress analysis was used to model half an experimental beam equivalent to Model A. This beam was loaded in a direction transverse to the corrugations, in three point bending. The analysis assumes plane strain, linear elastic materials and an adhesive with the properties given in table 4.4. Various packages are suitable but SESAM[28] was used in this case with three-dimensional 20-noded brick elements. The adhesive was incorporated into this model and was assumed to be 0.2mm thick, modelled by three layers of six elements through the thickness. The axial stress distribution across the surfaces of the plates of the sandwich beam, resulting from loading within the elastic limit, is illustrated in figure 4.11. It is clearly shown, see figure 4.12, that the stress variation across the plates does not follow simple beam theory. The maximum stress does not occur at the centre of the beam but one corrugation wavelength excluding the local effect of the load point. The bending stress in the surface of the skins alternates from tension to compression along the length of the beam indicating possible local instabilities. The positions of maximum stress occur at the bond edges and, across the bonds, there are high stress differentials.

4.7.2 Single Element

In an attempt to investigate further the behaviour of the bonds in the corrugated core sandwich beam a finite element stress analysis was used in a preliminary investigation to study the sensitivity of bond area on sandwich performance.

A single unit of corrugated core and the upper face plate was modelled using PAFEC[29] in a finite element stress analysis, see figure 4.13. The single unit of corrugation was dimensionally identical to the half beam previously analysed. To simulate a similar axial stress distribution to that found in the bonds at the face plate/adhesive interface of the 1/2 scale model, the boundary conditions and loading of this element were found through several iterations. Comparison

of the two axial stress plots is shown in figure 4.14. The sensitivity of this result was then studied by doubling the bond area. The resultant stress distribution is shown in figure 4.15, which shows that the stress level at the bond edge decreases and a larger proportion of the centre of the joint is carrying a low stress level for the same given load conditions.

4.8 Discussion

The parametric study section 4.4 demonstrated the structural benefits of using a corrugated core sandwich construction with the corrugations orientated in the longitudinal direction. The depth and web angle of the core were shown to be the most influential parameters on structural efficiency for a given thickness, if face plate thickness remains constant. A web angle of 30 degrees will produce a sandwich of good structural efficiency and high stiffness. The study also showed that flange size and core plate thickness to be relatively weak variables in sandwich design for high efficiency. Several other independent studies have realised the structural benefits of corrugated cored sandwich construction. An experimental study at Manchester University[13] concluded that there are several apparent advantages of panels of this type including high strength to weight and high stiffness to weight. In a computational optimisation study on three types of panelling, (a conventional stiffened panel, a corrugated panel and a corrugated sandwich panel) Sen et al[5] find that if low volume is important then corrugated sandwich structures should be seriously considered. Corrugated panels offer attractive combinations of low cost and low weight. This could have important implications for space limited ships such as RoRo vessels where plane surfaces may also be an advantage. Conventional stiffened plating tends to be bulky and cost reduction is incompatible with weight saving. In this work, it was shown that a corrugated sandwich for a given stiffness is nearly half the depth of a conventional stiffener and plate arrangement. Finally, Wiernicki et al[4] concluded that lightweight metallic corrugated core sandwich construction has the potential to become a more attractive alternative to conventional plate stiffener steel structure when all performance characteristics are considered on a total system basis.

The corrugated core is highly directional and is generally stiff enough to make a distinct contribution to the flexural rigidity in the longitudinal direction but it is more compliant in the transverse direction. Design tables and software for corrugated core sandwich are commercially available from ESDU International Ltd[30]. A particular case that the ESDU sheets do not cover is bending in the direction transverse to the corrugations[24] probably due to the complex nature of the analysis. Much of current research has therefore concentrated on obtaining performance characteristics in the transverse corrugation direction. Overall elastic deformation occurs in the transverse direction as if it were a

continuous medium. This response was also found by other workers[31] who tested corrugated panels under dynamic and impact loading transverse to the corrugations in bending. However, the core structure is a series of plate elements and, as such, permits local instabilities in both core and face components[31]. This is reflected in the detailed stress distribution found with finite element stress analysis, see figure 4.11. The axial stress distribution across the surfaces of the face plates of the sandwich beam resulting from loading within the elastic limit is illustrated in figure 4.11. It is clearly shown that the stress variation across the plates does not follow simple beam theory, compare to figure 4.12. The maximum stress does not occur at the centre of the beam (excluding the local effect due to the load point) but at one corrugation wavelength from centre. The bending stresses on the surface of the face plates alternate from tension to compression along the length of the beam. The axial stress is obviously being disturbed by the alternating presence of the single and double thickness of the plate due to the presence of the core. In a similar finite element stress analysis of a corrugated sandwich panel, Tan et al[10] found that the locations of the troughs has an influence on the stress and strains transverse to the corrugations, but very little influence on the stress patterns parallel to the corrugations. The positions of maximum stress occur at the bond edges whilst across the bonds there are high stress differentials. The transverse stress distribution across the lower and upper plate surface demonstrates that each face plate section, between the crowns of the corrugated core, act as a separate entity within the global structure and are liable to local buckling instabilities. Across the surface of the lower face plate, the stress alternates between compression and tension, unlike beam theory where the lower plate should be wholly in tension, see figure 4.12. Despite the detailed variation in stress, the general trend for stresses in the lower plate is predominantly tensile (at a higher tensile stress level than those in the upper plate) and for the upper plate surface are for low tensile and compressive stresses, as might be expected from curvature developed in bending. Thus, in general, the finite element stress analysis indicates that buckling of an element in the upper face plate is more likely. Tan et al[10] report a similar result from finite element analysis on corrugated sandwich panels. They found that the strain contours transverse to the corrugations showed a zig zag pattern with the peaks lying in the regions in contact with double plate thickness due to the core. Similarly, high membrane stresses occur in these regions. They also suggest that local bending can occur in the wide unsupported plate between the corrugation crowns. Although, if the corrugated panel is orientated such that

the panel is used in the longitudinal length, it is believed that both the outside and inside surface stresses will be, in general, small and therefore there will be little local bending. Figure 4.9 is a load displacement plot for the four beams tested in bending transverse to the corrugations demonstrating model A, B, C and D to be listed in order of decreasing order of stiffness. The calculated experimental rigidity value, assuming the beams initially deform as a global structure, follow a similar trend although Model C and D are in reverse order, see table 4.1. This change in order is believed due to experimental error as model C and D load displacement plots are very similar. Several modes of failure may occur in sandwich beams subjected to flexural loading, depending on sandwich geometry and core and skin properties[22]. There are two basic failure modes of a corrugated sandwich construction - a) face failure, b) core failure.

Failure of the faces occurs when the initial transverse stress is insufficient to cause failure of the core i.e. where the corrugated core is strong due to shallow web angle, low pitch etc. If the integrity of the core is maintained, and the faces are maintained the correct distance apart throughout bending, very large face plate stresses are generated. Two important modes of failure, tensile or compressive, of the skin material can occur at the beam surface where stresses in flexure are highest[22] as was indicated by the current experimental and numerical results. If the inner face plate is relatively thin, local instabilities will cause buckling of the compressive face due to the axial stresses. This can happen between the crowns of the corrugation. Tan et al[10] found similar evidence, experimentally and numerically, for local bending occurring in the wide unsupported plates between stiffeners in the transverse direction. In the longitudinal direction Tan et al[10] reported that the compression plate showed clear kinks, especially near the centre of the length and it might be deduced that buckling is occurring. These kinks represent the slow growth of the initial flatness imperfections in the compression plate which remain entirely stable although obviously experiencing a local reduction in longitudinal stiffness. If the faces are relatively thick, as in this current experimental study, and failure of the core has not occurred, overall global bending of the beam element will occur above the yield stress of the plate to cause plastic permanent deformation of the beam. Thus the type of face plate failure is governed by the relative thickness of the face plate material. Generally buckling of the face plate will not be expected in marine type structures as the face plate material must be of a minimum thickness to resist impact damage such as dropped gas cylinders,

debris in the sea and severe corrosion/erosion. Neither therefore will a tensile face plate failure be expected. None of these failure modes were seen here as the face plate materials were all relatively thick. Models C and D both demonstrated a face plate failure caused by plastic deformation of the whole structure, see figure 4.16. Table 4.1 shows that the calculated web stiffness of models C and D are the highest of the four beams indicating a relatively stiff strong core. In both cases the thickness of the face plate is such that local buckling of the inner face plate does not occur. In summary, Model C and D geometry has a relatively strong core, thus high face plate stresses are developed. The face plate thickness is great enough not to permit a buckling failure or a tensile failure and therefore becomes permanently deformed.

Core failure will occur if the core is weak relative to the material of the face plates. The failure of the core can also occur in two different modes. One mode of collapse results in large interfacial slip. As this occurs, the bonds between the face plate and core fail. The other mode of collapse is caused by web buckling. As soon as a critical stress is exceeded, the core buckles in one or more of its elements. This type of failure was also reported by Clark[24] in an experimental and numerical analysis of corrugated core bonded aluminium structure intended for automobile applications. These types of failures occur when the geometry of the core is relatively easy to crush, e.g. large corrugation pitch and thin core plates. Model B geometry demonstrates a core failure by web buckling, see figure 4.17. Model B has a weak core as indicated by the low calculated buckling load of the web. (See table 4.1.) Model A fails by large interfacial slip causing shear failure of the bonds, see figure 4.18. Thus ultimately the face plates will work as two separate beams and the sandwich effect will be lost. The stiffness of this core is also relatively low compared to the plate stiffness which is used.

The failure of the corrugated sandwich panel in bending transverse to the corrugations is governed by a combination of face and core geometry. There is no single predominant factor. The core and face plate failures are mutually exclusive since the mechanism of face failure requires that the core integrity remains intact to develop very high axial stresses in the faces. This can only occur at moderate curvatures provided the skins remain a large distance from the neutral axis[31]. The switch between the two failure types is subtle and thus a detailed understanding of the core geometry and localised deformation effects is necessary to permit design for a specific mode of failure. Further

evidence for this was also found in a numerical study by Clark[24] who carried out a sample parametric study indicating how the properties of a panel change if its weight is kept constant but the ratio of the skin gauge to corrugation gauge is varied from 1:1 to 3:1. He found that for ratios 1:1, 1.5:1 and 2:1 the failure was by local buckling in the skin. For the skins with ratio 2.5 and 3 times the thickness of the corrugation, the thin webs buckled first. For Clark's particular case, the optimum method to distribute weight was to have twice the face plate thickness the of the core plate thickness. He concluded that this is not a universal law, but it depends on the specific case. Furthermore, he concluded that by using by finite element analysis, he could predict failure loads of this kind to within 20%, but that design is still a case of trial and error.

For marine applications, the skin thickness will be kept high to allow for corrosion and to guard against accidental penetration damage from local impact. This may limit the attainable weight efficiency of a sandwich panel. As Sen et al[5] reported, the weight efficiency is critically dependent on the permissible minimum plate thickness and this form of panel will only offer significant weight saving if the minimum thickness can be reduced. Similarly, for automobile applications, sandwich optimum skin thickness are too thin[22] and hence are susceptible to damage or corrosion. However, weight savings are possible with sandwich panels with skins thicker than the optimum may require. Thus, failure of the skins is relatively unlikely and the geometry of the core will be the important design parameter. As previously stated, two modes of core failure can occur. Interfacial slip of the core is determined by the performance of the core and adhesive bonds. Finite element stress analysis has demonstrated the bond area to be in levels of high varying stress, especially at the edge of the bond, and also that complicated stress distributions are present in a corrugated panel. Across the adhesive bond, there are high stress differentials and peak stresses occurred at the bond edge. The axial stresses are mobilised in the supported plate/adhesive to limit the local bending curvature in the unsupported face plate between the troughs[10]. The single corrugation element model showed there was a small difference in the stress pattern at the bond edge when the length of the flange is increased. The resultant stress distribution is shown in figure 4.15, which shows that the stress level at the bond edge decreases and a larger proportion of the joint in the centre is carrying a low stress level. Thus stabilising the local bending curvature. The flange size has been shown to be not very influential in the structural efficiency of the overall sandwich beam in the longitudinal direction. In a previous section

(2.6.2), it was shown that increasing the overlap length of lap shear joints did not increase the ultimate load carrying capacity proportionally. Hart Smith[32] demonstrated that joint strength is initially proportional to the short overlap length. Then, as the overlap is increased further, the central portion of a joint is under a very low level of stress and is effectively redundant. Ultimately, no matter how much longer an overlap is made in a double strap joint, the joint strength remains the same and so does the maximum adhesive stress and strain. The flange must therefore be of an optimum length where the maximum stress and strain performance are attained for the adhesive. Increasing the flange length will slightly increase the sandwich longitudinal stiffness and efficiency and may increase the ultimate transverse capacity of the sandwich structure where a core failure through interfacial slip might be expected. A balance has to be drawn between the joint carrying capacity and axial stress levels along the adhesive layers and face plate, so that the optimum geometry may be obtained in the corrugated core sandwich panel. That is, if the flange length increases, intuitively there is a greater likelihood of local face plate buckling between troughs. Norris et al[13] drew a similar general conclusion, that the degree of local bending increased as the ratio of the distance between spot welding at the flanges (effectively flange length) to plate thickness increased.

Ideally, more experiments on thick section corrugated core sandwich panels should be undertaken to verify optimum design characteristics of the detailed core geometry, bond and face plates. The manufacturing of a continuous corrugated core of the required dimensional tolerance was impractical and outwith the scope of the University workshops and many commercial fabricators. Thus the experimental testing was to a degree limited to the type of cores which were available.

Static three point bend tests did not highlight any substantial benefits in terms of static strength and stiffness from using adhesive bonding or laser welding as a joining method, apart from the practical fabrication methods as mentioned previously. It must be noted that the specimens tested were not specifically designed to increase performance through using adhesive bonding i.e. the bond area could be further optimised to increase strength and stiffness of the structure. Furthermore, due to the intimately connected adherends when using adhesive bonding there is less likelihood of crevice corrosion as might be found in a laser welded construction. The true benefits from adhesive bonding are shown under fatigue loading. The fatigue performance of spot welds have been

found wanting by some investigators[14] and require further study in the context of corrugated panels which would be subjected to fatigue loading[13]. The fatigue tests on the Model A beam, (see figure 4.10) showed the improved fatigue performance of the adhesively bonded beam relative to a laser welded beam. The calculated gradient of the SN line through the limited experimental data points for the laser welded construction is 2.7. Most experimental data for crack growth in structural steels is given a exponent of curve gradient[33], m = 3. In metals, from fracture mechanics theory of fatigue, it is known that if the crack initiation phase is negligible the slope parameter of the SN curve is identical to the crack growth power law. This parameter depends mainly on the material property and hence all SN curves for a given material should be essentially parallel. In the experimental adhesively bonded model here the calculated gradient, using regression analysis, was 8.067. This value is high compared to fatigue crack growth in steel. This is similar to the gradients calculated in the previous section for fatigue of bonded composite pultrusion attachments and as discussed in the previous sections has implications in design (see section 3.6.6).

In a computational study[24] it has been shown that a finite element stress analysis model can predict stresses to within 5% of those obtained in the laboratory. And stiffnesses in the direction parallel to the corrugations can be predicted to within 10% using simple beam theory and neglecting the adhesive bonds. Furthermore, it has been shown that panel analysis in the longitudinal direction is predicting a structural action for a panel like that of a simply supported beam with stresses and strains indicating anticlastic bending curvature[10]. Only two bending experiments in the longitudinal direction were undertaken in this current study. The calculated experimental stiffness/rigidity values were found to be low compared to those calculated using beam theory in the longitudinal direction, see table 4.1 and 4.2. In fact, they were in error in excess of 50%. These errors are believed to be due to inadequate experimental beam elements. Model C failed through crushing of the core under the load point causing web buckling. It is thought therefore that the length of this beam was too short to develop true bending stresses. Model B also showed a much lower value of experimental stiffness than which was calculated through beam theory. It was felt that the beam was subject to boundary instabilities due to it only being one unit of corrugation wide. Other workers[12] reported that if a panel is simply supported all round it improves performance significantly. Despite relatively poor structural properties of the panel transverse to the

corrugations, a reduction in deflections brought about by supporting both orthogonal directions is significant. Despite the low values obtained for experimental rigidity/stiffness, when they are compared to the transverse rigidity values they are still significantly greater. Thus longitudinal and transverse static bending tests indicated the high directional characteristics of the corrugated core. To utilise a panel to its best advantage the core should be oriented such that the predominant load is carried in the longitudinal direction.

This work has shown that adhesively bonded steel corrugated core are feasible for marine applications and compare favourably with other fabrication methods available, especially in fatigue loading situations. They have been shown to have structural benefits over conventional stiffened panelling but are highly orthotropic and have a complex behaviour pattern transverse to the corrugations. To maximise structural capabilities the corrugated sandwich panel should be orientated such that the lines of corrugations are parallel to the maximum load. Further testing is required to produce comprehensive design tables transverse to the corrugations. From this study several conclusions can be drawn and follow in the next section.

4.9 Conclusion

(i) Heavy grade steel sandwich construction using adhesives has been shown to be possible using a single part hot cure epoxy adhesive. This laboratory fabrication method could easily be scaled up using heating pads (like those used for removing welding distortion) for use in the offshore fabrication and shipbuilding industries.

(ii) The required weight of material i.e. thickness of material for offshore applications makes steel sandwich construction only possible using through thickness laser welding or adhesive bonding technology. Adhesive bonding has distinct practical advantages over laser welding.

(iii) The fatigue performance of adhesively bonded construction in the low stress, high cycle fatigue regime is superior to laser welded construction.

(iv) Failure mechanisms and theory to predict corrugated core sandwich performance transverse to the corrugations are complicated due to (a) the faces are thick and no allowance is made for their local bending stiffness about their own centroidal axes and (b) the core is stiff enough to contribute to the overall stiffness of the sandwich construction. These factors would indicate that practical steel corrugated sandwich panels would not conform to established theories and their assumptions.

(v) Detailed stress distributions in the corrugated construction may be predicted using appropriate finite element analysis.

(vi) Many variables influence the performance of a corrugated sandwich panel. In the direction parallel to the corrugation, the web angle and core depth are the most influential.

(vii) Corrugated cored sandwich construction is a structurally efficient and volume efficient form of stiffened panelling.

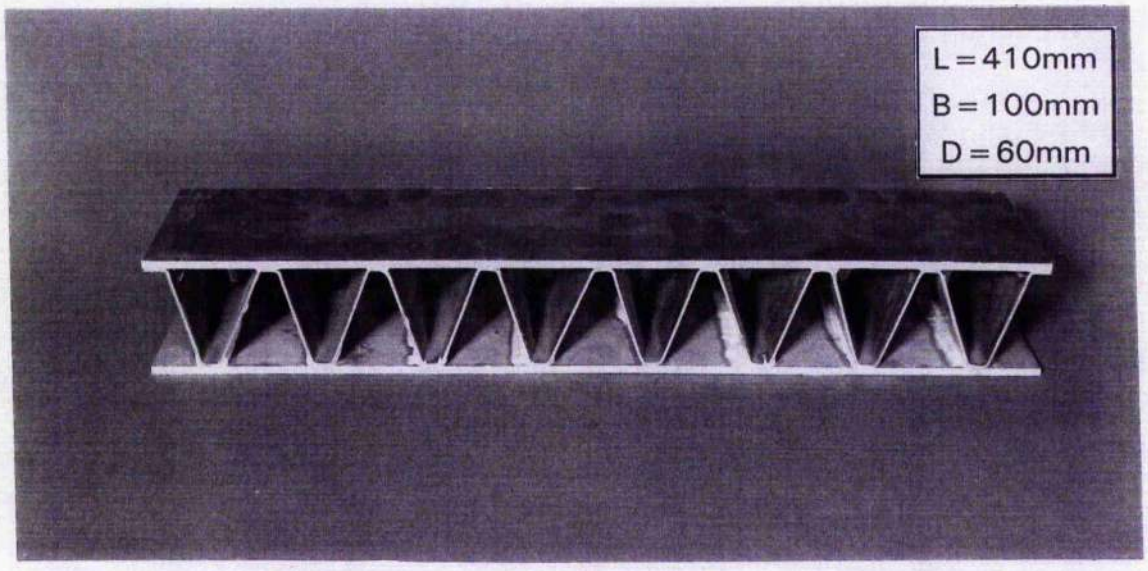

Figure 4.1 All steel adhesively bonded (Araldite 2007) corrugated core sandwich beam

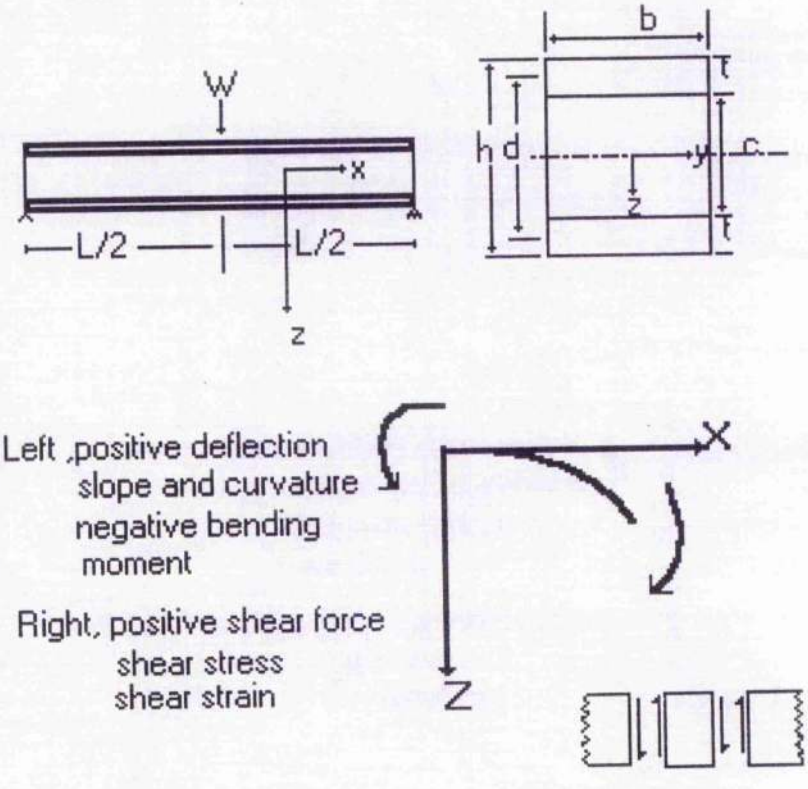

Figure 4.2 Simple sandwich beam and sign convention for sandwich theory

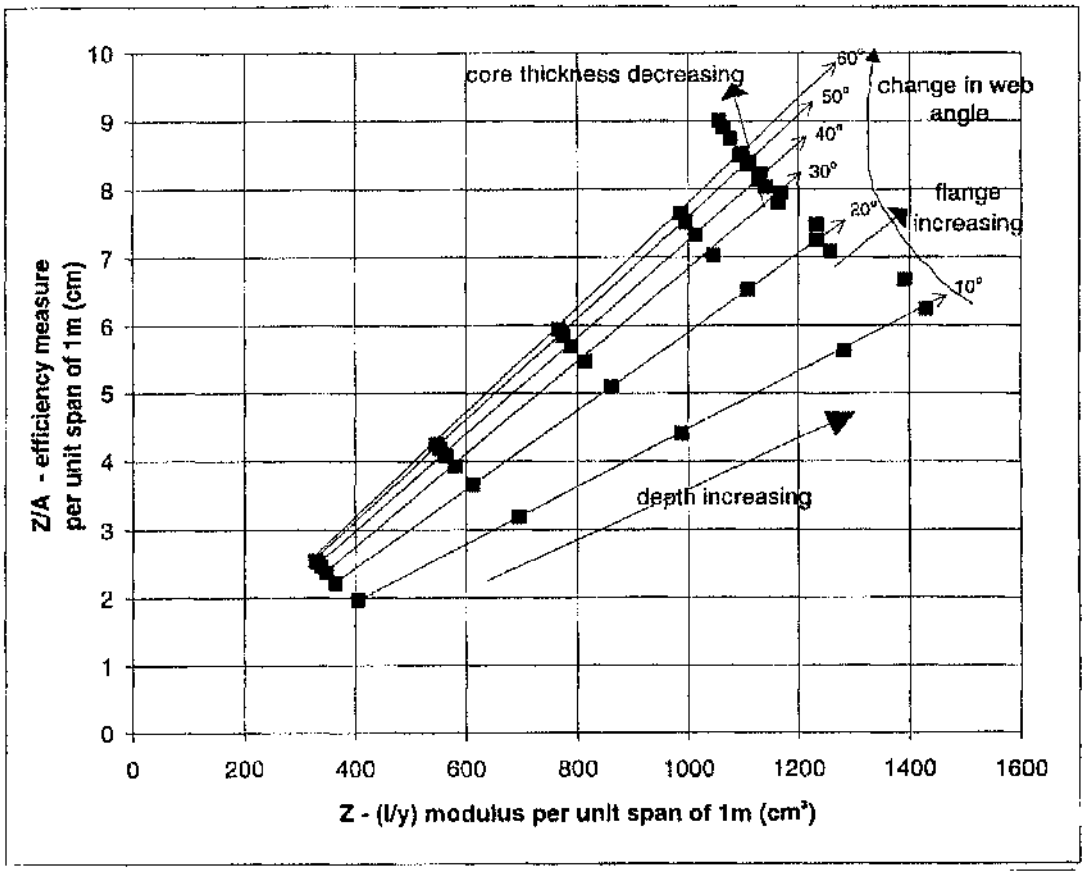

Figure 4.3 Influence of various parameters on the longitudinal structural efficiency of the corrugated core

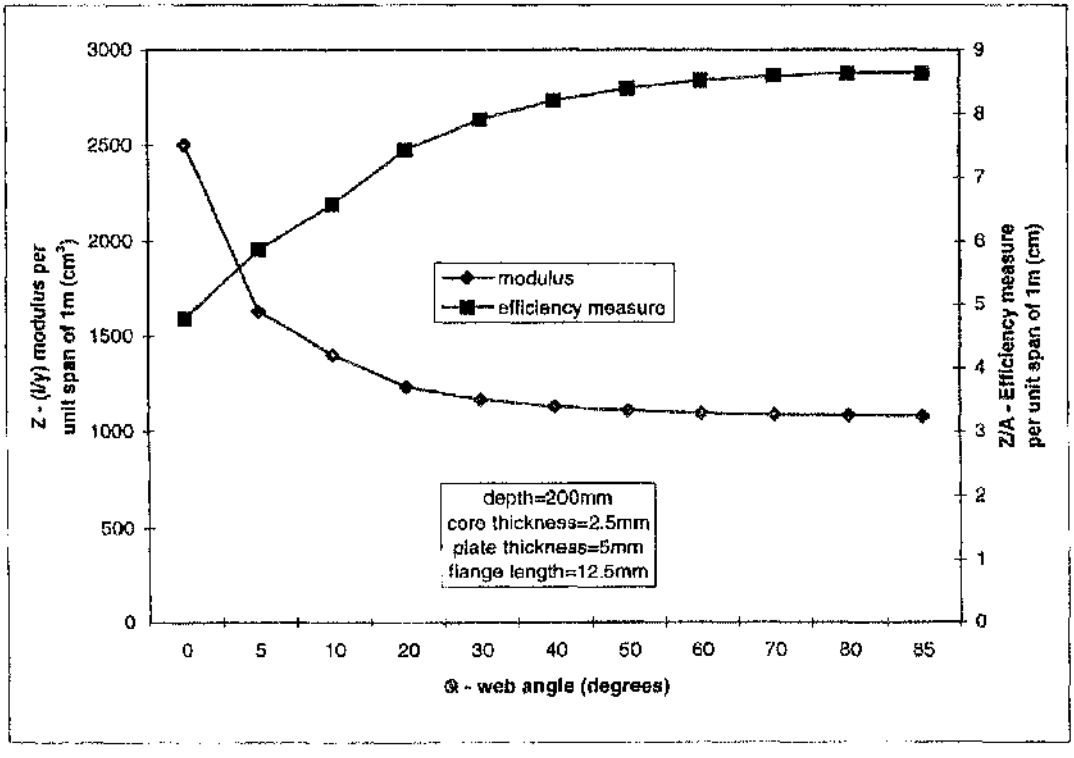

Figure 4.4 Effect of core web angle on longitudinal modulus and structural efficiency for a given core depth, face plate thickness and flange length

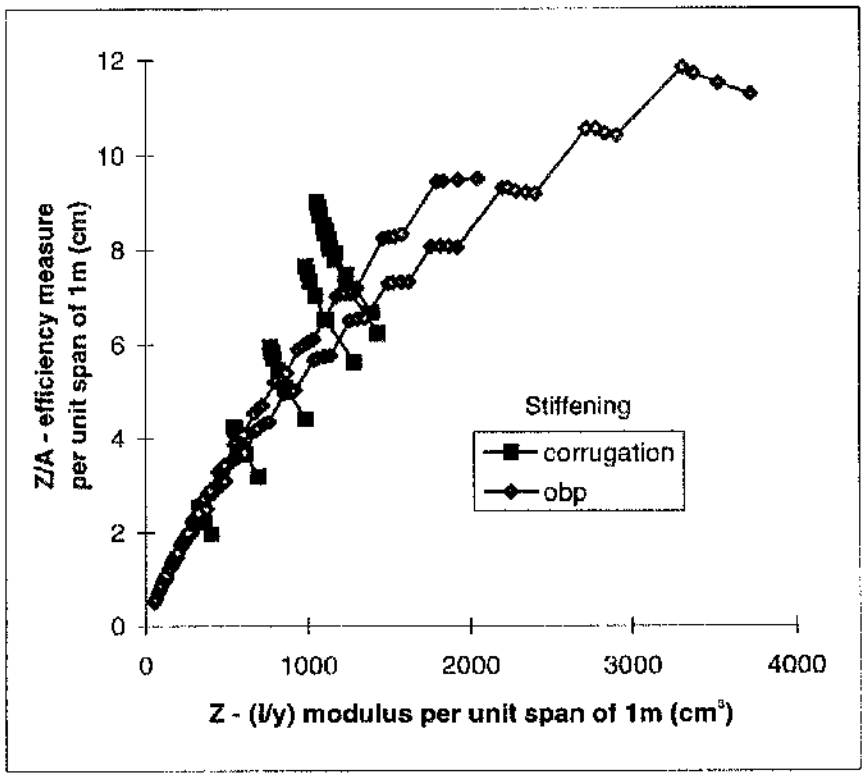

Figure 4.5 Comparison of the longitudinal structural efficiency of the corrugated sandwich structure versus traditional single sided stiffening

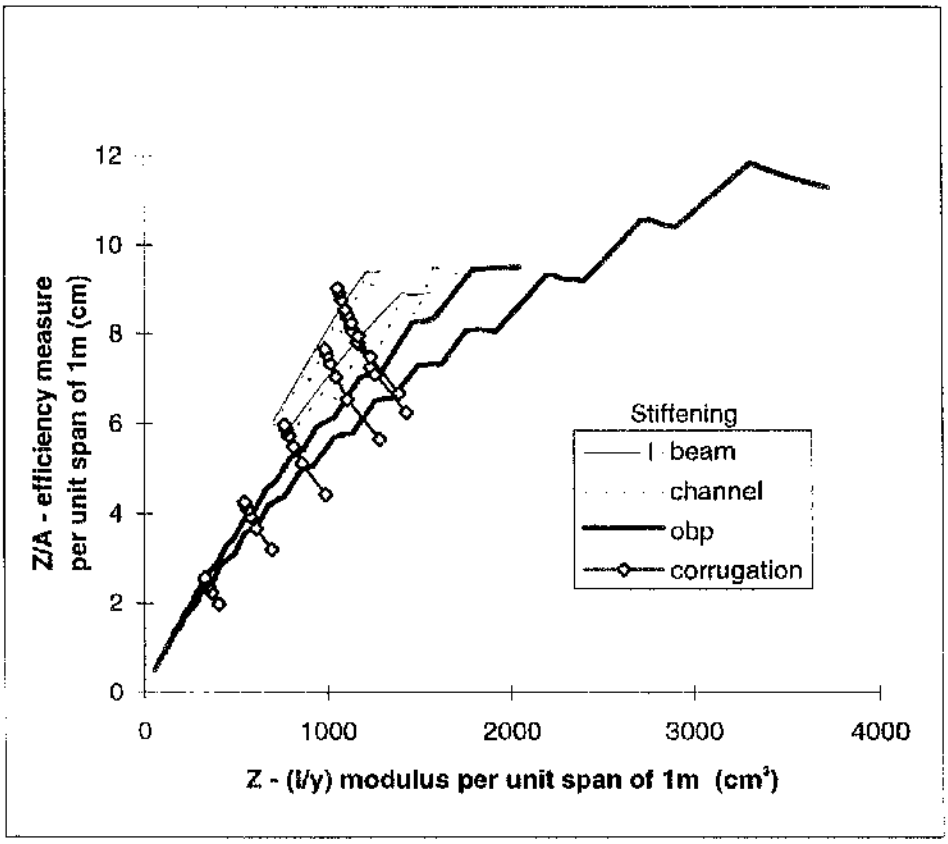

Figure 4.6 Comparison of the longitudinal structural efficiency of the corrugated sandwich structure versus alternative forms of stiffening

Three point bend test	units	model A	model B	model C	model D
length	mm	410	500	500	410
breadth	mm	100	100	100	100
depth	mm	60	75	86	80
span between supports	mm	350	350	330	370
plate thickness	mm	4	2.03	4	2.65
core plate thickness	mm	1.5	1.14	2.5	1.8
flange length	mm	5	5.25	40	12.5
web length	mm	53	74.4	90	77.6
core height	mm	52	69.9	78	75
web angle	deg	18	20	30	25
adhesive area	mm2	1000	1057	8000	x
adhesive area/metre	mm2	16400	20019	32000	x
unit span	mm	50	52.8	250	130
units/beam	-	8.2	9.47	2	3.15
units /metre	-	20	18.94	4	7.69
mass	kg	3.83	3.015	4.58	2.725
mass/metre	kg/m	9.34	6.03	9.16	6.65

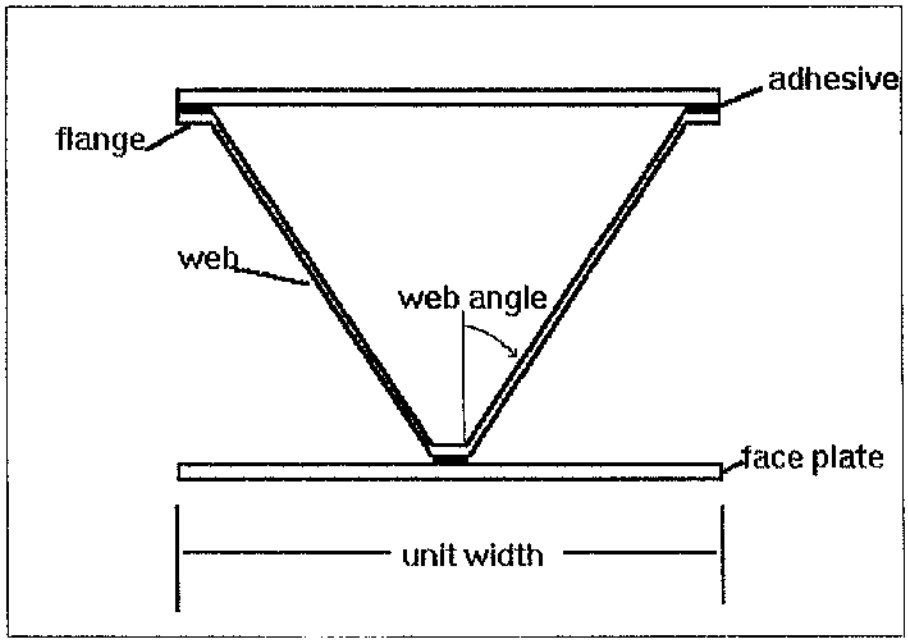

Figure 4.7 Terminology diagram and experimental sandwich dimensions

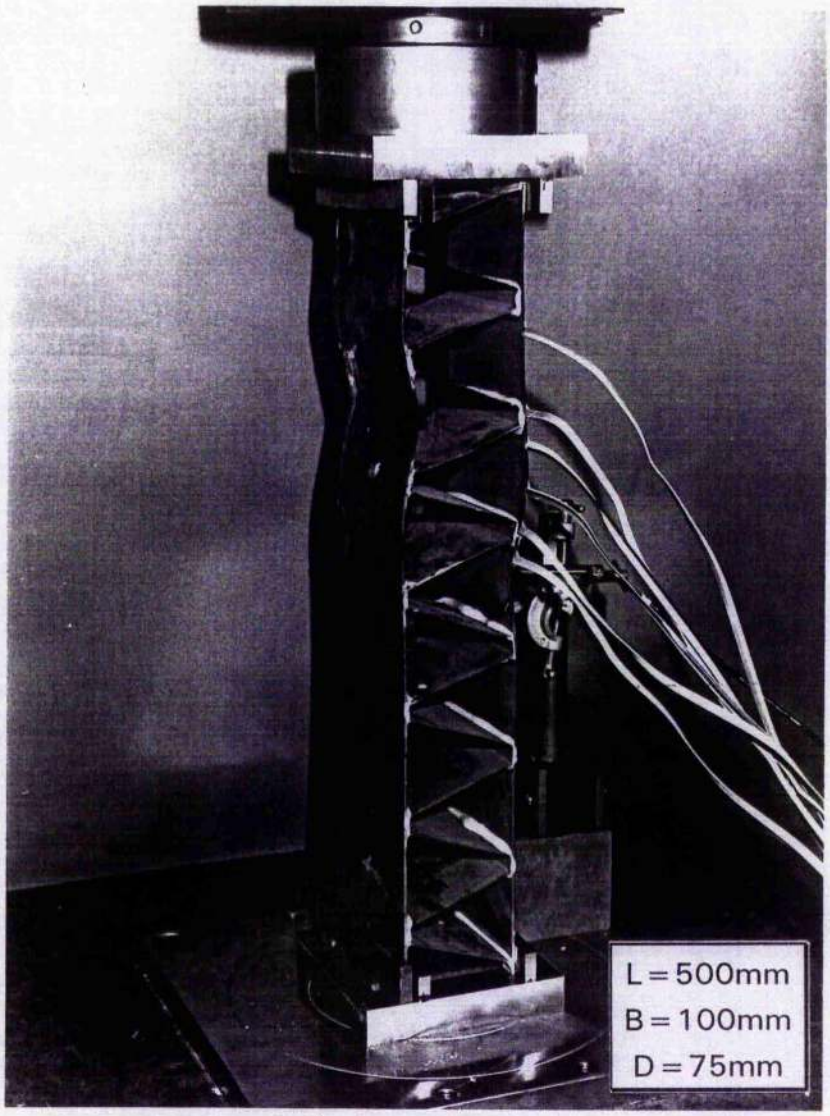

Figure 4.8 Axial compression test

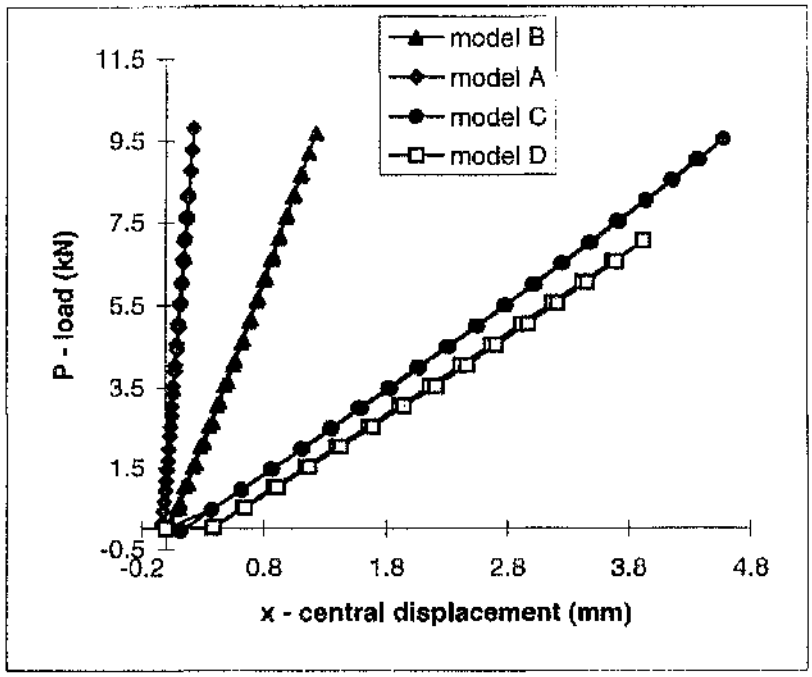

Figure 4.9 Load versus displacement curves for experimental sandwich beams tested in static three point bending transverse to the corrugations

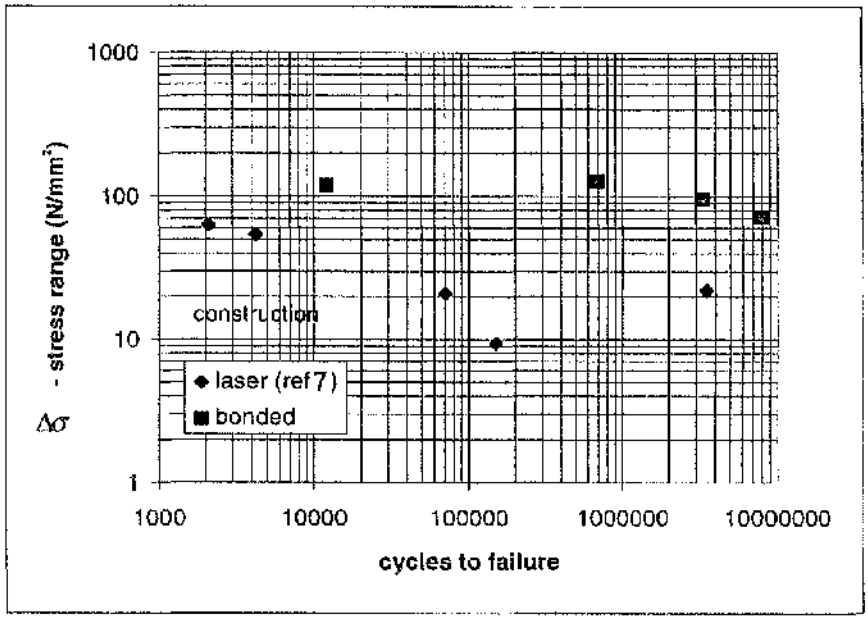

S - N Experimental Curves

Adhesive Beam = $\log N = 22.015 - 8.067 \log \Delta\sigma$

Laser Beam = $\log N = 8.596 - 2.7 \log \Delta\sigma$

Figure 4.10 Fatigue experimental results of sandwich beams in the form of a S-N diagram tested in bending transverse to the corrugations

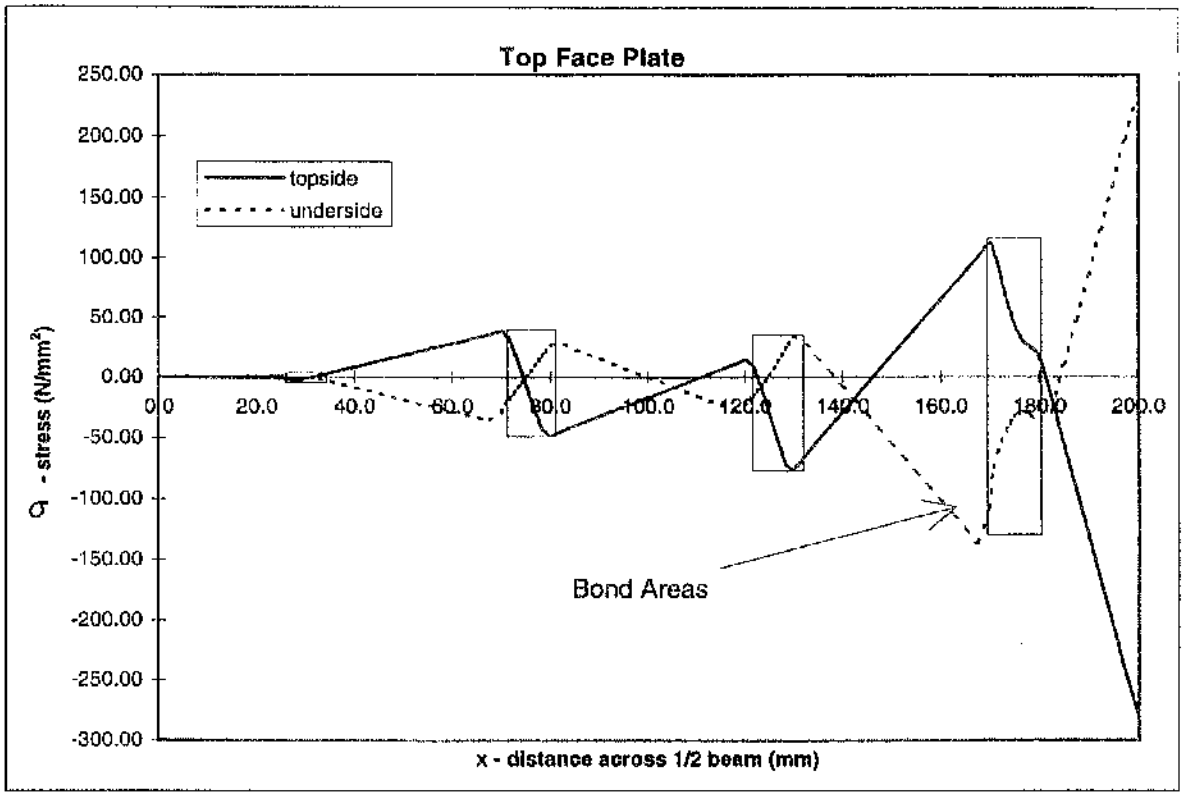

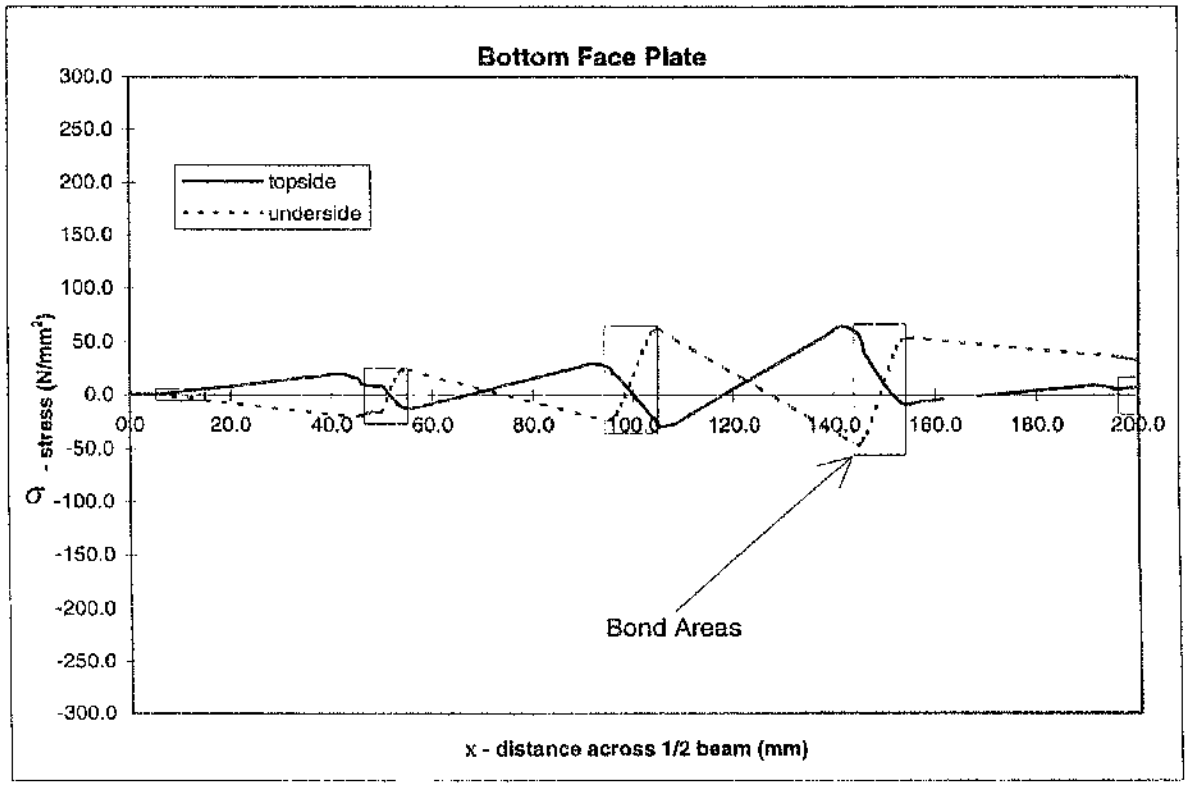

Figure 4.11 Finite element transverse in plane stress distribution across the face plate surfaces of a bonded steel corrugated core sandwich construction

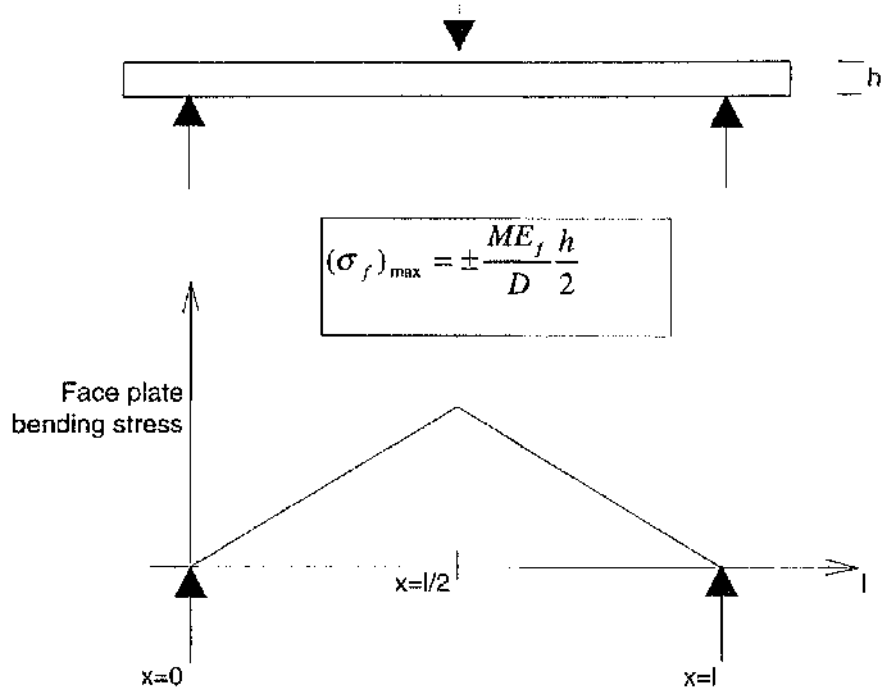

Figure 4.12 Schematic representation of the tensile transverse bending stress from simple sandwich beam theory.

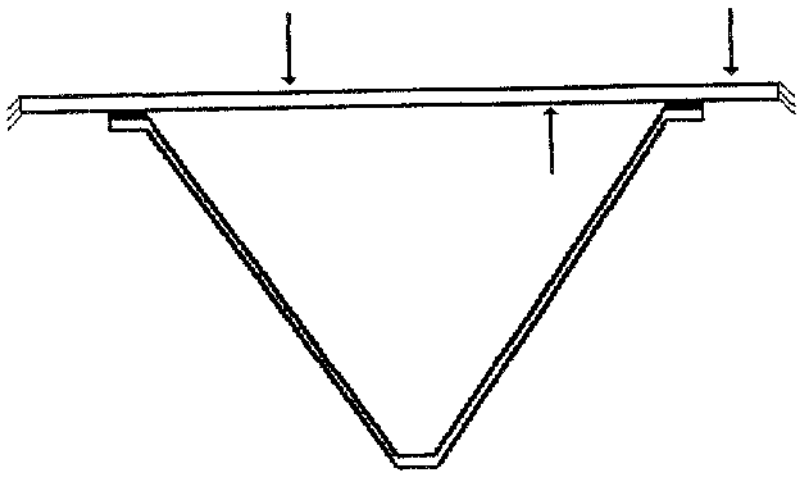

Figure 4.13 Single element model for finite element stress analysis

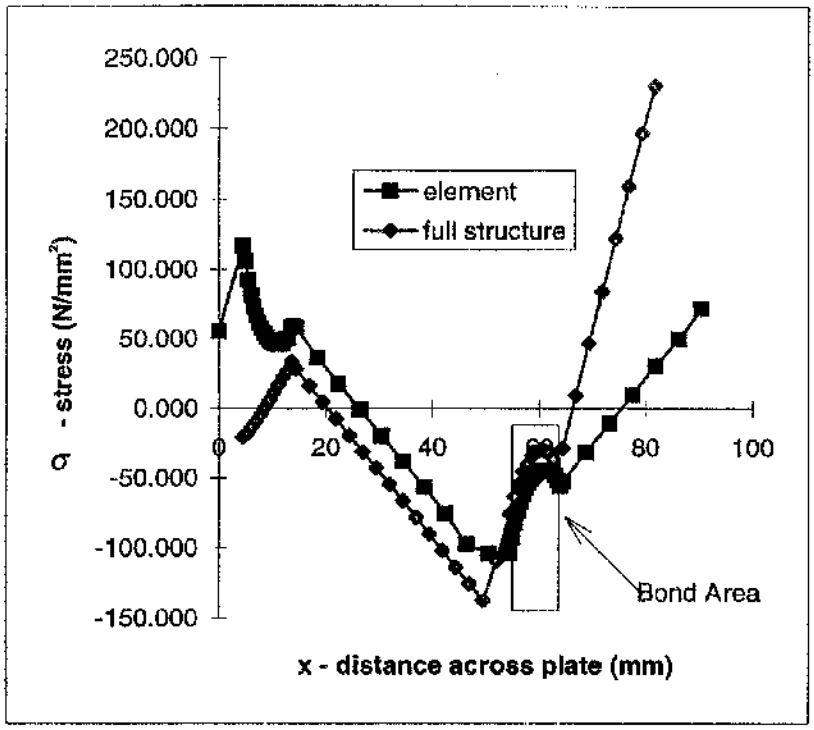

Figure 4.14 Finite element axial stress results for a single corrugation unit

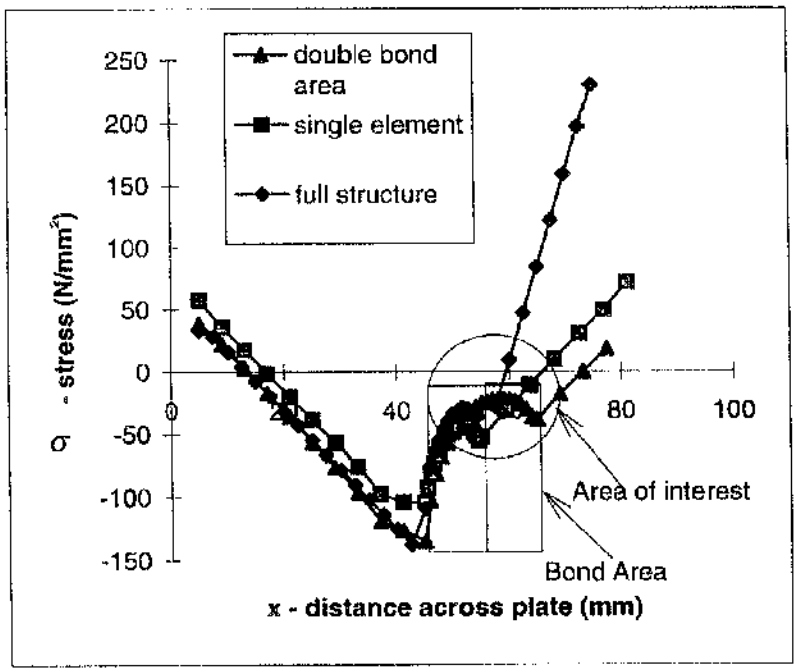

Figure 4.15 Resultant axial stress distribution at bond edge for an increase in flange length

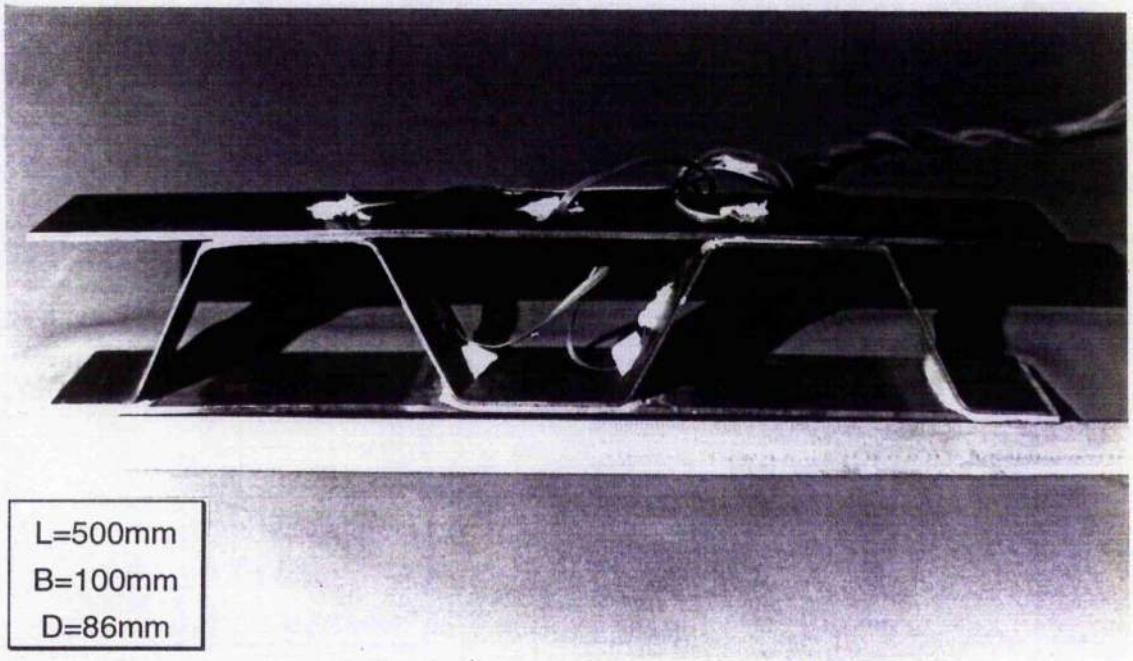

Figure 4.16 Model C demonstrating permanent plastic deformation of the beam element after loading transverse to the corrugations in bending

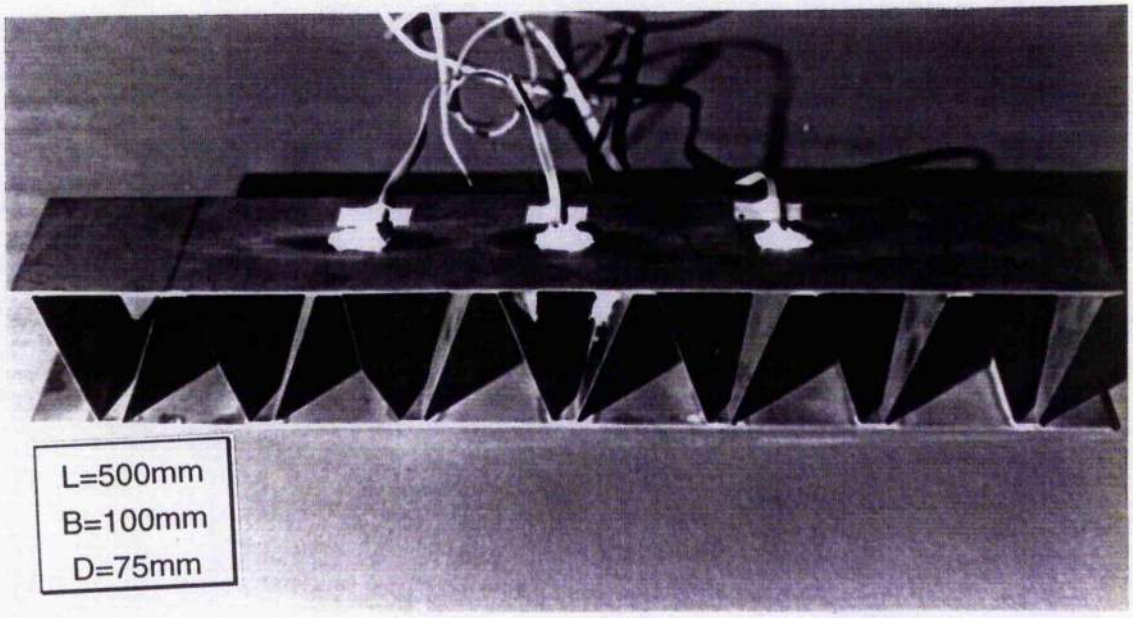

Figure 4.17 Model B demonstrating failure by web buckling after loading transverse to the corrugations in bending

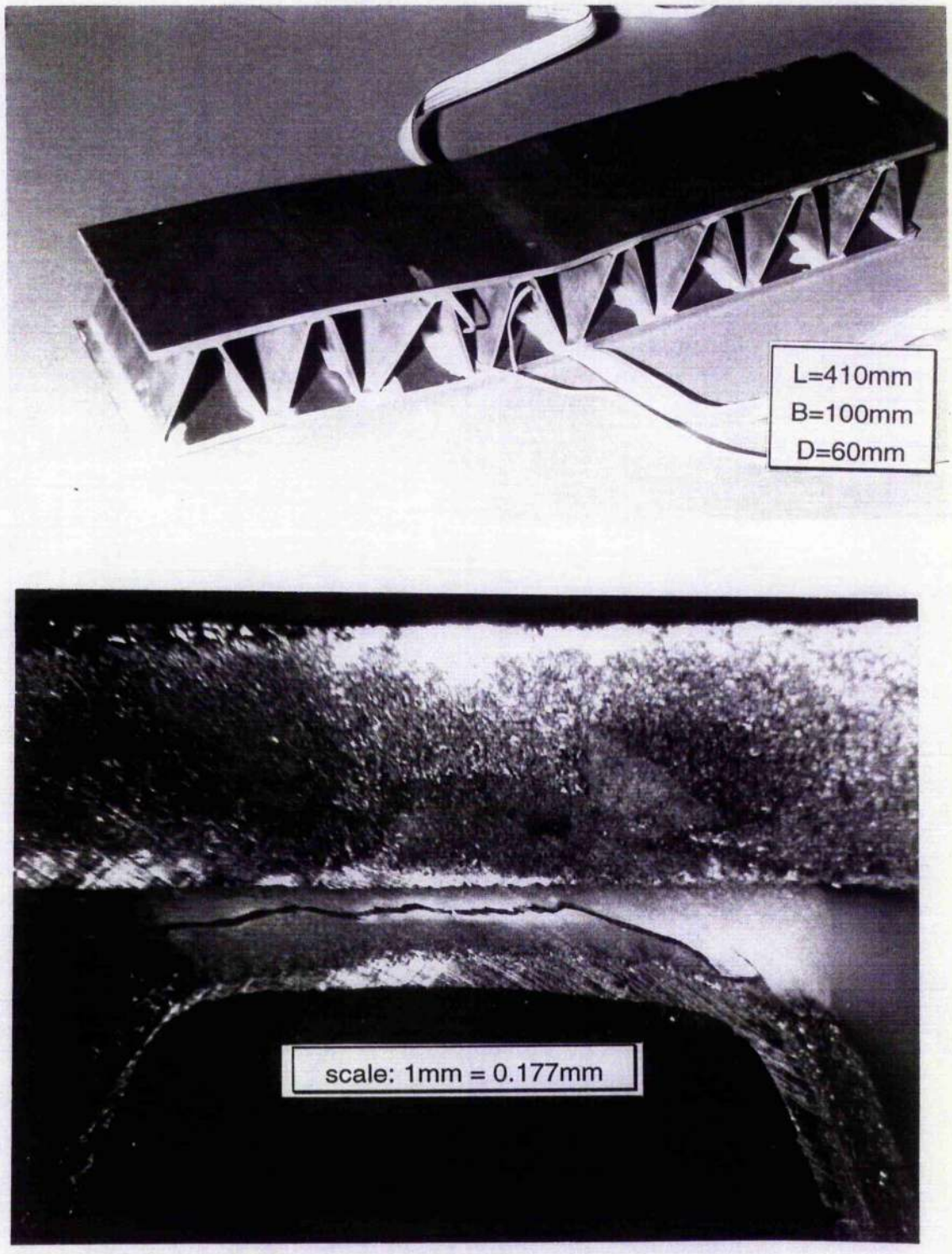

Figure 4.18 Model A demonstrating shear failure of a bond to allow the face plate to slip after loading transverse to the corrugations in bending

Model	A	B	C	D
plate stiffness(mm4)	6.28E+05	5.25E+05	1.35E+06	7.99E+05
web stiffness (mm4)	1.68E+04	3.45E+04	1.14E+05	5.76E+04
longitudinal unit stiffness(mm4)	6.66E+05	6.24E+05	2.23E+06	1.05E+06
longitudinal stiffness/metre(mm4)	1.33E+07	1.18E+07	8.90E+06	8.08E+06
web buckling stiffness(mm4)	28	12	130	49
web critical buckling load(kN)	21	5	33	17
transverse experimental rigidity(Nmm2)	3.91E+10	7.04E+09	1.57E+09	1.90E+09
transverse experimental stiffness (mm4)	1.96E+05	3.52E+04	7.85E+03	9.50E+03
failure mode	bond	web	face plate	face plate
failure load(kN)	25	24.55	14.61'	12.5'
failure displacement(mm)	1.853	3.35	8.28	9.74

' test stopped due to large deformation

Table 4.1 Sandwich static performance transverse to corrugations (three point bend)

Model	B	C
Span (mm)	350	360
Experimental rigidity(Nmm2)	6.93E+10	9.42E+10
Experimental stiffness(mm4)	3.47E+05	4.71E+05
Failure type	bond	web buckle
Failure load(kN)	14.25	119.57
Failure displacement(mm)	0.2	0.86

Table 4.2 Sandwich static performance parallel to corrugations (three point bending)

model	failure	load(kN)
A	face plate	235
B	bond failure	56
C	face plate	74

Table 4.3 Sandwich static performance (axial compression)

MATERIAL	YOUNG'S MODULUS (N/mm2)	POISSONS RATIO
Mild steel	210000	0.3
Epoxy adhesive Araldite 2007[34]	5000	0.37

Table 4.4 Data input for finite element stress analysis

5.0 Conclusion

This work has demonstrated that adhesive bonding technology has great potential for use in the marine and offshore industry. There are distinct practical and performance advantages when adhesive technology is used to fabricate corrugated core steel sandwich structures. Such constructions offer better structural efficiency when compared to single sided traditional fabrications. The performance of a corrugated core sandwich construction is dependent on the combination of face and core geometry. The bonded panels demonstrate increased fatigue durability when compared to the equivalent laser welded construction.

Structural bonding of grp sections has been shown to be effective, simple and fairly tolerant to the processing parameters and environment. The choice of the adhesive for the appropriate application is important. The performance of the adhesive in a composite joint does not appear to be the issue. In most cases in this study, in fatigue loading, high strength butt joints and durability performance in a wet environment the performance of the interlaminar strength or the adhesion of the resin to the fibres is the factor which dominates joint performance.

It has been shown that thick adherend steel bonded joints are affected by humidity or liquid water. A surface preparation which gives adequate short term strength (shot blasting) can be improved to increase long term strength in a humid environment by the use of a primer. The overall joint performance may be increased by leaving the spew fillet intact while also considering joint design to ensure that water cannot condense on the glueline. The application of a low nominal load reduces the durability performance of a bonded joint while in the case of a bulk adhesive, the durability performance is improved as long as the preload level is relatively low. It is understood that the bulk adhesive undergoes creep deformation in a humid environment and thus the level of preload is critical.

The interface is the determining parameter in the durability performance and the degradation of the adhesive is a secondary effect. It is believed that the liquid water diffuses not only through the adhesive but along the adhesive-adherend interface of a shot blasted steel adherend. As the interface had been established as the deciding factor in durability performance a novel rapid method of grading the interface performance was successfully developed for metallic adherends.

Adhesive technology has been shown to have distinct practical potential for marine applications and this work has allayed many previous concerns and uncertainties for its use.

6.0 References

1.0 Introduction

1. Kinloch, A.J., (1987) *Adhesion and Adhesives Science and Technology,* University Press, Cambridge, ISBN 0 412 274440 X.
2. Glagow Marine Technology Centre (1996) *Adhesives Bibliography,* Glasgow University, Glasgow, G12 8QQ.
3. Bell, J. (1996) High-power lasers weld ship-shape structures. *OLE,* May, pp17-21.

2.0 Section A: Durability Performance of Adhesively Bonded Joints

1. Kinloch, A.J. (1983) *Durability of Structural Adhesives* (ed. A.J. Kinloch), Elsevier Applied Science Publishers, ISBN 0 85334 214 8, chap 1.
2. Volkersen, O.R. (1938) *Luftfahrforschung* **15**(112), pp41-47.
3. Goland, M. and Reissner, E.J. (1944) *Applied Mech. Trans. ASME* **66,** A17 417.
4. Crocombe, A.D. (1989) Global yielding as a failure criterion for bonded joints. *Int. J. Adhesives and Adhesion* **9**(3), pp145-153.
5. Lubkin, J.L. and Reissner, E. (1956) *Trans. ASME* **78**, p1213.
6. Kinloch, A.J. (1987) Mechanical behaviour of adhesive joints. *Adhesion and Adhesives Science and Technology,* Chapman and Hall, ISBN 0 412 27440 x, chap 6, p223.
7. Adams R.D. (1986) The mechanics of bonded joints. *Structural Adhesives in Engineering* C180/86, I. Mech. E., pp17-24.
8. Kinloch, A.J., (1980) Review: The science of adhesion part 1. Surface and interfacial aspects. *J.Mat. Sci.* **15**, pp2141-2166.
9. Voyutskii, S.S. (1963) *Autohesion and Adhesion of High Polymers,* John Wiley/ Interscience, New York.
10. Deryaguin, B.V. and Smilga V.P. (1969) *Adhesion Fundamentals and Practise,* McLaren, London, p152.
11. Staverman A.J. (1965) *Adhesion and Adhesives* 1 (ed R. Houwink and G. Salmon), Elsevier, Amsterdam, p9.
12. Kinloch, A.J. (1980) Review: The science of adhesion part 2. Mechanics and mechanisms of failure. *J.Mat. Sci.* **17**, pp617-651.
13. Hashim, S.A. and Cowling, M.J. (1995) Aspects of testing and failure surface analysis related to thick adherend steel bonded joints. Proc. *Structural Adhesives in Engineering IV,* Bristol, U.K., Inst. of Materials, ISBN 0901716 91 x, pp245-250.

14. Comyn, J. (1983) Kinetics and mechanisms of environmental attack. *Durability of Structural Adhesives* (ed. A.J. Kinloch), Elsevier Applied Science Publishers, ISBN 0 85334 214 8, chap 3.
15. Ning, S.U., Mackie, R.I. and Harvey, W.J. (1992) The effects of aging and environment on the fatigue life of adhesive joints. *Int. J. Adhesion and Adhesives* **12**(2), pp85-93.
16. Zanni-Deffarges, M.P. and Shanahan, M.E.R. (1993) Evaluation of adhesive shear modulus in a torsional joint: influence of aging. *Int. J. Adhesion and Adhesives* **13**(1), pp41-45.
17. Davis, R.E. and Fay, P.A. (1990) The effect of a tropical environment and stress on bonded steel joints. Proc. *Adhesion'90,* Cambridge, U.K., The Plastics and Rubber Institute, ISBN 1 871571 21 9, pp27/1-27/6.
18. Kinloch, A.J. (1983) *Durability of Structural Adhesives* (ed. A.J. Kinloch), Elsevier Applied Science Publishers, ISBN 0 85334 214 8.
19. Gledhill, R.A. and Kinloch, A.J. (1974) Environmental failure of structural adhesive joints. *J. Adhesion* **6**, pp315-330.
20. Zanni-Deffarges, M.P and Shanahan, M.E.R. (1995) Diffusion of water into an epoxy adhesive:comparison between bulk behaviour and adhesive joints. *Int. J. Adhesion and Adhesives* **15**(3), pp3-15.
21. John, S.J., Kinloch, A.J. and Mathews, F.L. (1991) Measuring and predicting the durability of bonded carbon fibre/epoxy composite joints. *Composites* **22**(2), pp121-127.
22. DeNeve, B., Auriac, Y. and Shanahan, M.E.R (1993) Degradation of an epoxy resin in a water environment. Proc. *Adhesion'93*, York, U.K., Int. of Mat., pp159-164.
23. Apicella, A., Migliaresi, C., Nicolais, L., Iaccarino, L. and Roccotelli, S. (1983) The aging of unsaturated polyester based composites: influence of resin chemical structure. *Composites* **14**(4), pp387-392.
24. Gledhill, R.A. Kinloch, A.J. and Shaw, S.J. (1980) A model for predicting joint durability. *J. Adhesion* **11**, pp3-15.
25. Brockmann, W. (1983) *Durability of Structural Adhesives* (ed. A.J. Kinloch), Elsevier Applied Science Publishers, ISBN 0 85334 214 8, chap 7, p306
26. Ripling, E.J., Mostovoy, S. and Patrick, R.L. (1964) Measuring fracture toughness of adhesive joints. *Mat. Res. Std.* **4**, pp129-134.
27. Mostovoy, S. and Ripling, E.J. (1969) Influence of water on stress corrosion cracking of epoxy bonds. *J. of Applied Polymer Science* **13**, pp1083-1110.
28. Cherry, B.W. and Thomson, K.W. (1977) The effect of stress on water induced failure of epoxy/aluminium joints. *Adhesion 1*, (ed K.W. Allen), Applied Science Publishers, London, p251-267.
29. Davis, R.E. and Fay, P.A. (1993) The durability of coated steel joints. *Int. J. Adhesion and Adhesives* **13**(2), pp97-104.

30. Kinloch, A.J. (1979) Interfacial fracture mechanics aspects of adhesive bonded joints - a review. *J. Adhesion* **10,** pp193 - 219.
31. Brewis, D.M., Comyn, J. and Tegg, J.L (1980) *Int. J. Adhesion and Adhesives* **1,** p35
32. DeNeve, B. and Shanahan, M.E.R. (1992) Effects of humidity on an epoxy adhesive. *Int. J. Adhesion and Adhesives* **12,** pp191-196.
33. Bowditch, M.R., Hiscock, D. and Moth, D.A. (1992) The role of the substrate in the hydrolytic stability of adhesive joints. *Int. J. Adhesion and Adhesives* **12**(3), pp164-170.
34. Crank, J. (1975) *The Mathematics of Diffusion.* 2nd ed. Oxford University Press.
35. Bowditch, M.R., Hiscock, D., and Moth, D.A. (1990) The relationship between hydrolic stability of adhesive joints and the equilibrium water content. Proc. *Adhesion'90*, Cambridge, U.K., The Plastics and Rubber Institute, ISBN 1 871571 21 9, pp18/1-18/8.
36. Brewis, D.M., Comyn, J., Kinloch, A.J. and Ravall, A.K. (1990) Is there a critical relative humidity For the weakening of joints in wet air? Proc. *Adhesion'90*, Cambridge, U.K., The Plastics and Rubber Institute, ISBN 1 871571 21 9, pp28/1-28/6.
37. Kinloch, A.J. (1987) *Adhesion and Adhesives Science and Technology.* Chapman & Hall, London, ISBN 0 412 27440 x, p364, table 8.3.
38. Brockmann, W. (1983) *Durability of Structural Adhesives* (ed. A.J. Kinloch), Elsevier Applied Science Publishers ISBN 0 85334 214 8 chap7 fig 3&4
39. Brockmann, W. (1969) *Adhasion*, (1969)345, 448, (1970) 52, 250.
40. Brockmann, W. (1983) *Durability of Structural Adhesives* (ed. A.J. Kinloch), Elsevier Applied Science Publishers, ISBN 0 85334 214 8, chap 7, fig 2.
41. Fay, P.A. and Maddison, A. (1989) Durability of adhesively bonded steel under salt spray and hydrothermal stress conditions. Proc. *Structural Adhesives in Engineering II,* Bristol, U.K., Butterworths Scientific, pp112-121.
42. Hercules, D.M. (1974) *J. Electron Spectrosc*, Rel. Phen. **5**, 811.
43. Gledhill, R.A., Shaw, S.J. and Tod, D.A. (1989) Organosilanes for durability enhancement. Proc. *Structural Adhesives in Engineering II,* Bristol, U.K., Butterworths Scientific, pp133-140
44. Comyn, J. (1989) Surface treatment and analysis for adhesive bonding. Proc. *Structural Adhesives in Engineering II,* Bristol, U.K., Butterworth Scientific, pp41-45.
45. Tod, D.A., Atkins, R.W. and Shaw, S.J. (1992) Use of Primers to Enhance Adhesive Bonds. *Int. J. Adhesion and Adhesives* **12**(3), pp159-163.
46. Gettings, M. and Kinloch, A.J. (1977) Surface analysis of polysiloxane/metal oxide interfaces. *J. Mat. Sci* **12,** pp2511-2518.

47. Minford, J.D. (1983) Adhesives. *Durability of Structural Adhesives* (ed. A.J. Kinloch), Elsevier Applied Science Publishers, ISBN 0 85334 214 8, chap 4.
48. Minford, J.D. (1982) Durability of aluminium bonded joints in long term tropical exposure. *Int J. Adhesion and Adhesives* **2**, pp25 - 32.
49. Ciba Geigy Polymers, Duxford, Cambridge, CB2 4QA.
50. Autostic, Carlton Brown and Partners, Netherthorpe Rd. Sheffield SE 7EY
51. Union Carbide, Silane Coupling Agents Methods of Application, Technical Literature published by Union Carbide.
52. SIP, Technical Data Sheet, Permabond, 1986.
53. Albritec, Technical Note, Albright and Wilson, 1989.
54. Accomet C, Technical Note, Albright and Wilson, 1988.
55. SESAM, Developed by Det norske Veritas, marketed by Veritec, Marine Technology Consultants A.S., Veritec, Hovik, Oslo, Norway.
56. Adams, R.A. and Wake, W.C. (1984) *Structural Adhesive Joints in Engineering*, Elsevier Applied Science Publishers, ISBN 085334 263 6, chap 2, fig 26.
57. Jennings, C.W. (1972) *J.Adhesion* **4**, 25
58. Kinloch, A.J. (1987) *Adhesion and Adhesives Science and Technology*, Chapman and Hall, ISBN 0 412 27440 x, chap 3 fig 3.1.
59. Kinloch, A.J. (1987) *Adhesion and Adhesives Science and Technology*, Chapman and Hall, ISBN 0 412 27440 x, chap 3 p61.
60. Brockmann, W. (1983) *Durability of Structural Adhesives* (ed. A.J. Kinloch), Elsevier Applied Science Publishers, ISBN 0 85334 214 8, chap 7 fig 15
61. Brockmann, W. (1983) *Durability of Structural Adhesives* (ed. A.J. Kinloch), Elsevier Applied Science Publishers, ISBN 0 85334 214 8, chap 7 fig 10.
62. October, N. (1992) Private communication. Ciba Geigy Polymers, Duxford Cambridge.
63. Kinloch, A.J. (1987) *Adhesion and Adhesives Science and Technology.* Chapman & Hall, ISBN 0 412 27440 x, chap 4 p140.
64. Jackson, P.A. (1994) Private communication. Courtaulds Coatings (Holdings)Ltd.
65. Adams, R.D and Zhao, X. (1992) The significance of local effects on the strength of bonded joints. Proc. *Structural Adhesives in Engineering III* Bristol, U.K., The Plastics and Rubber Institute, ISBN 1 87 4667 00 4, pp1/1-1/5.
66. Adams, R.D. and Wake, W.C. (1984) *Structural Adhesive Joints in Engineering*, Elsevier Applied Science Publishers, ISBN 0 85334 263 6 p40 fig 21.
67. Adams, R.D. and Panes, G.A. (1993) Crack initiation in adhesively bonded joints. Proc. *Adhesion'93*, York, U.K., The Inst of Materials, pp216-218.

68. Zhao, X. and Adams, R.D. (1989) Adhesive Joint Strength Predictions for Real Boundary Conditions. Proc. *Structural Adhesives in Engineering II*, Bristol, U.K., Butterworth Scientific, pp55-61.
69. Adams, R.D. and Wake, W.C. (1984) *Structural Adhesive Joints in Engineering,* Elsevier Applied Science Publishers, ISBN 0 85334 263 6, pp49-51.
70. Hart Smith, L.J. (1981) Further developments in the design and analysis of adhesively bonded structural joints. *Joining of Composite Materials* (ed. K.T. Kedwards), ASTM STP **740**.
71. Mallick, V. and Adams, R.D. (1989) Strength predictions of lap joints with elasto-plastic adhesives using linear closed formed methods. Proc. *Structural Adhesives in Engineering II,* Bristol, U.K., Butterworth Scientific, pp160-165.
72. Richardson, G., Crocombe, A.D. and Smith, P.A. (1995) Failure prediction in adhesive joints by various techniques including the modelling of crack development. Proc. *Structural Adhesive in Engineering IV,* Bristol, U.K., Inst. of Materials, ISBN 0901716 91 x, pp45-50
73. McCarthy, J. (1996) Some studies of failure criteria for adhesive joints. Proc. *Stress Analysis and Fracture in Adhesive Joints* London, U.K., Inst. of Materials, pp1-3
74. Adams, R.D. and Wake, W.C. (1984) *Structural Adhesive Joints in Engineering,* Elsevier Applied Science Publishers, ISBN 0 85334 263 6, chap 2 fig 30.
75. Chiu, K.W. and Jones, R. (1992) A numerical study of adhesively bonded lap joints. *Int. J. Adhesion and Adhesives* **12**(4), pp219-225.
76. Winkle, I.E., Cowling, M.J., Hashim, S.A. and Smith, E.M. (1991) What can adhesives offer shipbuilding? *J. of Ship Production* **7**(3), pp137-152
77. Wilcox R.P. (1991) Performance of joints under cryogenic conditions. Student Final Year Project Report, Dept. of Mech. Eng, Glasgow University.
78. Bikerman, J.J. (1968) *The Science of Adhesive Joints,* 2nd Edition, Academic Press, New York.
79. Sharpe, L.H. (1972) The interphase in adhesion. *J.Adhesion* **4**, pp51-6
80. Adams, R.D. and Peppiat, N.A. (1974) *J. Strain Analysis* **9**, p185.
81. MTS Project 3, (1994) Environmental durability of adhesive bonds. Task 2 Development of Experimental Database Interim Progress Report Feb 94.
82. Hashim, S.A. (1992) Assessment of adhesive bonding for structural design with thick adherends. *PhD thesis,* Glasgow University, Glasgow, U.K..
83. Smith, C.S. (1990) *Design of Marine Structues in Composite Materials,* Elsevier Applied Science, ISBN 1 85166 416 5, chap 3 p99.
84. Adams, R.D. and Wake, W.C. (1984) *Structural Adhesive Joints in Engineering,* Elsevier Applied Science, ISBN 0 85334 263 6, p250.

85. Brockmann, W. (1974) The environmental resistance of metal bonds in new industries and applications for advanced materials technology. *19th Sampe Symp. Exhibition,* Azuza California.
86. Arnold, D.B. (1981) Mechanical test methods for aerospace bonding. In *Developments in Adhesives-2* (ed. A.J. Kinloch), Applied Science Publishers, London, pp207-241.
87. Small, G.D. and Fay, P. (1990) Creep of adhesive lap joints in dry and high humidity environments. Proc. *Adhesion'90,* Cambridge, U.K., The Plastics and Rubber Insitute, ISBN 1871571 21 9, pp25/1-25/7.
88. Gledhill, R.A. (1979) A self toughening mechanism in epoxide resins. *J.Mat. Sci* **14,** Letters, p1769.
89. Arrowsmith, D.J. and Maddison, A. (1987) The use of the perforated lap shear specimens to test the durability of adhesive bonded aluminium. *Int. J. Adhesion and Adhesives* **7**(1), pp15-24.
90. Pluedemann, E. (1991) *Silane Coupling Agents*, Second Edition, Plenum Press, New York and London, ISBN 0/306/43473/3, p161.
91. Lees, W.A. (1990) *The Design and Assembly of Bonded Composites.* Permabond Division National Starch and Chemical, February 1990.
92. Bowditch, M.R. and Stannard, K.J. (1982) Adhesive bonding of GRP. *Composites* **13**, pp298-304.
93. Kinloch, A.J. (1987) The service life of adhesive joints. *Adhesion and Adhesives Science and Technology,* Chapman and Hall, ISBN 0 412 27440 x, chap 8.
94. Parker, B.M. (1978) Proc. Conf. *Jointing in Fibre Reinforced Plastics*, London p95.
95. Kinloch, A.J. (1987) Mechanical behaviour of adhesive joints. *Adhesion and Adhesives Science and Technology,* Chapman and Hall, ISBN 0 412 27440 x, chap 6.
96. Hodgkiess, J., Cowling, M.J. and Mulheron, M. (1994) Durability of glass reinforced polymer composites in marine environments. Proc. *Structural Materials in Marine Environments.* London, Royal Society, London, U.K., Inst. of Materials, pp58-72.
97. Althof, W. (1979) *Aluminium* **55**, p600.
98. Work ongoing at Glasgow Marine Technology Centre, Glasgow University Glasgow, G12 8QQ, 1996.
99. Hashim, S.A. (1988) Private communication. Glasgow University, Glasgow, U.K.

3.0 Section B: Application of Adhesives for Joining Grp

1. Gibson, A.G. and Spagni, D.A. (1991) Recent developments in the use of composite materials offshore. Proc. *Polymers in a Marine Environment*, London, U.K., Inst. of Marine Engineers, pp1.1-1.7.
2. Grim, G.C. and Bliault, A. (1991) The use of GRP piping in the oil and blast water systems of Draugen gravity base structure. Proc. *Polymers in a Marine Environment*, London, U.K., Inst. of Marine Engineers, pp3.1-3.7.
3. Gibson, A.G. and Spagni, D.A. (1991) The cost effective use of fibre reinforced composites offshore, multi sponsor research programme *Phase I Final Report*, Marinetech North, Coupland III Building, The University Manchester, M13 9PL.
4. Smith, C.S. (1990) *Design of Marine Structues in Composite Materials,* Elsevier Applied Science, London, ISBN 1 85166 416 5, chap 1 p13.
5. Keylock Fitting, Ameron Bondstrand Product Data FP329 Appendix 9, Ameron Fibreglas Pipe Division, Churchill House, Bridgewater Court, Weston-Super-Mare, Avon.
6. Ulfvarson, A.Y.J. (1989) Superstructures of large ships and floating offshore platforms bulit in FRP-composite -A feasibility study. *Sandwich Constructions 1* (eds. K.A. Olsson and R.P. Reichard), EMAS, ISBN 0 947817 37 9, pp469-483.
7. Norwood, L.S. (1989) The use of tough resin systems for improved frame to hull bonding in GRP ships. *Sandwich Constructions 1* (eds. K.A. Olsson and R.P. Reichard), EMAS, ISBN 0 947817 37 9, pp279-292.
8. Dow, R.S. and Bird, J. (1994) The use of composites in marine environments. Proc. *Structural Materials In Marine Environments*, Royal Society, London, U.K, Inst. of Materials, pp1-34.
9. Helbrat, S.E. and Gullbwerg, O. (1989) The development of the GRP sandwich technique for large marine structures. *Sandwich Constructions 1* (eds. K.A. Olsson and R.P. Reichard), Emas, ISBN 0 947817 37 9, pp425-442.
10. Kristiansen, U. (1989) Experience of FRP sandwich in Norwegian ship building. *Sandwich Constructions 1* (eds. K.A. Olsson and R.P. Reichard), EMAS, ISBN 0 947817 37 9, pp459-467.
11. Robson, B.L. (1989) The Australian Navy inshore minehunter - lessons learned. *Sandwich Constructions 1* (eds. K.A. Olsson and R.P. Reichard), EMAS, ISBN 0 947817 37 9, pp395-423.
12. Le Lan J.Y., Livory, P. and Parneix, P. (1992) Steel/composite principle used in the connection of composite superstructure to a metal hull.

Sandwich Constructions-2 **II** (eds. D. Weissman-Berman and K.A. Olsson), EMAS, ISBN 0 947817 514, pp857-873.

13. Cahill, P. (1992) Composite materials and naval combatants: The integrated technology deckhouse project. *Journal of Ship Production* **8**(1), pp1-7.
14. Motherwell Bridge Pushes Structural Pultrusion (1995) *Reinforced Plastics,* October, Elsevier Science Ltd, ISBN 0034-3617, pp38 - 40.
15. NCE Bridges Link to a Tee (1992) *New Civil Engineering,* August, pp20-23.
16. Mottran, J.T. (1993) Short and long term structural properties of pultruded beam assemblies fabricated using adhesive bonding. *Composite Structures* **25** pp387-393.
17. Hart - Smith, L.J. (1987) Design of adhesively bonded joints. *Joining Fibre Reinforced Plastics* (ed. F.L. Mathews), Elsevier Applied Science, ISBN 1-85166-019-4, chap 7.
18. Thomason, J.L. (1995) The interface region in glass reinforced epoxy resin composites: 3 Characterisation of fibre surface coatings and the interphase. *Composites* **26**(7), pp487-498.
19. Thomason, J.L. (1995) The interface region in glass reinforced epoxy resin composites: 1 Sample preparation, void content and interfacial strength. *Composites* **26**(7), pp487-498.
20. Adams, R.D. and Wake, W.C. (1984) *Structural Adhesive Joints in Engineering,* Elsevier Applied Science Publishers, ISBN 0 85334 2636, chap1 p4.
21. Hashim, S.A., Cowling M.J. and Winkle, I.E. (1990) Adhesion mechanisms between grp and steel for sandwich construction. Proc. *Adhesion'90* Cambridge, U.K. The Plastics and Rubber Institute, ISBN 1 871571 21 9, pp38/1-38/7.
22. Dalling, J. (1989) Refridgerated vehicle construction. Proc. *Structural Adhesives in Engineering II,* Bristol, U.K., Butterworth Scientific, pp272-278.
23. Lees, W.A. (1988) Designing for adhesives. Presented at the *Materials and Engineering Design Conference,* 9-13 May.
24. Lees, W.A. (1990) *The Design and Assemble of Bonded Composites,* Permabond Division, National Starch and Chemical, Feb., p12.
25. Shenoi, R.A., Read, P.J.C.L. and Hawkins, G.L. (1995) Fatigue failure mechanisms in fibre reinforced laminated T-joints. *Int. J. of Fatigue* **17**(6), pp415-426.
26. Smith, C.S. (1990) *Design of Marine Structues in Composite Materials,* Elsevier Applied Science, London, ISBN 1 85166 416 5, chap 4 p285 fig 4.74.
27. Hart Smith, L.J. (1973) Adhesive bonded double lap joint. NASA CR112235 NASA Contractor Report.

28. Hart Smith, L.J. (1985) Designing to minimize peel stresses in adhesive joints delamination and debonding of materials. ASTM STP876 (ed. W.S. Johnson).
29. Hart Smith, L.J. (1987) Stress analysis: a continuum mechanics approach. *Adhesives Developments - 2* (ed. A.J. Kinloch), pp238 - 266.
30. Hart Smith, L.J. (1981) Further developments in the design and analysis of adhesive bonded structural joints. *Joining of Composite Materials* (ed. K.T. Kedward), ASTM STP 747 pp3-31.
31. Holloway, L. (1993) *Polymer Composites for Civil and Structural Engineering,* Blackie Academic & Professioinal, ISBN 0 75 140028 9, chap. 8 p190.
32. Adams, R.D. and Wake, W.C. (1984) *Structural Adhesive Joints in Engineering,* Elsevier Applied Science Publishers, ISBN 085 334 263 6, chap 2 p107.
33. Thamm F. (1976) *J. Adhesion* **7**, p301.
34. *International Convention for Safety of Life at Sea* (1986) International Maritime Organisation (IMO) London.
35. Yeow, Y.T., (1978) *PhD. Dissertation,* Virginia Polytechnic Institute and State University, Blacksburg, VA USA.
36. Tanimoto,T. and Amijima, S. (1975) Progressive nature of fatigue damage of glass fibre reinforced plastics. *J. of Composite Materials,* **9**(4), pp380-390.
37. Smith, C.S. (1990) *Design of Marine Structues in Composite Materials* Elsevier Applied Science London ISBN 1 85166 416 5, chap 3 p87.
38. Agarwal, B.D. and Broutman, L.J. (1980) *Analysis and Performance of Fibre Composites,* Wiley, New York, USA.
39. Tsai, S.W. and Wu, E.M. (1971) *J. Comp Materials* **5,** p58.
40. Chandler, H.D., Campbell, I.M.D. and Stone, A.N. (1995) Assesment of failure criteria for fibre reinforced composite laminates. *Int. J. Fatigue* **17**(7), pp513-518.
41. Hashim S.A., Winkle, I.E., Knox, E.M. and Cowling M.J. (1993) Advantages of adhesives for bonding offshore and structural applications. Proc. *Integrity of Offshore Structures* (eds. D. Faulkner, M.J. Cowling, A. Incecik and P.K. Das), EMAS, ISBN 0 947817581, pp417-438.
42. Cowling, M.J., Hashim S.A., Smith E.M. and Winkle, I.E. (1991) Adhesive bonding for marine structural applications. Proc. *Polymers in a Marine Environment,* London, U.K., Inst. of Marine Engineers, pp7.1-7.9.
43. Winkle, I.E., Cowling, M.J. and Hashim, S.A. Lightweight, Fire Resistant, Frp/Steel Composites for Topsides, Phase 1 Composites Offshore Managed Programme, Glasgow Marine Technology Centre, table 2.
44. Abaqus V5.4, Hibbitt, Karlsson and Sorensen, 100 Medway Street, Providence, Rhode Island U.S.A.

45. Patran v2.1, MSC, MSC House, Lyon Way Frimley, Camberley, Surrey, GU16 5ER.
46. Smith, C.S. (1990) *Design of Marine Structures in Composite Materials,* Elsevier Applied Science, ISBN 1 85166 416 5, p26 table 2.1.
47. Koch, S. (1995) Design of structural joints with P.U. adhesives. Proc. *Structural Adhesives in Engineering IV,* Bristol, U.K., Inst. of Materials, ISBN 0901716 91 x, pp101-110.
48. Hashim, S.A. (1992) Assesment of Adhesive Bonding for Structural Design with Thick Adherends. *PhD. Thesis,* Glasgow University, Glasgow, U.K., table 3.3.
49. Redux 420 A/B Ciba Geigy Structural Adhesives May 1992 Instruction Sheet No. A/61a.
50. Lees, W.A. (1991) *Recent Developments in Composite Bonding with Particular Reference to Large Structures and Unprepared Surfaces.* Permabond Division, National Starch and Chemical Ltd.
51. Hashim, S.A. and Cowling, M.J. (1995) Aspects of testing and failure surfaces analysis related to thick adherend steel bonded joints. Proc. *Structural Adhesives in Engineering IV,* Bristol, U.K., Inst. of Materials, ISBN 0901716 91 x, pp245-250.
52. Adams, R.D. and Wake, W.C. (1984) Service Life. *Structural Adhesive Joints in Engineering,* Elsevier Applied Science, ISBN 0 85334 263 6, chap 7.
53. Adams, R.D., Coppendale, J., Mallick, V. and Al-Hamden, H. (1992) The effect of temperature on the strength of adhesive joints. *Int. Journal of Adhesion and Adhesives* **1**(3), pp185-190.
54. Al-Hamden, H. (1989) Thermal stresses in bonded joints. *M.Sc. Thesis* University of Bristol, Bristol, U.K.
55. Wake, W.C. (1982) *Adhesion and the Formulation of Adhesives,* 2nd ed., Applied Science Publishers, London.
56. Kinloch, A.J. (1987) *Adhesives and Adhesion Science and Technology,* Chapman and Hall, ISBN 0 412 27440 X, chap 7 p329.
57. Smith,C.S. (1990) *Design of Marine Structures in Composite Materials,* Elsevier Applied Science, ISBN 1 85166 416 5, p97 figure 3.44.
58. Holloway, L. (1978) *Glass Reinforced Plastics in Construction Engineering: Engineering Aspects,* Surrey University Press, ISBN 0 903384 21 3, chap 5 p69 table 5.2.
59. Winkle, I.E., Cowling, M.J. and Hashim, S.A. (1991) *Lightweight, Fire Resistant, Frp/Steel Composites for Topsides,* Phase 1 Composites Offshore Managed Programme, Glasgow Marine Technology Centre , p12 & table 6.

60. Allen, K.W. and Shanahan, M.E.R. (1976) The creep behaviour of structural adhesive joints-I *J.Adhesion* **8**(1), pp43-56.
61. Allen, K.W. and Shanahan, M.E.R. (1976) The creep behaviour of structural adhesive joints. *J.Adhesion* **7**(3), p161-174.
62. Smith, G.D. and Fay, P. (1990) Creep of adhesive lap joints in the dry and high humidity environments. Proc. *Adhesion'90,* Cambridge, U.K., The Plastics and Rubber Insitute, ISBN 1871571 219, pp 25/1-25/7.
63. Hashim, S.A. (1992) Assesment of adhesive bonding for structural design with thick adherends. *PhD. Thesis,* University of Glasgow, Glasgow, U.K., p60.
64. Winkle, I.E., Cowling, M.J. and Hashim, S.A. (1991) *Lightweight, Fire Resistant, Frp/Steel Composites for Topsides,* Phase 1 Composites Offshore Managed Programme, Glasgow Marine Technology Centre, table 7.
65. Winkle, I.E., Hashim, S.A., and Cowling, M.J. (1991) Composite panel performance in offshore fire conditions. Proc. *Polymers in a Marine Environment*, London, Inst. of Marine Engineers, pp12/1-12/6.
66. Hilderbrand, M. (1994) Non linear analysis and optimization of adhesively bonded single lap joints between fibre reinforced plastics and metals. *Int. J. of Adhesion and Adhesives* **14**(4), pp261-267.
67. Young, N.K, Chen, C.C. and Cheng W.L., Joining sections of thick fibreglass laminate. pp209-216.
68. Hull, D. (1981) *An Introduction to Composite Materials,* Cambridge University Press, ISBN 0521 283922, p126 table 7.1.
69. Smith, C.S. (1990) *Design of Marine Structures in Composite Materials,* Elsevier Applied Science, ISBN 1 85166 416 5, p84 fig 3.36.
70. Hart Smith, L.J. (1987) *Joining Fibre Reinforced Plastics* (ed. F.L. Mathews), Elsevier Applied Science, ISBN 1 85166 019 4, chap 7 p276 fig 4.
71. Mayer, R.M. (1993) *Design with Reinforced Plastics,* The Design Council, ISBN 0 85072294 2.
72. Hertzberg, R.W. and Mason, J.A. (1980) *Fatigue of Engineering Plastics,* Academic Press, ISBN 0 12 343550 1, chap 5 p246 fig 5.47.
73. Dharan, C.K.H. (1974) In *Failure Modes in Composites II* (eds. J.N. Fleck and R.L. Mehen), The Metallurgical Society, AIME, New York, p144.
74. Johnson, W.S. and Mall S.M. (1985) TM86443, NASA Washington D.C. U.S.A.
75. Smith, C.S. (1990) *Design of Marine Structues in Composite Materials,* Elsevier Applied Science, London, ISBN 1 85166 416 5, chap 3 p87 fig 3.38.
76. Lotsberg, I. and Andersson, H. (1985) *Fatigue Handbook Offshore Steel Structures* (ed. A. Almar-Naess), Tapir, ISBN 82 519 0662 8, chap 11 p464 table 11.1.

77. Hertzberg, R.W. and Manson, J.A. (1980) *Fatigue of Engineering Plastics,* Academic Press, ISBN 0 12 343550 1, p235 fig 5.37.
78. Luckyram, J. and Vardy, A.E. (1988) Fatigue performance of two structural adhesives. *J. Adhesion* **26**, pp273-291.
79. Liechti, K., Johnson, W.S. and Dillard, D.A. (1987) Experimentally determined strength of adhesively bonded joints. In *Joining of Fibre Reinforced Plastics* (ed. F.L. Mathews), Elsevier Applied Science, ISBN 1 85166 019 4, chap 4 p144.
80. Smith, C.S. (1990) Structural analysis and design. *Design of Marine Structures in Composite Materials,* Elsevier Applied Science, London, ISBN 1 85166 416 5, chap 4.
81. Smith, C.S. (1990) *Design of Marine Structures In Composite Materials,* Elsevier Applied Science, London, ISBN 1 85166 416 5, chap 3 p79.
82. Hashim, S.A. (1992) Assesment of adhesive bonding for structural design with thick adherends. *PhD. Thesis,* University of Glasgow, Glasgow, U.K., table 1.1.

4.0 Section C: Steel Corrugated Core Sandwich Construction

1. Bukowski, P. and Conway, P. (1989) The application of extruded polystrene foam as an insulating core material. *Sandwich Constructions-1* (ed. K.A.Olsson and R.P. Reichard), EMAS, ISBN 0 947817 37 9, pp529-554.
2. Tollouka, J.A. (1990) Potential sandwich structure applications offshore. *Sandwich Structure Newsletter* **1**(1), p7.
3. Turner, A.F. (1993) Composites and Laminates. *British Steel Technical Information Sheet*, Swindon, Moorgate, Rotheram, S60 3AR.
4. Wiernicki, C.J., Franz Liem, P.E., Gregory, P.E., Woods, D. and Furio, A.J. (1991) Structural analysis methods for lightweight metallic corrugated core sandwich panels subjected to blast loading. *Naval Engineers Journal,* May, pp192-303.
5. Sen, P., Shi, B.W. and Caldwell, J.B. (1989) Efficient design of panel structures by general multiple criteria utility. *Eng. Opt.* **14,** pp287-310.
6. Czaplicki, R.M. (1992) Cellular core structure providing gridlike bearing surfaces of opposing parallel planes of the core. *Sandwich Constructions-2* **II** (ed. D. Weissman-Berman and K.A. Olsson), EMAS, ISBN 0 947817 53 0, pp721-736.
7. Hoare, J. (1988) The application of sandwich structures to ship design. *Phase 4 Summary Report,* University of Newcastle Upon Tyne, U.K.
8. Barnes, T.A.L. (1985) Redesign of ships structures to facilitate auto methods of production. *M.Sc Thesis,* University of Newcastle Upon Tyne, U.K.
9. Bird, J. (1990) Private communication. DRA, Dumferline, Fife, U.K.

10. Tan, K.H., Montague, P. and Norris, C. (1989) Steel sandwich panels: finite element, closed solution and experimental comparison on a 6m x 2.1m panel. *The Structural Engineer* **67**(9/2), pp159-165.
11. Norris, C. (1987) Spot welded corrugated core steel sandwich panels subjected to lateral loading. *PhD thesis,* University of Manchester, U.K.
12. Montague, P. and Norris C. (1987) Spot welded corrugated core steel sandwich panel subjected to lateral loading. *Steel and Aluminium Structures Int. Conference* Papers, Elsevier, pp564-574.
13. Norris C., Montague, P. and Tan, K.H. (1989) All steel structural panels to carry lateral load: experimental and theoretical behaviour. *The Structural Engineer* **67**(9/2), pp167-189.
14. Chandel, R.S. (1985) Resistance spot welding of mild steel sheets. A literature review. *Indian Welding Journal* **17**(2), pp27-32.
15. Rahimi, H. and Hutchinson, A.R. (1995) Flexural strengthening of concrete beams with externally bonded CFRP and GFRP plates. Proc. *Structural Adhesives in Engineering IV*, Bristol, U.K.,Inst. of Materials, pp177-182.
16. Allen, H.G. (1969) *Analysis and Design of Structural Sandwich Panels,* Permagon Press, 08 012870.
17. Platema, F.J. (1966) *Sandwich Construction,* John Wiley and Son, New York.
18. Reissner, E. (1948) Finite deflection of sandwich plates. *J. Aero Sci* **15**(7), pp435-440.
19. Libove, C. and Batdorf, S.B. (1948) A general small deflection theory for flat sandwich plates. NACA TN1526.
20. Libove, C. and Hubka, R.E. (1951) Elastic constants for corrugated core sandwich plates. NACA TN2289.
21. Harris, L.A. and Auelmann, R.R. (1960) Stability of flat, simply supported corrugated core sandwich plate under combined loads. *J. of the Aero/space Sciences*, July, pp525-534.
22. Johnson, A.F. and Sims, G.D. (1986) Mechanical properties and design of sandwich materials. *Composites* **17**(4), pp321-328.
23. Sowerby, J.G. (1989) Mechlad, Mechtool Engineering Ltd, Mechtool House, Mains Works, Whessoe Road, Darlington, Co. Durham, U.K.
24. Clark, J.D. (1987) Predicting the properties of adhesively bonded corrugated core sandwich panels. Proc. *Adhesion'87*, York, U.K., The Plastics and Rubber Inst., ppw1-w6.
25. Cowling M.J., Smith, E.M., Hashim, S.A. and Winkle, I.E. (1989) Performance of adhesively bonded steel connections for marine structures. Proc. *Evalmat'89*, JISI, Kobe, Japan, pp827-834.

26. Tillman, S.C. and Williams, A.F. (1987) Buckling under compression of simple and multi-cell plate columns. ECCS Colloquim on *Stability of Plate and Shell Structures,* Ghent University, 6-8 April 1987, pp225-234.
27. Kinloch, A.J. (1987) *Adhesion and Adhesives Science and Technology,* Chapman & Hall, ISBN 0 412 27440 X, chap 7.
28. SESAM, Developed by Det norske Veritas, marketed by Veritec, Marine Technology Consultants A.S., Veritec, Hovik, Oslo, Norway.
29. Pafec, Pafec Ltd, Strelley Hall, Strelley, Nottingham, U.K.
30. ESDU (1980) Data Sheets, Structures Subseries Vol 3, London: ESDU International Ltd.
31. Rollins, M.A. and Xia, Y.R. Dynamic failure of sandwich structures. *Structures Under Shock and Impact,* pp335-344.
32. Hart - Smith, L.J. (1987) Design of adhesively bonded joints. *Joining Fibre Reinforced Plactics* (ed. F.L. Mathews), Elsevier Applied Science, ISBN 1 85 166 0194, chap 7.
33. Lotsberg, I. and Andersson, H. (1985) *Fatigue Handbook Offshore Steel Structures* (ed. A. Almar-Naess), Tapir, ISBN 82 519 0662 8, chap 11, table 11.1, p464.
34. Hashim, S.A. (1988) Private communication. Glasgow University, Glasgow, U.K.